N. M. NEWMARK

CIVIL ENGINEERING STUDIES
STRUCTURAL RESEARCH SERIES NO. 201

STRENGTH AND BEHAVIOR OF PRESTRESSED CONCRETE BEAMS WITH WEB REINFORCEMENT

By
J. G. MAC GREGOR
M. A. SOZEN
and
C. P. SIESS

Issued as a Part
of the
Ninth Progress Report
of the
INVESTIGATION OF PRESTRESSED CONCRETE
FOR HIGHWAY BRIDGES

UNIVERSITY OF ILLINOIS
URBANA, ILLINOIS
AUGUST 1960

STRENGTH AND BEHAVIOR OF PRESTRESSED CONCRETE BEAMS WITH WEB REINFORCEMENT

by

J. G. MacGregor
M. A. Sozen
and
C. P. Siess

Prepared as a Part of an Investigation
Conducted by

THE ENGINEERING EXPERIMENT STATION
UNIVERSITY OF ILLINOIS
In Cooperation with
THE DIVISION OF HIGHWAYS
STATE OF ILLINOIS

and

U.S. DEPARTMENT OF COMMERCE
BUREAU OF PUBLIC ROADS

Project IHR-10
INVESTIGATION OF PRESTRESSED CONCRETE
FOR HIGHWAY BRIDGES

Urbana, Illinois
August 1960

CONTENTS

CONTENTS (Cont'd)

LIST OF TABLES

LIST OF FIGURES

LIST OF FIGURES (Cont'd)

Figure No.

LIST OF FIGURES (Cont'd)

Figure No.

LIST OF FIGURES (Cont'd)

Figure No.

LIST OF FIGURES (Cont'd)

Figure No.

LIST OF FIGURES (Cont'd)

APPENDIX A - LIST OF FIGURES

Figure No.

APPENDIX A - LIST OF FIGURES (Cont'd)

Figure No.

1. INTRODUCTION

1.1 Object and Scope

Tests of prestressed concrete beams conducted in the last few years have shown consistently that reinforcement should be provided in prestressed members to resist inclined tensile stresses as well as horizontal tensile stresses. Two different types of reinforcement are commonly used for this purpose: stirrups and draped reinforcement. The term "draped reinforcement" refers to longitudinal prestressed reinforcement which is curved in elevation so that its centroid is closer to the top of the beam at the supports than it is at midspan.

Stirrups are used primarily to transfer shearing forces across inclined cracks and to restrain the opening of such cracks. While stirrups have little effect on the load at which inclined cracks form, the presence of stirrups in a beam with inclined cracks makes it possible for the beam to carry load beyond inclined cracking. If inclined cracks develop in a beam without web reinforcement or with just a small amount of web reinforcement, the beam will fail in shear at a smaller load and a much smaller deflection than those corresponding to a flexural failure. By providing a sufficient number of properly designed stirrups, it is possible to make the beam fail in flexure at a load and deflection corresponding to those expected in a flexural failure.

Draped reinforcement primarily affects the shear strength of a prestressed concrete beam by means of changes in the inclined cracking load. Depending on the manner in which inclined cracks form, draped reinforcement may act to increase or decrease the inclined cracking load. While stirrups are provided solely to carry shear, the longitudinal reinforcement may be

draped primarily to relieve high tensile and compressive stresses resulting from the effect of the prestress at the end of the beam or to alleviate anchorage stresses.

The tests described in this report were carried out to study the effect of stirrups and draped reinforcement on the shear strength of prestressed concrete beams. Tests of 87 simply-supported beams are reported. The principal variables were the amount, type and spacing of the stirrups and the profile of the longitudinal reinforcement. Sixty-one beams had web reinforcement and straight longitudinal reinforcement. Fourteen had draped longitudinal reinforcement but no web reinforcement, and five had both stirrups and draped wires. The remaining seven beams had neither web reinforcement nor draped wires. The other variables included: shape of cross section, prestress level, amount of longitudinal reinforcement, concrete strength, and type of loading.

At the University of Illinois, tests of the shear strength of prestressed concrete beams started in 1952 with tests on rectangular post-tensioned beams without web reinforcement. The observations from these tests led to a fundamentally new explanation of the strength of beams failing in shear.(1)* Tests on I-beams in the following years increased the understanding of the failure mechanism and emphasized the importance of the inclined cracking load in beams without web reinforcement.(2) Means of preventing shear failures were studied next, and from 1956 to 1958, 38 I-beams with web reinforcement were tested and analyzed; and the strength of the web reinforcement was related for the first time to the difference between

*Numbers in parentheses refer to corresponding entries in the References.

the shears at inclined cracking and at ultimate. (3) Subsequent tests have served to broaden the range of variables in the tests of beams with web reinforcement, adding draped reinforcement and moving loads among other things to the list of variables considered.

The results from all the tests of beams with web reinforcement, draped reinforcement, and the beams tested under moving loads are presented and discussed in this report. The observed patterns of behavior are discussed and classified, with special attention being paid to the manner in which inclined cracking develops and the mode of failure. Finally, based on expressions developed to predict the cracking loads and failure loads, design recommendations are presented.

1.2 Outline of Tests

This report is based on the results of tests on 87 simply-supported prestressed concrete beams both with and without web reinforcement. The basic cross-sectional dimensions were 6 by 12 in. in all cases, although two beams had a 2 by 24-in. composite slab cast on top. Five beams were rectangular in section, 43 were I-beams with 3-in. thick webs, and 29 were I-beams with 1 3/4-in. thick webs. The two composite beams had 1 3/4-in. webs. The nominal dimensions of the beams are shown in Fig. 1, and the beam properties are listed in Table 1.

The majority of the beams had web reinforcement composed of one, two, or three-leg vertical stirrups. The nominal dimensions of the stirrups are shown in Fig. 2 and the properties of the web reinforcement are summarized in Table 2. Nineteen beams had some or all of the wires draped in the shear spans. In every case, the drape profiles consisted of straight-line segments with the wires deflected under the load points as shown in Fig. 3. The

properties of the various drape profiles are listed in Table 3. Seven other beams were tested under moving loads.

The ranges of variables covered in this series of 87 beams are indicated below.

Beams With Straight Longitudinal Reinforcement

Beams Without Web Reinforcement (3 beams)

Web Thickness:

3 in. . . . . 2 beams

1 3/4 in. . . . . 1 beam

Concrete Strength: 2640 to 3730 psi

Longitudinal Reinforcement Ratio: 0.29 to 0.41 percent

Prestress: 119 to 127 ksi

Shear Spans:

36 in. . . . . 2 beams

27 in. . . . . 1 beam

Beams With Web Reinforcement

Rectangular Beams (4 beams)

Concrete Strength: 2800 to 5470 psi

Longitudinal Reinforcement Ratio: 0.71 percent

Prestress:

120 ksi . . . . . 2 beams

60 ksi . . . . . 2 beams

Shear Span: 36 in.

Stirrups:

Spacing: 6.5 in.

Ratio $(\frac{A_v}{bs})$: 0.256 percent

Yield Stress: 53.7 ksi

I-Beams with 3-in. Webs (23 beams)

Concrete Strength: 2680 to 7630 psi

Longitudinal Reinforcement Ratio: 0.19 to 0.61 percent

Prestress:

120 ksi . . . . . 21 beams

60 ksi . . . . . 2 beams

Shear Spans:

36 in. . . . . 15 beams

48 in. . . . . 2 beams

54 in. . . . . 1 beam

70 in. . . . . 4 beams

78 in. . . . . 1 beam

Stirrups:

Spacing: Uniform - 2.5 to 10.5 in. . . . . 19 beams

Variable. . . . . 4 beams

Ratio $(\frac{A_v}{bs})$: 0.038 to 0.196 percent

Yield Stress: 34 to 79.5 ksi

I-Beams With 1 3/4-in. Webs (29 beams)

Concrete Strength: 2310 to 7420 psi

Longitudinal Reinforcement Ratio: 0.19 to 0.59 percent

Prestress:

120 ksi . . . . . 27 beams

65 ksi . . . . . 2 beams

Shear Spans:

28 in. . . . . 2 beams

36 in. . . . . 24 beams

70 in. . . . . 3 beams

Stirrups:

Spacing: Uniform - 2.25 to 9.0 in. . . . . 28 beams

Variable. . . . . 1 beam

Ratio $(\frac{A_v}{bs})$: 0.048 to 0.382 percent

Yield Stress: 34.0 to 79.5 ksi

I-Beams With 1 3/4-in. Webs and Cast-in-Place Slab (2 beams)

Concrete Strength: 3520 and 3910 psi

Longitudinal Reinforcement Ratio: 0.082 percent

Prestress: 120 ksi

Shear Span: 36 in.

Stirrups:

Spacing: 2.5 and 3.0 in.

Ratios $(\frac{A_v}{bs})$: 0.277 and 0.327 percent

Yield Stress: 36.8 and 41.2 ksi

Beams With Draped Longitudinal Reinforcement

Beams Without Web Reinforcement (14 beams)

Web Thickness:

6 in. . . . . 1 beam

3 in. . . . . 10 beams

1 3/4 in. . . . . 3 beams

Concrete Strength: 2560 to 6280 psi

Longitudinal Reinforcement Ratio: 0.30 or 0.40 percent

Prestress: 81 to 124 ksi

Shear Spans:

27 in. . . . . 2 beams

36 in. . . . . 12 beams

Drape Angle: 1.5 to 10 degrees

Beams With Web Reinforcement (5 beams)

Web Thickness: 3 in.

Concrete Strength: 2910 to 4600 psi

Longitudinal Reinforcement Ratio: 0.40 percent

Prestress: 120 ksi

Shear Span: 36 in.

Drape Angle: 2.25 to 6.80 degrees

Stirrups:

Spacing: Uniform - 3.5 to 5.0 in.

Ratio $(\frac{A_v}{bs})$: 0.137 to 0.196 percent

Yield Stress: 36.8 ksi

Beams With Straight Longitudinal Reinforcement, Moving Loads

Beams Without Web Reinforcement (4 beams)

Web Thickness:

3 in. . . . . 2 beams

1 3/4 in. . . . . 2 beams

Concrete Strength: 3660 to 5200 psi

Longitudinal Reinforcement Ratios: 0.30 and 0.40 percent

Prestress: 120 ksi

Beams With Web Reinforcement (3 beams)

Web Thickness:

3 in. . . . . 1 beam

1 3/4 in. . . . . 2 beams

Concrete Strength: 3970 to 4650 psi

Longitudinal Reinforcement Ratio: 0.30 and 0.40 percent

Prestress: 120 ksi

Stirrups:

Spacing: 4.5 in. . . . . 1 beam

Variable. . . . . 2 beams

Ratio: 0.072 to 0.154 percent

Yield Point: 36.8 to 37.2 ksi

1.3 Acknowledgements

This study was carried out as a part of the research under the Illinois Cooperative Highway Research Program Project IHR-10. "Investigation of Prestressed Reinforced Concrete for Highway Bridges". The work on the project was conducted by the Department of Civil Engineering of the University of Illinois in cooperation with the Division of Highways, State of Illinois, and the U.S. Department of Commerce, Bureau of Public Roads.

On the part of the University, the work covered by this report was carried out under the general administrative supervision of W. L. Everitt, Dean of the College of Engineering, Ross J. Martin, Director of the Engineering Experiment Station, N. M. Newmark, Head of the Department of Civil Engineering, and Ellis Danner, Director of the Illinois Cooperative Highway Research Program and Professor of Highway Engineering.

On the part of the Division of Highways of the State of Illinois, the work was under the administrative direction of R. R. Bartelsmeyer, Chief Highway Engineer, Theodore F. Morf, Engineer of Research and Planning, and W. E. Chastain, Sr., Engineer of Physical Research

The program of investigation has been guided by an Project Advisory Committee consisting of the following:

Representing the Illinois Division of Highways

W. E. Chastain, Sr., Engineer of Physical Research

Illinois Division of Highways

W. J. Mackay, Bridge Section, Bureau of Design, Illinois Division of Highways

C. E. Thunman, Jr., Bridge Section, Bureau of Design, Illinois Division of Highways

Representing the Bureau of Public Roads

Harold Allen, Chief, Division of Physical Research, Bureau of Public Roads

E. L. Erickson, Chief, Bridge Division, Bureau of Public Roads

Representing the University of Illinois

C. E. Kesler, Professor of Theoretical and Applied Mechanics

Narbey Khachaturian, Associate Professor of Civil Engineering

Fred Kellam, Bridge Engineer, Bureau of Public Roads, and G. S. Vincent, Chief, Bridge Research Branch, Bureau of Public Roads, also participated in the meetings of the Advisory Committee and contributed materially to the guidance of the program.

The investigation was directed by Dr. C. P. Siess, Professor of Civil Engineering, as Project Supervisor and as ex officio chairman of the Project Advisory Committee. Immediate supervision of the investigation was provided by Dr. M. A. Sozen, Associate Professor of Civil Engineering, as Project Investigator.

With the exception of Lot 14, the prestressing reinforcement used in this investigation was donated by the American Steel and Wire Division of the United States Steel Corporation. The Lot 14 wire was obtained from the Union Wire Rope Corporation.

Thanks are extended to C. J. Fleming and L. Hognestad, formerly Research Assistants in Civil Engineering, for their valued assistance in

connection with the tests and analyses and to Dr. G. Hernandez, formerly Research Assistant in Civil Engineering, who tested 37 of the beams described in this report, and analyzed the results and reported them in his Ph.D. thesis (3).

This report is based on a doctoral dissertation prepared by Mr. MacGregor under the direction of Professors Siess and Sozen.

1.4 Notation

(a) Designation of Test Specimens*

Although the specimens were numbered originally according to the order of testing, they have been regrouped for easier reference according to the major variables. Each beam is designated by one or two letters and two pairs of numerals; for example, BD.14.26. The letters and numerals have the following significance:

First letter (BD.14.26)

A - Rectangular beam

B - I-Beam, 3-in. web

C - I-Beam, 1 3/4-in. web

F - I-Beam, 1 3/4-in. web with 2 by 24-in. composite slab

Second letter (BD.14.26)

D - Draped reinforcement

V - Draped reinforcement and web reinforcement

---

*The designation of test specimens in Ref. 2 was the same as this system except for the second numeral (B.12.26) which represented:
1 - 54 in. shear span;
2 - 36-in. shear span;
3 - 28-in. shear span;
4 - 24 in. shear span.
The designation of the test specimens in Ref. 6 differs from this system except in the meaning of the first pair of numerals.

W - Web reinforcement

(The second letter is excluded if the beam has neither draped reinforcement nor web reinforcement).

First Numeral (BD.14.26)

1 - Prestress greater than 90,000 psi

2 - Prestress less than 90,000 psi

Second Numeral (BD.14.26)

0 - Beams tested under moving loads

3 - 27 or 28-in. shear span, approximately 3/12 span length

4 - 36-in. shear span, 4/12 span length

5 - 48-in. shear span, approximately 5/12 span length

6 - 54-in. shear span, 6/12 span length

8 - 70-in. shear span, approximately 8/12 span length

9 - 78-in. shear span, approximately 9/12 span length

The second pair of numerals (BD.14.26) represents the value of $Q = pE_s/f'_c$ to two significant figures.

Most of the specimens in the high and medium prestress levels (designated 1- and 2-) were prestressed to about 120,000 psi and 60,000 psi, respectively. The beams with 27, 54, 70 and 78-in. shear spans were loaded with a single load. The others had two loads symmetrically located about midspan. All beams had a span of 9 ft except those with 27-in. shear spans which had a span of 8 ft 6 in.

(b) Symbols

Cross-sectional Constants and Dimensions

A_s = total area of prestressed longitudinal reinforcement

A_{slab} = area of cast-in-place slab

A_v = total cross-sectional area of one stirrup

a = length of shear span

b = top flange width of precast beam

b' = web thickness

d = effective depth of the longitudinal reinforcement

h = overall depth of beam

I_t = transformed moment of inertia of uncracked section

n = number of stirrups crossed by a crack with horizontal projection of z

x = $h/4 + a/6$ = distance from load to assumed location of initiating flexural crack

y_b = distance from elastic centroid to bottom fiber

z = 1.5 x = horizontal projection of inclined crack

Loads, Moments and Forces

C = total compressive force in the concrete in a beam without stirrups

C' = total compressive force in the concrete in a beam with stirrups

M_{cf} = flexural cracking moment

M_{cs} = inclined cracking moment

M_D = dead load moment

M_{uf} = computed ultimate moment for flexural failure

M_{us} = computed ultimate moment for shear failure

M_{ut} = measured ultimate moment

M_w = maximum bending moment from one H-S truck on a span

P_s = force caused by differential shrinkage in slab and beam

T = tensile force in longitudinal reinforcement

V_c = computed inclined cracking shear

V'_c = computed inclined cracking shear for hypothetical beam with straight wires

V_{cm} = measured inclined cracking shear

V_{conc} = shear carried by concrete in a beam without stirrups

V'_{conc} = shear carried by concrete in a beam with stirrups

V_d = upward component of prestressing force, drape shear

V_f = computed initiating flexural cracking shear, corresponding to flexural cracking at $\underline{x}$ from given section in direction of diminishing moment

V'_f = computed shear corresponding to flexural cracking at $\underline{d}$ from given section in direction of diminishing moment

V_n = net shear at inclined cracking

V_s = computed shear corresponding to web-shear cracking

V_u = shear corresponding to failure load

V_v = shear carried by stirrups

Stresses

Concrete

f_b = computed failure stress in indirect tension test

f'_c = compressive strength determined from 6 by 12-in. control cylinders

f_{cu} = average concrete stress in compression zone at failure

f^b_F = stress in bottom fiber due to prestress

f_r = modulus of rupture determined from 6 by 6 by 22 in. control beams loaded at the thirdpoints of an 18-in. span

f_t = assumed tensile strength

f_1 = normal stress at a point

f_2 = vertical stress at a point

v = shear stress

Steel

f'_s = tensile strength of longitudinal reinforcement

f_{sc} = stress in longitudinal reinforcement at inclined cracking

f_{se} = effective prestress after losses

f_{su} = stress in longitudinal reinforcement at failure

f_y = stress in web reinforcement at one percent strain

Strains

Concrete

ϵ_c = concrete strain

ϵ_{cc} = concrete strain at top of beam at inclined cracking

ϵ_{ce} = concrete strain at level of longitudinal reinforcement due to effective prestress

ϵ_u = limiting strain at which concrete crushes in a beam

Steel

$\epsilon_{se} = \epsilon_{su} - (\epsilon_{se} + \epsilon_{ce})$ = increase in steel strains beyond zero concrete strain at level of longitudinal reinforcement

$\epsilon'_{sa} = \epsilon_{sa} - \epsilon_{sc}$ = increase in steel strain after inclined cracking

ϵ_{sc} = steel strain at inclined cracking

$\epsilon'_{sc} = \epsilon_{sc} - (\epsilon_{se} + \epsilon_{ce})$

ϵ_{se} = steel strain corresponding to effective prestress

ϵ_{su} = steel strain at ultimate

Dimensionless Factors

F = apparent strain compatability factor

F_1 = strain compatibility factor before inclined cracking

F_2 = strain compatibility factor after inclined cracking

j = ratio of length of internal lever arm to effective depth

k_c = ratio of neutral axis depth at inclined cracking to effective depth

k_u = ratio of neutral axis depth at ultimate to effective depth

k_2 = ratio of depth of the resultant compressive force to depth of neutral axis

$p = A_s/bd$ = reinforcement ratio

$Q = pE_s/f'_c$

$r = A_v/bd$ = web reinforcement ratio, based on flange width

Miscellaneous

E_c = assumed modulus of elasticity of concrete

E_s = modulus of elasticity of steel

φ = drape angle, angle between the resultant prestressing force and the horizontal

2. MATERIALS, FABRICATION, AND TEST SPECIMENS

2.1 Materials

(a) Cement

Marquette brand Type III portland cement was used for all the specimens. The cement was purchased in paper bags from local dealers in lots of 20 to 40 bags.

(b) Aggregates

Wabash River sand and pea gravel were used in all the beams. Both aggregates have been used in this laboratory for many previous investigations and have passed the usual specification tests. The sand had a fineness modulus of 3.0 to 3.3. The maximum size of the gravel was 3/8-in. The absorption of both the fine and coarse aggregate was about one percent by weight of the surface dry aggregate.

The aggregates were from a glacial outwash of the Wisconsin glaciation. The major constituents of the gravel were limestone and dolomite with minor quantities of quartz, granite and gneiss. The sand consisted mainly of quartz.

(c) Concrete Mixes

Mixes were designed by the trial batch method. Two batches were used in each beam, Batch 1 being in the lower half to two-thirds of the beam. Table 4 lists the proportions of the concrete batches used in each beam along with the slump, compressive strength, modulus of rupture and age of test. Proportions are in terms of oven dry weights.

Each compressive strength listed in Table 4 is the average from at least four tests on 6 by 12-in. cylinders. The increase in concrete strength with age, expressed as a ratio of the seven-day strength is shown in Fig. 4.

The modulus of rupture of each batch was determined from the test of one 6 by 6-in. beam, loaded at the third-points of an 18-in. span. The moduli of rupture are compared with compressive strengths in Fig. 5. Since a measure of the tensile strength and the modulus of rupture of the concrete in each beam was necessary for the interpretation of the test results, and since the scatter in the measured modulus of rupture data did not warrant use of the results of individual control beams, the statistical expression developed in Ref. 2 was selected to represent the test data. For concrete with small-size coarse aggregate this expression was:

$$f_r = \frac{3000}{4 + \frac{12{,}000}{f'_c}} \qquad (1)$$

where f_r and f'_c are both in pounds per square inch. This expression is plotted in Fig. 5 and is compared to the following expression which is commonly used to express the modulus of rupture of concrete.

$$f_r = 6\sqrt{f'_c} \qquad (2)$$

The values of f_r used in this study were all computed from Eq. 1 and were not the observed values.

A limited number of "Brazilian" or "Indirect Tension Tests" were made by loading 6 by 12-in. cylinders along their diameter. In this test a cylinder was placed on its side between the heads of the testing machine and 12 by 3/8-in. strips of card board were placed between the cylinder and the heads to distribute the load evenly along the length of the specimen. Under this loading the middle 4/5ths of the vertical diameter of the cylinder is stressed almost uniformly in tension and the specimen fails by splitting along this diameter. The computed stresses corresponding to the failure load are included in Table 4.

The modulus of elasticity for the concrete was determined by measuring the stresses and the corresponding strains in a 6 by 12-in. cylinder. The modulus was defined as the slope of a secant passing through the origin and the point on the stress-strain curve corresponding to 1000 psi. The measured values of the modulus of elasticity are plotted in Fig. 6. Equation 3, also plotted on this figure represents a modified form of Jensen's expression for the modulus of elasticity of concrete.

$$E_c = \frac{30,000,000}{6 + \frac{10,000}{f'_c}} \qquad (3)$$

where E_c and f'_c are both in pounds per square inch.

(d) Prestressing Reinforcement

Cold-drawn and stress-relieved high tensile strength single wire meeting the requirements of ASTM-A-421-59T was used for longitudinal reinforcement. The wires used were received in six shipments designated as Lots 8, 10, 11, 12, 13 and 14. Lots 8 through 13 were manufactured by the American Steel and Wire Division of the United States Steel Corporation and were designated as "Hard Drawn Stress Relieved Super-Tens Wire". The wire in Lot 14 was manufactured by the Union Wire Rope Corporation and was designated as "0.196-in. Tufwire". The manufacturing process for the AS and W wire consisted of the following steps: (1) hot rolling, (2) load patenting, (3) cold drawing, and (4) stress relieving. The heat analyses furnished by the manufacturers, the diameters, and strength properties of each wire are listed in Table 5.

The stress-strain relationships for the different lots determined from tests of samples cut from different portions of each coil are shown in

Figs. 7, 8 and 9. All samples were tested in a 120,000-lb capacity Baldwin-Southwark-Tate-Emery hydraulic testing machine, and the strains were measured with an 8-in. extensometer employing a Baldwin "microformer" coil and recorded by an automatic device.

To improve the bond, the cut lengths of wire were wiped with a rag dipped in a solution of hydrochloric acid and then rusted by storing in a moist room for one to three weeks. This produced a slightly pitted surface which improved the bond characteristics. The intended locations of the electric strain gages were protected from rusting by wrapping them with insulating tape. All wires were cleaned with a wire brush to remove loose rust before they were used in a beam.

(e) Web-Reinforcement

In all but four of the beams with web-reinforcement the stirrups were made of black annealed wire of six different nominal diameters. This wire was received in straight pieces, 5 or 15 ft long, in three shipments, designated as A, B and C.

In the remaining four beams, the stirrups were made from 0.129-in. square cold finished bars of AISI C-1018 steel. These wires were received in straight pieces, 12-ft long.

After cutting the wires to the proper lengths for stirrups, they were rusted and samples were tested in the same way as described for the prestressing steel. The stress-strain characteristics together with the diameters and yield-point stresses are shown in Figs. 10 through 13. The type of wire used for the stirrups of each particular beam is listed in Table 2.

In the analysis of the test results the yield point stress for the stirrup steel has been defined as the stress corresponding to one

percent strain, since strains of at least this magnitude were present in the stirrups when failure occurred. If a stirrup crossed by a crack is assumed to be unbonded for a quarter of its length on each side of the crack, a one-percent strain spread over the unbonded length of the stirrup would result in a crack which is 0.05 in. wide. The actual widths of the inclined cracks were often 0.05 in. or greater at ultimate indicating strains in the stirrups of one percent or more. The successive development of a number of adjacent inclined cracks in the webs of many of the beams tested would indicate better bond than assumed here. The stresses corresponding to one percent strain in the stirrup steel ranged from 2 to 11 percent greater than the stress at first yield. The stresses corresponding to one percent strain are listed with the stress-strain curves in Figs. 10 through 13.

(f) Reinforcing Bars

Intermediate grade No. 3 deformed bars were used to reinforce the slabs cast on the tops of two beams. These bars were taken from the laboratory stock and samples were tested in the same way as indicated in Section 2.1(d). A typical stress-strain curve is shown in Fig. 12.

2.2 Description of Specimens

(a) Over-all Dimensions

All the beams were modificiations of a basic member 6 by 12-in. in cross section and 10 ft 1 1/2 in. to 10 ft 8 in. in over-all length. Of the 87 beams reported, 43 had 3-in. webs, 39 had 1 3/4 in.-webs and 5 were rectangular in cross section. The webs were formed by metal inserts placed in rectangular forms. Rectangular end blocks 12 to 18 in. in length were provided at each end of the beams.

The nominal dimensions of the beams are shown in Fig. 1. Although the specimens were cast in metal forms, the dimensions varied slightly from beam to beam. The measured dimensions are listed in Table 1.

Two of the beams had 2 by 24-in. slabs cast on top. The continuity of shear flow between the slab and the beam was maintained by using longer stirrups with the upper ends protruding from the beam (Type B, Fig. 2) and shear keys along the top of the beam. The shear keys for both beams were 3/4 in. deep, 2 in. long in the direction of the length of the beam, and extended the full width of the upper flange. The center-to-center spacing of the shear keys was 5 in. in G43 and 6 in. in G38. The shear keys and protruding stirrups are shown in Fig. 14(a).

(b) Details of Longitudinal Reinforcement

The longitudinal reinforcement consisted of 4 to 12 single wires, pretensioned, and anchored by bond. Bond slip was observed after inclined cracking in a few of the beams with draped wires but not in beams with straight wires. The prestressing wires were placed in one or two horizontal rows of 2, 4 or 6 wires per row. The wires were spaced at 0.70 in. center to center in the horizontal direction and 0.75 in. in the vertical direction.

In the beams with draped wires the wire profiles consisted entirely of straight line segments, the wires being draped from the load points in every case. The prestressing wires were either all draped parallel to one another or some of the wires were draped and the rest were straight. The vertical and horizontal spacing of the wires was the same as in beams with straight wires. In all, twelve reinforcement profiles were used. These are described in Table 3 and Fig. 3.

In the two beams with composite slabs, the slabs were reinforced by intermediate grade No. 3 deformed bars at 6-in. spacing in both directions. The bars were placed at mid-height of the slab. Figure 14(b) shows the slab form and slab reinforcement in place prior to casting the slab.

(c) Details of Web Reinforcement

Vertical stirrups having one, two or three legs were used in all the 63 beams which had web reinforcement. The nominal dimensions of the stirrups are shown in Fig. 2 and their spacings in Figs. 15 through 22. Details of the stirrup percentages, spacings, type of wire and type of stirrups are summarized in Table 2.

Stirrup spacings ranged from 2 1/4 in. to 10 1/2 in. In the majority of the beams, a uniform stirrup spacing was used throughout the length of the beam. In seven beams, however, the spacing was varied along the length of the beam. In the first beams tested, stirrups were provided only in the shear spans (Beams CW.14.15, CW.14.18 and CW.14.45). However, horizontal cracks were observed between the web and the upper flange near midspan of two of these beams before and during the tests. Consequently, stirrups were used throughout the constant flexure region in all the other beams to prevent the development of these cracks. Cracks of this type were not observed in beams with stirrups in the flexure span. In the beams loaded with a single load placed away from the midspan the stirrup spacings were different in the two shear spans.

2.3 Prestressing

(a) End Details of Wires

Threaded connections were used to grip both ends of the wires during the tensioning process and until "transfer" took place. Threads were cut

on the end 3 in. of the wires with an automatic threading machine using specially heat-treated chasers with 24 threads to the inch. Despite the heat-treatment, the chasers required resharpening after threading about twenty wires. The threads on the wires were cut to provide a medium fit with the thread in the nuts, requiring a thread slightly larger than a No. 10 which has a basic major diameter of 0.190 in. The nominal diameter of the wires was 0.196 in.

The nuts used to anchor the wires were 5/8-in. long and octagonal in section. They were specially manufactured in the laboratory machine shop. The hole was sub-drilled with a No. 18 tap drill and tapped with a standard No. 12, 24 threads to the inch, tap. This provided a full No. 12 thread in the nuts. Nuts with a No. 10 thread required too much material to be cut from the wires to be practical. The thread cut on the wires to fit the No. 12 thread in the nuts is sufficient to develop at least 160,000 psi in the wires and was considered most suitable.

The nuts were made from 1/2 in. octagonal "Buster" alloy punch and chisel steel having the following analysis range: Carbon 0.56-0.60 percent; silicon 0.60-0.80 percent; chromium 1.10-1.30 percent; tungsten 2.00-2.30 percent; vanadium 0.20-0.30 percent. The hardening process involved six steps: (1) packing in charcoal in a closed steel box, (2) heating for 20 minutes at 1200 F, (3) heating for 45-60 minutes at 1650F, (4) oil quenching to slightly above room temperature, (5) tempering at 1000F for 30 minutes, and (6) removal from furnace and air cooling.

(b) Tensioning Apparatus

Since the beams in this series were all pre-tensioned, a pre-stressing frame was necessary to provide a reaction for the tensioning

force. The frame consisted of two 11 ft 6-in. lengths of extra-heavy 3-in. diameter pipe and two bearing plates, 2 by 6 by 20-in. It was built to fit around the form for the beam. The bearing plates had six rows of 0.206-in. diameter holes to accomodate the various positions of the wires. The holes were 0.70 in. apart horizontally and 0.75 in. vertically.

A 30-ton capacity Simplex center-hole hydraulic ram operated by a Blackhawk pump was used to tension the wires. A U-shaped jacking frame fitted between the pretensioning frame and the jack. To tension the wires, the ram reacted against the frame and a 5/8-in. diameter rod. The thrust was transferred from the ram to the rod through washers and a nut. The rod in turn extended through the center hole in the ram and was directly connected to the wires by means of a heat-treated nut welded to the rod. After the wire was tensioned to the desired stress the nut on the wire was turned up against a shim and the jack was released allowing the nut and shim to bear on the pretensioning frame. The complete tensioning setup is shown in Fig. 23.

(c) Draping Apparatus

The reinforcing wires were tensioned in their uppermost position and then were pulled down to their final position by two draping saddles, one at each load point. The draping saddles consisted of two long threaded 3/8-in. diameter rods with two 2 1/2-in. lengths of 1/2-in. diameter rod welded across them at one end. (See Fig. 24). The cross-bars and the threaded vertical rods were arranged to allow the wires to pass between them in their normal spacing. The lower ends of the vertical rods passed through holes in the bottom of the form and the saddles were held in position by nuts bearing on the bottom of the form. No provisions was made

for longitudinal movements of the wires during draping since the saddles were flexible enough in that direction. This caused no trouble in draping the wires.

The form members rested on a stiffening beam built up from plates and two 15-in. channels. The form and the stiffening beam are shown in Fig. 25. This beam was necessary to prevent the forms from warping when the prestressing wires were draped.

For low drapes, it was possible to do all the draping by screwing nuts onto the threaded rods. A hydraulic jack was used to pull down the saddles for the higher drapes.

(d) Tensioning, Draping, and Releasing of the Reinforcement

(1) Beams with Straight Reinforcement. The reinforcement was tensioned in the prestressing frame prior to casting the beam. The ends of the wires were slipped through the end plates of the form and through the bearing plates of the prestressing frame. Calibrated aluminum dynamometers were then slipped into one end of the wires and the anchoring nuts were put on each end of the wire. The reinforcement was tensioned one wire at a time with a hydraulic jack and anchored by tightening the nuts on the wire to bear on the prestressing frame. Shims were added between the nuts and the frame where necessary. Since the prestressing frame underwent an elastic shortening with the tensioning of the wires, the first wires tensioned were overstressed a certain amount, dictated by the experience with previous beams. Minor adjustments in the wire stresses were normally necessary after tensioning all the wires.

After all the wires had been tensioned, the frame and the wires were moved to the form and set in place. The prestressing frame was large

enough to fit around the form for the beams. The stirrups were wired in place after the longitudinal reinforcement was tensioned and before it was placed in the form.

When the concrete in the beam was strong enough, the prestress was transferred to the concrete beam. This was accomplished by loosening the nuts slowly so that the tension in each of the wires was approximately equal at all times. In a very few cases, wires fractured at the threads during this operation. When this occurred, the behavior of this wire was observed carefully in the test to detect possible bond failures. Where necessary, the beams were prestressed externally at the top to counteract the tensile stresses in the top fibers caused by the prestressing force. The "top prestress" was removed either before the test was started or after the first few increments of load were applied.

(2) Beams with Draped Reinforcement. In a beam with draped reinforcement, the prestressing wires were tensioned in their uppermost position and then were pulled down to their final position by a welded steel saddle at each load point. The initial prestress in the wires was chosen so that the additional increment added by draping brought the total prestress up to the desired level. An allowance was made for the shortening of the prestressing frame. In drape profiles F and G, the draping process alone would have stressed the wires to more than the desired stress and it was necessary to release some stress at intervals to have the desired prestress in the finished beam.

After initial tensioning, the prestressing frame and wires were transported to the form and the ends of the saddles were fitted through holes in the bottom of the form. The end plates were bolted to one sideform to prevent being pulled out of line during the draping procedure.

The other side-form was not in place during draping to facilitate measurement of the height of the wires. The wires were then pulled down into position with saddles. Dynamometer and steel strain gage readings were taken before and after the draping operation.

Two days before testing, the tension was released, the end anchorages being released first. This release sequence was followed so that the beam would be prestressed before the vertical reaction of the draping saddles was transferred to the beam.

(c) Measurement of Prestress

During prestressing, draping, and release, the force in each wire was determined by measuring electrically the compressive strain in calibrated aluminum dynamometers, slipped on the wire between the nut and the bearing plate at the end opposite to the one where the tension was applied as shown in Fig. 23. The dynamometer consisted of two-in. length of 1/2-in. aluminum rod with a 0.2-in. diameter hole drilled through its center. Strains were measured by means of two Type A7 SR-4 electric strain gages mounted on opposite sides of each dynamometer and wired in series. This arrangement gave a strain reading which was the average of the strains in the two gages thereby compensating for small eccentricities of load that might occur. The dynamometers were calibrated using the 6000-lb range of a 120,000-lb capacity Baldwin hydraulic testing machine. The calibration constants of the dynamometers were very nearly the same; the strain increment necessary to measure a tensioning stress of 120 ksi in the wire was about 2000 millionths. This large increment of strain allowed a precise measurement of stress in the wires, since the strain indicator used had a sensitivity of two or three millionths.

Strains in the wires were measured at various points along the beam with Type A7 SR-4 electric strain gages during the draping operation to check the dynamometer readings and to check the uniformity of the prestress inside and outside of the drape points. Measurements taken during this operation showed that the average stress at the jacking end and at the dynamometer end were 100 and 101 percent, respectively, of the stress in the flexure span.

The instantaneous losses at release were measured with Type A7 SR-4 electric strain gages mounted on the wires at midspan. The computed elastic losses and the losses measured at the time of release by the gages on the wires compared fairly well. The losses due to creep, shrinkage, and relaxation were estimated using data obtained from previous tests on concrete cylinders, prestressed beams and wire specimens (4) (5). In a number of specimens, the estimates of total losses were corrobrated by measurement of the increase in midspan deflection between the times of release and test. The effective prestress levels listed in Table 1 were obtained by subtracting the total losses from the initial prestress.

(f) Stirrups

The Type A, B, and D stirrups were slipped on the prestressing wires before these were inserted in the prestressing frame. After tensioning the wires, the position of each stirrups was marked on the longitudinal reinforcement and each stirrup was tied in position using baling wire (Fig. 26). Type E stirrups were made of a type D stirrup to which a third leg was added. Type C stirrups could be placed in position after tensioning the longitudinal steel because they had only one leg. The position of the stirrups was always carefully referred to the prestressing frame before

casting the beam. When the forms were stripped, the position of each stirrup was marked on the sides of the beam by vertical broken lines which can be seen in all photographs of the beams with web reinforcement.

A reinforcing bar was tied to the top of all the stirrups to keep them vertical and at the proper spacing. After the first batch of concrete had been placed and vibrated this bar was removed.

2.4 Casting and Curing

After prestressing the wires and tying the stirrups in position, the prestressing frame was placed around the form and the wires were correctly aligned inside the form. Metal forms were used to cast all the beams, although wooden forms were used to cast the composite deck slabs used on two beams. Removable metal inserts were used to shape the I-Beam.

All concrete was mixed three to six minutes in a non-tilting drum type mixer of 6-cu ft capacity. A butter mix of one cu ft preceded two 4 cu ft batches which were used in the specimens. Before batching, samples of the aggregates were taken for free moisture tests. The slump was determined immediately after mixing. Since the clear distance between the wires was about one-half inch, pea gravel with a maximum size of 3/8 in. was used in all beams.

Two batches of concrete were required in each beam. The first batch was placed in a layer of uniform height through the beam and filled a half to three quarters of the depth. The second batch was placed on top of the first batch. Consequently, all the concrete in the compression zone of the beam was from the same batch. Six 6 by 12-in. control cylinders and one 6 by 6 by 20-in. modulus of rupture beam were cast from each batch.

Several hours after casting, the top surface of the beam was trowelled smooth and the cylinders were capped with neat cement paste. The

forms of the beam and the control specimens were removed after one day and the beam and control specimens were wrapped in wet burlap for several days. The burlap was removed two to three days before testing to allow the concrete surface to dry before electrical strain gages were applied.

The beams which were to have a slab cast on top were manufactured in the same manner as indicated in the preceding paragraphs, except for the following difference. Beveled pieces of wood were pressed into the concrete at the top of the beam to form the shear keys and the top of beam was not trowelled smooth. After transfer, the protruding parts of the stirrups were thoroughly cleaned and the coarse aggregate of the concrete was exposed on the top of the beam using a special hammer and a wire brush. Finally the top surface was cleaned by compressed air (Fig. 14a). At this stage the beam was supported at two points, the span being the same as that for the test and the form for the slab was built around the beam (Fig. 14b). The slab reinforcement was placed and the top surface of the beam was wetted before casting the slab. One batch of concrete was used for the entire slab, including four 6 by 12-in. control cylinders, and one 6 by 6 by 20-in. control beam. The slab was finished and cured according to the procedure already outlined for the beams.

3. INSTRUMENTATION, LOADING APPARATUS, AND TEST PROCEDURE

3.1 Strain Gages and Load Cells

(a) Strain Gages on Reinforcing Wire

Two wires in each beam were instrumented with Type A7 SR-4 electric strain gages which have a nominal gage length of 1/4 in. and a minimum trim width of 3/16 in. Type A7 gages were chosen for their narrow width, short length and flexibility. These gages were placed at midspan in all the beams tested under two-point loads and moving loads. In beams loaded with a single concentrated load, the gages were under the load point. In eight of the beams with draped wires, additional gages were mounted three inches inside and outside of each drape-point to measure the uniformity of the stress in the draped spans and the flexure span. These gages were carefully placed on the same side of the wire and at equal distances from the drape point so that both would be affected equally by any curvature or other disturbance resulting from the bend in the wire at the drape point. In beams with two layers of steel, one instrumented wire was placed in each layer.

The surface of the wire was prepared for gage application by using fine emery cloth and acetone. Duco cement or Eastman 910 cement was used as the bonding agent. In the case of Duco cement, heat lamps were used to hasten the drying of the cement. After several hours of air-drying, and after the lead wires had been soldered to the gages and insulated with tape, the gages were waterproofed with a coating of Petrolastic* or Epoxoid**. The Petrolastic compound was applied in the following manner: After attaching

---

* An asphaltic compound manufactured by Standard Oil of California.

** An adhesive produced by the International Prestressing Corporation of Los Angeles, California.

and insulating the lead wires, the gage was given a thin coating of Petrosine wax. A 1/2 by 1/2 by 1 1/2 in. open-topped box made of cardboard or light sheet metal was then placed around the gage and molten Petrolastic was poured into this box and allowed to cool. The prestressing wire was kept warm until this operation was started in order to improve the bond between the wire and the Petrolastic. The method of waterproofing using Epoxoid adhesive was as follows: After attaching the lead wires and wrapping the bare portions with insulating tape, a small amount of adhesive was mixed and trowelled over the surface of the gage and wire taking care to cover the entire surface. Approximately six hours were required for it to set completely. Although the Petrolastic solidified quickly and was more flexible then the Epoxoid, the latter was easier to apply and bonded better with the prestressing wire.

The lead wires from the gages ran along the bottom of the beam or at the level of the wires to one end of the beam and then were brought up and out of the top flange.

(b) Electric Strain Gages on Concrete

Strains in the concrete at the top of the beam were measured with Type A3 SR-4 electric strain gages which have a nominal gage length of 3/4 in. and a width of 3/8 in. A portable grinder was used to smooth the top surface of the beam at the desired locations. A thin layer of Duco cement was applied to the smoothed surface and allowed to dry for several minutes. A layer of Duco cement was applied on the gage which was then mounted in place. Care was taken to remove all air bubbles from under the gage. One pound steel weights were left on the gages for about half an hour with a sponge rubber cushion under each gage. The gages were usually mounted 1 to 2 days before the test. The concrete surface was allowed to air-dry 2 to 3 days before the gages were mounted. No waterproofing or curing was used.

From 12 to 19 strain gages were placed on the top surface of each specimen at a 3-in. spacing near the load points and at 6 or 12 in. elsewhere. Typical gage patterns are shown in Fig. 27. The location of the gages was changed as the tests progressed to suit the different loading patterns and to obtain a better picture of the strain distribution. The gages were placed along the longitudinal center line of the beams except for those placed immediately around the load point. As shown in Fig. 28, additional strain gages were mounted on the two composite beams. Wherever strain distributions are presented in the text, the locations of the gages are indicated.

(c) Mechanical Strain Gages

A 10-in. Whittemore strain gage was used to measure the distribution of concrete strain in the pure flexure region of the beams with cast-in-place slabs. Although these measurements were not strictly related to the shear strength of these beams, it was considered that they would be helpful in obtaining a better understanding of the behavior of these specimens. The Whittemore gage was equipped with a 0.001-in. dial indicator which was read to about one-tenth of one division and, since a 10-in. gage length was used, the strains measured were estimated to one millionth. Measurements on all the gage lines were taken twice and if both readings did not agree to 10 millionths, additional readings were taken until agreement was reached. A steel standard bar was used to compensate for temperature changes during the test.

Six gage-lines were placed symmetrically on each side of the specimen as shown in Fig. 28. These gage-lines were established by cementing 3/8 by 1/4 in. long steel plugs to the sides of the specimen. Each plug had a cylindrical gage hole drilled to a depth of about 1/8 in.

(d) Load Cells

Load cells designed for a working load of 35 kips were used to measure the loads applied in the moving load tests and the tests in which unsymmetrically placed concentrated loads were used. These cells consisted of cold-drawn seamless metal tubes machined to a wall thickness of 0.10 in. in the zone where measurements were made. Each load cell had eight Type A7 SR-4 electric strain gages mounted at mid-height and wired to form a "four-arm bridge" with a strain magnification factor of about 2.6. In addition to the instrumented cylinder, a protective cover and handles were included in the design as shown in the cross section in Fig. 29. This type of load cell was used to provide remote measurement with reasonable precision. They were found to have long-time dependability.

The load cells were calibrated in a 120,000 lb. Baldwin hydraulic testing machine. Prior to calibration, they were loaded in excess of their expected working load several times so that all zero-shift in the gages which might result from local inelastic action would be eliminated. The load cells had a sensitivity of 134 lb. per dial division on the strain indicator.

3.2 Loading Apparatus

(a) Two-Point Loads

The beams tested under two-point loads were tested in a specially constructed frame employing a 30-ton capacity Simplex hydraulic ram operated by a Blackhawk pump. Details of the frame are shown in Fig. 30. The load was applied to the specimen by a steel distributing beam which applied equal loads at two symmetrically located points on the top of the beam being tested. A 50,000-lb capacity elastic ring dynamometer was used to measure the loads. It was equipped with a dial indicator and was calibrated at 110.8 lb. per dial division.

The specimen rested on two 6 by 8 by 2-in. bearing blocks attached to the bottom of the beam with hydrocal plaster. These in turn rested on a "half-round" at one end and a roller at the other. The loading blocks were also 6 by 8 by 2-in. plates but these rested on 4 by 4 by 1/4-in. squares of leather. Leather was used to distribute the load rather than hydrocal so that electric strain gages could be placed close to the point of loading. The loading blocks received the load from the distributing beam through a ball at one end and a roller at the other.

(b) Moving Load Tests

The frame used to test beams under two-point loads was modified as shown in Fig. 31 to allow the application of simulated moving loads. The beam to be tested was supported on concrete piers so that its longitudinal center-line was directly below that of the longitudinal beam in the testing frame. By placing jacks between the longitudinal beam and the specimen, loads could be applied at any point along the beam being tested.

Loads were applied by two 20-ton Blackhawk rams held below the loading beam by a supporting device composed of a 6 in. by 3/16 in. plate 7 ft 5 in. long which was held 7/8 in. below the bottom of the loading beam by 7/8-in. square bars running across the plate at 8 in. on centers. Slots, into which the rams fitted, were cut in the plate at 8-in. centers. The ends of the slots were circular to position the rams accurately. The hydraulic rams, in turn, had 6 by 6 by 3/4-in. shoes which fitted loosely into the space between the supporting plate and the reaction beam. In this way, the rams could be easily moved and placed accurately in eleven successive positions, each 8 in. apart. The center load position was at midspan of test beam. Thus, the "moving load" consisted of a series of concentrated loads applied one after the other at positions 8 in. apart along the beam.

Two hydraulic rams were used in the test to facilitate the transfer of load from point to point. Each of the hydraulic rams was operated by a separate jack. The load applied was measured by a load cell between each ram and the beam. A 5-in. square of leather was placed between the load cell and the beam. To prevent tangling of the hydraulic lines, the slots in the plate supporting the rams were cut on alternate sides of the plate and the hoses and the load cell connections for each of the two rams were on opposite sides of the loading beam.

Tests of beams under single unsymmetrically placed concentrated loads were made using the moving-load testing frame with a single 20-ton hydraulic ram in one of the eleven load positions. A load cell was used to measure the magnitude of the applied load.

3.3 Measurements

The applied load was measured by means of a 50,000-lb elastic ring dynamometer or by specially constructed load cells in tests of beams loaded with two-point loads and tests of beams under simulated moving loads, respectively. The ring dynamometer and load cells have been described in Sections 3.2(a) and 3.1(d).

In the tests with two-point loads, deflections were measured at midspan and at the third-points with 0.001 in. dial indicators. In the moving load tests, five 0.001-in. dials were used to record the deflection at midspan and at 18 and 36 in. on either side of midspan. Two deflection dials were used in the tests of beams under unsymmetrically placed loads, one at midspan and one under the load.

Strains in the longitudinal reinforcement and on the top surface of the beam were measured by electrical resistance strain gages.

After each increment of loading, the cracks were marked and the number of the load increment was marked on the beam opposite the end of the pertinent cracks. Photographs were taken at various stages during the test to serve as a permanent record of the development of cracking.

After failure, the dimensions of the region of failure were carefully measured. Immediately after testing, the control cylinders and beams were tested for compressive strength, modulus of elasticity, and modulus of rupture. Some of the moving load tests on beams took two days to run. In such cases, part of the control specimens were tested each day.

3.4 Testing Procedure

(a) Beams Loaded at Two Points

The failure load was usually reached in five to ten increments. Load and deflection readings were taken at frequent intervals during the application of each increment of load. After a load increment, all deflection, load, and strain measurements were taken and the cracks were marked. Load and midspan deflection were measured again immediately before the resumption of loading since a drop-off in load and an increase in deflection occurred during the interval between load increments.

The flexural cracking load was reached in two or three increments. After flexural cracking, the magnitude of the load increments depended on the development of the crack pattern. The beams were loaded until they ruptured completely or failed to develop increased resistance to large deformation. Each test took about four hours to complete. Control specimens were tested immediately after the beam test.

(b) Beams Tested with Moving Loads

There were two stages in the testing of a beam under moving loads. In the first stage, the beam was loaded with a concentrated load at midspan

until flexural cracks developed or until some predetermined load level was reached. Normally, this took three load increments. Load and deflection readings were taken at frequent intervals as each increment of load was applied. After each load increment the strain gages and deflection dials were read and the cracks were marked. This initial stage of loading was carried out to obtain data about the uncracked beam in a short time, since it was felt that there were no critical questions about the behavior of an uncracked beam under moving loads.

The second stage of loading consisted of a number of increments of "moving load". In this stage, one "load increment" consisted of applying the same load successivly in each of the eleven loading positions from the south end of the beam to the north end. Two rams were used so that when the load was transferred from one position to the next, the load could be decreased gradually in the first ram as it was increased in the second. In this way, the load acting on the beam was never entirely removed as it was transferred from one position to the next. The total load acting on the beam during a transfer rarely fell below 70 percent of the nominal "moving load" for that increment.

At each loading position, a complete set of readings were taken and the cracks were marked. Thus, one load increment consisted of eleven separate loadings and took approximately two and a half hours to complete. It was possible to test a beam without web reinforcement in one day, but the beams with stirrups took up to twenty hours to test and were each tested over a two day period.

Each load increment was from 5 to 20 percent greater than the preceding one. The actual magnitudes of the load increments applied depended

both on the computed beam strength and the observed crack patterns and deflections of the beam in the test.

(c) Unsymmetrically Loaded Beam Tests

Two of the beams with draped wires, and one beam with straight wires, CD.13.24, CD.13.25 and C.13.23, were tested on a 8 ft 6-in. span with a single concentrated load placed 2 ft 3 in. from the reaction. One end was loaded until inclined cracking occurred. Following this, the load was removed and reapplied at a point 2 ft 3 in. from the other end of the beam which was then loaded to failure. During the second loading, external stirrups were used to restrain the inclined cracks which had developed under the first loading. The test results for these beams are listed as CD.13.24a and CD.13.24b etc. for the two ends.

Eight beams with straight wires and web reinforcement were tested to failure with a single concentrated load placed either 30 in. or 38 in. from the south end of a 9 ft span.

4. BEHAVIOR OF TEST BEAMS

4.1 Introductory Remarks

In addition to functional requirements such as size or shape, a well designed structure must be strong enough to support all the loads which might reasonably be expected to occur, and its behavior or response to these loads should not be undesirable. The first of these requirements, that of adequate strength, is obvious and in ultimate strength design is satisfied by designing the structure for the expected loads multiplied by a load factor. The second criterion for a well designed structure is that it should behave in a desirable manner when loaded. That is, the deflections and cracking at working loads or reasonable overloads must not be undesirable, unsightly, or dangerous, the structure must be sufficiently ductile to absorb impulse loadings, and, finally, the mode of failure should be such that adequate warning is given of impending failure. Only after considering all of these aspects of the behavior of a member is it possible to determine the range of safe working loads and therefore the factor of safety required.

Chapter 4 consists of a discussion of the behavior of prestressed concrete beams loaded to failure, with emphasis on the behavior of beams subjected to combined flexure and shear. Section 4.2 is a general discussion of the behavior of a prestressed beam to illustrate the various stages in the loading history. This description of beam behavior is based primarily on the relationship between loads and deflections, and strains and crack patterns are mentioned only briefly to illustrate stages in the load-deflection diagram. In Section 4.3 the development of cracking is discussed, and the types of cracks occurring in each type of beam are described and classified.

Concrete and steel strains and the relationship between them are considered in Section 4.4. The various modes of failure are defined and discussed in Section 4.5

4.2 General Characteristics of Behavior of Prestressed Concrete Beams

Although this report is concerned primarily with the strength of prestressed concrete beams having web reinforcement, an understanding of the behavior of a member is fundamental to any discussion of its strength. In the case of beams, the best way to study behavior is by means of load-deflection diagrams taking into account the other phenomena observed during testing. In this section the discussion of beam behavior is based on such diagrams.

The load-deflection curves for all the specimens are presented in the Appendix. The curves have been grouped according to web thickness, level of prestress and type of loading by means of the notation system used to classify the beams. All the curves, except those for beams with cast-in-place slabs, are plotted to the same scale so that direct comparisons can be made among them. Different symbols are used to differentiate the type of failure, and the points corresponding to the observed flexural and inclined cracking loads are indicated on each curve. In all curves, except those for beams loaded with a single concentrated load, the deflections measured at midspan are plotted versus the total live load, omitting the weight of the test beam. In the case of beams loaded with a single concentrated load, the deflections plotted are those measured beneath the load.

The load-deflection curve for beam BW.14.22 in Fig. 32 is similar in most respects to the load-deflection diagram for a typical practical beam. This beam failed in flexure, as would be required in practice, and its longitudinal steel ratio was comparable to that used in a practical beam. This

load-deflection curve can be divided into three distinct stages of behavior which are indicated on the figure as AB, BE and EG. The letters C, D and F refer to specific points in the loading history and will be discussed later. The first stage, AB, covers the response of the beam prior to flexural cracking; the second stage, BE, covers the response of the beam during the development of flexural cracking; and the third stage, EG, refers to the response of the beam after the longitudinal reinforcement has yielded at sections of maximum moment.

The first stage of loading, from A to B, is marked by "elastic" behavior in which the deflections are proportional to the loads. This stage ends with the formation of one or more vertical flexural cracks in the region of maximum moment. The computation of the load corresponding to flexural cracking is discussed in Chapter 5. Prior to cracking, the deflections can be estimated with reasonable accuracy using an elastic analysis.

The second stage of loading starts with the formation of vertical flexural cracks in the region of maximum moment. With further loading, additional flexural cracks occur in the shear spans, the portions of the beam between the loads and the supports. These cracks extend vertically to the level of the reinforcement and then bend over toward the load points. The crack pattern of beam BW.14.22 corresponding to point C on the load-deflection curve in Fig. 32 is shown in Fig. 33(a).

During this stage of loading, the rate of increase in deflection with respect to load increases continually as the load is increased. This phenomenon is due to such factors as the formation of new flexural cracks, a continuing rise in the position of the neutral axis as the cracks extend higher into the beam, and inelastic action in the concrete above the cracks.

The distribution of strains and stresses corresponding to point C on the load-deflection curve in Fig. 32 is shown in Fig. 33(b) and (c). The section shown is in the constant moment region of the beam. At this stage of loading, the flexural cracks have extended quite high into the beam and the stresses in the concrete above the cracks are becoming inelastic. The distribution of concrete strains along the top of the beam, shown in Fig. 33(d), resembles the shape of the moment diagram in the portion of the span where flexural cracking has occurred.

The third stage in the behavior of a beam failing in flexure is initiated by inelastic straining of the tension reinforcement and is marked by a rapid increase in deflection with respect to load. Since the steel stress-strain curve is relatively flat after the yield stress of the reinforcement is reached, any increase in moment is a result of large additional steel strains which result in large angle changes and deflections but only small increases in the steel stress and the length of the internal lever arm. The crack pattern and the distribution of strains and stresses over the depth of beam BW.14.22 are shown in Fig. 34(a) (b) and (c) for a load corresponding to point F on the load-deflection curve in Fig. 32. At this stage of loading, the flexural cracks have extended higher into the beam, and the inclined cracks shown in Fig. 34(a) have developed in the shear spans. The inclined cracks were sufficiently restrained by web reinforcement that the behavior of this beam remained that of a beam failing in flexure. The inclined cracking load is marked in Fig. 32 by the letter D.

As shown in Fig. 34(b) and (d), the sum of ϵ_{se}, the effective steel strain due to prestressing, and ϵ_{sa}, the additional steel strain developed during the test, exceeds the yield strain of the wire. At this stage of

loading, the steel has become inelastic and large steel strains and consequently large deflections are necessary to increase the tension force and the internal moment. At the same time, the concrete in the compression zone has also become inelastic as shown in Fig. 34(c).

The ductility of beams failing in flexure will vary considerably depending on the relative values of the longitudinal steel ratio, p, and the concrete strength, f'_c as expressed by the ratio $Q = pE_s/f'_c$. Thus, for the beams described in this report, there were two general types of load-deflection diagrams depending on whether Q was large or small. The load-deflection curves for two beams failing in flexure are shown in Fig. 35. These beams represent two types of behavior observed in flexural failures. The letters, B, D, and E on the load-deflection curves mark the first flexural cracking, inclined cracking, and first yielding, respectively, as they did in Fig. 32.

In beam CW.14.19, the steel stress at failure exceeded the yield strength of the reinforcement, and the resulting large inelastic strains in the steel were the primary cause of failure. Final failure occurred by crushing of the compression zone but only after large deflections had developed. The load-deflection curve for this beam is typical for a "tension" failure and the beam is said to be "under-reinforced" since the longitudinal reinforcement reached its yield stress before the compression zone crushed.

Beam CW.14.40 had "balanced" tension reinforcement. That is, the amount of longitudinal reinforcement was such that failure occurred in the compression zone just as the stress in the steel reached the yield stress for the wire. The load-deflection curve for this beam is typical for a "balanced" beam. If the beam had still more longitudinal reinforcement, and the same concrete strength, failure would occur by crushing of the concrete before the stress in the longitudinal reinforcement reached the yield

stress. A failure of this type is called a "compression" failure. Such a beam would be called an "over-reinforced" beam and would not be acceptable in the present design philosophy which requires that a beam have both strength and ductility.

Whether a beam will fail in compression or tension and the ductility at failure is a function of the ratio $Q = pE_s/f'_c$. In the comparisons made above, the differences in behavior were caused by variations in the steel percentage in beams which had similar concrete strengths. Variations in the concrete strength in beams with the same longitudinal steel percentage will also produce a variation in the behavior of the beam. Thus, beam BW.14.22 in Fig. 32 was under-reinforced while beam CW.14.40 in Fig. 35 was balanced, although both beams had the same amount of longitudinal reinforcement. The concrete strength in BW.14.22 was 7200 psi as compared to 3010 psi in CW.14.40. To ensure ductility in structures, current design specifications place upper limits on the ratio p/f'_c which can be used in a beam.

An important development in the flexural cracking stage of behavior was inclined cracking. Inclined cracking was sometimes accompanied by a slight drop in load but in general the occurrence of inclined cracks could not be detected by any specific change in the load-deflection curves. Some of the beams failing in flexure never developed inclined cracks, and in a few beams with thin webs and high prestressing forces, inclined cracking occurred before flexural cracks had been observed.

If inclined cracks occur in a beam without web reinforcement, its strength and ductility are reduced. This is illustrated by the load-deflection curves for beams failing in flexure and shear in Figs. 36(a) and (b). Properties of the beams are listed in each figure. All five beams were

loaded at the third-points of a nine-foot simple span. Beams BW.14.41 and CW.14.42 had sufficient stirrups to prevent shear failures, beam CW.14.39 had half as much web reinforcement as CW.14.42, and beams B.14.41 and C.12.44* had no web reinforcement. The inclined cracking loads are marked on all five load-deflection curves. Before inclined cracking, the differences between the curves for beams failing in flexure and shear can be attributed to differences in concrete strength, the amount and location of longitudinal reinforcement, and the number and location of cracks.

The load-deflection curves for the I-beams with 3-in. webs in Fig. 36(a) indicate that inclined cracking marked the end of the useful life of beam B.14.41, since failure occurred after only a small additional load and deflection. On the other hand, the inclined cracks in BW.14.41 were restrained by stirrups and this beam developed its flexural capacity and the corresponding deflection. Similarly in Fig. 36(b), beam C.12.44, which had no stirrups, failed at inclined cracking. Beam CW.14.42 had enough web reinforcement to induce a flexural failure and carried twice as much load and had four times the ultimate deflection of C.12.44. Another interesting comparison can be made using the curves for C.12.44 and CW.14.39 which had half as much web reinforcement as CW.14.42. Although beam CW.14.39 failed in shear, its strength and ductility were almost as great as for CW.14.42, showing the effect of even a small amount of web reinforcement on the behavior of a beam.

Except for almost negligible differences in the moment of inertia of the uncracked section, the web thickness had no effect on the load-deflection curves other than governing the inclined cracking loads and consequently affecting the amount of web-reinforcement needed to avoid a shear failure.

* This beam had 36-in. shear spans. It was originally reported in Ref. 2 and in the beam notation system used in that paper, the numeral 2 in C.12.44 referred to a 36-in. shear span.

The type of loading influenced the ultimate deflections for beams failing in flexure by changing the length of the region of constant moment. Since this region becomes "plastic" at ultimate and most of the rotations take place there, the closer the loads are to each other the smaller the deflection is for a constant span length. The beams with a single concentrated load developed the smallest deflections. It has not been possible to compare directly the relative ductilities of a beam tested under moving loads and a beam tested under stationary loads. However, because flexural cracking tends to be more widespread in the case of a beam tested under moving loads, it would seem probable that, for beams with web reinforcement, the ductility and energy absorbing capacity of a beam tested under a single moving load would be greater than that of a beam tested under a single stationary load.

The effect of the drape angle on the ductility of the beams with all wires draped is illustrated by the load deflection diagrams in Fig. 37. The curve for beam BW.14.18 has been included in this figure for comparison. This beam had straight wires and enough stirrups to ensure a flexure failure. It should be pointed out that the first break in each curve does not reflect any effects of draping because it corresponds to first flexural cracking in the constant moment region where the reinforcement was parallel to the longitudinal axis of the beam. For beams having the same shear spans, the effect of increasing the drape angle is indicated by the reduction in both the inclined tension cracking load and the ductility.

4.3 Crack Patterns

(a) Introduction

Since concrete is inherently weak in tension and strong in compression, cracks will form in a beam in regions of tensile stress long before

the compressive stresses in the beam are large enough to become critical. In a reinforced concrete member, steel tensile reinforcement is provided to prevent the total collapse of the member after cracking occurs. However, the reinforcement does not prevent the cracking of concrete although it may tend to restrain the opening of cracks. A study of the cracks in a test specimen is essential in determining the behavior of the member and the adequacy of its reinforcement. Thus, the location, width, and shape of cracks can indicate the location of maximum tensile stresses in the beam, whether the reinforcement was placed in the proper location, and the state of the bond between the reinforcement and the concrete. During each test the location of the cracks was marked carefully and recorded in photographs.

Two types of cracks commonly occur in prestressed concrete beams: flexural cracks, which result from horizontal tensile stresses caused by flexure; and inclined or "shear" cracks, which result from the inclined tensile stresses in a region of combined bending and shear.

(b) Flexural Cracks

Usually the first cracks observed in testing a prestressed concrete beam occurred at the section of maximum moment. These cracks, called flexural cracks, resulted from tensile stresses caused by bending. Since these tensile stresses acted parallel to the axis of the beam and were a maximum in the bottom fiber, the cracks started at the bottom of the beam and were essentially vertical. The load corresponding to the formation of flexural cracks is computed and discussed in Section 5.2. In the beams tested, the spacing between flexural cracks was about 6 in. Typical flexural cracks are shown in Fig. 33.

After the formation of cracks at the point of maximum moment, and throughout the constant moment region, if one existed, further loading

caused flexural cracks in the shear spans. These cracks were initiated by horizontal flexural tensions and thus started in the bottom fiber as vertical cracks. However, as they extended into regions of combined shear and flexural stresses, they tended to bend over toward the load point, a major change in direction occurring at the junction of the web and the lower flange where the shearing stresses first became significant. In a number of beams, inclined cracks occurred in the web before flexural cracks had formed in the shear spans, and in some of these beams failure occurred before flexural cracks could occur in the shear spans.

Initially, a flexural crack extends into the beam across the longitudinal reinforcement and continues to extend until the tension in the longitudinal steel and the internal moment arm are sufficient to restore moment equilibrium. The height to which the crack must extend for a given moment is primarily a function of the amount of longitudinal reinforcement, the prestressing force and the effective depth. If the longitudinal reinforcement is draped in the shear span, the height to which a flexural crack in the shear span will extend initially is greater than in a beam with straight wires. In general, a flexural crack will extend highest in a beam with a small amount of reinforcement and a small prestressing force. Thus, in beams with small steel percentages it was not uncommon for flexural cracks to develop suddenly from the bottom fiber to about mid-depth of the beam. On the other hand, the greater the steel percentage the more uniform was the progress of the cracks with respect to load.

The occurrence of flexural cracks decreased the stiffness of the beam, in every case resulting in a definite reduction in the slope of the load-deflection curve. This reduction in slope was greatest for beams with low values of Q. Flexural cracking was accompanied by an increase in the

rates of increase of steel and top concrete strains with load. However, flexural cracks did not greatly disturb the linearity of the strain distribution over the depth of the cross section, and beam action was preserved throughout all stages of the development of a flexural crack.

(c) Inclined Cracks

In regions of combined bending and shear, the combination of flexural stresses, shear stresses, and direct stresses due to prestressing results in principal tensile stresses at various angles with the horizontal. The load at which the principal tensile stresses become excessive and cause cracking represents a major turning point in the life of a prestressed concrete beam. The resulting cracks, known as "inclined tension" cracks or "shear" cracks, propagate rapidly, particularly in beams without web reinforcement. In contrast to flexural cracks which are essentially perpendicular to the longitudinal reinforcement and hence are directly restrained by it, inclined cracks form at an angle to the longitudinal steel and thus can be only partially restrained by it. Consequently, in beams without web reinforcement, the formation of inclined cracks marks the useful limit of the beams as indicated by the load deflection diagrams for B.14.41 and C.14.44 in Fig. 36(a) and (b).

An inclined tension crack eliminates the inclined principal tensile stresses necessary for beam action in the shear spans and thus forces a redistribution of stresses and strains over the depth of the section. After the full development of the inclined crack, beam action is replaced by arch action and the member may fail in a manner associated with the latter. A shear failure in a beam without web reinforcement will occur at a load less than the flexural ultimate and with a ductility much less than that anticipated for a flexural failure. If the beam has web reinforcement,

however, its presence across the inclined cracks partially restores beam action by providing a path for the shear flow between the upper flange and the longitudinal reinforcement. If the beam has sufficient web reinforcement, enough beam action may be restored for the beam to fail in flexure.

In the beams tested, inclined cracks occurred in two different ways which are discussed below. The strength and behavior were different for the two types of inclined cracking.

(1) Web-Shear Cracking. In beams with high prestress, thin webs, and short shear spans, the principal tensile stresses in the web may exceed the tensile strength of the concrete before flexural cracks occur in the shear span. An inclined crack which occurs in the web before flexural cracks appear in its vicinity is referred to as a "Web-Shear Crack." This type of inclined crack is shown in Fig. 38. Web-shear cracks occurred in over half the beams with 1 3/4-in. webs and shear spans of 36 in. or less which are reported herein but did not occur in the rectangular beams or the I-beams with 3-in. webs.

The first web-shear crack generally occurred along a radial line through the load point at an angle approximately equal to that predicted in the computation of the principal tensile stresses in the web. For beams in the CW.14 series this angle was about 30 deg. with the horizontal. In beams with web reinforcement, further loading often caused additional cracks parallel to the first inclined crack. If the shear span was shorter than about two times the over-all height of the beam, vertical stresses near the load and reaction affected the stresses in the web, resulting in a larger angle between the crack and the horizontal. In such beams, the web-shear crack formed along a line very close to the diagonal line joining the load and the reaction.

A special type of web-shear crack was observed in some of the beams with 1 3/4-in. webs and high values of Q. This type of crack consisted of a series of small inclined cracks which appeared suddenly at the junction of the web and the upper flange near the reaction as shown in Fig. 38(c). This type of crack is shown as a "Secondary Inclined Crack." Although the formation of a secondary inclined crack is rapidly followed by failure of the beam in beams without web reinforcement, the presence of adequate stirrups seemed to be effective in stopping the propagation and opening of these cracks.

(2) Flexure-Shear Cracks. In beams with moderate prestress, relatively thick webs, and relatively long shear spans, flexural cracks will occur in the shear span before the principal tensile stresses in the web are high enough to cause web-shear cracks. If an inclined crack does occur in such a beam, normally it is the extension of a flexural crack in the shear span or it occurs over or beside such a flexural crack. This type of inclined crack will be referred to as a "Flexure-Shear Crack," since the flexural cracks in the shear span were necessary as stress-raisers in the development of the crack. The critical flexural crack which influenced the formation of the inclined crack, will be referred to as the "Initiating Crack." In a typical beam, the initiating crack develops, crosses the steel and bends over toward the load point. The action of this crack eventually raises the stresses in the web to a critical value, precipitating the rapid formation of the flexure-shear crack.

In the tests outlined in this report, flexure-shear cracks developed in all the rectangular beams, all the I-beams with 3-in. webs, and about a third of the I-beams with 1 3/4-in. webs. In general, the

I-beams with 1-3/4-in. webs which developed flexure-shear cracks had low values of Q or shear spans longer than 36 in.

Three typical flexure-shear cracks and the corresponding initiating flexural cracks are shown in Fig. 39. The first of these, shown in (a), represents the type of crack which occurs when the shear required to cause flexural cracks in the shear span is very much less than that required to cause a web-shear crack. In such a beam, the initiating crack extends high into the beam before the flexure-shear crack forms. The inclined crack normally forms as an extension of the initiating crack. If web reinforcement is not present, the final development of the inclined crack occurs abruptly and often disastrously. The presence of web reinforcement, however, moderates the rate of development of this crack to the extent that it is often difficult to determine the load at which the crack began to act as an "inclined crack". Flexure-shear cracks of the type shown in (a) occur in beams with large ratios of moment to shear, beams with thick webs, and beams with low prestress levels. A photograph of this type of flexure-shear crack is shown in Fig. 40.

The inclined crack shown in Fig. 39(c) represents a transition between the flexure-shear crack and the web-shear crack. This type of inclined crack occurs if the shear required to cause the initiating crack is only slightly less than that required to cause a web-shear crack. In such a beam, a short flexural crack, as shown in Fig. 39(c), is sufficient to cause a web-shear type of crack in the web above it. This type of flexure-shear crack occurs in beams with relatively thin webs, high prestressing forces and short shear spans. Figure 41 shows such a crack in beam CW.14.40.

An intermediate and more typical type of flexure-shear crack is shown in Fig. 39(b). In this case, the inclined crack formed adjacent to the initiating crack. An example of this type of crack is shown in Fig. 40.

In each of the three variations of the flexure-shear crack shown in Fig. 39, the critical stage in the formation of the inclined crack was the opening of the initiating flexural crack. Generally, the initiating crack was located at a distance from the load point ranging from one-third the length of the shear span (a/3) to one-half the height of the beam (h/2). The location of the initiating crack is discussed further in Section 5.3(b).

The shape of a flexure-shear crack depended to some extent on the properties of the beam and the way in which the crack developed. Thus, if an inclined crack developed in the manner shown in Fig. 39(a), its slope was steeper in the lower part of the web than in beams similar to Fig. 39(b) or (c) because the shearing stresses in the web did not become significant until the crack had penetrated about half the height of the web. The horizontal projection of the inclined crack was generally less in beams with low prestress levels than in beams with higher prestress levels.

The presence of web reinforcement affected the shape of the top of a flexure-shear crack to a small degree. In a beam without web reinforcement, the top of the crack extended well into the compression zone under the load points. This was especially true in beams with long shear spans where the inclined crack often penetrated half the thickness of the flange before stopping. On the other hand, if the web reinforcement was sufficient to prevent shear failures, the inclined cracks did not extend appreciably higher than the flexural cracks, even in beams with long shear spans.

In previous tests of beams with high values of Q and no web reinforcement (2), the inclined crack was often followed by a single horizontal crack or a series of short almost horizontal inclined cracks at the junction of the web and flange. These cracks extended from the inclined crack toward the reaction, and, when fully developed, transformed a bonded beam

into essentially an unbonded beam. In the beams described in this report, this type of cracking, which will be referred to as "splitting", was especially serious in beams which had draped longitudinal reinforcement passing through the web as shown in Fig. 42(a). The rate of splitting depended on the angle of the drape, the beams with high drape splitting faster than the beams with low drapes. Splitting also occurred in the rectangular beam with draped wires.

The presence of web reinforcement at reasonably close spacings prevented splitting from occurring or spreading extensively. However, if the stirrup spacing was large, as for example in BW.14.31 shown in Fig. 42(b), splitting was still a problem.

(d) Crack Patterns Observed in Tests

(1) Beams with Straight Wires with One or Two Concentrated Loads. Typical crack patterns for beams loaded with two concentrated loads are shown in Fig. 43(a) and (b). In all cases, the two loads were symmetrically placed so that the central portion of the beam was subjected to pure flexure and the regions between the loads and the supports were subjected to combined flexure and shear. In all the beams with straight wires and two loads, the first cracks were flexural cracks in the constant moment region. In most cases these were followed by flexural cracks in the shear spans, and, with the increased load, flexure-shear cracks developed. In about half of the I-beams with 1 3/4-in. webs, web-shear cracks developed before flexural cracks had formed in the shear spans.

Figure 43(c) shows a typical crack pattern for a beam loaded with a single unsymmetrically placed concentrated load. In these beams, the first crack was a flexural crack under the load. As the load was increased,

flexural cracks occurred in the shear spans at spacings of about six inches. The transformation of a flexural crack in the long shear span into a flexure-shear crack was gradual, partly because the shear in the long shear-span was small, and partly because the stirrups crossing the crack transferred stress across the crack and thus hindered its development.

(2) Beams with Draped Wires. The crack patterns for the beams with draped wires which were loaded with third-point loads are similar to the crack patterns for beams with straight wires except that more splitting occurred. The distance from the load to the initiating cracks tended to increase as the drape angle increased. One of the beams loaded at the third-points developed a web-shear crack; the others developed flexure-shear cracks as shown in Fig. 43(d). Three beams were loaded alternately at one end and then the other and developed web-shear cracks in the short spans as shown in Fig. 43(e).

(3) Beams Loaded with Simulated Moving Loads. The development of cracks in beam BW.10.22 is shown diagramatically in Fig. 44. The drawing at the bottom of the figure shows the cracks in this beam after failure and the chart at the top compares the loadings applied and the computed cracking and ultimate loads. The vertical axis of this chart indicates the load magnitude and the horizontal axis the load position. The heavy lines indicate the level of the applied load. Load increments 1, 2 and 3 were applied with the load at midspan. Load increment 4, which was the first increment of moving load, is represented by the lowest heavy horizontal line. This line joins the ordinates of the maximum load applied at each load position during increment 4. The computed beam strengths are shown by curved dotted lines which represent from bottom to top: (a) the computed

flexural cracking load, (b) the computed flexure-shear cracking load, (c) the computed ultimate shear capacity, and (d) the computed load corresponding to a flexural failure. The loads at which flexural cracking, inclined cracking and crushing of the concrete were observed are also indicated in the figure.

In beam BW.10.22, seven flexural cracks occurred under the load points 2 and 4 through 9 at load increments 3, 4, 6 and 8. These cracks extended vertically until they crossed the reinforcing steel. The subsequent development of these cracks was influenced by the varying shear and moment acting at each crack as the load was moved across the beam. The cracks which developed under a given load extended toward the point of application of the load. Since the load was applied at eleven separate positions for each load increment, a very complicated branching crack pattern developed as shown in the lower part of Fig. 44. At least eight flexure-shear cracks formed in this beam but because they formed in a region of many flexural cracks it was difficult to determine when they became inclined cracks. Beam BW.10.22 failed in flexure with the load at midspan. It had web reinforcement designed to allow a flexure failure.

Typical crack patterns are shown in Fig. 45 for beams tested under moving loads. Beam C.10.28, shown in Fig. 45(a) had a thin web and no web reinforcement. It developed a web-shear crack with the load in Position 2, close to the support, and as this load was moved from Position 2 to Position 3 and from 3 to 4, etc., nearly flat cracks occurred in the upper part of the web and extended the existing inclined tension crack toward the new load position. Eventually the thrust line was well below the inclined crack and the upper flange cracked and buckled upwards.

The beams shown in Fig. 45(b) and (c) had thicker webs and did not develop web-shear cracks. Beam BW.10.22 in Fig. (c) had web reinforcement. This beam is also shown in Fig. 44 and discussed above.

Beam CW.10.27, shown in Fig. 45(d) had a thin web and web reinforcement. Web-shear cracks developed near the reactions before flexural cracks developed. The presence of web reinforcement prevented these cracks from extending in the manner shown in Fig. 45(a). With further loading, flexural cracks and flexure-shear cracks occurred. Ultimate failure occurred in flexure with the load at midspan.

4.4 Measured Strains

(a) Measurements

As described in Sections 3.1(a) and (b), electric strain gages were used to measure strains on the top surface of the concrete and strains in the longitudinal reinforcement at midspan. No attempt was made to measure strains in the web reinforcement. Mechanical strain gages were used to measure the strain distribution over the depth of the beams with cast-in-place slabs. These measurements agreed fairly accurately with those given by the electric strain gages on these beams. Warwaruk (6), in tests of rectangular beams with aggregate similar to that used in these beams, also found that the readings of the one-inch electric strain gages were closely corroborated by those of mechanical strain gages.

The measured strains from each gage were plotted against the midspan deflection to determine if the readings were consistent, to estimate the values of the strains at failure by extrapolation from the measured values, and to observe possible trends in the data. Figure 46 shows several of these plots for the north span of CW.14.21. Several points of

interest can be observed. At a deflection of about 0.11 in., the first flexural crack was observed and the slope of the curves changed. This was caused by the upward displacement of the neutral axis and the decrease in beam stiffness which resulted from flexural cracking. Another change in slope for the gages near the load point occurred when the first inclined crack was formed at a deflection of 0.46 in. At flexural cracking, the slope of the strain-deflection curves decreased, while at inclined cracking it increased, owing to the concentration of concrete strains near the load. Other inclined cracks occurred at deflections of 0.68 in. and 1.10 in. The inclined cracks caused a redistribution of the stresses in the shear spans and, because there could be no shear flow between the tension and compression flanges across the inclined crack, beam action ceased and the beam carried load as a "tied arch." The compression thrust line over the inclined crack was close to the crack and almost parallel to it. Hence, the thrust acted with a considerable eccentricity on the portion of the beam over the crack near the reactions causing tensions in the top surface. This was evidenced by the decrease in the strains in gage B and by the tensile strains recorded by gage A. In a number of beams these strains led to cracking in the top flange and failure by distortion of the web. At a deflection of 1.6 in. crushing was observed in the south half span, the strains for which are not shown in this figure. Consequently, most of the deflection beyond this stage was due to rotations in the crushing zone, and the deflections increased faster than the strains, resulting in a decrease in slope of the strain-deflection curves for the north end of the beam. In the last stages of the test, the loads and the strains at the north end were almost constant.

(b) Concrete Strain at First Crushing

Figure 47 shows the measured concrete strains at crushing plotted against the compressive strength of the control cylinders. The data in

this plot were obtained from the beams which failed in flexure or in shear-compression. When the concrete started to crush but collapse did not follow immediately, the crushing strain was recorded directly, while in other cases, it was determined by extrapolation. The strains were recorded at the location where crushing took place and at the load at which crushing was first observed with a magnifying glass. In some cases, greater strains were recorded at other locations, usually at the loading points. Apparently the confinement of the concrete under the loads prevented its crushing in spite of the greater strains.

The crushing strain ranged from 0.003 to 0.007 and seemed to be independent of the concrete strength and the other variables studied. The crushing strain in the four beams with moving loads was less than 0.004 in each case, probably because these beams were loaded and unloaded a number of times in the application of the "moving loads". A value of 0.004 has been adopted as the crushing strain of concrete in flexure. This value is conservative for these test data but is in good agreement with the crushing strains reported in other investigations of the strength of prestressed beams failing in flexure and shear (6) (2).

(c) Distribution of Concrete Strain on Top Surface of Beam

The distribution of concrete strains on the top surface of the beams, measured by SR-4 gages, was useful in interpreting the behavior of the beams. The strain distributions at different stages of loading are presented in Figs. 48, 49 and 50 for beams CW.14.40, BW.14.42 and CW.14.39, respectively. Three strain distributions and the corresponding crack patterns are shown for each beam, the one at the top of each figure corresponding to a load before inclined cracking, the one in the middle to a load after inclined cracking, and the bottom one to the ultimate load.

Some of the strains in the last distribution were obtained by extrapolation. Beams CW.14.40, BW.14.42 and CW.14.39, respectively, had about 2.23, 1.54 and 0.69 times the minimum amount of web reinforcement needed to prevent a shear failure. Although CW.14.39 was the only one of the three which failed in shear, there were many indications that BW.14.42 was close to the transition range between shear and flexural failures. Photographs of the failures of these three beams are shown in Fig. 51.

Before inclined cracking, the strain distribution varied approximately as the moment diagram except that the strains were small in the uncracked regions at the ends of each beam. In beam CW.14.40, the opening of the inclined cracks was restrained by the heavy web reinforcement and the strain distribution remained unaltered. At loads approaching ultimate, the strains became greater and crushing occurred at a point between the loads, presumably where the concrete was weakest.

The behavior of beam CW.14.39 was different because the stirrups were not adequate to prevent a shear failure. After the formation of inclined cracks in such a beam, two phenomena cause a redistribution of stresses in the shear spans. The angle-changes resulting from steel strains under the entire horizontal projection of the inclined crack are concentrated under the load point since the depth of the compression zone is least at this point and thus the compression zone is most flexible here. This results in large concentrations of compressive strain under the load points as shown in Fig. 50. The intensity of this strain concentration varies with the severity of the inclined crack and the restraint imposed on the inclined crack by the web reinforcement. Over the rest of the length of the inclined crack, the strains at the top of the beam tend to decrease because the line of action of the compression thrust is lowered. While this is not evident from the

strain measurements plotted in Fig. 50, the presence of high tensile stresses in the top of the beam is shown by the crack in the top flange at the left end of the beam.

Beam BW.14.42 (Fig. 49) was an intermediate case; it failed in flexure but the stirrups permitted some opening of the inclined cracks with the related concentrations of strains. In this respect it resembles a shear failure. On the other hand, the stirrups transmitted sufficient shear across the crack that the compression thrust line remained close to the top of the beam. Thus, tensile stresses did not develop at the top of the beam in the shear spans after inclined cracking.

The three examples presented do not cover all possible cases. Some beams which failed by distortion of the web did not develop high strain concentrations under the loads since they failed before such concentrations could develop. However, these examples are sufficient to show that there is no clear-cut boundary between shear and flexural failures. Instead, there is a transition range and the beams that fall in this range display hybrid characteristics involving properties of both shear and flexural failures. In this transition zone the behavior changes gradually from one type of failure to the other.

In the case of beams loaded with one concentrated load, it is very difficult to determine the mode of failure from the strain distribution along the top of the beam because the maximum strains from the flexural cracks and from the inclined cracks in the two spans are concentrated under the load point. Furthermore, because of the length of the shear spans, the thrust line over the inclined cracks is not much lower than it would be in a beam failing in flexure and, as a result, tensile strains do not usually develop in the top flange.

For any given load position, the distribution of concrete strains along the top of a beam loaded with a moving load is similar to that for a comparable beam with a concentrated load at the same point. The strain concentrations at the load are less severe in the beam which is loaded with the moving load, however, as is shown in Fig. 52. Because of the differences in concrete strengths and loadings, beam B.10.23, with a moving load, developed an inclined crack at 12 kips as compared to the cracking load of 14 kips for beam B.11.29* which was loaded at midspan. The network of flexural and inclined cracks in B.10.23 joined together to separate the top flange from the web over the middle third of the span as the failure load was approached. This made the top flange more flexible for a greater length and allowed the compression strains to be spread over a greater length of beam, thus reducing the strain concentrations under the load. The total concrete strain for the two beams in Fig. 52, as measured by the area under the strain distribution curves, was practically the same in both cases, but the maximum strain for the beam loaded with the concentrated load was about 25 percent greater than for the beam with moving loads. Thus, a beam loaded with a single moving load should be more ductile in its behavior than a similar beam loaded to failure with a single concentrated load at midspan.

(d) Relationship between Concrete and Steel Strains

A fundamental assumption in the theory of flexure is that strains vary linearly over the depth of the beam. Prior to cracking, the strains in a bonded beam do vary linearly as assumed, and, after flexural cracking, the average strains measured over a considerable length of beam are also linear.

*This beam was loaded at midspan. It was originally reported in Ref. 2 and in the beam notation used in that paper, the second 1 in B.11.29 referred to a 54-in. shear span.

However, at any given section, as for example, a section containing a flexural crack, the strains will normally be non-linear to a small degree. This phenomena is discussed in detail by Warwaruk (6). For the purpose of computing the strength of a beam failing in flexure, the results are sufficiently accurate if the strain distribution is assumed to be linear, provided that good bond exists between the steel and concrete and provided that unrestrained inclined cracks have not formed in the shear spans.

On the other hand, inclined cracks lead to a severely non-linear distribution of strains over the depth of the section and this has a large effect on the strength of beams failing in shear. The inclined crack comes closest to the top of the beam under the load, and large compressive strains occur in the concrete in this region where the upper flange is most flexible. This concentration of compressive strains is illustrated in Fig. 49 or 50. The tensile steel strains corresponding to these high concrete strains are spread over the entire horizontal projection of the inclined crack. As a result, when the concrete reaches its limiting strain and crushes, the steel strains and stresses are much lower than they would be if the strains were linearly distributed and the ultimate strength of the beam is reduced below its flexural capacity. The presence of web reinforcement tends to restore the condition of linear strains.

To study the influence of the crack pattern on the relationship between the steel strains and the concrete strains at the top of the beam, plots like those in Fig. 53 were prepared. This figure shows the relationship between the steel strain measured at midspan and concrete strains measured at the three points indicated in the figure. Before flexural cracking, the relation was linear and the concrete strain increased rapidly.

After flexural cracking but before inclined cracking, the concrete strain increased more slowly than the steel strain because cracking shifted the neutral axis toward the top of the beam.

Three different beams were used to plot the curves in this figure. There are two curves for beam CW.14.45, one corresponding to a point a mid-span and the other to a loading point. This beam failed in flexure and the amount of web reinforcement in it was enough, not only to prevent a shear failure, but also to prevent any appreciable opening of the inclined cracks. Consequently, the two curves are almost identical and are fairly straight for the full range beyond first flexural cracking.

Beam CW.14.39, also shown in Fig. 50, failed in shear and had a very small amount of web reinforcement. It is seen that after the formation of the inclined cracks the concrete strain increased at a faster rate than before although there was no definite break in the curve, probably because of the presence of stirrups. The increase in concrete strain is a result of the non-linear distribution of strain previously discussed.

Beam CW.14.17 also failed in shear. However, the amount of web reinforcement in this beam was only slightly less than that required for a flexural failure. Thus, the inclined cracks affected the relationship between concrete and steel strains to a smaller extent than they did in CW.14.39. These trends agree in general with the results reported in Ref. 2 where these phenomena are described in more detail for beams without web reinforcement.

4.5 Mode of Failure

(a) Flexural Failures

A flexural failure is one caused primarily by bending stresses. For a given beam and loading, the load and deflection corresponding to

flexural failure represent the maximum load and deflection which the beam can sustain. A flexural failure occurs by crushing of the concrete over a flexural crack or by fracture of the longitudinal reinforcement at such a crack. Half of the 88 beams described in this report failed in flexure.

If failure occurred by crushing of the compression zone, the crushing started at the top of the beam and progressed downward, while the load dropped as a consequence of the reduction in the internal lever arm. However, when the neutral axis moved down further and entered the web, the compression zone was drastically reduced and the remaining portion of the compression zone crushed suddenly. This type of failure was typical of the beam with small values of Q and is illustrated in Fig. 54.

In the case of I-beams with high values of Q, the neutral axis was in the web before crushing started. Therefore, as soon as the concrete started to crush, the compression zone was greatly reduced and the crushing progressed downward violently. This type of failure was sudden, without warning and was quite different from the flexural failures of rectangular beams in which the area of the compression zone remained almost constant as the neutral axis moved down in the beam. This fact must be kept in mind when flexural and shear failures are compared, especially for beams with high values of Q. Figure 55 shows a photograph of one of these failures and another similar failure is shown in Fig. 43(b).

Photographs of beam FW.14.07 are shown in Figs. 56 and 57 as an example of a very ductile flexural failure. This beam was very much underreinforced, with a value of Q = 7. After a small amount of crushing, the beam failed by fracture of six of the eight wires in it. Figure 56 shows the well developed crack pattern after failure and Fig. 57 shows the crushing in the slab. In these figures, the large opening of the cracks in which the wires fractured can also be seen.

In tests of beams loaded with a single concentrated load or single moving load, it was difficult to define "failure" since the beams failed by crushing of the compression zone under the load where the concrete was restrained and hence strengthened by the load. In such cases, the development of serious crushing was taken as failure although the load could often be increased an additional five percent before collapse occurred. In addition, it was difficult to define the mode of failure because the compression forces balancing the prestressing force were lost when the compression zone crushed, and to regain statical equilibrium, the part of the beam between the load and the reaction slid up and inward toward the load point along an existing inclined crack until the unbalanced prestressing force had been dissipated. This action, which gave the appearance of a violent shear failure, occurred with both flexural and shear failures and is believed to have been secondary to the actual type of failure. Thus, in beams with long shear spans, it was difficult to determine the type of failure by observation of the beam after failure had occurred. An example of this type of failure is shown in Fig. 58 for beam CW.18.15 which failed in flexure. The stirrups in this beam were made of high strength cold drawn wire and could not undergo the deformations involved in this over-riding action.

(b) Shear Failures

Shear failures result from a combination of bending and shear stresses. Such failures are characterized by a major inclined crack in the shear span which disrupts beam action and results in a failure load and deflection which are both smaller than anticipated if the beam were to fail in flexure. Shear failures may occur in a number of ways, but it is always possible to recognize the effects of a well developed inclined crack.

The development of inclined cracking and the resulting redistribution of stresses in the shear spans is discussed in Sections 4.3(b) and 4.4. If the inclined cracks in a beam are all crossed by a sufficient amount of web reinforcement, "beam-like" action can be restored and flexural failures will occur. On the other hand, beams with less than adequate amounts of web reinforcement will fail in shear after the stirrups crossing the inclined cracks have yielded. Final collapse was a result of one of the following phenomena:

(1) Failure by Crushing and Distortion of the Web. As inclined cracks developed in a specimen, beam action ceased because the shear flow between the tension and compression flanges was destroyed by the inclined crack and the specimen carried load as a tied arch in the region of these cracks. Consequently, the compression thrust line moved down over the inclined cracks until it was relatively close and almost parallel to them. If the inclined crack reached almost to the reaction, as was normally the case with web-shear cracks, the thrust line acted with considerable eccentricity on the portion of the beam over the inclined crack, inducing large compressive stresses in the web and large tensile stresses in the top flange. As a result, tensile cracks formed in the upper flange and were followed immediately by crushing of the web as illustrated in Figs. 43(b), 45(a), 50 and 51(c).

(2) Shear-Compression Failures. In beams with long shear spans or thick webs, failure most often occurred by crushing of the concrete at or near the top of an inclined crack which extended to the vicinity of the load point. Typical failures of this type are shown in Fig. 43(a) and Fig. 45(b). At failure, the distribution of top concrete strains over the

length of the span showed peaks at locations corresponding to the tops of the inclined cracks, as discussed in Section 4.4(c) and shown in Fig. 49. This type of failure generally resulted from a flexure-shear crack.

(3) Failure by Separation of the Tension Flange from the Rest of the Beam. If the prestressing steel becomes unbonded in the neighborhood of a flexure-shear crack, the non-linearity of strains is magnified even more since the length over which the steel strains are distributed is increased by the additional unbonded length. If the tension reinforcement is "unbonded" by separation of the tension flange from the rest of the beam, this may constitute the primary failure before a shear-compression failure can occur. This type of splitting occurred in about half of the draped beams, especially in the beams with wires passing through the web. In beams with closely spaced stirrups, the development of cracks along the steel or along the junction of the web and flange was checked by the web reinforcement. This was not true in the case of widely spaced stirrups, however, as shown in Fig. 42.

(4) Failure by Fracture of the Stirrups. In beams with very small amounts of web reinforcement, the inclined cracks continued to open until some stirrups fractured. Usually, however, the deformations required to break mild steel stirrups are so large that crushing would occur under the load points or tensile cracks would occur in the top flange before the stirrups broke. This would not necessarily be true in the case of beams with stirrups made of the more brittle high strength cold-drawn steel.

Stirrups fractured in four beams: CW.14.23, BW.18.15, BW.19.28 and CW.18.15. Beam CW.14.23 failed by web distortion. Beam BW.18.15 failed suddenly and completely when the capacity of the stirrups was

reached, presumably because the brittle, high-strength steel stirrups broke almost immediately after they yielded. However, the load and deflection for BW.18.15 were close to those expected in a flexural failure. Stirrups were also broken in beams BW.19.28 and CW.18.15 as the end of the beam slid inward along an inclined crack after the compression zone had been destroyed by crushing. Beam CW.18.15 shown in Fig. 58 had high strength stirrups.

Beam CW.13.28 failed in a somewhat different manner. This beam had a shear span of 28 in., a web thickness of 1 3/4 in., and eight longitudinal prestressing wires. After inclined cracking, one of the inclined cracks developed faster than the others until it extended from the lower region of the end block to a point below the loading block. As the load increased, tensile cracks formed in the upper flange near the end-block and slight crushing was observed in the flexure span near the load. With further load, the beam failed very violently as shown in Fig. 59. In this beam the concrete crushed below the upper end of the major inclined crack; this may or may not have been the initial cause of failure. If it were, however, it may indicate that the strength of the "cantilever" below the inclined crack represents an upper limit on the amount of shear which can be transferred by web reinforcement. This possibility is discussed in more detail in Section 5.5(a).

(c) Transition Failures

In eight of the beams tested, the failure could not be classified as either a flexural or a shear failure but rather appeared to have enough of the properties of both types of failures to fall between the two groups. These beams were designated as transition failures. In general, all these beams behaved as if they were going to fail in flexure up to the time that

failure occurred. They exhibited all the properties of beams with flexural failures except for their appearance after failure. For structural purposes, these beams were as good as those which failed in flexure.

5. STRENGTH OF PRESTRESSED CONCRETE BEAMS WITH WEB REINFORCEMENT

5.1 Introductory Remarks

By far the most important property of any structural member is its strength. Four different strength properties enter into a consideration of the strength and behavior of a prestressed concrete beam. These are the flexural cracking load, the flexural failure load, the inclined or shear cracking load, and the shear failure load. The relationship between these four strength properties defines the behavior of a beam. In all cases, flexural cracking will occur before the flexural capacity is reached. However, inclined cracking may occur before or after cracking or not at all. If inclined cracks do occur before the ultimate load is reached in beams without web reinforcement, shear failures will result. However, if sufficient web reinforcement is provided in these beams it may be possible to change the mode of failure from shear to flexure.

Chapter 5 consists of a discussion of the four analyses used to correlate the test results. The analysis for the flexural cracking load is presented in Section 5.2. In Section 5.3, the inclined cracking load is discussed from a semi-rational standpoint and following this, an empirical expression is derived for the inclined cracking load. The flexural capacity of prestressed concrete beams is considered in Section 5.4. Finally, the effect of web reinforcement on the ultimate strength of prestressed concrete beams is considered in Section 5.5. In each section, the analysis is compared to the pertinent test results.

5.2 Flexural Cracking Load

The development of cracks in a prestressed concrete beam marks the end of the "elastic" stage of behavior. In beams of practical proportions,

the first cracks to form are flexural cracks. In Section 4.3 it was noted that inclined cracks frequently result from flexural cracks in the shear span and, as will be discussed in Section 5.3, the prediction of this type of inclined crack, the flexure-shear crack, is based in part on the flexural cracking load at a given point in the shear span.

(a) Assumptions

The computation of the flexural cracking load is based on the following assumptions:

1. The concrete in the beam is assumed to have a linear stress-strain curve with the same modulus of elasticity in tension and compression. The assumption of linearity is essentially true in compression since the compressive stresses are normally in the "elastic" range at the flexural cracking load. It is not true in tension since tests have shown that the tensile stress-strain curve for concrete is not linear up to failure (7). However, the assumption of linear strains is compatible with the linear stress-strain relationship implicitly assumed in using the equation $f = My/I$ to evaluate the modulus of rupture from the cracking load in the standard test for modulus of rupture.

2. The ultimate tensile strength of concrete in flexure is assumed to be equal to the modulus of rupture as expressed by Eq. 1. In addition to the error in the tensile strength resulting from assuming a linear stress-strain curve for concrete in tension, it has been shown that the modulus of rupture from a beam test is affected by the length and shape of the specimen and the type of loading applied (8). In this analysis, no allowance was made for size and shape effects because in a prestressed beam the bending moment required to overcome the tensile strength of the concrete

is only 20 to 30 percent of the total applied moment required to overcome the combined effects of the tensile strength and the prestress at the bottom of the beam.

The modulus of rupture used in computing the flexural cracking load was the value computed from the compressive strength using Eq. 1 rather than the measured value, since the compressive strength of the concrete is the basic property assumed in design and under normal circumstances is the only concrete property checked by control specimens.

3. The section is assumed to act as a transformed section. The transformed area of the prestressing wires and the slab reinforcement was computed using the ratio of modulus of elasticity of steel to modulus of elasticity of concrete given by Eq. 3. No allowance was made for possible differences in the modulus of elasticity of the slab and beam concrete for the beams with composite slabs since there was little difference in compressive strength.

(b) Method of Computation

For all the beams in this series except the two composite beams FW.14.06 and FW.14.07, the flexural cracking moment was computed by the conventional method for an uncracked section as given by Eq. 4.

$$\frac{M_{cf} y_b}{I_t} = f_F^b + f_r \qquad (4)$$

where: M_{cf} = total live and dead load moment at flexural cracking

y_b = distance from the centroid of the transformed section to the bottom fiber

I_t = transformed moment of inertia

f_F^b = stress at the bottom of the beam resulting from the prestressing force

f_r = computed modulus of rupture of the concrete at the bottom of the beam

In the case of the two beams with cast-in-place slabs, the term f_F^b included an allowance for the stresses resulting from the differential shrinkage of the prestressed beam and the cast-in-place slab. The effect of shrinkage was taken into account by considering the composite section as an eccentrically loaded column loaded with a load applied at the centroid of the slab. The magnitude of this shrinkage "load" was assumed to be:

$$P_s = 0.0001\, E_c\, A_{slab} \qquad (5)$$

where: P_s = differential shrinkage force, lb.

E_c = modulus of elasticity of concrete from Eq. (3)

A_{slab} = Area of concrete in slab

The coefficient 0.001 represented the amount of differential shrinkage strain between the beam and the slab at the time of testing, estimated from previous studies of shrinkage (4).

(c) Comparison of Measured and Computed Values of Flexural Cracking Moment

The measured and computed values of the flexural cracking moment are listed and compared in Table 6. The values listed for the beams with draped wires correspond to the flexural cracking moment in the constant moment region. The agreement between the measured and computed cracking loads was excellent as shown in the table below.

Ratio of Measured to Computed Flexural Cracking Moment

	Mean	Maximum	Minimum	Mean Deviation
Using Computed f_r	1.03	1.16	0.72	0.046
Using Measured f_r	1.02	1.19	0.71	0.054

To compare the effects of basing the flexural cracking moment on the computed rather than the measured values of the modulus of rupture, flexural cracking moments based on both values are listed in Table 6 and in the table above. It is interesting to note that for the beams in this test series, the mean deviation from the average ratio of measured to computed flexural cracking moments was lower for the values predicted with the computed modulus of rupture than for the values predicted using the actual measured modulus of rupture.

5.3 Inclined Cracking Load

The load at which inclined cracks form in a prestressed concrete beam marks a critical stage in its behavior. As shown in Fig. 36, the strength and ductility of a beam without web reinforcement are seriously limited by the formation of inclined cracks and, for practical purposes, the inclined cracking load represents the ultimate capacity of a beam without web reinforcement. In the design of beams with web reinforcement, a knowledge of the inclined cracking load is essential since the web reinforcement does not act before an inclined crack has formed.

The prediction of the web-shear and flexure-shear cracking loads will be discussed separately in parts (a) and (b) since these loads represent the limiting conditions for the inclined cracking load. In parts (c) and (d) the inclined cracking loads of beams with draped wires and beams tested under moving loads will be discussed.

(a) Web-Shear Cracks

A web-shear crack has been defined in this report as an inclined crack which develops in the web of a beam before flexural cracks develop in its vicinity. Therefore, in the case of web-shear cracking, and only in

this case, the principal tensile stresses computed for an uncracked section will approximate the stresses in the web of the beam at the time of inclined cracking. If it is assumed that web-shear cracking is a stress phenomenon and that the critical tensile strength of the concrete in the web can be determined or estimated, it should then be possible to compute the web-shear cracking load.

All but two of the beams described in this report were symmetrical about both axes of the cross-section; the remaining two beams were composite T-beams which were symmetrical about the vertical axis only. The method of calculation and the critical value of the tensile strength of the concrete will be evaluated first for doubly symmetrical beams and the value thus obtained will be assumed to apply to beams which are symmetrical only about the vertical axis.

1. Cross Sections Symmetrical About Two Axes. The principal tensile stresses in the web of a beam are computed by the usual methods of strength of materials, assuming that the concrete in the beam remains elastic until web-shear cracks develop. The maximum principal tensile stress at any given point in a beam is given by the following expression:

$$f_t = \sqrt{v^2 + \frac{f_1 - f_2}{2}} - \left[\frac{f_1 + f_2}{2}\right] \qquad (6)$$

where: f_t = maximum tensile stress at the point

f_1 = normal stress at the point

f_2 = vertical stress at the point

v = shearing stress at the point

The term f_2 has been included in this equation to indicate the effect of the vertical bearing stresses which act near the loads and reactions. For very short beams, the shearing forces tend to be transmitted

to the supports by these vertical stresses as shown by Timoshenko and Goodier (9) or Laupa, Siess, and Newmark (10). The zone in which vertical stresses exist extends about 0.7h to h on either side of the load point and thus, if the shear span is shorter than 1.5h to 2h, bearing stresses will affect the principal tensile stresses in the region where the web-shear cracks start. However, in more practical beams, with shear spans longer than twice the overall depth, the bearing stresses can be neglected in the computation of the stresses in the part of the web affected by web-shear cracking.

The constantly changing combinations of shearing stress, flexural stress, and the bearing stress which acts near the loads and reactions, makes it very tedious to determine the location and magnitude of the maximum principal tensile stress in a beam at the time of inclined cracking. The inclined crack may originate at, above, or below the elastic centroid, and anywhere along the length of the shear span where the stresses are large enough. However, since the web-shear cracks observed in the tests formed presumably where the stresses were most critical, it should be possible to determine the critical point for the beams tested by computing the stresses acting in the uncracked web along the trajectory of the actual web-shear crack, at the inclined cracking load. Computations of this sort have shown that in beams with short shear spans and thin webs, and with symmetrical cross sections similar to those tested, the maximum principal tensile stress along the potential inclined crack occurs at the centroid of the cross section. As the shear span gets longer or the web thickness increases, flexural stresses have a greater effect on the magnitude of the principal tensile stresses and the point of maximum stress along the potential web-shear crack tends to move toward the tension flange. At the same time, however, the properties of the beam become such that flexural cracks develop in the shear span before

inclined cracking, and the computed stresses in the uncracked web cease to have any significance at the time of inclined cracking.

The distribution of principal tensile stresses along the trajectory of the inclined crack is illustrated in Fig. 60 for three typical cases. Web-shear cracks developed in beams CW.13.38 and CW.14.47, while beam BW.14.41 developed a flexure-shear crack. In the first beam the maximum principal tensile stress along the actual crack trajectory occurred at the centroid. In beam CW.14.47, the maximum tensile stress was about 102 percent of that at the neutral axis. While this beam did develop a web-shear crack, the cracking load was only a little less than the predicted flexure-shear cracking load and, as expected, flexural stresses had a larger effect on the tensile stresses in the web than in the first case. In beam BW.14.41, flexural stresses predominated and the maximum principal tensile stress in the web occurred at the junction of the web and the lower flange. However, before the stresses at this level could become critical, an initiating flexural crack occurred at the bottom of the beam and a flexure-shear crack developed. For the two beams in Fig. 60 which developed web-shear cracks, it can be assumed with little error that the maximum principal tensile stress acted at the centroid. In similar computations for all of the beams in this report and in Ref. 2 which developed web-shear cracks, the average ratio of maximum principal tension to that at the centroid was 1.03. These ratios are listed in Table 7. In 20 of the 30 beams listed in this table, the maximum principal tensile stress actually occurred at the centroid while in the others the maximum principal tensile stress ranged from 1.00 to 1.23 times that at the centroid. Thus, in symmetrical I-beams similar to those tested, it can be assumed that the web-shear cracking load can be determined by considering only the principal tensile stresses at the elastic centroid of the uncracked section.

Since no test data for the tensile strength of the concrete were obtained, this quantity was estimated on the basis of modulus of rupture tests. The true tensile strength of concrete would be the same as that measured in a beam test if the stress-strain curve in tension were linear all the way to rupture, as is nearly the case for very high strength concrete. For normal concretes, however, the tensile strength is less than the conventional modulus of rupture because the tensile stress-strain curve is nonlinear. The actual tensile strength of concrete lies somewhere between 60 and 100 percent of the modulus of rupture depending on the degree of nonlinearity of the tensile stress-strain curve.

To determine the tensile strength of concrete corresponding to web-shear cracking, the tensile stresses at cracking were computed at the centroid of each of the test beams in this report and in Ref. 2 which developed this type of inclined crack. The ratio ranged from 0.53 to 1.07 with a mean value of 0.79 for beams without web reinforcement* and 0.90 for beams with web reinforcement. These ratios are listed in Table 7.

In computing the web-shear cracking load the tensile strength of the concrete has been taken as 80 percent of the modulus of rupture computed from Eq. 1. This value has been chosen to fit the data for beams without web reinforcement since one result of adding web reinforcement was a small increase in the apparent tensile strength of the concrete. In Fig. 61 the ratio of the apparent tensile strength at cracking, for the beams with web reinforcement, to that assumed for a beam without web reinforcement is plotted against the ratio of the transformed area to the gross area of the web

---

*In beams C.12.40, C.12.44, and C.22.40, a spacer made of 1/2-in. pipe was placed across the top flange at the middle of the shear spans to keep the forms 6 in. apart. The first inclined cracks in these beams occurred immediately under these pipes. If these beams are omitted, the ratios ranged from 0.64 to 1.07 with a mean value of 0.83 for beams without web reinforcement.

along a horizontal section. The low point corresponds to beam CW.14.35 which as discussed in Section 5.5(e), had weak concrete in one shear span. As indicated by the points falling above the inclined line in this figure, the increase in the apparent tensile strength is greater than that attributed to the transformed area of the stirrups. The presence of the web reinforcement may have permitted a greater degree of inelastic redistribution of the tensile stresses in the web before failure, thus increasing the apparent tensile strength of the concrete. Also, part of the increase in the cracking load may have resulted from a delay in the time when the first crack was visible. There did not seem to be any correlation between the increase in the apparent tensile strength of the concrete and the spacing of the stirrups.

No attempt has been made to evaluate the vertical compression stress f_2 for beams with a/h less than two. Shear span to depth ratios significantly less than two occurred only in the beams loaded with moving loads and in these tests inclined cracks did not initiate with the loads closer than 1.83h to the supports. However, presumably because of the vertical stresses, the loads which caused web-shear cracks at load position 2, (a/h = 1.83), previously acted at load position 1, (a/h = 1.17) without causing cracking. The shear resulting from this load at load position 1 is 9 percent greater than for the same load at position 2.

Using 80 percent of the computed modulus of rupture as the tensile strength of the concrete in the web, the inclined cracking loads were computed for the symmetrical I-beams in this report and in Ref. 2 which developed web-shear cracks, by determining the shear required to raise the principal tensile stresses at the elastic centroid to the critical values. The computed cracking loads are listed and compared with the measured loads in Table 7. The agreement between the measured and computed web-shear cracking loads will be summarized in Section 5.3(e).

For general application, a lower limiting value of the tensile strength should be used. It is recommended that the value of the tensile strength of the concrete be taken as 1/2 to 2/3 the modulus of rupture rather than 80 percent as used in the analysis of these tests which were made under laboratory conditions.

2. Cross Sections Symmetrical About One Axis. So far in this discussion the web-shear cracking load of cross sections symmetrical about both axes has been considered although composite beams and T-beams are much more common in practice. The inclined cracking loads of such beams can be computed by a simple extension of the procedure just described. The effect of torsion in sections unsymmetrical about both axes will not be considered.

Two beams, FW.14.06 and FW.14.07, were initially constructed as symmetrical I-beams with 1 3/4-in. webs with a cast-in-place slab added after release. In the complete beam, the dead load stresses and the stresses resulting from prestressing were carried on the I-section while the live load stresses and shrinkage stresses from the slab acted on the entire composite section, leading to a complex distribution of direct and shear stresses in the member.

The web-shear cracking load of unsymmetrical beams can be predicted in the same way as for symmetrical beams if the centroid is in the web of the beam. However, the centroid of the beam tested was in the upper flange; therefore the critical conditions for web-shear cracking were assumed to occur at the point in the web closest to the centroid along a 45 deg. line passing through the top of the beam at the load point. This line was assumed to be at 45 deg. for simplicity; actually, a web-shear crack would occur at a flatter angle if prestress were present and if vertical bearing stresses

were not appreciable. By assuming a 45 deg. line in finding the critical section, however, the flexural tension at the assumed critical section was over-estimated and, as a result, the predicted inclined cracking load should be less than the actual cracking load. The distribution of principal tensile stresses along a 45 deg. line through the load point in beam FW.14.06 is shown in Fig. 62.

Based on this analysis, the ratios of observed to computed web-shear cracking loads were 1.10 and 0.96, respectively, for FW.14.06 and FW.14.07. Both beams developed web-shear cracks and in both the first inclined cracks appeared at the juncture of the web and the upper flange.

(b) Flexure-Shear Cracks

An inclined crack which develops after flexural cracks have formed in the shear span in its vicinity is defined in this report as a flexure-shear crack. When a flexural crack forms in the shear span of a beam, it acts as a stress raiser and forces a redistribution of the principal tensile stresses in the uncracked part of the beam above or adjacent to it. If these stresses are high when the flexural crack forms, the stress redistribution in the web is often such that the inclined crack forms at a load equal to or only slightly larger than the load causing the critical flexural crack in the shear span. In other cases, depending on the properties of the prestressed beam, the inclined cracking load may be as much as 20 to 30 percent greater than the load at which the critical flexural crack forms.

The flexural crack which critically affects the inclined cracking load is called the "Initiating Crack". Its location is influenced by such factors as the length of the shear span and the relative magnitudes of the flexural cracking load and the web-shear cracking load. By examining the shape of the flexure-shear cracks which developed in tests of 139 beams with

straight wires, reported in this paper and in Ref. 2, it was found that the initiating flexural crack generally started at the bottom of the beam at a distance ranging from one-half the height of the beam (h/2) to one-third the shear span (a/3) from the load point. This distance approached h/2 as the load causing the initiating crack approached the computed web-shear cracking load, and approached a/3 if the load causing the initiating crack was small compared to the web-shear cracking load. The location of the initiating crack was also influenced to a small degree by the effective depth, and by random variations in the location of the first flexural crack in the beam. In all subsequent computations of the loads required to cause the initiating crack, the distance x from the load point to the critical initiating crack has been assumed to be the average of a/3 and h/2 as represented by the following equation:

$$x = a/6 + h/4 \qquad (9)$$

The effect of the initiating crack on the stresses in the shear span can be shown by the following analysis. Figure 63(a) shows a portion of a beam in a region of both shear and moment. The sections AC and $A'C'$ are cut on the two sides of an opening, CB $B'C'$, of width Δx, in the bottom of the beam. In the limiting case, as this gap is made narrower, it can be considered to represent the initiating flexural crack.

The forces acting on sections ABC and $A'B'C'$ are shown in Fig. 63(b). Under the loading considered, the moments on the two faces are different since shearing forces act on both faces. However, the stress in the tension reinforcement crossing the gap cannot change from one side of the gap to the other, and therefore, the normal forces in the concrete on both sections are equal. The change in moment between the two sections is accomplished by a change in the distribution of stresses and a shift in the

location of the resultant compressive force in the concrete. In the general case, the stress distributions on the two faces will be similar to those shown in Figure 63(c) and the difference in the stresses on the two faces will resemble Fig. 63(d).

Since the tension force in the steel must remain constant across the width of the crack, there is no resultant horizontal shear on Section BB'. Since no "faulting" of the vertical crack can be visualized, it can be assumed that the steel does not transfer shear across the crack by doweling. Therefore, all the shearing forces on the vertical sections must act on the uncracked concrete AB and A'B' above the initiating crack. From elementary mechanics it can be shown that the shear stresses acting at any level on the cut surfaces AB or A'B' may be found by integrating the difference between the direct stresses on the two faces of the element above the level. The resulting shearing stresses are shown in Fig. 63(e). Finally, by combining the effect of the direct stresses and the shearing stresses it is possible to compute the principal tensile stresses acting on the face A'B' as shown in Fig. 63(f). In this figure the maximum principal tensile stress acts at the top of the crack and corresponds presumably to the tensile strength of the concrete in flexure. High tensile stresses also exist at some point D as a result of the combined shearing stresses and direct stresses.

With further loading, the flexural crack CBB'C' extends vertically into the beam under the influence of the tensile stresses at the top of the crack, and as a result, the depths of the incracked section AB or A'B' are reduced. As the crack extends vertically, the principal stresses at point D increase rapidly and eventually reach a critical value at which an inclined crack resembling a web-shear crack should develop. Examples of this type of flexure-shear crack are shown in Figs. 39(c) and 41.

As the load is increased in the interval between the formation of the initiating crack and the inclined crack, the height of the initiating crack increases rapidly, compounding the already difficult problem of computing stresses in the beam. For a given cross section, the height of the flexural crack and the magnitude of the stresses corresponding to a given value of the applied moment can be evaluated if a stress-strain relationship is assumed for the concrete. By trying a number of crack heights it is then possible to determine the load at which the principal tensile stresses become critical in the uncracked portion of the beam above the crack. The resulting distributions of the principal tensile stresses in a given beam are shown in Fig. 64 for a beam without a crack, a beam with a 2.65-in. crack, and a beam with a 4.15-in. crack. A linear distribution of direct stresses was assumed in computing the stress distributions shown in this figure.

This analysis is by no means considered to be a complete explanation of the phenomenon of flexure-shear cracking. It does not explain, for example, why a flexural crack in the shear span tends to bend over toward the load point. However, the analysis does emphasize the major effect that an initiating flexural crack has on the principal tensile stresses in its vicinity, and for this reason it has been included in this report. If the principal tensile stresses in the web are large when the initiating crack develops, or in other words, if the web-shear cracking load is only slightly greater than the load causing the initiating crack, the increase in the principal tensile stresses in the web due to the formation of the initiating crack may be enough to cause the immediate formation of an inclined crack. On the other hand, if the web-shear cracking load is much greater than the load required to cause the initiating flexural crack, the initiating crack will extend some distance into the beam before an inclined crack will develop.

Since the determination of the actual stresses above a crack involves assumptions about the behavior of the beam which may never be sufficiently accurate to justify such a stress analysis, the determination of the flexure-shear cracking load for the beams in this test series has been approached on an empirical level. The basis of this method of computing the flexure-shear cracking load is the relationship between the inclined cracking load, the load causing the initiating flexural crack, and the load theoretically required to cause a web-shear crack.

Figure 65 shows the relationship between the computed loads corresponding to the initiating flexural cracks and the inclined cracking loads for beams developing flexure-shear cracks. In this figure, the ordinate of each point is the applied shear at inclined cracking, V_{cm}, and the abscissa is the shear, V_f, at the computed load required to cause a flexural crack in the shear span at a distance x from the load point, where x is given by Eq. 9. This flexural crack is assumed to be the critical initiating crack. The plotted points lie above the 45-degree line since the inclined cracking loads are greater than the load assumed necessary to cause the initiating crack.

Figure 65 does not include data for beams with web-shear cracks. If the load required to cause an initiating crack exceeds the web-shear cracking load, a web-shear crack will develop before a flexure-shear crack. In this case, the inclined cracking load is not related to the initiating flexural crack. Figure 65 can be changed to the more general form shown in Fig. 66 by dividing both the abscissas and ordinates of Fig. 65 by the shear V_s, corresponding to web-shear cracking, computed for an uncracked section as previously discussed. The results of 168 tests of prestressed

concrete beams with straight longitudinal wires,* both with and without web reinforcement are plotted in this manner in Fig. 66.

When, V_f, corresponding to the initiating crack is less than that for a web-shear crack, V_s, the inclined cracking shear, V_c, is related to V_f. This relation is represented by the 45-degree line in Fig. 66 which corresponds to $V_c = V_f$. The test results for flexure-shear cracks, plotted with solid points, fall in a band parallel to but slightly above this 45-degree line. If V_f is greater than V_s, the inclined crack should theoretically be a web-shear crack and V_c should equal V_s as indicated by the horizontal line in Fig. 66. The agreement of this line with the test data for beams with web-shear cracks (open symbols) appears reasonable, especially since the web-shear cracking load is strongly affected by variations in the tensile strength of the concrete.

The relationship shown in Fig. 65 and 66, between the flexure-shear cracking load and the load corresponding to the formation of the initiating flexural crack, suggests that the inclined cracking load could be expressed in terms of V_f, the computed shear corresponding to the initiating crack, and V_s, the computed shear corresponding to the formation of a web-shear crack. Accordingly, the line given by Eq. 10 was passed through the points in Fig. 66 which represent flexure-shear cracks.

$$V_c = V_f + 1/15\ V_s \leq V_s \qquad (10)$$

where:

V_c = shear at formation of flexure-shear crack

V_f = shear corresponding to formation of initiating flexural crack

V_s = shear corresponding to formation of a web-shear crack as computed in Section 5.3(a).

---

*Ninety-nine of these beams were reported in Ref. 2.

The data used to derive Eq. 10 was obtained from tests of beams which were essentially similar in most respects. All the beams were 6 by 12 in. in over-all cross section, although the web thickness varied from 0.3 to 1.0 times the flange width. The effective depth, d, varied from 8 to 11 in. and the range of a/d varied from 2.8 to 7.8 (a/h = 2.0 to 6.5). The prestress level and concrete strengths were both varied over a wide range. In addition, the shear was practically constant throughout the shear spans of the beams tested since the dead load shear was negligible in comparison to the live load shears. Although all of the beams used to derive this expression were symmetrical I-beams, it is expected that this method of predicting the flexure-shear cracking load would apply to other reasonably similar cross sections. The accuracy of Eq. 10 in predicting the inclined cracking load of beams subjected to loadings other than concentrated loads has not been considered.

The measured and computed values of the flexure-shear cracking load for beams with straight reinforcement are presented and compared in Table 8(a) for beams included in this report and in Table 8(b) for beams reported in Ref. 2. The results of these comparisons will be summarized in Section 5.3(e).

(c) Inclined Cracking Load of Beams with Draped Reinforcement

Both web-shear and flexure-shear cracks occurred in the tests of beams with draped reinforcement, although the properties of the beams tested were such that most of them developed flexure-shear cracks. Draping the longitudinal reinforcement appeared to increase the inclined cracking load in the beams which developed web-shear cracks, and appeared to decrease the inclined cracking load for the beams which developed flexure-shear cracks. In this section, the web-shear cracking load of beams with draped wires will be discussed first, followed by a discussion of the flexure-shear cracking load.

In a beam with draped wires, the upward component of the prestressing force counteracts some of the dead and live load shear so that the "net" shear force acting at any point in the shear spans at inclined cracking may be stated as:

$$V_n = V_c - V_d \qquad (11)$$

where:

V_n = net shear at inclined cracking

V_c = total applied shear at inclined cracking

V_d = upward component of prestressing force at that point

(1) Web-Shear Cracks. In computing shear stresses and principal stresses, only the net shear is considered. Since the web-shear cracking load is a function of principal tensile stresses, draping the longitudinal reinforcement should increase the web-shear cracking load. Beams CD.13.24 and CD.13.25 were tested to check the validity of this concept. Beam CD.13.24 was tested with a load first near one end and then near the other, giving two values of the web-shear cracking load. The data from these two tests and the test on CD.13.25 are plotted in Fig. 67(a) and (b) along with the web-shear cracking data obtained from tests of beams with straight wires. The ordinates in Fig. 67(a) and (b) are the ratio of V_{cm} or V_n, the observed gross or net shear at inclined cracking, to V_s, the web-shear cracking load as computed in Section 5.3(a). The abscissas represent the angles of drape for the various beams plotted. Figure 67(a) is plotted for the gross shear, V_{cm}, while Fig. 67(b) is plotted for the net shear, V_n. The points plotted at $\varphi = 0$ compare the measured and computed web-shear cracking loads for 27 beams with straight wires and are the same on both figures since the gross and net shears are the same in a beam with straight wires. (Beam CD.14.34 which is also plotted in Fig. 67 will be discussed later.)

From Fig. 67(a) it appears that the gross shear at web-shear cracking is increased by draping the wires, although the three points for beams CD.13.24 and CD.13.25 all fall within the range of the data for beams with straight wires. If this figure is replotted in terms of net shear, as shown in Fig. 67(b), the test data for the draped beams agree more closely with the average for the beams with straight wires. From these two figures, it appears that the inclined cracking strength of beams developing web-shear cracks is increased by draping the wires. Since flexural cracks do not influence the development of this type of crack, the "net shear capacity" of beams developing web-shear cracks depends only on the principal stresses in the web and, therefore, remains constant as the drape angle increases. Accordingly, the shear corresponding to the web-shear cracking load of a beam with draped wires is the sum of the cracking shear for a beam with straight wires, computed according to Section 5.3(a) and the upward component of the prestress. The measured and computed cracking shears for beams CD.13.24 and CD.13.25 are compared in Table 9(a). These beams are also listed in Tables 7 and 8(a).

If the draped wires enter the web in the shear span, the stress-concentrations introduced by shear transfer at the level of the steel or by the reduction of the concrete section may be sufficient to raise the principal tensile stresses at that location to a critical value. This condition did not exist in beams CD.13.24 and CD.13.25 since the draped wires did not enter the web. However, in CD.14.34 the web-shear crack originated approximately at the point where the wires entered the web and the load at inclined cracking was only 81 percent of the predicted value.

(2) Flexure-Shear Cracks. The properties of most of the beams with draped wires were such that flexure-shear cracks occurred. The close

relationship between flexural cracking and inclined cracking is very important in the interpretation of the behavior of these beams. When the reinforcement is draped in the shear spans, the moment required to cause the initiating flexural crack is smaller than in a beam with straight wires and, as a result, the flexure-shear cracking load is also decreased.

The ratio of the measured inclined cracking shear for the draped beams which developed flexure-shear cracks to the inclined cracking shear in an identical hypothetical beam with straight wires, computed from Eq. 10 is plotted against the angle of drape in Fig. 68 for the 17 beams which developed flexure-shear cracks. The corresponding shears are listed in Table 9(b).

The test results in Fig. 68 indicate a reduction in the flexure-shear cracking load as the drape angle of the longitudinal reinforcement is increased beyond 2 to 3 degrees.

It should be noted that the inclined cracking shear for the beams with draped wires in Fig. 68 is the total applied shear at a section. A similar plot based on the net shear as defined by Eq. 11 is shown in Fig. 69. Such a plot isolates the effects of the steel position on the cracking strength of the section, and the data in Fig. 69 emphasize the marked reduction in the net shear strength for draped beams which develop flexure-shear cracks. When the prestressing wires in the test beams were draped through the upper kern point at the support (φ = 10 deg.), the resulting net shear strength was only 30 percent of that for a beam with straight wires.

The considerable reduction in flexure-shear cracking load for the beams with draped wires can be explained in terms of the reduction in the load required to produce the initiating flexural crack. In the beams with draped wires, the eccentricity of the reinforcement was decreased in the shear span and the prestressing force was thus less effective in resisting

flexural tensions at the bottom of the beam. Consequently, initiating cracks formed at lower loads in the beams with draped wires than in similar beams with straight wires. In addition, the increment of load between the formation of the initiating crack and the inclined crack was decreased since in a beam with draped wires an initiating crack grows more rapidly and to a greater height because the centroid of the reinforcement is higher.

The development of splitting along the reinforcement adjacent to an inclined crack was adversely affected by draping the wires. This splitting results from the doweling action of the steel crossing the crack and from the large change in steel stress which occurrs adjacent to an inclined crack, as the behavior of the portion of the beam between the crack and the support tends to revert from "tied-arch action" to "beam action". The change in the tensile force must "flow" to the compression flange. This requires that, for the restoration of beam action, not only must there be adequate bond between the concrete and the steel, but the concrete section itself must be able to carry the shear flow from the tension to the compression flange. In a beam with straight wires, the junction of the web flange is the critical section in this transfer of shearing forces. In a beam with draped wires, the presence of wires in the web introduces another plane of weakness along which splitting can develop. Furthermore, the change in steel stress adjacent to an inclined crack tends to be higher in a beam with draped wires, because at an uncracked section, the tensile strains in the reinforcement are smaller the closer the reinforcement is to the neutral axis of the beam. Thus, in a beam with draped wires there is a greater variation in steel stress between a cracked section and an adjacent uncracked section than in a comparable beam with straight wires. This increased stress difference results in a large shear flow adjacent to the crack which may cause splitting along the wires.

By means of Eq. 10, developed in Section 5.3(b) the load corresponding to flexure-shear cracking was computed for all the draped beams which developed flexure-shear cracks. If the actual eccentricity of the draped wires at the location of the initiating crack is considered in computing the shear corresponding to the initiating cracking load, Eq. 10 will apply directly to beams with draped wires. The agreement of the test results and this equation are shown in Fig. 70. This figure is similar in construction to Fig. 66, discussed in Section 5.3(b). However, the ordinates of Fig. 70 represent the ratio of the net shear at inclined cracking, $V_n = V_c - V_d$, to the shear corresponding to web-shear cracking, V_s, so that the test results for web-shear cracks will fall along the line $V_n = V_s$. Similarly, the abscissa represents the ratio of the net shear corresponding to the formation of the initiating crack, $V_f - V_d$, to V_s, since initiating flexural cracks will occur before web-shear cracks if the term $V_f - V_d$ is less than V_s. The measured and computed values of the web-shear and the flexure-shear cracking loads for beams with draped wires are listed and compared in Table 9. The results of this comparison will be summarized in Section 5.3(e).

(d) Inclined Cracking Load of Beams Subjected to Moving Loads

A bridge beam is subjected to loads which move across the span from one end to the other. When the load acts near the ends of the span, high shears are produced and the web-shear type of crack may occur. When the load is near midspan, the shearing forces are lower but the combined effect of moments and shear is such that flexure-shear cracks can often develop. Consequently, both types of inclined cracks could occur in the same bridge beam. A beam with both web-shear and flexure-shear cracks is shown in Fig. 44(d).

For each section of a beam subjected to a moving load the web-shear cracking load can be computed by the procedure used to compute the cracking load for a beam with a stationary load. When the moving load comes onto or leaves the span, short a/h ratios exist, and a portion of shear in the short span is transferred to the supports by arch action. Allowance should be made for this in computing the web-shear load for sections near the supports.

Six web-shear cracks occurred in the tests of beams under moving loads, two each in beams CW.10.26 and CW.10.28 and one each in beams C.10.27 and C.10.28. The measured and computed cracking loads for these beams are tabulated and compared in Table 10 and are included in the comparisons made in Section 5.3(e).

The prediction of flexure-shear cracks in a beam loaded with a moving load is a more complex task since the zone in which flexural cracking occurs is longer than in a beam loaded with a single concentrated load. As the load moves away from the location of a given flexural crack, the crack tends to close; however, for a given load position, the number of flexural cracks which are open in a beam tested with moving loads is similar to the number of flexural cracks in a beam loaded at the same point with a single concentrated load. Equation 10, the empirical equation used to predict the flexure-shear cracking load for beams tested under stationary loads, was found to be sufficiently accurate in the case of beams loaded with moving loads.

A total of 25 flexure-shear cracks developed in beams B.10.23, B.10.24, BW.10.22, CW.10.26 and CW.10.27. The ratios of observed cracking load to predicted load for these cracks are listed in Table 10 and are discussed in the next section of this report.

(e) Comparison of Measured and Computed Values of Inclined Cracking Load

(1) Web-Shear Cracks. Web-shear cracks occurred in 21 beams included in this report and in 8 beams reported in Ref. 2. Most of these beams had straight wires and were loaded with stationary loads. Three web-shear cracks occurred in two beams with draped wires and a total of six web-shear cracks occurred in four of the beams loaded with moving loads. Sixteen beams had web reinforcement. The measured and computed values of the web-shear cracking loads for all the beams are listed in Table 7 and are summarized below. The web-shear cracking loads of the two beams with draped wires are listed in Table 9(a). In addition, the cracking loads for beams with stationary loads are included in Table 8(a).

Ratio of Measured to Computed Web-Shear Cracking Loads

	No. of Tests	Mean	Maximum	Minimum	Mean Deviation
I-Beams without Web-Reinforcement	15	0.99	1.21	0.74	0.091
I-Beams with Web-Reinforcement	15	1.07	1.19	0.82	0.060
Composite Beams	2	-	1.10	1.05	-
All beams	32	1.03	1.21	0.74	0.087

(2) Flexure-Shear Cracks. Flexure-shear cracks occurred in 61 beams described in this report and in 66 of the prestressed beams reported in Ref. 2. The majority of these beams had straight wires and were loaded with stationary loads. However, flexure-shear cracks occurred in 16 beams with draped wires and a total of 25 such cracks developed in 5 of the beams tested under moving loads. The measured and computed values of the flexure-shear cracking loads are given in Tables 8(a) and (b) for beams loaded with stationary loads and in Table 10 for beams loaded with moving loads. The results of all the tests are summarized in the following table.

Ratio of Measured to Computed Flexure-Shear Cracking Load

	No. of Cracks	Mean	Maximum	Minimum	Mean Deviation
Beams without Web Reinforcement					
Straight Wires, Fixed Loads	71	0.95	1.13	0.80	0.055
Draped Wires	12	1.03	1.19	0.81	0.091
Moving Loads (2 beams)	9	0.98	1.08	0.94	0.020
Beams with Web Reinforcement					
Straight Wires, Fixed Loads	52	1.03	1.33	0.89	0.064
Draped Wires	5	1.05	1.09	1.01	0.024
Moving Loads (3 beams)	11	0.97	1.07	0.88	0.044
All Beams	160	0.99	1.33	0.80	0.069

5.4 Flexural Strength

The maximum moment a beam can resist is that corresponding to its flexural capacity and for this reason, no amount of web reinforcement can increase the strength of a beam beyond this limiting value. It is important, therefore, to know this value in evaluating the effects of the web reinforcement in the test beams and in designing web reinforcement for prestressed concrete beams.

(a) Assumptions

The analysis of the flexural strength is based on the following assumptions:

1. Concrete is assumed to crush in flexure at a limiting strain of 0.004. The strains measured at crushing are plotted in Fig. 47 for all of the beams in this test series.

2. The steel and concrete strains are assumed to be linearly distributed over the depth of the beam. Measurements of concrete and steel

strains have shown that although the strains in the compression zone are linearly distributed, the tensile strains in the steel are generally less than the value corresponding to a linear distribution of strains. Analytical studies have shown, however, that the error in ultimate moment introduced by this assumption is small (6). It is necessary to consider the effects of the non-linear strain distribution in computing deflections and steel stresses.

3. The average stress in the concrete is assumed to be defined by the following equation, derived in Ref. 6.

$$f_{cu} = \frac{f'_c}{0.8 + 0.0001 f'_c} \qquad (12)$$

4. The ratio, k_2, of the depth to the centroid of the compression force to the overall depth of the compression zone is assumed to be $k_2 = 0.42$.

5. No tension is resisted by the concrete.

6. The stress-strain curve for the reinforcement is known.

(b) Analysis

The ultimate moment, M_u, of a beam failing in flexure or a beam failing in shear-compression can be expressed by the following equation.

$$M_u = A_s f_{su} d (1 - 0.42 k_u) \qquad (13)$$

where:

A_s = total area of longitudinal reinforcement

f_{su} = stress in longitudinal reinforcement at failure of beam

d = effective depth of the longitudinal reinforcement

k_u = ratio of neutral axis depth at failure to effective depth.

In evaluating the steel stress, f_{su}, a definite relationship is assumed to exist between the strains in the concrete and the steel. In the most general form, the distribution of stresses and strains across the

depth of the section of failure is similar to that shown in Fig. 71. At failure, the maximum strain in the concrete is ϵ_u, assumed to be 0.004, and the depth of the compression zone can be expressed as $k_u d$. For a non-prestressed beam, the strain in the steel at failure is expressed as:

$$\epsilon_{su} = \epsilon_{sa} = F\epsilon_u \left[\frac{1 - k_u}{k_u}\right] \tag{14}$$

where:

ϵ_{su} = steel strain at ultimate

ϵ_{sa} = steel strain due to flexure

ϵ_u = limiting strain in concrete

F = strain compatibility factor

The strain compatability factor, F, is close to unity for flexural failures of well bonded beams, but may be greater or less if the strains are not linearly distributed. In the analysis of the flexural strength of the beams reported in this paper, F was assumed equal to unity.

Equation 14 for the steel strain at failure may be modified to apply to beams with prestressed reinforcement by adding to the right hand side terms for the strain corresponding to the effective prestress and the compressive strain in the concrete at the level of the steel. The modified equation is:

$$\epsilon_{su} = \epsilon_{sa} + \epsilon_{se} + \epsilon_{ce} \tag{15}$$

or

$$\epsilon_{su} = F\epsilon_u \left[\frac{1 - k_u}{k_u}\right] + \epsilon_{se} + \epsilon_{ce} \tag{16}$$

where:

ϵ_{se} = steel strain corresponding to effective prestress

ϵ_{ce} = concrete strain at level of longitudinal reinforcement due to the effective prestress.

From the equilibrium of forces parallel to the axis of the beam, it can be shown that:

$$k_u = \frac{pf_{su}}{f_{cu}} \tag{17}$$

where:

p = longitudinal reinforcement ratio

f_{cu} = average concrete stress in the compression zone at failure, as defined by Eq. 12.

The steel stress at failure can be determined by a trial and error procedure using Eqs. 16 and 17, and the stress-strain curve of the steel. When the resulting values of f_{su} and k_u are substituted into Eq. 13 it is then possible to compute the ultimate moment capacity of a given beam.

If the neutral axis of an I-beam fell in the upper flange, the ultimate moment was not affected by the presence of the web. In a number of I-beams, however, the neutral axis was in the web, thus reducing the compression zone below that which would exist in a rectangular beam of similar dimensions. In analyzing these beams, the portions of the flange projecting from the web were assumed to be stressed to a constant stress of f_{cu}. It was then possible to compute the ultimate moment by assuming a value of f_{su}, assigning a certain amount of reinforcement to act with the flanges, and analyzing the web and the portion of the flange above the web as a rectangular beam reinforced with the remainder of the longitudinal steel. The value of f_{su} corresponding to this distribution of steel was then computed by the procedure described above for rectangular beams. In several trials, the assumed initial value of f_{su} and the value determined from this analysis converged and the resulting value of the steel stress was used to compute the flexural capacity of the beam. As a further simplification, the flange was assumed to be rectangular with a thickness equal to the average of the maximum and minimum thicknesses.

(c) Measured and Computed Quantities

The measured and computed values of the ultimate moment are tabulated and compared in Table 11. The mode of failure, either shear, flexure or transition is denoted by the letters S, F or T, respectively. The computation of M_{us}, the ultimate moment corresponding to a shear failure, is discussed in Section 5.5.

For the 45 beams failing in flexure listed in Table 11, the agreement between the measured and computed ultimate moments is excellent. The results of this comparison are summarized in the following table.

Ratio of Measured to Computed Ultimate Moment for Flexural Failures

	Mean	Maximum	Minimum	Mean Deviation
Neutral Axis in Flange	1.00	1.07	0.86	0.028
Neutral Axis in Web	0.99	1.03	0.92	0.026
All Beams	1.00	1.07	0.86	0.027

The agreement between the measured and computed steel stresses listed in Table 11 is not as good as for the ultimate moments. The average measured stress was about 95 percent of the computed value. While this is not a significant error in terms of stresses, a five percent decrease in f_{su} would require as much as a 45 percent decrease in ϵ_{sa}, the flexural strain in the steel. Thus, while we have assumed the strain concentration factor, F, to be unity, the actual value of F in the tests was often much lower.

5.5 Shear Strength of Prestressed Concrete Beams with Web Reinforcement

A prestressed concrete beam is designed to support a given load and its properties are limited in such a way by design specifications that the behavior of the beam will not be undesirable. Both the design procedure and the specifications are based on the assumption that the beam will fail

in flexure. If, however, an inclined crack occurs in a beam without web reinforcement, the beam will fail in shear with less than the desired factor of safety and much less than the desired ductility. By adding a sufficient amount of web reinforcement to such a beam, it is possible to restrain the opening of the inclined cracks and change the mode of failure from shear to flexure.

The effect of web reinforcement on the ultimate strength of a prestressed beam is considered in this section. Section 5.5 is divided into three main parts. In Section 5.5(a), two shear failure mechanisms are examined from a rational standpoint. In Section 5.5(b), an empirical expression is developed for the strength of beams with web reinforcement. Finally, in Sections 5.5(c) through (f), this expression is compared to test results and is applied to beams with draped wires and beams tested under moving loads.

(a) Qualitative Discussion of the Effect of Web Reinforcement on the Strength of Prestressed Concrete Beams

Shear failures occur in a number of different ways, the principal failure mechanisms being by crushing and distortion of the web of the beam and by shear-compression. The location of the actual failure and the manner in which failure occurs differs considerably for these two modes. Web-distortion failures occur by cracking of the top flange at a point close to the reaction and subsequent crushing of the web under this crack, while shear-compression failures occur by crushing of the compression zone at the upper end of an inclined crack close to the load. Generally, the former type of failure is an outgrowth of web-shear cracks while the latter generally results from flexure-shear cracks. Although it is not possible to place all shear failures in either one group or the other, or to say that a given type

of inclined crack will always result in a given mode of failure, these two types of shear failures will be considered separately when discussing the effect of web reinforcement.

Although shear failures may also occur by separation of the tension flange from the rest of the beam or by fracture of the stirrups, these modes of failure will not be discussed extensively in this section. The presence of web reinforcement prevents the spread of cracks which would otherwise separate the flange from the rest of the beam. Similarly, if the stirrups are made of a ductile metal with a well defined yield point, the large inelastic strains required to break the stirrup wire rule out fracture of the stirrups as a practical mode of failure. This is especially true if enough stirrups are provided to ensure a flexural failure.

(1) Web-Distortion Failures. No matter how an inclined crack forms, it causes a major redistribution of the stresses in its vicinity as shown in Fig. 72. The amount of redistribution that occurs depends on the shape of the inclined crack, the amount of web reinforcement crossing the inclined crack, and the stresses in the beam before the inclined crack forms.

To gain a clear understanding of the stresses in a beam with an inclined crack, consider first a beam without web reinforcement as shown in Fig. 72(a) neglecting the effects of the dowel action of the longitudinal reinforcement crossing the crack. After an inclined crack forms, horizontal shearing stresses can no longer be transferred across the web and, as a result, the magnitude of the compression and tension forces must remain constant along the full length of the inclined crack. For the moment to vary along the length of the shear span, the length of the moment arm must vary and, thus, the compression thrust line shifts to the position shown in Fig. 72(a). When this occurs, the load carrying mechanism within the beam

is said to have changed from "beam action" in which the compression and tension forces are parallel but vary in magnitude to bring a variation in the internal moment, to "tied-arch action" in which the compression and tension forces are constant in magnitude but vary in their distance apart to bring about the necessary variation in moment in the shear span.

The change from beam action to arch action occurs in all beams with inclined cracks. If these cracks extend over a large part of the length of the shear span, the location of the compression thrust line will have a large eccentricity with respect to the centroid of the concrete above the crack at a section near the reaction, as for example, Section AB in Fig. 72(a). The concrete above the crack acts as an eccentrically loaded plain concrete column or "arch rib", developing tensile stresses at the top surface and compression stresses in the web. The presence of tensile stresses at the top of the beam in the shear span has already been discussed in Section 44 and is illustrated by the deflection-strain curves shown in Fig. 46.

If these tensile stresses reach the tensile strength of the concrete, the arch rib will fail by cracking at the top of the beam followed by crushing of the web under this crack. This type of failure, designated as a "web-distortion" or "web-crushing" failure, is sudden and complete as shown in Fig. 43(b) and 51(c). In beams without web reinforcement, web distortion failures occur at a load only slightly greater than the inclined cracking load. In a number of beams, a failure resembling a web-distortion failure appeared to be initiated by crushing of the compression zone in the vicinity of the load point. In a number of such cases, the crushing was associated with an imminent flexural failure.

In drawing the compression thrust line in Fig. 72(a) it was assumed that there was no transfer of shearing force across the inclined

crack, either by web reinforcement or by dowel action of the longitudinal reinforcement crossing the crack, and as a result the compression thrust line is in its lowest possible position.

There is a twofold effect of transferring a shear force across an inclined crack by stirrups or dowel action. The presence of shear in the portion of the beam below the inclined crack gives rise to a moment in this portion which, at any section, resists some of the applied moment acting on that section. As a result, the compression thrust line rises to a new position more nearly parallel to the longitudinal reinforcement. At the same time, the magnitude of the thrust is reduced. The danger of a web-distortion failure is therefore reduced because the eccentricity of the thrust line with respect to the centroid of the arch rib is reduced and because the magnitude of the compression force acting on the arch rib is also reduced.

In a beam without web reinforcement, a certain amount of shear will be transferred across the inclined crack by dowel action of the longitudinal reinforcement, the actual moment being a variable and unreliable quantity. If no doweling force existed, the portion of the beam below the crack would not deflect and as a result there would be a "fault" in the longitudinal steel where it crosses the inclined crack as shown by Fig. 72(b). Since such a "fault" did not exist in the beams tested, some shear must be transferred across the inclined crack by dowel action. This was especially true in the 26 beams of this series in which the major inclined crack was a web-shear crack which never completely penetrated the lower flange.

The magnitude of the dowel force is extremely difficult to determine since it depends on such factors as the stiffness of the arch, of the portion of the beam below the crack, and of the reinforcement crossing

the crack. These factors are very difficult to evaluate even if the shape of the inclined crack is known. In addition, the doweling force often tends to destroy itself. As a result of the vertical tensile stresses induced between the web and the lower flange by doweling, horizontal cracks were observed in this region in many beams without web reinforcement and the presence of these cracks reduced the amount of doweling force which could be transferred. In the beams in which the inclined crack did not penetrate completely through the lower flange, the doweling force acted to extend the inclined crack toward the lower flange, thus reducing the concrete area available to transfer the doweling force.

Thus, while the doweling force may play a significant role in carrying the shear force in a prestressed concrete beam without web reinforcement, the magnitude of this force is variable and is not dependable. In beams with web reinforcement, the shear transferred by doweling is relatively unimportant since the shear transferred across the inclined crack by the web reinforcement deflects the portion of the beam under the inclined crack, thus reducing the magnitude of the "fault" which would occur where the longitudinal reinforcement crosses the crack. In the analysis of beams with web reinforcement, therefore, the doweling force is assumed to be negligible. This assumption is probably close to the truth for beams with flexure-shear cracks but may err on the conservative side for beams developing web-shear cracks which do not penetrate the lower flange.

Web reinforcement is placed in a prestressed concrete beam to increase the shear strength of the beam and make its behavior more desirable at high loads. There are two principal effects of such web reinforcement: it transfers shear across the inclined crack, improving the position of the

thrust line within the arch rib above the crack as shown in Fig. 72(c); and, at the same time, it restrains the opening of the crack, thus reducing the concentration of compressive strains above the upper end of the inclined crack. The first of these effects is more important in considering web-distortion failures. The second effect of web reinforcement, that of reducing the strain concentrations above the end of an inclined crack is more important in relation to shear-compression failures and will be discussed later in this section.

In a beam which otherwise would develop a web-distortion failure, web reinforcement transfers shear across the inclined crack and in doing so changes the location of the compression thrust line as shown in Fig. 72(c). As explained above, a part of the moment change along the horizontal projection of the inclined crack is resisted by the portion C, below the crack, acting as a "cantilever". To satisfy statics, the compression thrust need not be as large, and its line of action is more nearly parallel to the longitudinal reinforcement if web reinforcement is present in a beam. At each stirrup, the thrust line is bent through the angle resulting from the addition of the vectors representing the compression thrust and the shear force transferred by that stirrup. If the shear transferred across the inclined crack by the stirrups does not keep the thrustline far enough above the crack, a beam with web reinforcement will fail in shear. In such a case, the stirrups will usually yield and sometimes fracture.

In addition to transferring a vertical tension force across the crack, it is probable that the stirrups also transmit a horizontal dowel force because of the nature of the relative displacements of the arch rib and the portion of the beam below the crack. The over-all result of this dowel action is to restore beam action by moving the thrust line upward slightly.

If it were possible to know or estimate the length, shape, and height of the inclined cracks; the distribution of normal and shearing stresses on the sections at each end of the inclined crack; and the stresses in the stirrups at failure, it would then be possible to compute the web-distortion failure load for beams with and without web reinforcement. Such a computation would be based on the further assumption that the beam would fail when the eccentrically loaded "column" or "arch rib" above the crack developed flexural tension cracks in its top surface. This analysis of the ultimate strength is not presented here because of the large number of major variables which must be assumed and which could not be checked from the test data.

From this concept of the behavior of a beam failing in shear it can be seen that if the horizontal projection of the inclined crack is less than about one-half the length of the shear span, the eccentricity of the thrust line with respect to the centroid of the arch-rib above the crack is not sufficient to cause failure of this section. Thus, if the inclined crack originates as a flexure-shear crack, a web-distortion failure is not apt to occur unless splitting develops along the longitudinal reinforcement.

(2) Shear-Compression Failures. Beam action is destroyed in the shear spans of a beam after inclined cracks form and, as previously explained, the beam then carries load as a "tied-arch". In addition to failure of the arch rib under the eccentric thrusts which exist after inclined cracking, the tied arch structure will fail if excessive angle changes occur in the concrete above the inclined crack.

The inclined cracks penetrate closest to the top of the beam under the load points and, as a result, the arch rib is most flexible in this region. When the structure is loaded, the steel strains which occur along the entire horizontal projection of the inclined crack contribute to angle

changes occurring in this rather limited region of the compression flange. Thus, a small increase in steel strain over the projection of the crack is accompanied by a proportionately larger increase in concrete strain in the compression zone over the crack and when the concrete strains reach a limiting value, crushing occurs, destroying the beam. This type of failure is known as a "shear-compression failure".

Although the distribution of strains is not linear after inclined cracking, shear-compression failures occur in essentially the same way as flexural failures. In Section 5.4 and in Fig. 71, the distribution of strains across the depth of a beam failing in flexure is discussed and used as the basis of a trial and error procedure to determine the flexural capacity of prestressed concrete beam.

In computing the strength of a beam failing in shear-compression, it is again assumed that there is a definite relationship between the concrete and steel strains. This relationship is complicated by the fact that there is a great change in the strain compatibility factor, F, at the time of inclined cracking. During the flexural cracking stage prior to inclined cracking, strains are essentially linearly distributed and in most cases the compatibility factor is unity or close to it. After inclined cracking, however, the strains are no longer linearly distributed and the compatibility factor is considerably less.

Referring to Fig. 73(a), the steel strain in a prestressed concrete beam immediately prior to inclined cracking may be expressed as

$$\epsilon_{sc} = \epsilon_{se} + \epsilon_{ce} + \epsilon'_{sc} \qquad (18)$$

where ϵ'_{sc} = steel strain due to flexure at inclined cracking load.
Equation 18 can be written as:

$$\epsilon_{sc} = \epsilon_{se} + \epsilon_{ce} + F_1 \epsilon_{cc} \left[\frac{1-k_c}{k_c}\right] \tag{18a}$$

At ultimate, as shown in Fig. 73(b), the steel strain is:

$$\epsilon_{su} = \epsilon_{se} + \epsilon_{ce} + \epsilon'_{sc} + \epsilon'_{sa} \tag{19}$$

where ϵ'_{sa} = steel strain developed between inclined cracking and ultimate. Equation 19 can be expanded to the form:

$$\epsilon_{su} = \epsilon_{se} + \epsilon_{ce} + F_1 \epsilon_{cc} \left[\frac{1-k_c}{k_c}\right] + F_2 (\epsilon_u - \epsilon_{cc}) \left[\frac{1-k_u}{k_u}\right] \tag{19a}$$

Equation 19(a) and Eq. 17 can be solved to yield a steel stress, and the beam strength can be determined if F_1, F_2, k_c, k_u, f_{cu}, ϵ_{cc} and ϵ_u are known. The value of f_{cu}, ϵ_u and k_2 assumed in Section 5.4 in the analysis of flexural strength can be used in analyzing the strength of beams with inclined cracks. The depth to the neutral axis at the inclined cracking load, expressed by $k_c d$, will be assumed to be the same as that at ultimate, expressed by $k_u d$ and thus, $k_c = k_u$. In addition, it is assumed that $F_1 = 1.0$, such that a linear distribution of strains exists before inclined cracking. Based on these assumptions, Eq. 19(a) can be rearranged and simplified to the following form.*

$$\epsilon_{su} = \epsilon_{sc} + F_2 \left[\epsilon_u \left(\frac{1}{k_u} - 1\right) - \epsilon'_{sc}\right] \tag{20}$$

The value of the steel stress at inclined cracking can be determined from Eq. 21 using the cracking shear, V_c, computed from Eq. 10.

$$f_{sc} = \frac{V_c a}{A_s d(1-0.42\, k_u)} \tag{21}$$

---

*The various steps in deriving Eq. 20 are outlined in Ref. 2.

The ultimate steel stress can be determined by a trial and error procedure from Eq. 20 and 21 provided that the stress-strain curve for the steel, the ultimate concrete strain, and the value of the compatibility factor, F_2, are known or assumed. Once the steel stress is computed, the ultimate moment corresponding to a shear-compression failure can be computed from Eq. 13.

The major variable in the analysis presented above is the value of F_2, the strain compatibility factor which relates the concrete and steel strains after inclined cracking. The effect of variations in the value of F_2 on the ultimate strength of a beam is shown in Fig. 74. The curve in this figure describes a typical stress-strain relationship for prestressing wire.

In a moderately reinforced beam, the ultimate moment varies almost directly with the steel stress at ultimate (see Eq. 13). As a result, variations in the ultimate capacity of a beam can be discussed in terms of the steel stresses developed at failure. The various strain quantities in Eq. 19 are marked on this figure by the letters A, B, C, and F. The points on the curve corresponding to the prestrain, ϵ_{se}, and the compressive strain at the level of the longitudinal steel, ϵ_{ce}, are marked A and B, respectively. Point C in Fig. 74 refers to ϵ_{sc}, the total steel strain at the time of inclined cracking. The value of this strain is given by Eq. 18 and is similar for beams with and without web reinforcement.

After inclined cracking, the value of the strain compatibility factor, F_2, is a function of how much the opening of the inclined cracks is restrained by stirrups crossing the crack and the height to which the inclined crack extends. The points on Fig. 74, indicated by the letters F show the effect of various values of the strain compatibility factor F_2

on the steel stress at failure. If stirrups are present, they act to restrain the opening of the inclined cracks and distribute the angle changes over a greater length of the top flange, thus limiting the strain concentrations which can develop at the end of the crack. In addition, stirrups act to limit the height to which the inclined cracks develop and thus affect the value of k_u at failure. Since both of these actions tend to restore the linearity of strains, the presence of stirrups tends to increase F_2. If enough stirrups are provided, the steel and concrete strains at failure will be related almost linearly, and the strain compatibility factor F_2 will approach a value of 1.0, representing a linear strain distribution. This value of F_2 corresponds to a flexural failure and the maximum ultimate steel stress which can be developed in the beam. This condition is shown in Fig. 74 by the point $F_{1.0}$(for $F_2 = 1.0$).

On the other hand, F_2, may be as low as 0.10 or less if no web reinforcement is provided, and in this case the steel strain developed after inclined cracking is only a tenth as great as that occurring in a flexural failure. The ultimate steel stress corresponding to $F_2 = 0.1$, shown by $F_{0.1}$, is much less than that for $F = 1.0$ and as a result the ultimate moment is less than that for a flexural failure. As F_2 is increased, the total strain at ultimate will reach and exceed the yield strain of the prestressing wire. The rate of increase in ultimate steel stress and ultimate moment is high up to about $F_2 = 0.1$, but above a value of $F_2 = 0.3$, there is relatively little increase. Points representing $F_2 = 0.3$ and 0.5 are shown in Fig. 74 by the letters $F_{0.3}$ and $F_{0.5}$.

Values of F_2, the strain compatibility factor after inclined cracking, were computed for all of the test beams which failed in shear-compression. Since the strain and crack height data were not sufficiently

complete to allow a direct evaluation of F_2, this quantity was computed indirectly from load measurements made during the tests. The derivation of the compatibility factor was based on Eq. 20 and the idealized conditions of strain and stress shown in Fig. 73. Equation 20 can be rewritten as follows:

$$F_2 = \frac{\epsilon_{su} - \epsilon_{sc}}{\epsilon_u(\frac{1}{k_u} - 1) - \epsilon'_{sc}} \qquad (22)$$

All the quantities on the right hand side of Eq. 22 except ϵ_{su} were derived or assumed in accordance with the assumptions made in Section 5.4. The actual steel strains measured at cracking and at ultimate and the corresponding stresses were used. The ratio k_u was derived using Eq. 17 in which the average concrete strength was assumed to be that given by Eq. 12. The limiting concrete strain, ϵ_u, was assumed to be 0.004. The data pertinent to this assumption are shown in Fig. 47 and are discussed in Section 4.4(b). The term ϵ'_{sc} was obtained by subtracting the sum of ϵ_{se} and ϵ_{ce} from ϵ_{sc}.

Studies of the test data indicated that the compatibility factor F_2 was a function of the total force in the stirrups crossing a given inclined crack. In Fig. 75, values of the strain compatibility factor F_2 derived by the above analysis are compared to the total stirrup force $nA_v f_y$ crossing an inclined crack of length 1.5 x, where n is the number of stirrups crossing the assumed crack and x is given by Eq. 10. The line shown in this figure was fitted to the points by observation. Based on this line, it appears that the increase in F_2 is proportionately less for small amounts of web reinforcement than for large amounts. This trend is offset by the fact that the increase in the failure load is proportionately larger for small increases in F_2 than for large increases, as shown in

Fig. 24, and as a result the increase in ultimate load is nearly proportional to the shear transferred across the inclined crack by the stirrups.

(3) Limitations on the Effectiveness of Web-Reinforcement. The flexural capacity represents an upper limit on the strength which can be developed by a beam with web reinforcement and, clearly, no amount of web reinforcement can increase the strength of a beam beyond this value. A number of other limits on the effectiveness of web reinforcement are suggested by the analyses discussed above.

In a beam with web reinforcement, the stirrups transfer shearing forces across the inclined cracks which develop. These shearing forces act on the portion of the beam below the crack which acts as a "cantilever" fixed under the load point as shown in Fig. 72(c). Taking moments about the longitudinal reinforcement and assuming that no forces act on the cracked surface it can be seen that a compressive force is necessary below the crack for moment equilibrium of the cantilever. If the web is very thin and there is a large amount of web reinforcement, the primary cause of failure could be crushing of the concrete under the inclined crack in the zone D. The upper limit on the moment which can be carried by the "cantilever" corresponds to its compression failure moment, and thus, the moment about the end of the cantilever of the stirrup forces crossing the inclined crack should be less than the compression failure moment for that section.

Ratios of the stirrup moment, based on the estimated ultimate stirrup stress, to the compression failure moment, assuming a beam with a width equal to the web thickness and a depth equal to the effective depth minus the thickness of the upper flange, range from 0.02 to 1.04. After failure, crushing was observed under the inclined cracks in six beams (CW.13.28,

CW.14.35, CW.14.39, CW.14.51, CW.14.54, and the short span of CW.28.28). In these beams the ratio of stirrup moment to the web strength ranged from 0.46 to 1.04. However, all of these beams failed at loads close to those predicted in Section 5.5(c) and the crushing under the crack was probably secondary.

An examination of the strain conditions at failure shows that if the angle change in the upper flange required to produce the limiting strain in the concrete over the end of the crack is greater than that required to produce the limiting strain at the top of the "cantilever", it is conceivable that this type of failure could occur. In Fig. 72(c) the depth to the neutral axis of the cantilever corresponding to a compression failure of the cantilever is greater than the depth of the compression flange above the load and in this case, the necessary rotations are possible.

One upper limit on the effectiveness of web reinforcement is thus the flexural capacity of the web below the crack. This type of failure is especially serious in beams with thin webs and high values of Q.

Another limitation on the efficiency of the stirrups is defined by the crushing strength of the web under the inclined thrusts which exist in the "compression rods" between the inclined cracks in the web. This type of failure differs from a web-distortion failure in that a web-distortion failure is initially caused by the formation of tensile cracks at the top of the beam while this type of failure occurs by crushing of the compression rods at the junction of the rods and the upper flange. Two theories have been proposed to predict the strength of beams which develop this type of crushing. The first of these*, assumes that the inclined cracks radiate

---

*This theory was described in a letter from Y. Guyon to Professor C. P. Siess dated March 11, 1959.

from the load with a compression rod extending from the load to the bottom of each stirrup and states the strength of the web in terms of the strength of these rods. The second method of computing the crushing strength of the web is to assume that the web acts as a "compression-field beam" similar in behavior to the tension-field beams used in aircraft structures (11). Since this type of failure did not occur in this test series, these analyses could not be checked. Crushing of the compression rods in the web would only occur in short deep shear spans with very thin webs.

Tests of reinforced concrete beams reported by Hognestad and Elstner (12) indicated an upper limit to the shear strength of beams with vertical stirrups. For the beams in this test series, however, there was no apparent upper limit on the effectiveness of the stirrups in a prestressed concrete beam. For very small amounts of web reinforcement, the efficiency of the web reinforcement appeared to decrease as shown in Fig. 75. The minimum ratio of web reinforcement, $r = A_v/bs$, in this test series was 0.041 percent based on the total number of stirrups crossing the last crack to form in the long span of beam CW.28.26. This crack opened rapidly but the beam did not fail at this location. The ACI-ASCE Tentative Recommendation for Prestressed Concrete (13) requires a minimum web reinforcement ratio of $r = 0.25\ b'/b$ percent, which for beam CW.28.26 would be 0.073 percent.

(b) Quantitative Discussion of the Effect of Web Reinforcement on the Strength of Prestressed Concrete Beams

In the previous section, the strength of prestressed concrete beams with web reinforcement was discussed qualitatively and analyses based on observed modes of failure were presented for the two types of shear failure which are most likely to occur in prestressed concrete beams. Since the

determination of the actual conditions of stress and strain in a beam failing in shear involved assumptions about the behavior of the beam which may never be sufficiently accurate to justify the use of these analyses, the determination of the ultimate capacity of the beams in this test series has been approached on an empirical level.

The contribution of web reinforcement to the shear strength of a prestressed concrete beam can be considered in a number of different ways. Figure 76(a) shows a portion of a beam without stirrups. At failure, equilibrium for this beam can be expressed by Eq. 23 where it is assumed that the ultimate moment capacity of a beam without stirrups is equal to M_c, the inclined cracking moment.

$$V_{conc.}\, a = Cjd = M_c \tag{23}$$

If stirrups are added to the beam as shown in Fig. 76(b), the following equilibrium equations can be written

$$V_u = V'_{conc.} + V_v \tag{24}$$

$$M_u = V_u a = C' jd + V_v z \tag{25}$$

where: $V'_{conc.}$ = ultimate shear carried by the compression zone over the inclined crack in a beam with web reinforcement

V_v = ultimate shear carried by the stirrups = $A_v f_y\, z/s$

z = horizontal projection of the inclined crack

s = spacing of the stirrups

A_v = cross-sectional area of one stirrup

f_y = yield stress corresponding to one percent strain in the stirrup steel

C' = ultimate compression force carried by the compression zone over the inclined crack in a beam with web reinforcement.

Several assumptions may be made to simplify these equations. If C' is assumed equal to C, Eq. 25 may be written as:

$$M_u = M_c + V_v \, z/2 \tag{26}$$

By rearranging Eq. 26, it can be shown that for this assumption the shear carried by the concrete above the crack is less at ultimate in a beam with web reinforcement than in a beam without. Computed values of the ratio $(V_v \, z/2)/(M_u - M_c)$ based on the stirrups crossing the observed inclined cracks in the beams tested ranged from 0.17 to 1.38 with over half the values less than 0.50. Similar results are mentioned by Laupa, Siess and Newmark (10). Thus, Eq. 26 is not correct and C' must be greater than C.

Another assumption which could be used to simplify Eq. 24 and 25 would be that the shear carried by the compression zone above an inclined crack is the same whether stirrups are present or not. Eq. 24 can be written as:

$$V_u = V_{conc.} + V_v \tag{27}$$

where:

$$V_{conc.} = \frac{M_c}{a} \tag{28}$$

The value of C' at failure may be written as:

$$\frac{M_c + V_v \, (a - z/2)}{jd} = C' \tag{29}$$

Equation 29 implies that C' will be larger in a beam with web reinforcement than in a beam without web reinforcement. Observations of the inclined cracks showed that in general the depth of the compression zone over the crack increased when web reinforcement was added to a beam, thus making possible an increase in the force C'.

The difference between the ultimate shear and the shear corresponding to inclined tension cracking was found to be by far the most significant variable governing the amount of web reinforcement necessary to prevent a shear failure, and the following empirical expression relating these two variables was found:

$$V_u - V_c = 1.1\, A_v f_y \frac{d}{s} \qquad (30)$$

where: V_u = ultimate shear corresponding to flexural failure

V_c = shear corresponding to the inclined cracking load

d = effective depth of the beam

s = spacing of the stirrups

A_v = cross sectional area of one stirrup

f_y = yield stress, stress corresponding to one percent strain in the stirrup steel.

Equation 30 can also be written as follows:

$$r f_y = \frac{V_u - V_c}{1.1\, bd} \qquad (30a)$$

where: $r = A_v/bs$ = web reinforcement ratio based on flange width

b = flange width

Equation 30a is represented graphically in Fig. 77 and is compared with the observed data. It must be pointed out that Eq. 30a represents the locus of the points corresponding to balanced failures. Points corresponding to shear failures with less than the balanced amount of web reinforcement can lie to the left of that line but not far away from it. Points corresponding to flexural failures must be to the right of the plotted line. The distance such a point falls to the right of this line depends on the amount by which the web reinforcement is over-designed. A number of the

points representing shear failures fall considerably to the right of the line. This error was due, in part, to the assumption that the number of stirrups crossing the critical inclined crack was directly related to rf_y. In beams with large stirrup spacings or in beams in which the first stirrup was placed under the load point (Stirrup Arrangement 2, Fig. 15) the number of stirrups crossing the inclined crack was often less than implied by the nominal value of rf_y. For these beams, an effective value of rf_y based on the number of stirrups crossing an assumed inclined crack was computed using Eq. 31.

$$(rf_y)_{eff} = \frac{n A_v f_y}{1.5 x b} \qquad (31)$$

where: 1.5 x = assumed horizontal projection of the inclined crack, x given by Eq. 9.

n = number of stirrups crossing the assumed inclined crack for a given stirrup arrangement.

The data plotted in Fig. 77 have been replotted in Fig. 78 in terms of $(rf_y)_{eff}$. There is reasonable agreement between the plotted line and the test data.

The empirical coefficient, which is 1.1 in Eq. 30, presumably includes a term to relate the horizontal projection of the inclined crack to the effective depth, d, and also allows for the variations in the actual stress in the stirrups crossing the crack since some of the stirrups near the ends of the inclined crack may not be stressed to the yield point.

The relationship between the web reinforcement index, rf_y and the corresponding increment in total shear beyond inclined cracking is shown in Fig. 79. The abscissa represent the ratio between the nominal

value of rf_y corresponding to the stirrups actually present in each beam and the quantity $(rf_y)_{bal.}$ computed from Eq. 30 for a balanced shear and flexural failure. The ratios plotted as ordinates have in the numerator the difference between the observed shear at failure and the computed shear at inclined cracking, and in the denominator the difference between the computed shears at flexural failure and inclined cracking. By definition, any value of the ratio $(rf_y)/(rf_y)_{bal.}$ greater than 1.0 should refer to a flexural failure and should correspond to an ordinate equal to 1.0. The horizontal line on the figure represents the locus of the predicted flexural failures while the 45 deg. line represents the locus of the shear failure loads as predicted by Eq. 30.

In studying the scatter of the points in Fig. 79, it is important to note that the magnitude of the ordinates depends on the difference between the shear at failure and the shear at cracking. Since the difference between these quantities is small, any experimental error in the observed shear at failure will be magnified in this expression. In spite of this, the scatter is not great and in general the points lie close to the lines drawn on this figure.

Nine beams with ratios of $(rf_y)/(rf_y)_{bal.}$ greater than 1.0 developed either shear failures or transition failures.* In beam BW.14.60, the inclined crack appeared to follow a horizontal plane of weakness through the web, presumably along the joint between the two batches of concrete. The unusual shape of this crack greatly enhanced the conditions necessary for a web distortion failure and this type of failure ultimately occurred. The failure of beam CW.14.35 resembled a flexural failure and apparently was not

*In the order in which they will be discussed, these beams were: BW.14.60 and CW.14.35; BW.14.45, BW.14.58, and CW.14.21; CW.14.23, CW.14.47, CW.14.50, and CW.28.26s. The ratios of $(rf_y/rf_y)_{bal.}$ for these beams were respectively, 1.10, 1.37, 1.77, 1.14, 1.11, 1.23, 1.05, 1.46 and 1.15.

influenced by any inclined crack. This failure was classified as a transition failure because it took place outside the flexural span at a point where the bending moment was less than a maximum. It is conceivable that an unusually weak spot in the concrete triggered the failure at this location. This is borne out by the fact that the inclined crack formed in the region of the failure at a load less than that predicted.

The failure load for the remaining seven beams in which the mode of failure was predicted incorrectly ranged from 98 to 104 percent of the predicted flexural failure load and are classified as shear or transition failures primarily on the appearance of the beam after failure. These beams fall into two groups:

1. Failures resembling shear-compression failures occurred in three of these beams. First crushing developed near the load point in a region affected by both inclined cracks and flexural cracks.

2. Failures resembling web distortion failures occurred in the other four beams. These failures were preceded by a varying amount of crushing under the load point which may have triggered the web-distortion failure, and the final failure was sudden and destructive. Failure loads ranged from 90 to 98 percent of the computed shear strength.

The data used to derive Eq. 30 were obtained from tests of beams which were essentially similar in most respects. All the beams were 6 by 12 in. in overall cross section, and the web thickness varied from 0.3 to 1.0 times the flange width. The effective depth, d, varied from 8 to 11 in. and the ratio a/d varied from 2.8 to 7.8. The prestress level and concrete strength were both varied over a wide range. The yield stress of the stirrups varied from 34.0 to 79.5 ksi, and the stirrup spacing varied from 2.25

to 10.5 in. In addition, the shear was practically constant throughout the shear spans of the beams tested, since the dead load shear was negligible in comparison to the live load shears.

In some of the beams with 70 or 78-in. shear spans, the stirrup spacing was not constant throughout the length of each shear span. The stirrup design procedure for these beams was similar to that used in designing stirrups in the beams tested under moving loads as described in Section 5.5(e). In this procedure it is assumed that all sections subjected to inclined cracking should fail in shear at the load corresponding to flexural ultimate. Stirrups were provided for the difference between the inclined cracking shear and the ultimate shear at each section. As shown in Figs. 18 through 21 there were no stirrups in at least a third of the span in some of these beams. However, since no inclined cracks occurred in these regions in the tests, no stirrups were necessary. In calculating the ultimate capacity of the stirrups, the stirrup spacing adjacent to the load was considered to govern.

Two of the six beams with non-uniform stirrup spacings failed in shear at 102 and 105 percent the predicted shear capacity. In Fig. 85(a), the efficiency of the web reinforcement in these two beams is compared to the efficiency of the uniformly spaced stirrups in beams failing in shear. On the basis of the six beams with variable stirrup spacings, it appears that a variable stirrup spacing is as efficient as a uniform spacing in preventing shear failures. It should be noted that in all beams with variable stirrup spacings the amount of stirrups required at each point were extended a distance h (12 in.) beyond that point since it was assumed that an inclined crack would extend downward from each point at approximately 45 deg.

Eq. 30 is similar to the corresponding equation derived by Hernandez (3) using data from 37 of the beams reported in this paper, except that Hernandez derived an empirical coefficient equal to 1.25. The change in the coefficient used in this report is partly due to the more extensive data now available and partly a result of differences between the definitions of V_c and f_y used in the two papers.*

Measured and computed values of the ultimate load are presented and compared in Table 11. The results of these comparisons will be summarized in Section 5.5(f).

(c) Effect of Web Reinforcement on the Strength of Beams with Draped Reinforcement

When sufficient web reinforcement was added to beams with draped wires, the mode of failure changed from shear to flexure. The inclined cracking load was not greatly affected by the presence of stirrups but the ductility of the beams after cracking was improved. The development of splitting along the tension reinforcement was restrained and failures due to the separation of the wires from the beam were prevented.

To check the applicability of Eq. 30 to beams with draped wires, the five beams in the BV series were tested. Beams BV.14.32b (a retest of the intact end of BV.14.32a, BV.14.34, BV.14.35 and BV.14.42 were provided with 0.80, 1.04, 1.08 and 1.32 times the amount of web reinforcement required for a balanced shear and flexural failure. All four of these beams failed in flexure. In Fig. 80 the ratio $(V_{u\ test} - V_{c\ comp.})/(V_u - V_c)_{comp.}$

*In this report V_c is defined by Eq. 10 and f_y is defined as the stress corresponding to 1 percent strain in the stirrup wire. Hernandez used Eq. 6 from Ref. 2 to define the inclined cracking shear. The average ratio of measured to computed inclined cracking load for his beams using this equation was 1.13. Hernandez defined f_y as the initial deviation from the linear elastic stress-strain curve.

is compared to the angle of drape for these beams. The computed inclined cracking shear was computed with Eq. 10 using the reduced eccentricity of the draped wires as discussed in Section 5.3(c). The points plotted on the $\Phi = 0$ axis represent this ratio for beams with straight wires in the BW.14 series. Beams BV.14.30 and BV.14.32a failed at less than their flexural capacity due to a secondary failure in bond in the anchorages after inclined cracking. The bond strength of the draped wires might have been lower with respect to a beam with straight wires due to the settlement of a larger depth of concrete underneath the wires. It appears, therefore, that if the anchorage bond is adequate, Eq. 30 can be used to predict the additional strength provided by stirrups in a beam with draped wires and web reinforcement if the cracking load shear includes an allowance for the effect of draping the wires. Since the inclined cracking load is reduced by draping the wires in beams developing flexure-shear cracks, more web reinforcement is required to ensure a flexural failure in this type of beam with draped wires than is required in a similar beam with straight wires.

(d) Effect of Web Reinforcement on the Strength of Beams Tested Under Moving Loads

Three beams with web reinforcement were tested under moving loads. The web reinforcement was designed using the expression developed by Hernandez (3) which is similar to Eq. 30 except for the value of the constant. Beam CW.10.26 had uniformly spaced web reinforcement throughout, while the web reinforcement in beams BW.10.22 and CW.10.27 (Fig. 22) was varied according to the difference in the shear corresponding to the load required to cause a flexural failure at midspan and the inclined cracking shear at each section, as illustrated in Fig. 81 for beam BW.10.22. The

ordinates in this figure are values of the applied shear; the abscissae are the positions where loads are applied to the beam. The two lines near the top of the figure represent: (a) V_u, the ultimate shear resulting from the moving load which will just cause a flexural failure at midspan, and (b) V_c, the shear corresponding to the inclined cracking load. According to Eq. 30, the amount of web reinforcement required was proportional to the difference between V_u and V_c. This difference is plotted at the bottom of the figure as a solid line. The hatched area outlined by the dotted line represents the shear capacity of the stirrups actually placed in the beam. The amount of stirrups required at each point has been extended a distance h (12 in.) toward the reaction, since an inclined crack extends downward from the load at an angle of 45 deg. or less. In beam CW.10.27, the stirrup spacing decreased near the ends of the beam since the difference between the ultimate shear and the shear corresponding to web-shear cracking increases near the ends of a beam loaded with a moving load. The stirrups in beam BW.10.22 were designed for the actual ultimate load but those in CW.10.26 and CW.10.27 were over-designed.

All three of these beams failed in flexure although the appearance of the failure zone in CW.10.26 resembled a shear failure in some respects. Some difficulty was experienced in defining "failure" since crushing occurred at the point of maximum moment which was under the load point. Since the development of crushing was restrained by the vertical stresses from the load, the first major crushing was assumed to be failure, although beams CW.10.26 and CW.10.27 carried up to six percent more load after the first major crushing occurred.

Beam BW.10.22 developed severe crushing at load position 5 and failed in that region as the load was transferred from position 5 to 6.

At load position 5, the load was 99 and 98 percent, respectively, of the computed flexural and shear ultimate loads. The load record and crack pattern for this beam are shown in Figs. 44 and 45. There were no stirrups in the end 15 in. of the span and, since no inclined cracks formed, no web reinforcement was necessary. It should be pointed out that the distribution of web reinforcement in this beam is contrary to what would be required by the usual design procedures.

Beam CW.10.26 had a 1 3/4-in. web and as a result, developed web-shear cracks at the ends of the span and flexure-shear cracks near midspan. The stirrups in this beam were spaced uniformly at 4.5 in. and were over-designed at midspan but under-designed near the reactions. Severe crushing was first observed at load position 4 at a load equal to 87 and 93 percent, respectively, of the computed flexural and shear ultimate loads. Additional crushing occurred with the load at position 6 at 95 and 85 percent ultimate loads. Although this load was defined as the "failure" load in view of the severity of the crushing, collapse occurred under additional loading at position 6 at 101 and 89 percent, respectively, of the flexural and shear failure loads.

Beam CW.10.27 also had a 1 3/4-in. web but had a smaller stirrup spacing near the reactions than at midspan. Crushing was observed first at load position 5 at 97 and 91 percent of the flexural and shear failure loads. Additional crushing, which was defined as "failure" occurred at load position 6 at 98 and 88 percent, respectively, of the computed flexural and shear failure loads. Collapse occurred under additional loading at position 6 at 101 and 89 percent, respectively, of the flexural and and shear failure loads.

These three tests on beams tested with moving loads indicated that Eq. 30 could be used to compute the strength of stirrups in such beams. The measured and computed ultimate loads for beams tested under moving loads are listed and compared in Table 12.

(e) Comparison of Measured and Computed Ultimate Loads of Prestressed Concrete Beams with Web Reinforcement

Sixty-six beams in this test series had web reinforcement. Sixteen of these failed in shear and six failed in a manner intermediate between shear and flexure (transition failures). Two beams with draped wires developed secondary anchorage bond failures which resembled shear failures in appearance but not in behavior. These two tests have not been included in the various comparisons of measured and computed capacity. The remaining 42 beams and a retest on one of the bond failures failed in flexure.

The measured and computed ultimate loads for all the beams are listed and compared in Table 11 and the ratios for the beams with web reinforcement are summarized below.

Ratio of Measured to Computed Ultimate Loads for Beams with Web Reinforcement

	No. of Tests	Mean	Maximum	Minimum	Mean Deviation
Shear Failures	16	1.00	1.13	0.90	0.044
Transition Failures	6	0.95	1.06	0.85	0.055
Flexural Failures	43	1.00	1.07	0.86	0.027

The ratios of measured and computed ultimate loads for the beams failing in flexure are compared in more detail in Section 5.4(c). Equation 30 appeared to apply satisfactorily also to beams with draped wires and beams tested under moving loads, as discussed in Section 5.5(d) and (e).

(f) Discussion of the Variables Affecting the Strength of Prestressed Concrete Beams with Web Reinforcement

The effects of a number of variables on the strength of prestressed concrete beams with web reinforcement is studied in Fig. 82 through 85. The ratio of the failure moments to the computed moments corresponding to shear failures is plotted as the ordinates of these figures. Only beams developing shear or transition failures are plotted on these figures since beams failing in flexure may have failed before the entire capacity of the stirrups was utilized.

There was no definite trend to the variation in the predicted shear strength with variations in concrete strength (Fig. 82), prestressing force (Fig. 82), type of inclined cracking (plotted in terms of V_f/V_s in Fig. 83), stirrup yield point (Fig. 83), or rf_y (Fig. 84).

On the other hand, there did seem to be a downward trend in the efficiency of web reinforcement as the stirrups spacing was increased as shown in Fig. 85(a). In addition, the location of the stirrups with respect to the load also appeared to affect the efficiency of the stirrups. Stirrup Arrangement 2 (Fig. 15) in which the first stirrup in the shear span was located a distance s from the load appeared to be less efficient than Arrangement 1 in which the first stirrup was located a distance s/2 from the load. Thus, beam CW.14.54 which failed in shear at 105 percent of its computed shear capacity had Stirrup Arrangement 1 while CW.14.51 which failed in shear at 98 precent of its computed shear capacity had Arrangement 2. On the basis of these test results it is recommended that the stirrup spacing in prestressed concrete beams should not be allowed to exceed d/2.

There may have been a slight increase in the efficiency of the web reinforcement in these tests as the length of the shear span was decreased below 36 in., as indicated by beam CW.13.28, plotted at a = 28 in. on Fig. 85, and as indicated by the fact that beam CW.10.26 carried a load of 1.12 times the computed ultimate shear capacity at a shear span of 22 in. without showing signs of distress.

6. DESIGN OF WEB REINFORCEMENT IN PRESTRESSED CONCRETE BRIDGE BEAMS

6.1 Introductory Remarks

A basic assumption in the design of a bridge girder is that the ultimate mode of failure will be flexure. However, if inclined cracks occur in a prestressed concrete beam, it may fail at a small load and much smaller deflection than those associated with a flexural failure; in general, the failure will be sudden and complete. By providing enough properly designed web reinforcement, however, it is possible to change the mode of failure from shear to failure.

For the tests described in this report, the difference between the ultimate shear and the shear corresponding to inclined cracking was found to be the most significant variable governing the amount of web reinforcement necessary to prevent a shear failure, and in Section 5.5 the following empirical expression relating these two variables was derived:

$$V_u - V_c = 1.1\, A_v f_y\, d/s \qquad (30)$$

This expression seemed to apply for all the variables included in this series of tests, at least throughout the ranges involved. The procedure proposed for the design of web reinforcement in bridge members is based essentially on this equation although certain modifications are necessary in extrapolating from the test results to full scale members, especially since Eq. 30 represents an average of the test data while a design equation to be conservative should represent a reasonable lower limit to the test data.

The basis of the proposed method for designing web reinforcement for prestressed beams is outlined in Section 6.2. In Section 6.3, the

criteria recommended for the design of web reinforcement are set forth. Design examples for pretensioned beams with straight strands, draped strands, and partially unbonded strands are presented in Section 6.4. For these beams, the proposed design method is compared to the stirrup design requirements of current specifications.

6.2 Basis of Proposed Design Method

As stated above, the basis of the web reinforcement design method proposed in this report is the empirically developed Eq. 30 which states that the required amount of web reinforcement is a function of the difference between the shears at inclined cracking and ultimate. For use in design, it is recommended that this equation be simplified to the following form:

$$A_v = \frac{(V_u - V_c)\, s}{f_y d} \tag{32}$$

In going from Eq. 30 to Eq. 32 the coefficient 1.1 has been eliminated and, as will be discussed later, a more conservative definition of V_c has been adopted. As shown by the comparisons made in Section 5.5(e), Eq. 30 approximately corresponds to the mean of the test results for shear failures or transition failures. The minimum ratios of measured to computed ultimate load for the shear and transition failures, respectively, were 0.90 and 0.85 based on Eq. 30. The elimination of the coefficient 1.1 in Eq. 32 along with the change in the definition of V_c resulted in minimum ratios of measured to computed ultimate load of 0.95 and 0.90 for the shear failures and the transition failures.

In computing V_u, the shear carried by the beam at ultimate, it is assumed that the member is loaded with one dead load plus the number of live

loads required to cause a flexural failure at midspan. Although the resulting factor of safety of the member will exceed that recommended by the Joint Committee on Prestressed Concrete (13) in many cases, it is felt that the more ductile type of behavior associated with a flexural failure is essential in a bridge member. Furthermore, increasing the strength of the web reinforcement to allow the beam to carry its flexural capacity is a relatively inexpensive way of gaining additional overload capacity in a prestressed concrete beam.

The major difficulty in the application of Eq. 32 to design is related to the determination of the shear V_c, which corresponds to inclined cracking. In the previous discussions of inclined cracking (Section 4.3(c) and 5.3), two types have been distinguished. The first type, web-shear cracking, occurs in the webs of beams with short shear spans before flexural cracks occur in the shear span. In a bridge beam, the conditions necessary for this type of cracking may exist as the moving loads come on to, and leave the span. At these times the moving concentrated loads cause large shear forces but only small moments. The shear, V_s, corresponding to web-shear cracking, is a function of the principal tensile stresses in the web of the beam as discussed in Section 5.3(a).

The second type of inclined cracking, flexure-shear cracking, develops from flexural cracks in a region subjected to shear. In a bridge beam this type of inclined cracking occurs near midspan where the live load moments are close to a maximum value and where the shearing forces are small. A moving load may cause both web-shear and flexure-shear cracks in the same beam, as shown in Fig. 45. The shear at which such a crack forms is equal to the sum of the shear causing a flexural crack at a given point

in the shear span plus the increment of shear required to cause the flexural crack to penetrate sufficiently far into the web to initiate an inclined crack. In Eq. 10 (Section 5.3) this additional increment of shear after flexural cracking was expressed empirically in terms of the shear corresponding to web-shear cracking, as follows:

$$V_c = (V_f + \frac{1}{15} V_s), \text{ but not greater than } V_s \qquad (10)$$

where: V_f = shear assumed necessary to cause the initiating flexural crack; that is, the shear required to cause a flexural crack at a distance $x = \frac{a}{6} + \frac{h}{4}$ from the load point.

The essential part of this expression is the term V_f, since flexure-shear cracks cannot form if the initiating flexural cracks do not occur. For use in Eq. 32, V_c' will be defined by the following expression which represents a lower limit to the shear corresponding to flexure-shear cracking:

$$V_c = V_f' \leq V_s \qquad (33)$$

where: V_f' = shear required to cause a flexural crack at $\underline{d}$ from the load point

Equation 33 differs from Eq. 10 in that the empirically derived term $V_s/15$ has been dropped. For standard bridge sections the resulting values of V_c are about 10 to 20 percent lower than would be predicted using Eq. 10. In addition, the definition of V_f' has been simplified by introducing the assumption that the initiating flexural crack will occur at a distance $\underline{d}$ from the load point. For short shear spans, the resulting values of V_f' will be larger than those obtained in the analysis of the test results and for long shear spans they will be smaller. The correlation between V_c and V_f for beams developing flexure-shear cracks is shown in Fig. 65. In this figure, V_f was computed at a distance $\underline{x}$ (Eq. 9), rather than $\underline{d}$, from

the load point. For most of the beams in this figure the value of V_f based on $\underline{x}$ is about 4 percent less than that based on $\underline{d}$.

The measured inclined cracking loads for the beams in this test series and the cracking loads computed using Eq. 33 are compared in the table below. It should be noted that for web-shear cracks, Eq. 33 reduces to: $V_c = V_s$, where V_s is computed in the manner outlined in Section 5.3(a). For flexure-shear cracks, Eq. 33 reduces to: $V_c = V_f' < V_s$, using the value of V_f' defined above. In these computations, the modulus of rupture was computed using Eq. 1 and the tensile strength of the concrete was taken as 80 percent of this value, as was done in the analysis of the test results.

Ratio of Measured Inclined Cracking Load to Inclined Cracking Load Computed Using Equation 33

	Mean	Maximum	Minimum	Mean Deviation
Web-Shear Cracks	1.03	1.21	0.74	0.087
Flexure-Shear Cracks	1.13	1.57	0.90	0.116

The values listed above for web-shear cracks are the same as those listed in Section 5.3(e). The values for flexure-shear cracks in the above table are based on Eq. 33 and indicate that this equation represents a lower bound on the flexure-shear cracking load. On the other hand, Eq. 10 which is compared to the test results in Section 5.3(e) was chosen to fit the average of the test results. It should be noted that the inclined cracking load is only one of the terms in Eq. 32 and thus cannot be used directly as a measure of the safety of Eq. 32. The over-all ratios of measured ultimate load for the beams which developed shear or transition failures to that computed using Eq. 32 are compared in the table below.

Ratio of Measured Ultimate Load to Ultimate Load Computed Using Equation 32

	Mean	Maximum	Minimum	Mean Deviation
Shear Failure	1.06	1.19	0.95	0.051
Transition Failures	1.04	1.23	0.90	0.075

In Section 5.3(c) it was shown that while draping the longitudinal reinforcement increased the web-shear cracking load, it tended to decrease the flexure-shear cracking load. However, if the actual eccentricity of the longitudinal reinforcement at the location of the initiating crack was used in the computation of V_f', Eq. 10 could be used to predict the flexure-shear cracking load. Thus, for the design of stirrups, the inclined cracking shear V_c will be taken as:

$$V_c = V_f' \text{ but not greater than } (V_s + A_{sd} f_{se} \sin\varphi) \qquad (33a)$$

where: A_{sd} = cross sectional area of draped prestressed reinforcement

f_{se} = effective prestress in reinforcement

φ = angle between the centroid of the draped wires and the horizontal at the section considered.

In computing V_f' for a beam with draped wires, the initiating flexural crack may be assumed to occur at a distance from the section being considered equal to the effective depth at that section.

If the prestressing force in a pretensioned beam is varied by preventing bond in some of the strands at the ends of the beam, the actual prestressing force at each section should be used in computing V_s and V_f', except that, because an anchorage length of 1 to 3 ft is required to fully develop the prestress in a given strand, it is suggested that the prestressing force in a strand be disregarded for 3 ft from the point at which the unbonding ends.

Observations of the behavior of the beams tested under moving loads and studies of the shear and moment conditions existing under the wheels of an H-S type truck indicate that although inclined cracking will occur under both of the heavy truck axles at approximately the same load,

it is sufficiently accurate for design purposes to compute V_f' assuming that the rear axle of an H-S type truck is placed over the section being considered. Since there are no other loads acting between this wheel and the adjacent reaction, the shear, V_f', at flexure-shear cracking can thus be taken as the live load flexural cracking moment divided by a distance equal to d less than that from the reaction to the section considered.

For the beams in this series of tests, the modulus of rupture of the concrete was determined from tests, and Eqs. 10 and 33 were developed using values of the modulus of rupture and concrete tensile strength expressed in terms of Eq. 1. To allow for uncertainties in the strength of concrete produced and cured under field conditions and subjected to repetitive loading, the following more conservative expressions are recommended for use in computing V_s and V_f' for full-size beams made with normal-weight aggregates:

Tensile strength: $$f_t = 4\sqrt{f_c'} \qquad (34)$$

Modulus of rupture: $$f_r = 6\sqrt{f_c'} \qquad (2)$$

where f_t, f_r and f_c' are in psi. Equation 2 for the modulus of rupture is plotted in Fig. 5. The value of the modulus of rupture computed from Eq. 2 is less than that specified in Section 207.3.3 of the Joint Committee's "Tentative Recommendations for Prestressed Concrete" (13). Equation 2 has been chosen as a lower limit for use in computing strengths whereas the value given in Section 207.3.3 is closer to an average value since it is not used as a measure of the strength of the member.

For beams with shear spans shorter than d, a large portion of the shearing force is transferred by vertical stresses and arch action and as a result, the inclined cracking shear is much larger than the predicted

value of V_s based on the tensile strength given by Eq. 34. For such beams, the amount of web reinforcement required within a distance d from the reaction may be assumed to be no greater than the amount required at a distance d from the reaction.

Because of the nature and limited knowledge of shear failures, it is suggested that some web reinforcement be provided in all bridge members. In Ref. 14, the following expression is proposed for the minimum amount of web reinforcement which should be used in a prestressed concrete bridge beam.

$$A_{v\ min.} = \frac{A_s f'_s}{80}\sqrt{\frac{d}{b'}}\ \frac{s}{f_y d} \qquad (35)$$

where: A_s = area of longitudinal tension reinforcement

f'_s = breaking strength of longitudinal reinforcement

Equation 35 can be rearranged in the form given in Eq. 35(a):

$$(V_u - V_c)_{min.} = \frac{A_s f'_s d}{80\sqrt{b'd}} \qquad (35a)$$

where $A_s f'_s d$ is a measure of the ultimate moment capacity of the member and thus of the required value of V_u. As the web thickness, b', increases, the danger of inclined cracking decreases, and hence the need for web reinforcement decreases. The amount of web reinforcement computed by this equation is close to the maximum amount required by Eq. 32 for many bridge members.

It is recommended that the spacing of stirrups in bridge girders be no greater than 0.5d or the clear height of the web, whichever is smaller. These requirements are somewhat more rigid than those specified in the Tentative Recommendations of the Joint Committee (13) or in the Bureau of Public Roads "Criteria for Prestressed Concrete Bridges" (15), both of

which allow a maximum stirrup spacing of 0.75d. However, in Section 5.5(f) (Fig. 85) it was observed that the efficiency of the stirrups appeared to drop for spacings greater than 0.5d. This was especially true if the stirrups were not properly located with respect to the load position. In addition, splitting along the junction of the web and the lower flange rarely occurred if the stirrup spacing was less than 0.5d.

The web reinforcement computed by means of Eq. 32 for a given section is actually the amount of reinforcement required to prevent failure along an inclined crack which extends downward toward the reaction at an angle of 45 deg. or less with the horizontal. For this reason, it is necessary to continue the amount of web reinforcement required at each section for a distance of at least d in the direction of diminishing moment, unless the required amount of web reinforcement increases within this distance.

6.3 Recommendations for the Design of Web Reinforcement in Bridge Girders

The design recommendations discussed in the preceding section are summarized here. These recommendations are limited to the case of simply-supported beams loaded primarily with either stationary or moving concentrated loads. This design method has also been described in Ref. 14.

(a) Amount of Web Reinforcement

1. It is recommended that web reinforcement in a prestressed concrete bridge member subjected to combined bending and shear be provided according to the following expression:

$$A_v = \frac{(V_u - V_c)s}{f_y d} \qquad (32)$$

but not less than:

$$A_v = \frac{A_s f'_s}{80} \sqrt{\frac{d}{b'}} \frac{s}{f_y d} \qquad (35)$$

where: A_v = cross sectional area of web reinforcement at spacing s, placed perpendicular to the longitudinal axis of the member

V_u = maximum shear at the section considered corresponding to the ultimate load, defined in Section 6.3(b)

V_c = shear carried by the concrete at ultimate, defined in Section 6.3(c)

s = longitudinal spacing of web reinforcement

f_y = yield point or 0.2 percent offset stress of web reinforcement, but not greater than 60,000 psi

d = effective depth of a member at section considered

A_s = total cross sectional area of prestressed tensile reinforcement at section of maximum moment

f'_s = strength of the tensile reinforcement

b' = width of web

2. Between the reaction and a point d away from the reaction, it is not necessary to increase the amount of web reinforcement above that required at a distance d from the reaction.

(b) Calculation of V_u

The ultimate shear at each section, V_u, should be taken as the shear corresponding to the load required to cause a flexural failure at mid-span. For a highway bridge girder, the ultimate shear at each section should be taken as that resulting from the passage of a hypothetical truck with the same ratios of axle loads as a standard H-S truck (16) but with axle loads equal to $(M_u - M_D)/M_w$ times the standard H-S axle loadings, where:

M_u = ultimate flexural capacity of the beam, based on Section 209.2 of the Tentative Recommendations (13)

M_D = dead load moment at point of maximum live load moment

M_w = maximum bending moment for one H-S truck on the span considered.

(c) Calculation of V_c

1. The shear V_c should be taken as the smaller of the following values:

V_f' = shear which produces a net tensile stress of $6\sqrt{f_c'}$ in the extreme fiber in tension at a distance d in the direction of decreasing moment from the section considered. In computing V_f' for a highway bridge girder, the critical truck shall be placed with one axle at the section considered such that the live load shear between the reaction and that section is uniform and a maximum.

V_s = the shear which produces a net principal tensile stress of $4\sqrt{f_c'}$ at the elastic centroid. If the centroid is not in the web of the beam, the stress should be computed also at the intersection with the web of a line drawn with the slope h/d from the extreme fiber in compression of the section considered.

2. For beams with draped prestressed reinforcement, the value of V_c shall be taken equal to V_f' but not greater than

$$V_c = (V_s + A_{sd}\, f_{se} \sin\varphi) \qquad (36)$$

where: A_{sd} = cross sectional area of draped prestressed reinforcement

f_{se} = effective prestress in draped reinforcement

φ = angle between the centroid of the draped wires and the horizontal at the section

In computing V_f', the actual eccentricity of the draped reinforcement at a distance d from the section considered must be used.

3. For beams with prestressed reinforcement which is unbonded at the ends of the beam with bond prevention devices, V_c should be computed in the vicinity of the end of the unbonded section, except that it is recommended that the prestress in each tendon be disregarded for 3 ft from the point at which the unbonding ends.

(d) Spacing of Web Reinforcement

The amount of web reinforcement required at a given section, as determined from Eq. 32, should be kept constant over a distance of at least d, the effective depth at the section considered, in the direction of diminishing moment, unless the required amount of web reinforcement increases within this distance.

The spacing of web reinforcement should not exceed 0.5d or the clear height of the web, whichever is smaller. In cases where the effective depth varies along the span independently of the over-all height, the maximum spacing need not be less than 0.25h.

(e) General Requirements

1. In general, vertical stirrups are preferable in beams subjected to moving loads. If inclined stirrups are to be used in such beams, V_c must be evaluated for several different load positions corresponding to moment decreasing to both the left and right of the section considered, and separate inclined web reinforcement should be designed for cracks sloping to the right and to the left of each section.

2. Web reinforcement must be made of deformed bars having a minimum elongation equal to that specified in ASTM A15-58T but not less than 10 percent.

6.4 Design Examples

To provide examples of the use of the recommendations given in Section 6.3, designs for three 70-ft span, pretensioned concrete bridge girders are compared in this section. Each of these girders represents an interior stringer in a bridge with a 28-ft roadway and each has a 6-in. by 6 ft 6-in. cast-in-place composite deck slab. The design was based on the AASHO "Standard Specification for Highway Bridges" (14) and the "Tentative Recommendations for Prestressed Concrete" by ACI-ASCE Joint Committee 323 (13). In each case an H20-S16-44 truck loading was assumed in the design. The stirrup design procedure was based on the recommendations made in Section 6.3. This procedure is basically the same as that used to design the stirrups in the test specimens which had varied stirrup spacings (See Section 5.5(d) and Fig. 81).

Each of the three girders is a standard AASHO-PCI Type III Beam. The beams differ only in the profile and distribution of the prestressing force as shown in Fig. 86. Beam No. 1 has 46 straight 3/8-in. strands running the entire length of the beam. The eccentricity of the prestressing force is 10.44 in. throughout the length of this beam. Beam No. 2 has 36 strands of 3/8-in. diameter, 8 of which are deflected or draped at three-tenths of the span length from each end of the beam. At midspan, the eccentricity of the prestressing steel is 15.59 in. and at the reactions it is 8.93 in. Beam No. 3 also has 36 strands of 3/8-in. diameter with an eccentricity of 15.59 in. at midspan, but the variation in the prestressing force is accomplished by unbonding 6 strands in the end two-tenths of the span and an additional 10 strands in the end tenth of the span at each end.

In the design computations for these beams, the following properties were assumed:

Concrete strength in the pretensioned girder = 5000 psi

Concrete strength in the cast-in-place slab = 3000 psi

Modulus of elasticity of slab concrete = 85 percent of that for the girder concrete

Tensile strength of the strand = 250,000 psi

Final prestress = 80 percent of initial prestress

Direct comparisons of the amount of web reinforcement required in these three beams is not possible since the ultimate flexural capacity of Beam 1 is 1.0 Dead Load + 3.59 (Design Live Load + Impact) while the flexural capacities of Beams 2 and 3 are 1.0 Dead Load + 3.17 (Design Live Load + Impact).

The design of stirrups in the beam with straight wires (Beam No. 1) was carried out in the manner shown in Fig. 87. In Eq. 32, the ultimate shear, V_u, at each section was chosen as the maximum shear at that section resulting from a hypothetical H-S type truck (16) which was just heavy enough to cause a flexural failure at the point of maximum moment. This truck was assumed to be 3.59 times as heavy as an H20-S16-44 truck since, as explained above, the live load factor of safety for this bridge was 3.59. This factor of safety was not selected before the design. It resulted from the requirement that the beam should develop its full flexural strength. Thus, the live load factor of safety is computed as the ratio of the flexural failure moment minus the dead load moment to the maximum live load moment under a single design load. The line designated as V_u in Fig. 87 represents the maximum shear at each point caused by the passage of the critical truck over the span.

The curved line near midspan in Fig. 87 represents the live load shear, V_f', required to cause initiating flexural cracks at various points

along the span. This shear corresponds to that required to cause a flexural crack at a distance d from the section under consideration, assuming that cracking occurs when the net tensile stress in the bottom fiber reaches a value of $6\sqrt{f'_c}$. Since the shear corresponding to the ultimate load is plotted in terms of a live load shear, the dead load stresses at each section have been subtracted from the stresses due to prestressing when computing the flexural cracking moment. The cracking load shear, $V_c = V'_f$, was computed by dividing the flexural cracking moment by the distance from the reaction to a point d away from the section considered because the inclined crack is assumed to occur when the trailer wheel is over the section being considered with no wheels between the given section and the reaction.

Near the ends of the beam, inclined cracks may start as web-shear cracks and in this region it is necessary to investigate the shear, V_s, which corresponds to web-shear cracking. This shear is defined in Section 6.3(b) as the shear required to cause a principal tensile stress of $4\sqrt{f'_c}$ at the elastic centroid, or at a specified nearby point in the web if the centroid falls in a flange. For a monolithically-cast prestressed concrete beam the dead load shears should be subtracted from the computed value of the web-shear cracking shear, V_s, since the ultimate shear, V_u, in Fig. 87 is plotted in terms of live load shears only. For a composite beam, however, the maximum principal tensile stresses due to the dead load shears occur at the centroid of the precast section while those due to live load shears occur at the centroid of the composite section. In addition, flexural stresses due to the dead load acting on the precast section increase the compressive stresses at the centroid of the composite section. For this section it was conservative to disregard completely all

effects of the dead load when computing V_s, the shear corresponding to web-shear cracking and this has been done in all three examples. Furthermore, the increase in thickness of the web near the reaction was ignored.

The value of $(V_u - V_c)$ to be used in Eq. 32 for the design of web reinforcement can now be obtained directly from Fig. 87 for each section. The values of $(V_u - V_c)$ which is a measure of the required amount of web reinforcement are represented by the hatched area in this figure. It should be noted that according to Section 6.3(c), the amount of web reinforcement computed for a given section must be continued for a distance d in the direction of diminishing moment beyond that section. In addition, in Section 6.3(a) it is suggested that between the reaction and a distance d from it, it is not necessary to increase the amount of web reinforcement over the amount required at a distance d from the reaction.

The remaining three lines are plotted in Fig. 87 to show the amounts of web reinforcement required by other design procedures. In each case, the required amount of web reinforcement has been converted into a shear force using Eq. 32 and is plotted downwards from the V_u line. Thus, for example, the minimum amount of web reinforcement required by Eq. 35 is represented by the vertical distance from the line marked Eq. 35 to the line V_u. It can be seen that the minimum web reinforcement from Eq. 35 agrees with the amount computed by the above analysis except at midspan. The lines marked "Joint Committee" and "Joint Committee-Minimum" refer to the amounts of web reinforcement required by the Joint Committee (13). The comparison between these methods and the proposed method will be discussed later.

Figure 88 illustrates the design procedure for the stirrups required in a beam with draped reinforcement. Since Beam 2 has fewer strands

than the beam with straight wires, its ultimate strength is less. The line marked V_u represents the maximum shear at each point resulting from the truck which will cause flexural failure at the point of maximum moment. For this beam the critical H-S truck is 3.17 times as heavy as the standard H20-S16-44 truck.

The inclined cracking shear, $V_c = V_f'$, is shown by the solid curve near midspan in this figure. This line corresponds to the shear required to cause a net tensile stress of $6\sqrt{f_c'}$ in the bottom fibers at a distance $\underline{d}$ from the section under consideration. The actual eccentricity of the prestress at each section was used in computing this line. The upper curve in this figure, shown as a broken line, represents values of V_f' computed for a similar beam with straight cables. The distance by which the solid line falls below the broken line represents the additional web reinforcement required in a beam with draped reinforcement.

Near the ends of the beam, the sum of the shear V_s, corresponding to the shear causing a principal tensile stress of $4\sqrt{f_c'}$ at the centroid, and V_d, the upward component of the prestress, has been plotted disregarding dead load stresses. The variation in the eccentricity of the prestressing force was taken into account in computing V_s for the composite section. The value of V_s calculated for a beam with straight wires has also been plotted on this graph. This line falls considerably below the line corresponding to the beam with draped wires because of the different distribution of prestress in beams with and without draped wires and because there is no drape shear, V_d, in the beams with straight wires. Thus, in regions where the inclined cracks start as web shear cracks, draping the longitudinal reinforcement reduces the amount of web reinforcement required.

The amount of web reinforcement required in this beam can be computed from Eq. 32 using the difference between V_u and V_c from Fig. 88. This amount of web reinforcement is compared in this figure with the minimum amount of web reinforcement from Eq. 35 and the amount required by the Joint Committee (13), also expressed in terms of $(V_u - V_c)$. Again the minimum web reinforcement from Eq. 35 and the Joint Committee agree well with the amount computed by the above analysis. It should be noted that in a beam with draped reinforcement, the amount of web reinforcement required by Eq. 32 is decreased in zones of web-shear cracking and increased in zones of flexure-shear cracking, in relation to the amount required in a beam with straight wires. From a diagram of this type, it can be seen that the most advantageous place to drape the reinforcement in a prestressed concrete bridge member would be near the quarter points of the span since the strands would be straight throughout most of the zone where flexure-shear cracks occur so that the load at which such cracks occur is not reduced. At the same time, the upward component of the prestressing force and the increase in the compressive stress in the upper part of the web in the outer quarters of the span increase the web-shear cracking load in these regions, thus reducing the amount of web reinforcement required near the ends of the beam. For the same reason, a parabolic drape profile is advantageous since the major change in the eccentricity and slope of the wires occurs near the end of the span in such a profile.

Figure 89 illustrates the stirrup design procedure for a beam with "partially bonded" strands which are unbonded by plastic sleeves or some other method for a portion of the length of the beam. The line marked V_u corresponds to the maximum shears at each point in the span resulting from the critical H-S truck, which in this case weighs 3.17 times as much as a H20-S16 truck.

The jagged line, marked $V_c = V_f'$ corresponds to the shear required to cause a net tensile stress of $6\sqrt{f_c'}$ in the bottom fibers at a distance d from the section under consideration. The steps in the line occur at points d away from the points at which the wire becomes fully bonded. In this computation, as recommended in Section 6.3(b), it was assumed that each unbonded strand reaches its full stress abruptly at a point 3 ft from the point where the anchorage bond begins. Under this assumption, $V_c = V_f'$ is considerably less than V_u with the loads at 13.5 ft and 20.5 ft from the reaction and flexure-shear cracks presumably could occur with the loads in these positions. A somewhat more reasonable distribution of the cracking shears in the vicinity of the points of unbonding is shown by dashed lines which correspond to a linear increase in the prestressing force over a distance of 3 ft from the point where the anchorage bond begins.

In addition to reducing the value of $V_c = V_f'$ in the outer parts of the shear span, varying the prestressing force by means of bond prevention decreases the web-shear cracking shear, V_s, at the ends of the span as shown in Fig. 91 by the line $V_c = V_s$. The other lines in this figure compare the amount of web reinforcement just computed to the minimum from Eq. 35 and to the amounts required by other specifications. Comparison of Figs. 87, 88 and 89 taking into account the increased capacity of the beam with straight strands, shows that a beam prestressed by means of the bond prevention technique requires more web reinforcement than the other two types of beams considered. Coupled with the danger of premature inclined cracking in the zone in which the cut-off strands are anchored by bond, is the possibility of bond failure adjacent to either flexural or inclined cracks which might occur in these anchorage zones. Because of the increased possibility of shear and bond failures occurring in beams with cut-off strands, this

method of varying the prestress in a beam does not appear to be desirable for bridge members.

In Figs. 87, 88, and 89, the lines marked "Joint Committee" and "Joint Committee-Minimum" refer, respectively, to the maximum shear which could be transferred by stirrups designed according to Section 210.2.2 of the Tentative Recommendations for Prestressed Concrete of the Joint Committee (13) and the capacity of the minimum amount of web reinforcement required in Section 210.2.3. Similarly, the hatched areas refer to the shear transferred by stirrups designed according to the design procedure outlined in Section 6.3, and the line labeled Eq. 35 refers to the shear corresponding to the minimum amount of web reinforcement required by Eq. 35. In each case the web reinforcement has been expressed in terms of a shear computed from Eq. 32.

A comparison of Fig. 87, 88, and 89 indicates that the amount of web reinforcement required by the procedure outlined in Section 6.3 and that required by the Tentative Recommendations for Prestressed Concrete (13) are approximately equal, largely because the minimum amounts of web reinforcement are similar in both cases. The basic stirrup design equations in the two procedures differ considerably, however, the greatest differences occurring near midspan. In the Joint Committee design equation (Section 210.2.2), the shear carried by the concrete, V_c, is related directly to a shear force while in the proposed design method the shear carried by the concrete, V_c, is assumed to be equal to the inclined cracking shear, which is expressed in terms of either shear or moment. Near midspan inclined cracks are most likely to start as flexure-shear cracks and in this region the inclined cracking load is more closely related to moment than to shear. Although the Joint Committee stirrup design method is easier to use, it is felt

that the design procedure outlined in Section 6.3 is actually preferable since it is based on a more rational consideration of the behavior of beams subjected to combined bending and shear.

7. SUMMARY

7.1 Outline of Investigation

The purpose of this investigation was to study the behavior of simply-supported prestressed concrete beams with web reinforcement and/or draped reinforcement. Particular attention was paid to the development of inclined cracks and the modes of failure.

Tests of 87 beams, 6 by 12 in. in cross section and spanning 9 ft are reported. Five beams were rectangular, while the rest were I-beams with 3 in. or 1 3/4 in. thick webs. Two had 2 by 24 in. composite slabs. The beams were prestressed with 0.082 to 0.712 percent longitudinal reinforcement which was straight in 68 beams and draped under the load points in the rest. Concrete strengths ranged from 2310 to 7625 psi while the nominal prestress was 120,000 or 60,000 psi. Vertical stirrups were used, with web reinforcement ratios, based on the flange width and stirrup spacing, ranging from 0.038 to 0.327. The stirrup spacing varied from 2.25 to 10.5 in. All the beams were tested under one or two concentrated loads with shear spans of 28 to 78 in. In seven beams the load was applied successively at eleven points along the span to simulate a moving load.

Each beam was tested to failure. Records of load, deflection, concrete and steel strains and cracking were obtained at all stages of loading. Studies of the data resulted in empirical expressions for the inclined cracking and ultimate loads. In addition, design procedures are proposed for prestressed bridge girders.

7.2 Behavior of Test Beams

Of the 87 beams reported, 36 failed in shear, 43 in flexure, 6 in a "transition" failure and 2 in bond. Prior to the development of

inclined cracks, all the beams behaved in a similar fashion with "elastic" behavior before flexural cracking and an increasing rate of deflection after flexural cracking. Inclined cracks generally formed after some flexural cracking had occurred, although in a few cases the inclined cracks preceded flexural cracking.

Because of the different phenomena involved in their initiation, the inclined cracks were classified into two types: flexure-shear cracks which developed as a result of flexural cracks in a region of combined bending and shear; and web-shear cracks which originated in the web before any flexural cracking in their vicinity.

After inclined cracking in beams with web reinforcement, the stirrups controlled the opening of the inclined cracks, thus preventing immediate failure. With increased load, the beam failed in flexure before the stirrup failed, or the stirrups yielded or fractured resulting in a shear failure. In beams without web reinforcement, shear failures occurred with little or no increase in load beyond inclined cracking.

The flexural failures occurred by crushing of the concrete above a vertical flexural crack in the region of maximum moment. For beams with high longitudinal reinforcement ratios, these failures were often quite violent.

Beams failed in shear in several ways: (1) by crushing and distortion of the web due to the thrusts induced by arch action; (2) by crushing of the compression zone above the end of one of the inclined cracks; (3) by separation of the tension flange from the rest of the beam by cracks along the reinforcement; and (4) by fracture of the stirrups. In general, shear failures were violent, although in some cases the failure load and deflection were comparable to those for a flexural failure.

The development of inclined cracking and the observed modes of failure for the beams with draped wires and the beams tested under moving loads were essentially similar to those for beams with straight wires and stationary loads.

7.3 Test Results

The load corresponding to the formation of a flexure-shear crack was found to be closely related to the flexural cracking load near its point of origin. The load corresponding to web-shear cracking could be computed on the basis of an uncracked section analysis. Draped reinforcement tended to decrease the flexure-shear cracking load but tended to increase the web-shear cracking load. An empirical expression for the inclined cracking load, Eq. 10, was derived from the data. The average ratio of measured to predicted inclined cracking loads for 192 tests in this and another test series was 1.00 and the mean deviation was 0.071.

The strength of the beams with web reinforcement was computed on the basis of an empirically derived equation, Eq. 30, which related the additional strength after inclined cracking directly to the amount of web reinforcement. For the beams failing in shear, the average ratio of the measured to computed strength was 1.00 and the mean deviation was 0.044.

In general, it was concluded that, within the wide range of variables considered, it was possible to prevent shear failures by providing adequate amounts of vertical stirrups. The presence of even a small amount of web reinforcement improved both the strength and ductility of a beam failing in shear, but in the practical range of variables the maximum strength and ductility were attained only in the case of flexural failures. It is recommended, therefore, that prestressed concrete beams be provided with sufficient web reinforcement to ensure flexural failures.

8. BIBLIOGRAPHY

1. Zwoyer, E. M. and C. P. Siess, "The Ultimate Strength in Shear of Simply-Supported Prestressed Concrete Beams Without Web Reinforcement," Proceedings, American Concrete Institute, Vol. 51, pp. 181-200, October 1954.

2. Sozen, M. A., E. M. Zwoyer, and C. P. Siess, "Investigation of Prestressed Concrete for Highway Bridges, Part 1: Strength in Shear of Beams Without Web Reinforcement," Bulletin No. 452, University of Illinois Engineering Experiment Station, April 1959.

3. Hernandez, G., "Strength of Prestressed Concrete Beams With Web Reinforcement," Ph.D. thesis, University of Illinois, May 1958.

4. Murphy, P. E., "Behavior of Prestressed Concrete Beams Under Long-Time Loading", M.S. thesis, University of Illinois, September 1957.

5. Siess, C. P. and G. McLean, "Relaxation of High-Tensile-Strength Steel Wire for Use in Prestressed Concrete", Bulletin No. 211, American Society for Testing Materials, January 1956.

6. Warwaruk, J., "Strength and Behavior in Flexure of Prestressed Concrete Beams," Ph.D. thesis, University of Illinois, June 1960.

7. Johnson, J. W., "Relationship Between Strength and Elasticity of Concrete in Tension and Compression," Bulletin No. 90, Iowa State College, 1928.

8. Tucker, J. Jr., "Statistical Theory of the Effect of Dimensions and of Method of Loading Upon the Modulus of Rupture of Beams," Proceedings, American Society of Testing Materials, Vol. 41, p. 1072, 1941.

9. Timoshenko, S. and J. N. Goodier, "Theory of Elasticity," McGraw-Hill, 1951, pp. 99-107.

10. Laupa, A., C. P. Siess, and N. M. Newmark, "Strength in Shear of Reinforced Concrete Beams," Bulletin No. 428, University of Illinois Engineering Experiment Station, 1955.

11. Sethunarayanan, R., "Ultimate Strength of Pretensioned I-Beams in Combined Bending and Shear", Comite' Europeen du Beton, Paris, February 1959.

12. Hognestad, E. and R. C. Elstner, "An Investigation of Reinforced Concrete Beams Failing in Shear", Department of Theoretical and Applied Mechanics, University of Illinois, October 1951.

13. ACI-ASCE Joint Committee 323, "Tentative Recommendations for Prestressed Concrete," Proceedings, American Concrete Institute, Vol. 54, pp. 546-578, January 1958.

14. Hernandez, G., M. A. Sozen, and C. P. Siess, "Shear Tests on Beams with Web Reinforcing", Paper presented at New Orleans Regional Convention, American Society of Civil Engineers, March 8, 1960 and submitted for publication in the Journal of the American Concrete Institute.

15. Bureau of Public Roads, "Criteria for Prestressed Concrete Bridges," U. S. Government Printing Office, Washington, December 1954.

16. "Standard Specifications for Highway Bridges, Seventh Edition," adopted and published by the American Association of State Highway Officials, Washington, D. C., 1957.

TABLE 1

PROPERTIES OF BEAMS

Mark	Concrete Strength* f'_c psi	Flange Width b in.	Web Thickness b' in.	Effective Depth d in.	Steel Area A_{s_2} in.^{2}	Longit. Reinf. p %	Effective Prestress f_{se} ksi	Shear Span a in.	Wire Lot
AD.14.37	3260	6.00	--	10.15	0.242	0.398	106	36	11
AW.14.39	5470	6.00	--	8.53	0.362	0.708	120	36	8
AW.14.76	2800	6.00	--	8.48	0.362	0.712	118	36	8
AW.24.48	4400	6.00	--	8.48	0.362	0.712	58	36	8
AW.24.68	3170	5.95	--	8.54	0.362	0.713	62	36	8
B.10.23	5200	6.00	3.00	10.04	0.242	0.405	127.4	ML	12
B.10.24	3835	6.04	3.03	10.09	0.181	0.300	126.8	ML	12
B.14.34	2640	6.05	3.10	10.30	0.181	0.290	115	36	12
B.14.41	2890	6.05	3.00	10.00	0.242	0.399	114	36	12
BD.14.18	6280	5.95	2.86	10.11	0.237	0.386	123	36	13
BD.14.19	6280	5.95	2.90	10.20	0.242	0.398	112	36	12
BD.14.23	3870	6.00	3.00	10.10	0.181	0.300	99	36	11
BD.14.26	3460	6.00	3.00	10.10	0.181	0.298	116	36	11
BD.14.27	3400	6.00	3.00	10.10	0.181	0.298	111	36	11
BD.14.28	3320	6.00	3.00	10.10	0.181	0.300	118	36	11
BD.14.34	2700	6.05	3.00	10.22	0.181	0.293	110	36	11
BD.14.35	2610	6.05	2.95	10.10	0.181	0.297	108	36	11
BD.14.42	2870	6.00	2.90	10.10	0.242	0.400	107	36	11
BD.24.32	3800	6.05	3.00	10.10	0.242	0.395	81	36	11

TABLE 1 (Cont'd)

Mark	Concrete Strength * f'_c psi	Flange Width b in.	Web Thickness b' in.	Effective Depth d in.	Steel Area A_{s_2} in.	Longit. Reinf. p %	Effective Prestress f_{se} ksi	Shear Span a in.	Wire Lot
BV.14.30	4020	5.95	2.95	10.10	0.242	0.403	123	36	11
BV.14.32	3800	5.90	2.85	10.13	0.242	0.403	112	36	12
BV.14.34	3620	5.95	3.00	10.15	0.242	0.400	124	36	12
BV.14.35	3410	5.95	2.92	10.20	0.242	0.398	115	36	12
BV.14.42	2910	6.00	2.88	10.15	0.237	0.387	120	36	13
BW.10.22	3970	6.05	3.05	10.19	0.181	0.295	123	ML	12
BW.14.20	2870	6.00	2.95	10.47	0.121	0.192	126.8	36	10
BW.14.22	5430	6.00	3.00	10.10	0.242	0.399	119.7	36	11
BW.14.23	5520	5.90	3.02	9.97	0.242	0.410	119.1	36	12
BW.14.26	3510	6.00	2.86	10.11	0.183	0.302	121.0	36	14
BW.14.31	3870	6.00	3.00	10.02	0.242	0.402	116.8	36	11
BW.14.32	2830	5.88	2.86	10.21	0.177	0.294	123.1	36	13
BW.14.34	3560	5.90	2.90	10.10	0.237	0.390	122.6	36	13
BW.14.38	3110	6.00	2.95	10.11	0.242	0.398	120.0	36	10
BW.14.39	3050	5.95	2.90	10.11	0.242	0.401	120.6	36	10
BW.14.41	2860	6.00	2.95	10.15	0.242	0.397	121.8	36	10
BW.14.42	2810	5.98	2.96	10.14	0.242	0.398	121.0	36	10
BW.14.43	2780	6.00	2.95	10.12	0.242	0.397	120.3	36	10
BW.14.45	2680	6.00	3.00	10.03	0.242	0.402	120.4	36	11
BW.14.58	3165	6.00	2.91	9.97	0.366	0.611	109.4	36	14
BW.14.60	3025	6.04	2.89	9.98	0.366	0.608	109.8	36	14
BW.15.34	3550	6.00	3.00	10.15	0.242	0.397	122.4	48	11
BW.15.37	3210	6.00	3.00	10.12	0.242	0.398	122.5	48	11
BW.16.38	3160	6.00	3.00	10.05	0.242	0.401	122.0	54	11

TABLE 1 (Cont'd)

Mark	Concrete Strength* f'_c psi	Flange Width b in.	Web Thickness b' in.	Effective Depth d in.	Steel Area A_s in.^{2}	Longit. Reinf. p %	Effective Prestress f_{se} ksi	Shear Span a in.	Wire Lot
BW.18.15	7625	6.06	3.00	10.04	0.237	0.378	105.6	70	13
BW.18.27	4340	6.03	3.00	10.15	0.242	0.397	122.1	70	12
BW.19.28	4080	6.15	3.15	10.15	0.242	0.386	120.0	78	12
BW.28.26	3425	5.95	3.05	10.20	0.177	0.292	59.6	70	13
BW.28.28	3120	5.88	2.95	10.18	0.177	0.296	64.1	70	13
C.10.27	3660	5.95	1.68	10.12	0.181	0.302	123.0	ML	12
C.10.28	4300	6.00	1.88	10.06	0.242	0.400	113.0	ML	12
C.13.23	3730	6.05	1.79	10.38	0.181	0.288	118.9	27	12
CD.13.24	3670	5.92	1.77	10.56	0.181	0.290	124.5	27	12
CD.13.25	3460	6.07	1.82	10.46	0.181	0.286	118.2	27	12
CD.14.34	2560	6.00	1.75	10.22	0.181	0.296	105.0	36	11
CW.10.26	4650	5.90	1.73	10.00	0.242	0.410	119.8	ML	12
CW.10.27	4530	6.00	1.72	9.96	0.242	0.405	119.1	ML	12
CW.13.28	4330	6.00	1.75	10.03	0.242	0.402	118.5	28	11
CW.13.38	3200	6.00	1.80	10.03	0.242	0.402	119.0	28	11
CW.14.14	7200	5.92	1.72	10.05	0.242	0.405	111.5	36	12
CW.14.15	3280	6.00	1.70	10.50	0.121	0.192	125.5	36	10
CW.14.16	3230	6.00	1.75	10.47	0.121	0.193	127.3	36	11
CW.14.17	3140	6.00	1.76	10.49	0.121	0.192	125.9	36	10
CW.14.18	3100	6.00	1.70	10.50	0.121	0.192	125.5	36	10

TABLE 1 (Cont'd)

Mark	Concrete Strength* f'_c psi	Flange Width b in.	Web Thickness b' in.	Effective Depth d in.	Steel Area A_s $in.^2$	Longit. Reinf. p %	Effective Prestress f_{se} ksi	Shear Span a in.	Wire Lot
CW.14.19	3080	6.00	1.78	10.48	0.121	0.192	125.9	36	10
CW.14.20	3020	6.00	1.70	10.49	0.121	0.192	127.1	36	10
CW.14.21	2990	6.00	1.70	10.52	0.121	0.191	125.7	36	10
CW.14.22	4660	5.95	1.71	10.14	0.242	0.400	121.6	36	10
CW.14.23	2690	6.00	1.75	10.48	0.121	0.192	125.8	36	10
CW.14.24	2680	6.05	1.75	10.47	0.121	0.191	125.5	36	10
CW.14.25	5050	6.00	1.80	10.15	0.242	0.397	121.2	36	11
CW.14.26	2310	6.00	1.70	10.50	0.121	0.192	126.1	36	10
CW.14.35	3420	6.05	1.75	10.06	0.242	0.398	118.5	36	11
CW.14.36	3300	6.00	1.86	10.11	0.242	0.399	112.5	36	10
CW.14.37	3240	5.95	1.70	10.11	0.242	0.401	120.8	36	10
CW.14.39	3010	6.00	1.75	10.12	0.242	0.397	119.8	36	10
CW.14.40	3010	6.00	1.75	10.14	0.242	0.397	120.2	36	11
CW.14.42	2840	5.95	1.70	10.10	0.242	0.402	116.5	36	10
CW.14.45	2640	6.00	1.65	10.13	0.242	0.397	119.2	36	10
CW.14.47	2535	6.00	1.70	10.14	0.242	0.396	118.8	36	10
CW.14.50	2400	6.00	1.75	10.15	0.242	0.397	121.5	36	10
CW.14.51	3260	6.03	1.80	9.92	0.355	0.593	115.9	36	13
CW.14.54	3300	6.00	1.78	9.96	0.355	0.595	107.4	36	13
CW.18.15	7420	6.08	1.73	10.10	0.232	0.374	126.4	70	13
CW.28.26	3370	6.00	1.78	10.09	0.177	0.291	63.7	70	13
CW.28.28	3080	6.00	1.84	10.18	0.177	0.290	66.0	70	13
FW.14.06	3910	24.0	1.75	12.30	0.242	0.082	117.8	36	11
FW.14.07	3520	24.0	1.85	12.30	0.242	0.082	123.0	36	11

*Strength of concrete in top flange.

TABLE 2

PROPERTIES OF WEB REINFORCEMENT

Mark*	Web Reinf. Ratio r %	Yield Stress f_y ksi	Stirrup Spacing s in.	Stirrup*** Arrangement	Type of+ Stirrup	Wire Lot
AW.14.39	0.256	53.7	6.5	2	A	2 bar C
AW.14.76	0.256	53.7	6.5	2	A	2 bar C
AW.24.48	0.256	53.7	6.5	2	A	2 bar C
AW.24.68	0.256	53.7	6.5	2	A	2 bar C
BV.14.30	0.137	36.8	5.0	6	D	8A
BV.14.32	0.154	36.8	4.5	1	D	8A
BV.14.34	0.152	36.8	4.5	1	D	8A
BV.14.35	0.196	36.8	3.5	1	D	8A
BV.14.42	0.170	36.8	4.0	1	D	8A
BW.10.22	0.072**	37.2	Varies	15	C'	10B
BW.14.20	0.048	43.5	5.0	6	C	10A
BW.14.22	0.139	36.8	5.0	6	D	8A
BW.14.23	0.076	79.5	3.75	1	C'	H.S.
BW.14.26	0.106	43.0	4.5	1	D	10C
BW.14.31	0.147	41.2	10.0	1	E	6B
BW.14.32	0.069	36.8	5.0	1	C'	8A
BW.14.34	0.063	34.0	10.5	1	D	4B
BW.14.38	0.095	43.5	2.5	4	C	10A
BW.14.39	0.193	35.7	2.5	4	C	6A
BW.14.41	0.139	36.8	5.0	6	D	8A
BW.14.42	0.139	36.8	2.5	4	C	8A
BW.14.43	0.196	41.2	5.0	6	D	6B
BW.14.45	0.131	41.2	7.5	2	D	6B
BW.14.58	0.095	43.0	5.0	1	D	10C
BW.14.60	0.095	43.0	5.0	2	D	10C
BW.15.34	0.097	37.2	5.0	6	D	10B
BW.15.37	0.139	36.8	5.0	6	D	8A
BW.16.38	0.097	37.2	5.0	6	D	10B
BW.18.15S*	0.069**	79.5	Varies	9	C'	H.S.
L*	0.038**	79.5	Varies		C'	H.S.
BW.18.27S*	0.194	41.2	5.0	10	D	6B
L*	0.080**	37.2	Varies		C	10B
BW.19.28S*	0.191	41.2	5.0	11	D	6B
L*	0.070**	37.2	Varies		C	10B

TABLE 2 (Cont'd)

Mark*	Web Reinf. Ratio r %	Yield Stress f_y ksi	Stirrup Spacing s in.	Stirrup*** Arrangement	Type of+ Stirrup	Wire Lot
BW.28.26S*	0.162**	37.2	Varies	12	D	10B
L*	0.089**	37.2	Varies		C	10B
BW.28.28S*	0.174	36.8	4.0	8	D	8A
L*	0.090	37.2	5.5		D	10B
CW.10.26	0.154	36.8	4.5	7	D	8A
CW.10.27	0.151**	36.8	Varies	16	D	8A
CW.13.28	0.277	36.8	2.5	4	D	8A
CW.13.38	0.327	41.2	3.0	5	D	6B
CW.14.14	0.102	79.5	2.75	1	C'	H.S.
CW.14.15	0.277	36.8	2.5	3	D	8A
CW.14.16	0.077	36.8	9.0	1	D	8A
CW.14.17	0.048	43.5	5.0	6	C	10A
CW.14.18	0.382	35.7	2.5	3	D	6A
CW.14.19	0.095	43.5	2.5	4	C	10A
CW.14.20	0.095	43.5	5.0	6	D	10A
CW.14.21	0.069	36.8	5.0	6	C	8A
CW.14.22	0.193	35.7	2.5	4	C	6A
CW.14.23	0.069	36.8	5.0	6	C	8A
CW.14.24	0.108	41.2	9.0	1	D	6B
CW.14.25	0.277	36.8	2.5	4	D	8A
CW.14.26	0.139	36.8	2.5	4	C	8A
CW.14.35	0.230	44.5	7.5	2	D	2B
CW.14.36	0.261	41.2	3.75	2	D	6B
CW.14.37	0.140	36.8	2.5	4	C	8A
CW.14.39	0.095	43.5	2.5	4	C	10A
CW.14.40	0.347	44.5	5.0	6	D	2B
CW.14.42	0.192	43.5	2.5	4	D	10A
CW.14.45	0.277	36.8	2.5	3	D	8A
CW.14.47	0.191	35.7	5.0	6	D	6A
CW.14.50	0.261	34.0	5.0	6	D	4B
CW.14.51	0.135	36.8	5.0	2	D	8A
CW.14.54	1.136	36.8	5.0	1	D	8A
CW.18.15S*	0.100**	79.5	Varies	13	C'	H.S.
L*	0.055**	79.5	Varies		C'	H.S.
CW.28.26S*	0.203**	37.2	Varies	14	D	10B
L*	0.107**	37.2	Varies		C'	10B
CW.28.28S*	0.210	36.8	3.25	8	D	10B
L*	0.110	37.2	4.38		C'	10B
FW.14.06	0.277++	36.8	2.5	4	B	8A
FW.14.07	0.327++	41.2	3.0	5	B	6B

* In beams loaded with a single unsymmetrically placed load, S refers to the short shear span, L to the long one.

** At midspan or adjacent to load point.

*** Numbers correspond to stirrup arrangements in Fig. 15 through 22.

\+ Letters correspond to types of stirrups shown in Fig. 2.

++ Based on flange width of precast section.

TABLE 3

PROPERTIES OF DRAPE PROFILES

Drape* Profile	Mark	No. of Wires	No. of Draped Wires	Height of Center of Gravity of Steel At Support: Draped Wires, in.	At Support: All Wires, in.	At Midspan: All Wires, in.	Angle of Draped Wires, deg.	Drape Angle φ deg.
A	BD.14.28	6	6	2.96	2.96	2.0	1.53	1.53
B	BD.14.27	6	6	3.40	3.40	2.0	2.22	2.22
	BD.14.42	8	8	3.50	3.50	2.0	2.38	2.38
C	CD.13.24	6	6	3.23	3.23	1.63	3.40	3.40
D	BD.14.19	8	8	5.14	5.14	2.0	5.00	5.00
	BV.14.35	8	8	5.36	5.36	2.0	5.36	5.36
	AD.14.37	8	8	6.07	6.07	2.0	6.45	6.45
E	BD.24.32	8	8	6.07	6.07	2.0	6.45	6.45
(Mid Height)	BD.14.35	6	6	5.96	5.96	2.0	6.28	6.28
	BV.14.42	8	8	6.30	6.30	2.0	6.80	6.80
F	BD.14.23	6	6	7.8	7.8	2.0	9.13	9.13
G	BD.14.26	6	6	8.33	8.33	2.0	9.95	9.95
W	BD.14.34	6	4	4.14	3.04	1.87	3.42	1.88
	CD.14.24	6	4	4.14	3.04	1.87	3.42	1.88
X	BD.14.18	8	4	5.37	3.69	2.0	5.36	2.70
	BV.14.34	8	4	5.37	3.69	2.0	5.36	2.70
Y	CD.13.25	6	4	3.23	2.47	1.67	4.44	2.85

TABLE 3 (Cont'd)

Drape* Profile	Mark	No. of Wires	No. of Draped Wires	Height of Center of Gravity of Steel At Support: Draped Wires, in.	At Support: All Wires, in.	At Midspan: All Wires, in.	Angle of Draped Wires, deg.	Drape Angle φ deg.
Z	BV.14.30	8	4	6.07	4.04	2.0	6.45	3.25
	BV.14.32	8	4	6.07	4.04	2.0	6.45	3.25
S (Straight)	B.14.34	6	-	1.87	1.87	-	-	-
	B.14.41	8	-	2.00	2.00	-	-	-
	C.14.34	6	-	1.64	1.64	-	-	-

*Profiles A through G have only draped wires.
Profiles W through Z comprise both straight and draped wires.
Profile S designates straight reinforcement only.
Profiles C and Y have 27-in. shear spans.

TABLE 4(a)

PROPERTIES OF CONCRETE MIXES

Mark	Compressive Strength f'_c psi		Modulus of Rupture f_r psi		Cement:Sand:Gravel by weight	Water/Cement by weight		Slump in.		Age at Test days
Batch	1	2	1	2	1 and 2	1	2	1	2	
AD.14.37	2700	3260	300	282	1:4.2:4.6	0.91	0.91	1.5	2	12
AW.14.39	5470	5560	510	-	1:3.3:3.5	0.83	0.83	3.5	3	19
AW.14.76	2765	2795	385	-	1:3.7:3.9	1.06	1.06	8	8	6
AW.24.48	4900	4400	525	-	1:3.3:3.5	0.69	0.69	2.5	6	8
AW.24.68	2510	3170	400	-	1:4.1:4.3	0.96	0.96	5.5	6	10
B.10.23	5205	5200	425	462	1:3.9:4.2	0.85	0.85	1	2	36
B.10.24	3720	3835	375	342	1:4.1:4.4	0.82	0.87	2	1.5	18
B.14.34	3090	2640	340	275	1:4.1:4.4	0.79	0.79	1	1	8
B.14.41	3000	2890	358	358	1:4.1:4.4	0.79	0.79	1	1	7
BD.14.18	6390	6280	517	438	1:2.9:3.2	0.72	0.71	3	2	6
BD.14.19	6720	6280	519	519	1:2.8:3.0	0.72	0.74	3	3	7
BD.14.23	4210	3870	337	310	1:4.0:4.3	0.78	0.78	2	1.5	15
BD.14.26	3160	3460	383	392	1:4.2:4.6	0.84	0.84	1.5	1	8
BD.14.27	3850	3400	442	416	1:4.3:4.6	0.79	0.79	1.5	2	9
BD.14.28	4230	3320	457	367	1:4.0:4.4	0.77	0.78	2	2	8
BD.14.34	2720	2700	404	350	1:4.2:4.6	0.79	0.79	3	2.5	8
BD.14.35	2610	2610	375	400	1:4.2:4.6	0.92	0.92	1	1	8
BD.14.42	2980	2870	491	491	1:4.2:4.5	1.00	1.00	3	2	8
BD.24.32	3090	3800	416	375	1:4.3:4.6	0.81	0.81	2	2	8
BV.14.30	4200	4020	346	350	1:3.9:4.2	0.82	0.82	2	3	20
BV.14.32	4210	3800	420	451	1:3.9:4.2	0.84	0.83	2	3	6
BV.14.34	3800	3620	500	416	1:4.0:4.2	0.86	0.85	2	2	5
BV.14.35	3340	3410	508	425	1:3.9:4.2	0.83	0.83	3	3	5
BV.14.42	3090	2910	455	450	1:3.9:4.2	0.90	0.90	2.5	3	6
BW.10.22	4150	3970	466	469	1:4.1:4.4	0.91	0.85	2	2	13
BW.14.20	2840	2870	333	350	1:4.1:4.4	0.80	0.83	1.5	1	7
BW.14.22	5520	5430	517	475	1:3.2:3.5	0.65	0.62	3	2.5	10
BW.14.23	5360	5523	500	520	1:2.2:2.6	0.72	0.74	4	6	7
BW.14.26	3471	3507	400	400	1:3.9:4.2	0.82	0.82	3	3	7
BW.14.31	3190	3870	383	425	1:4.1:4.4	0.79	0.76	7	3	11
BW.14.32	2838	2829	308	350	1:3.9:4.2	0.90	0.90	3	3	6

TABLE 4(a) (Cont'd)

Mark	Compressive Strength f'_c psi		Modulus of Rupture f_r psi		Cement:Sand:Gravel by weight	Water/Cement by weight		Slump in.		Age at Test days
Batch	1	2	1	2	1 and 2	1	2	1	2	
BW.14.34	3452	3559	366	358	1:3.9:4.2	0.83	0.83	2	2.5	7
BW.14.38	2890	3110	342	316	1:4.1:4.5	0.91	0.91	1.5	1	7
BW.14.39	3120	3050	358	392	1:4.2:4.5	0.86	0.86	2	1	8
BW.14.41	3050	2860	466	359	1:3.9:4.2	0.87	0.85	2.5	2.5	8
BW.14.42	2870	2810	338	342	1:4.1:4.5	0.84	0.84	2	2	8
BW.14.43	2910	2780	346	392	1:4.1:4.4	0.88	0.88	1	3	8
BW.14.45	3100	2680	304	304	1:4.1:4.3	0.80	0.79	2.5	3.5	9
BW.14.58	3387	3165	416	358	1:4.0:4.3	0.82	0.83	2	3	7
BW.14.60	2730	3025	358	350	1:4.0:4.3	0.89	0.89	2	2	7
BW.15.34	3620	3550	375	392	1:4.1:4.3	0.75	0.75	4	2	11
BW.15.37	3300	3210	417	392	1:4.2:4.4	0.87	0.83	3	3.5	8
BW.16.38	3800	3160	383	267	1:4.0:4.3	0.88	0.91	1.5	2.5	10
BW.18.15	7265	7626	618	558	1:2.2:2.6	0.59	0.59	3.5	4	18
BW.18.27	4655	4342	533	512	1:4.0:4.3	0.80	0.80	2	2	12
BW.19.28	4420	4080	444	438	1:4.1:4.4	0.89	0.86	2	2	12
BW.28.26	3201	3425	458	366	1:3.9:4.2	0.86	0.86	2	2	8
BW.28.28	3365	3120	450	413	1:3.9:4.2	0.85	0.86	2	3	6
C.10.27	3300	3661	275	300	1:4.1:4.4	0.85	0.82	2	2	14
C.10.28	4250	4300	412	316	1:3.9:4.2	0.89	0.85	1	1	25
C.13.23	3460	3730	495	425	1:4.4:4.4	0.87	0.83	1	1.5	13
CD.13.24	3850	3670	467	437	1:4.4:4.4	0.90	0.90	1	1.5	14
CD.13.25	3020	3460	408	417	1:4.4:4.4	0.85	0.85	1	1.5	11
CD.14.34	2660	2560	417	420	1:3.8:4.2	0.91	0.94	2	3	6
CW.10.26	4160	4650	456	460	1:4.1:4.4	0.84	0.85	2	2	20
CW.10.27	4235	4529	408	417	1:3.8:4.4	0.94	0.85	1	1.5	16
CW.13.28	3860	4330	408	433	1:3.9:4.2	0.82	0.82	1.5	1.5	11
CW.13.38	3290	3200	333	367	1:4.0:4.3	0.86	0.83	4.5	2.5	11
CW.14.14	6732	7203	504	541	1:2.2:2.6	0.59	0.59	2	2	13
CW.14.15	2750	3280	342	433	1:4.2:4.4	1.02	1.02	4	5	9
CW.14.16	3170	3230	466	396	1:3.7:3.9	0.81	0.78	5	3	7
CW.14.17	2870	3140	333	371	1:4.2:4.5	0.84	0.84	2	2	8

TABLE 4(a) (Cont'd)

Mark	Compressive Strength f'_c psi		Modulus of Rupture f_r psi		Cement:Sand:Gravel by weight	Water/Cement by weight		Slump in.		Age at Test days
Batch	1	2	1	2	1 and 2	1	2	1	2	
CW.14.18	2950	3100	408	442	1:4.2:4.4	0.94	0.94	6	3.5	7
CW.14.19	2875	3080	333	366	1:4.2:4.6	0.86	0.86	2	1.5	8
CW.14.20	2950	3020	400	-	1:4.2:4.5	0.86	0.86	2	1.5	8
CW.14.21	2580	2990	350	416	1:4.2:4.4	0.86	0.89	1	1.5	8
CW.14.22	4660	4660	484	458	1:2.6:3.1	0.70	0.67	7	7	8
CW.14.23	2800	2690	375	342	1:3.8:4.1	0.87	0.87	1.5	2	7
CW.14.24	2900	2680	416	400	1:3.7:3.9	0.94	0.94	2.5	4	8
CW.14.25	5420	5050	518	492	1:3.2:3.5	0.67	0.67	1	2	11
CW.14.26	2415	2310	410	348	1:4.2:4.5	0.91	0.87	6	2	8
CW.14.35	3260	3420	433	508	1:3.7:4.0	0.87	0.83	6	2	9
CW.14.36	3280	3300	383	425	1:3.7:4.0	0.75	0.75	1	2	8
CW.14.37	4460	3240	408	425	1:4.2:4.5	0.93	0.91	6	1.5	6
CW.14.39	3360	3010	408	425	1:4.2:4.5	0.93	0.91	1	3	8
CW.14.40	3040	3010	421	383	1:3.7:4.0	0.80	0.80	2	2.5	8
CW.14.42	3180	2840	375	342	1:4.2:4.5	0.89	0.89	3	8	8
CW.14.45	3160	2640	333	366	1:4.3:4.5	0.95	0.95	5	3	9
CW.14.47	2635	2535	366	317	1:4.2:4.5	0.91	0.95	1	1	8
CW.14.50	2450	2400	400	367	1:3.9:4.2	0.92	0.88	4.5	2.5	8
CW.14.51	3505	3258	333	266	1:3.9:4.2	0.88	0.89	3	3.5	13
CW.14.54	3501	3300	358	342	1:3.9:4.2	0.82	0.83	2	2.5	8
CW.18.15	7619	7424	633	609	1:2.2:2.6	0.59	0.60	2.5	2.5	19
CW.28.26	3902	3372	433	292	1:3.9:4.2	0.80	0.81	2	3	10
CW.28.28	3172	3083	433	334	1:4.0:4.2	0.86	0.86	2	2.5	8
FW.14.06	3320	3910	425	362	1:4.1:4.3	0.82	0.79	3	2	12
	3000	-	383	-	1:3.9:4.0	0.78	-	2.5	-	6
FW.14.07	4030	3520	433	275	1:4.1:4.3	0.80	0.79	2.5	4.5	15
	3280	-	333	-	1:3.8:4.1	0.75	-	1	-	9

TABLE 4(b)

PROPERTIES OF CONCRETE MIXES: INDIRECT TENSILE STRENGTH

Mark	Indirect Tensile Strength f_b psi		Modulus of Rupture f_r psi	
Batch	1	2	1	2
BW.14.26	409	412	400	400
BW.14.32	314	305	308	350
BW.14.34	380	316	366	358
BW.14.45	324	354	304	304
BW.14.58	413	354	416	358
BW.14.60	297	362	358	350
BW.15.34	424	367	375	392
BW.15.37	356	345	417	392
CW.14.51	292	276	333	266
CW.14.54	336	354	358	342
FW.14.06	211	206	425	362

TABLE 5

PROPERTIES OF REINFORCEMENT

Lot	Manufacturer	Heat Analysis					Diam.	Stress at 1 % Strain	Strength
		C	Mn	P	S	Si			
		%	%	%	%	%	in.	ksi	ksi
8	AS and W	0.83	0.75	0.010	0.035	0.20	0.196	217	255
10	AS and W	0.81	0.76	0.010	0.027	0.23	0.196	222	267
11	AS and W	0.85	0.65	0.010	0.027	0.18	0.196	219	256
12	AS and W	0.88	0.79	0.024	0.033	0.25	0.196	228	255
13	AS and W	0.82	0.72	0.018	0.032	0.21	0.194	218	258
14	Union	0.85	0.84	0.010	0.029	0.18	0.197	242	280

TABLE 6

MEASURED AND COMPUTED FLEXURAL CRACKING MOMENTS

Mark	Prestress in Bottom Fiber f_F^b psi	Modulus of Rupture f_r psi		Computed Flexural Cracking Moment k-in.		Measured Cracking Moment k-in.	Meas./Comp. Flexural Cracking Moment	
		Comp.*	Meas.	Comp. f_r	Meas. f_r		Comp. f_r	Meas. f_r
AD.14.37	988	356	300	208	198	236	1.13	1.19
AW.14.39	1,352	485	510	271	277	196	0.72	0.71
AW.14.76	1,304	355	385	246	251	236	0.96	0.94
AW.24.48	640	466	525	164	173	169	1.03	0.98
AW.24.68	703	342	400	156	164	153	0.98	0.93
B.10.23	1,407	475	425	266	265	298	1.12	1.12
B.10.24	1,066	419	375	206	200	229	1.11	1.14
B.14.34	961	381	340	194	188	188	0.97	1.00
B.14.41	1,210	368	358	231	230	228	0.99	0.99
BD.14.18	1,330	510	519	265	266	267	1.01	1.00
BD.14.19	1,274	519	517	258	258	262	1.01	1.01
BD.14.23	895	438	337	191	177	174	0.91	0.98
BD.14.26	976	402	383	199	196	215	1.08	1.10
BD.14.27	950	421	442	197	200	186	0.94	0.93
BD.14.28	999	438	457	206	209	195	0.95	0.93
BD.14.34	948	356	404	188	195	190	1.01	0.98
BD.14.35	912	348	375	182	186	172	0.98	0.92
BD.14.42	1,189	369	491	228	246	202	0.89	0.82
BD.24.34	904	381	416	189	194	190	1.00	0.98
BV.14.30	1,370	438	346	261	248	268	1.02	1.08
BV.14.32	1,254	438	420	244	241	270	1.11	1.12
BV.14.34	1,392	409	500	259	272	276	1.06	1.01
BV.14.35	1,310	396	508	247	263	288	1.16	1.09
BV.14.42	1,408	380	455	256	267	276	1.08	1.03
BW.10.22	1,058	435	466	213	218	227	1.06	1.04
BW.14.20	786	367	333	161	156	166	1.03	1.06
BW.14.22	1,385	488	517	266	270	277	1.04	1.03
BW.14.23	1,334	481	500	256	259	272	1.06	1.05
BW.14.26	1,060	418	400	208	206	210	1.01	1.02

TABLE 6 (Cont'd)

Mark	Prestress in Bottom Fiber f_F^b psi	Modulus of Rupture f_r psi		Computed Flexural Cracking Moment k-in.		Measured Cracking Moment k-in.	Meas./Comp. Flexural Cracking Moment	
		Comp.*	Meas.	Comp. f_r	Meas. f_r		Comp. f_r	Meas. f_r
BW.14.31	1,336	387	383	244	244	237	0.97	0.97
BW.14.32	1,056	364	308	204	192	214	1.05	1.11
BW.14.34	1,386	401	366	254	249	288	1.13	1.15
BW.14.38	1,374	368	342	250	246	265	1.06	1.08
BW.14.39	1,337	383	358	246	243	258	1.05	1.06
BW.14.41	1,410	378	466	256	268	258	1.01	0.96
BW.14.42	1,396	366	338	253	248	260	1.04	1.06
BW.14.43	1,385	369	346	252	248	258	1.02	1.04
BW.14.45	1,370	381	304	251	240	256	1.02	1.07
BW.14.58	1,840	398	416	328	331	352	1.07	1.06
BW.14.60	1,845	357	358	324	324	330	1.07	1.02
BW.15.34	1,412	410	375	262	256	246	0.94	0.96
BW.15.37	1,410	393	417	258	261	258	1.00	0.99
BW.16.38	1,384	418	383	259	253	267	1.03	1.06
BW.18.15	1,222	530	618	247	259	261	1.06	1.00
BW.18.27	1,379	456	533	265	276	287	1.08	1.04
BW.19.28	1,379	440	444	258	259	279	1.08	1.08
BW.28.26	508	389	458	130	137	145	1.14	1.05
BW.28.28	540	396	450	134	141	155	1.16	1.10
C.10.27	1,110	393	275	210	194	---	---	---
C.10.28	1,282	490	412	249	245	---	---	---
C.13.23	1,100	402	495	216	229	224	1.04	0.98
CD.13.24	1,183	421	467	230	237	226	0.98	0.95
CD.13.25	1,111	403	417	217	219	217	1.00	0.99
CD.14.34	942	352	417	186	195	---	---	---
CW.10.26	1,424	436	456	264	267	265	1.05	1.05
CW.10.27	1,410	439	408	262	258	260	1.05	1.05
CW.13.28	1,430	421	408	260	258	258	0.99	1.00
CW.13.38	1,420	390	333	257	249	264	1.03	1.06
CW.14.14	1,343	520	504	261	259	267	1.02	1.03
CW.14.15	815	358	342	162	160	164	1.01	1.03

TABLE 6 (Cont'd)

Mark	Prestress in Bottom Fiber f_F^b psi	Modulus of Rupture f_r psi		Computed Flexural Cracking Moment k-in.		Measured Cracking Moment k-in.	Meas./Comp. Flexural Cracking Moment	
		Comp.*	Meas.	Comp. f_r	Meas. f_r		Comp. f_r	Meas. f_r
CW.14.16	822	386	466	167	178	169	1.01	0.95
CW.14.17	813	366	333	158	158	166	1.05	1.05
CW.14.18	815	372	408	164	169	167	1.02	0.99
CW.14.19	813	368	333	163	158	168	1.03	1.06
CW.14.20	825	372	400	165	169	176	1.07	1.04
CW.14.21	816	347	350	161	161	175	1.09	1.09
CW.14.22	1,490	456	484	273	277	265	0.97	0.96
CW.14.23	813	362	375	162	164	176	1.09	1.07
CW.14.24	812	369	416	163	169	163	1.00	0.97
CW.14.25	1,489	483	518	277	281	287	1.04	1.02
CW.14.26	819	335	410	160	171	168	1.05	0.98
CW.14.35	1,425	390	433	258	264	261	1.01	0.99
CW.14.36	1,360	392	383	249	248	255	1.02	1.03
CW.14.37	1,460	448	408	271	265	301	1.11	1.14
CW.14.39	1,445	396	408	262	263	269	1.03	1.02
CW.14.40	1,461	380	421	262	267	280	1.07	1.05
CW.14.42	1,405	386	375	254	253	270	1.06	1.07
CW.14.45	1,450	386	333	260	253	252	0.97	1.00
CW.14.47	1,441	351	366	255	264	253	0.99	0.96
CW.14.50	1,475	338	400	258	266	255	0.99	0.96
CW.14.51	1,980	405	333	346	335	393	1.13	1.17
CW.14.54	1,840	405	358	326	319	357	1.09	1.12
CW.18.15	1,467	540	633	281	294	301	1.07	1.02
CW.28.26	567	410	433	136	139	136	1.00	0.98
CW.28.28	622	484	433	155	144	149	0.99	1.03
FW.14.06	1,357**	394	425	373	379	373	1.00	0.98
FW.14.07	1,428**	430	433	395	396	374	0.95	0.95

* Computed using Eq. 1.
** Includes shrinkage stresses.

TABLE 7

MEASURED AND COMPUTED VALUES OF WEB-SHEAR CRACKING LOAD

Mark	Maximum Tensile Stress / Tensile Stress at Centroid	Cracking Tensile Stress at Centroid f_t psi	Tensile* Stress / Modulus of Rupture f_t/f_r	Shear Span a in.	Web-Shear Cracking Shear: Meas.** V_{cm} kips	Comp. V_s kips	Meas./Comp. V_{cm}/V_s
C.10.27a	1.00	310	0.79	22	7.17	7.27	0.99
C.10.27b	-	(355)	(0.90)	14	(7.82)	-	-
C.10.28a	1.00	319	0.73	22	8.90	9.59	0.93
C.10.28b	-	(355)	(0.81)	14	(9.56)	-	-
C.13.23a	1.00	259	0.64	27	6.61	7.91	0.84
C.13.23b	1.00	430	1.07	27	10.0	8.26	1.21
CD.13.24a	1.00	337	0.80	27	9.35*	8.40	1.11
CD.13.24b	1.00	327	0.78	27	7.76*	7.93	0.98
CD.13.25	1.02	367	0.91	27	8.78*	7.95	1.10
CW.10.26a	1.00	391	0.90	22	9.50	8.80	1.08
CW.10.26b	1.00	348	0.80	30	8.74	8.80	0.99
CW.10.26c	-	(448)	(1.03)	14	(10.50)	-	-
CW.10.27	1.00	432	0.98	22	9.84	8.98	1.10
CW.13.28	1.00	408	0.97	28	9.90	8.70	1.14
CW.13.38	1.00	335	0.85	28	8.90	8.40	1.06
CW.14.22	1.00	417	0.92	36	9.45	9.05	1.04
CW.14.35	1.00	227	0.58	36	6.65	8.15	0.82
CW.14.37	1.00	392	0.88	36	9.40	8.78	1.07
CW.14.39	1.00	366	0.92	36	9.10	8.29	1.11
CW.14.42	1.11	394	1.02	36	9.25	7.82	1.18

TABLE 7 (Cont'd)

Mark	Maximum Tensile Stress / Tensile Stress at Centroid	Cracking Tensile Stress at Centroid f_t psi	Tensile Stress* / Modulus of Rupture f_t/f_r	Shear Span a in.	Web-Shear Cracking Shear: Meas.** V_{cm} kips	Web-Shear Cracking Shear: Comp. V_s kips	Web-Shear Cracking Shear: Meas./Comp. V_{cm}/V_s
CW.14.45	1.02	385	1.00	36	8.90	7.66	1.16
CW.14.47	1.02	366	1.04	36	8.80	7.50	1.17
CW.14.50	1.23	309	0.91	36	8.15	7.47	1.09
CW.14.51	1.00	333	0.82	36	9.99	9.80	1.02
CW.14.54	1.00	358	0.88	36	10.05	9.42	1.07
FW.14.06	-	398	1.01	36	10.25	9.33	1.10
FW.14.07	-	433	1.00	36	9.71	9.26	1.05
C.12.32	1.18	237	0.82	36	6.75	6.72	1.00
C.12.33	1.16	440	0.91	36	12.25	11.36	1.08
C.12.40	1.08	178	0.53	36	5.10	6.85	0.74
C.12.44	1.00	236	0.60	36	6.42	7.91	0.81
C.12.50	1.10	321	0.84	36	9.05	8.91	1.01
C.12.57	1.00	357	0.94	36	10.50	9.66	1.09
C.22.40	1.06	340	0.75	36	9.00	9.50	0.95
C.22.73	1.00	256	0.76	36	6.67	6.90	0.97

* Modulus of Rupture computed with Eq. 1.

** Values listed for beams with draped wires are net shears at cracking.

TABLE 8(a)

SHEAR AT INCLINED CRACKING: BEAMS TESTED WITH STATIONARY LOADS

Mark	Initiating Cracking Shear V_f kips	Web-Shear Cracking Shear V_s kips	Inclined Cracking Shear: Comp. V_c kips	Inclined Cracking Shear: Meas. V_{cm} kips	Inclined Cracking Shear: Meas./Comp.	Type of* Cracking: Observed	Type of* Cracking: Predicted
AD.14.37(a)	6.70	20.18	8.04	6.55	0.81	F	F
(b)	7.65	20.18	8.99	9.45	1.05	F	F
AW.14.39	10.00	29.60	11.97	11.25	0.94	F	F
AW.14.76	9.00	23.65	10.58	10.60	1.00	F	F
AW.24.48	5.96	23.62	7.54	10.02	1.33	F	F
AW.24.68	5.66	19.00	6.93	8.21	1.18	F	F
B.14.34	7.19	11.46	7.95	8.49	1.07	F	F
B.14.41	8.56	12.42	9.39	9.21	0.98	F	F
BD.14.18	9.34	15.27	10.36	10.85	1.05	F	F
BD.14.19	8.81	15.37	9.83	11.16	1.13	F	F
BD.14.23	5.43	12.81	6.28	5.60	0.89	F	F
BD.14.26	6.04	12.26	6.86	6.38	0.93	F	F
BD.14.27	7.00	12.61	7.84	8.95	1.14	F	F
BD.14.28	7.41	13.25	8.29	(10.00)	1.20	-	F
BD.14.34	6.75	11.19	7.50	7.90	1.05	F	F
BD.14.35	5.96	10.70	6.67	6.49	0.97	F	F
BD.14.42	8.08	11.89	8.87	9.95	1.12	F	F
BD.24.32	6.15	11.56	6.92	7.45	1.08	F	F
BV.14.30	9.15	14.18	10.09	10.20	1.01	F	F
BV.14.32	8.60	13.18	9.48	10.37	1.09	F	F
BV.14.34	9.05	13.86	9.97	10.48	1.05	F	F
BV.14.35	8.19	12.91	9.05	9.80	1.08	F	F
BV.14.42	8.40	12.60	9.24	9.60	1.04	F	F
BW.14.20	5.96	10.49	6.66	(8.25)	1.24	-	F
BW.14.22	9.85	15.50	10.88	10.60	0.97	F	F
BW.14.23	9.48	15.34	10.50	10.25	0.98	F	F
BW.14.26	7.70	12.25	8.52	7.99	0.94	F	F
BW.14.31	9.04	13.10	9.91	10.20	1.03	F	F
BW.14.32	7.55	11.20	8.30	9.54	1.15	F	F
BW.14.34	9.41	13.10	10.28	10.37	1.01	F	F
BW.14.38	9.26	12.56	10.10	10.40	1.03	F	F
BW.14.39	9.10	12.56	9.94	10.50	1.06	F	F
BW.14.41	9.48	12.84	10.34	9.90	0.96	F	F

TABLE 8(a) (Cont'd)

Mark	Initiating Cracking Shear V_f kips	Web-Shear Cracking Shear V_s kips	Inclined Cracking Shear: Comp. V_c kips	Inclined Cracking Shear: Meas. V_{cm} kips	Inclined Cracking Shear: Meas./Comp.	Type of* Cracking: Observed	Type of* Cracking: Predicted
BW.14.42	9.36	12.55	10.20	9.35	0.92	F	F
BW.14.43	9.32	12.60	10.16	10.70	1.05	F	F
BW.14.45	9.30	13.20	10.18	9.90	0.97	F	F
BW.14.58	12.15	14.50	13.12	14.00	1.07	F	F
BW.14.60	12.00	13.30	12.89	12.76	0.99	F	F
BW.15.34	7.08	13.81	8.00	8.15	1.02	F	F
BW.15.37	6.96	13.41	7.88	8.35	1.06	F	F
BW.16.38	6.16	14.01	7.09	7.00	0.99	F	F
BW.18.15 S	8.63	15.85	9.69	9.50	0.98	F	F
L	4.46	15.85	5.52	5.93	1.07	F	F
BW.18.27 S	9.25	14.85	10.24	10.80	1.05	F	F
L	4.80	14.85	5.79	5.63	0.97	F	F
BW.19.28 S	11.71	15.15	12.72	12.81	1.01	F	F
L	4.16	15.15	5.17	5.28	1.02	F	F
BW.28.26 S	4.55	11.10	5.29	6.18	1.17	F	F
L	2.35	11.10	3.09	3.43	1.11	F	F
BW.28.28 S	4.84	11.70	5.62	5.75	1.02	F	F
L	2.50	11.70	3.38	3.46	1.02	F	F
C.13.23(a)	11.12	7.91	7.91	6.61	0.84	W	W
(b)	11.12	8.26	8.26	10.00	1.21	W	W
CD.13.24(a)	11.35	8.40	9.74	10.69	1.10	W	W
(b)	11.35	7.93	9.27	9.10	0.98	W	W
CD.13.25	10.81	7.95	9.06	9.89	1.09	W	W
CD.14.34	6.70	5.85	6.59	5.45	0.83	W	W
CW.13.28	12.79	8.70	8.70	9.90	1.14	W	W
CW.13.38	12.65	8.40	8.40	8.90	1.06	W	W
CW.14.14	9.67	9.65	9.65	9.60	0.99	F	W
CW.14.15	6.00	6.30	6.30	6.25	0.99	F	F
CW.14.16	6.19	6.86	6.65	6.75	1.02	F	F
CW.14.17	5.85	6.63	6.29	5.95	0.95	F	F
CW.14.18	6.08	6.50	6.50	6.50	1.00	F	F
CW.14.19	6.04	6.72	6.49	6.94	1.07	F	F
CW.14.20	6.11	6.50	6.50	6.45	0.99	F	F

TABLE 8(a) (Cont'd)

Mark	Initiating Cracking Shear V_f	Web-Shear Cracking Shear V_s	Inclined Cracking Shear			Type of* Cracking	
			Comp. V_c	Meas. V_{cm}	Meas. / Comp.	Observed	Predicted
CW.14.21	5.96	6.17	6.17	6.05	0.98	F	F
CW.14.22	10.10	9.05	9.05	9.45	1.04	W	W
CW.14.23	6.00	6.55	6.44	7.40	1.14	F	F
CW.14.24	6.04	6.64	6.48	6.20	0.96	F	F
CW.14.25	10.25	9.89	9.89	10.50	1.06	F	W
CW.14.26	5.92	5.99	5.99	6.45	1.08	F	F
CW.14.35	9.56	8.15	8.15	6.65	0.82	W	W
CW.14.36	9.22	8.29	8.29	8.65	1.04	F	W
CW.14.37	10.05	8.78	8.78	9.40	1.07	W	W
CW.14.39	9.70	8.29	8.29	9.10	1.11	W	W
CW.14.40	9.70	8.08	8.08	9.15	1.13	F	W
CW.14.42	9.40	7.82	7.82	9.25	1.18	W	W
CW.14.45	9.64	7.66	7.66	8.90	1.16	W	W
CW.14.47	9.45	7.36	7.50	8.80	1.17	W	W
CW.14.50	9.56	7.47	7.47	8.15	1.09	W	W
CW.14.51	12.80	9.80	9.80	9.99	1.02	W	W
CW.14.54	12.09	9.42	9.42	10.05	1.07	W	W
CW.18.15 S	9.80	10.21	10.21	9.55	0.93	F	F
L	5.09	10.21	5.77	5.20	0.90	F	F
CW.28.26 S	4.75	6.75	5.20	5.74	1.10	F	F
L	2.46	6.75	2.91	2.88	0.99	F	F
CW.28.28 S	5.27	6.70	5.72	5.75	1.00	F	F
L	2.74	6.70	3.19	2.83	0.89	F	F
FW.14.06	13.80	9.33	9.33	10.25	1.10	W	W
FW.14.07	14.25	9.26	9.26	9.71	1.05	W	W

* F:Flexure-shear crack; W:Web-shear crack; -:No inclined crack.

TABLE 8(b)

SHEAR AT INCLINED CRACKING: PRESTRESSED BEAMS
FROM REFERENCE 2

Mark	Initiating Cracking Shear V_f kips	Web-Shear Cracking Shear V_s kips	Inclined Cracking Shear			Type of* Cracking	
			Comp. V_c kips	Meas. V_{cm} kips	Meas. / Comp.	Observed	Predicted
A.11.43	7.60	42.5	10.43	9.50	0.91	F	F
A.11.51	4.65	26.2	6.40	6.50	1.02	F	F
A.11.53	6.50	49.9	9.82	8.50	0.87	F	F
A.11.96	7.29	31.7	9.40	8.50	0.90	F	F
A.12.23	9.47	36.4	11.89	11.50	0.97	F	F
A.12.31	8.85	28.1	10.72	10.00	0.93	F	F
A.12.34	11.73	44.6	14.71	14.00	0.95	F	F
A.12.36	8.19	28.7	10.10	10.40	1.03	F	F
A.12.42	11.19	41.3	13.94	13.50	0.97	F	F
A.12.46	10.42	37.2	12.90	11.50	0.89	F	F
A.12.48	11.81	39.0	14.41	(15.05)	1.04	-	F
A.12.53	8.00	23.2	9.55	9.00	0.94	F	F
A.12.56	10.13	26.6	11.90	11.00	0.92	F	F
A.12.60	11.32	32.4	13.48	13.50	1.00	F	F
A.12.69	8.85	29.6	10.82	10.50	0.97	F	F
A.12.73	10.30	32.9	12.49	11.50	0.92	F	F
A.12.81	9.85	28.8	11.77	10.75	0.91	F	F
A.14.39	11.00	27.6	12.84	14.00	1.09	F	F
A.14.44	11.62	28.4	13.51	13.75	1.02	F	F
A.14.55	14.30	30.0	16.30	16.50	1.01	F	F
A.14.68	11.76	25.0	13.43	14.50	1.08	F	F
A.21.29	2.74	23.3	4.29	3.50	0.82	F	F
A.21.39	3.00	23.4	4.56	4.00	0.88	F	F
A.21.51	5.10	35.5	7.46	7.00	0.94	F	F
A.22.20	4.89	30.4	6.91	6.00	0.87	F	F
A.22.24	4.00	23.5	5.57	5.00	0.90	F	F
A.22.26	4.55	24.2	6.16	7.00	1.03	F	F
A.22.27	4.40	25.4	6.09	6.00	0.99	F	F
A.22.28	4.40	23.8	5.99	5.50	0.92	F	F
A.22.31	5.07	25.7	6.78	5.65	0.83	F	F
A.22.34	5.00	26.6	6.77	6.50	0.96	F	F
A.22.36	5.74	23.0	7.27	6.00	0.83	F	F
A.22.39	3.59	19.2	4.87	5.00	1.03	F	F
A.22.40	7.85	36.1	10.26	10.50	1.02	F	F
A.22.49	6.77	27.6	8.61	8.00	0.93	F	F

TABLE 8(b) (Cont'd)

Mark	Initiating Cracking Shear V_f kips	Web-Shear Cracking Shear V_s kips	Inclined Cracking Shear: Comp. V_c kips	Inclined Cracking Shear: Meas. V_{cm} kips	Inclined Cracking Shear: Meas./Comp.	Type of* Cracking: Observed	Type of* Cracking: Predicted
B.11.07	4.57	14.70	5.55	(6.28)	1.13+	-	F
B.11.20	5.20	14.70	6.18	6.00	0.97	F	F
B.11.29	6.29	14.21	7.24	6.75	0.93	F	F
B.11.40	8.66	16.00	9.73	8.90	0.92	F	F
B.12.07	7.26	14.60	8.23	(9.10)	1.11+	-	F
B.12.10	6.81	13.29	7.69	7.00	0.91	F	F
B.12.12	6.75	12.30	7.57	7.45	0.99	F	F
B.12.14	6.52	11.76	7.30	7.06	0.97	F	F
B.12.19	6.26	10.40	6.95	7.15	1.03	F	F
B.12.26	8.90	14.25	9.85	9.17	0.93	F	F
B.12.29	9.40	14.51	10.37	9.80	0.95	F	F
B.12.34	11.95	16.90	13.08	12.55	0.96	F	F
B.12.35	9.37	13.56	10.27	9.00	0.88	F	F
B.12.50	11.26	13.40	12.15	11.43	0.94	F	F
B.12.61	12.00	14.80	12.99	11.93	0.92	F	F
B.13.07	9.75	14.98	10.75	(11.74)	1.09+	-	F
B.13.16	11.20	14.81	12.19	12.35	1.01	F	F
B.13.26	13.02	15.20	14.03	13.20	0.94	F	F
B.13.41	17.90	16.58	16.58	15.05	0.90	F	W
B.21.26	3.79	11.80	4.58	4.28	0.94	F	F
B.22.09	4.83	12.00	5.65	6.35	1.12	F	F
B.22.23	5.81	12.59	6.65	6.40	0.96	F	F
B.22.30	4.63	10.61	5.34	5.50	1.03	F	F
B.22.41	5.30	11.47	6.06	6.00	1.01	F	F
B.22.65	5.07	9.05	5.67	5.40	0.95	F	F
B.22.68	7.44	11.74	8.22	7.85	0.95	F	F
C.12.09	7.15	8.29	7.70	7.25	0.94	F	F
C.12.18	7.70	8.30	8.25	7.25	0.88	F	F
C.12.19	9.52	9.57	9.57	8.50	0.89	F	F
C.12.32	7.70	6.72	6.72	6.75	1.00	W	W
C.12.33	15.00	11.36	11.36	12.25	1.08	W	W
C.12.40	7.55	6.85	6.85	5.10	0.74	W	W
C.12.44	8.51	7.91	7.91	6.42	0.81	W	W
C.12.50	11.60	8.91	8.91	9.05	1.01	W	W
C.12.57	13.30	9.66	9.66	10.50	1.09	W	W
C.22.29	3.58	5.28	3.93	3.75	0.95	F	F
C.22.31	5.55	6.75	6.00	5.75	0.96	F	F

TABLE 8(b) (Cont'd)

Mark	Initiating Cracking Shear V_f kips	Web-Shear Cracking Shear V_s kips	Inclined Cracking Shear			Type of* Cracking	
			Comp. V_c kips	Meas. V_{cm} kips	Meas. / Comp.	Observed	Predicted
C.22.36	6.18	7.39	6.67	5.30	0.80	F	F
C.22.39	3.54	3.74	3.74	3.60	0.96	F	F
C.22.40	11.20	9.50	9.50	9.00	0.95	W	W
C.22.46	6.75	7.32	7.24	6.00	0.83	F	F
C.22.62	4.63	6.35	5.05	4.25	0.84	F	F
C.22.73	8.20	6.90	6.90	6.67	0.97	W	W

*F:Flexure-shear crack; W:Web-shear crack; -:No inclined crack.

TABLE 9

EFFECT OF DRAPED REINFORCEMENT ON SHEAR AT INCLINED CRACKING

(a) Web-Shear Cracking

Mark	Measured Total Cracking Shear V_{cm} kips	Vertical Component of Prestress V_d kips	Net Cracking Shear V_n kips	Computed Cracking Shear V_s kips	Meas. Cracking Shear / Comp. Cracking Shear V_{cm}/V_s	V_n/V_s	Drape Angle φ deg.
CD.13.24(a)	10.69	1.34	9.35	8.40	1.27	1.11	3.40
CD.13.24(b)	9.10	1.34	7.76	7.93	1.15	0.98	3.40
CD.13.25	9.89	1.11	8.78	7.95	1.24	1.10	2.85
CD.14.34	5.45	0.74	4.71	5.85	0.93	0.81	1.88

(b) Flexure-Shear Cracking

Mark	Cracking Shear: Computed for Straight Wires V'_c kips	Cracking Shear: Measured V_{cm} kips	$\frac{V_{cm}}{V'_c}$	Drape Shear $\frac{A_s f_{se} \sin\varphi}{V_d}$ kips	Net Shear V_n kips	$\frac{V_n}{V'_c}$	Drape Angle φ deg.
AD.14.37(a)	9.04	6.55	0.72	2.75	3.80	0.42	6.45
AD.14.37(b)	10.12	9.45	0.93	2.75	6.70	0.66	6.45
BD.14.18	10.84	10.85	1.00	1.31	9.54	0.88	2.70
BD.14.19	10.58	11.16	1.05	2.45	8.21	0.82	5.00
BD.14.23	7.92	5.60	0.71	2.86	2.74	0.34	9.13
BD.14.26	8.19	6.38	0.78	3.63	2.75	0.34	9.95
BD.14.27	8.14	8.95	1.10	0.78	8.17	1.00	2.22
BD.14.28	8.51	-	1.16+	0.57	-	1.09+	1.53
BD.14.34	7.71	7.90	1.02	0.79	7.11	0.92	1.88
BD.14.35	7.45	6.49	0.87	2.14	4.35	0.58	6.28
BD.14.42	9.23	9.95	1.08	1.07	8.88	0.96	2.38
BD.24.32	7.77	7.45	0.96	2.20	5.25	0.68	6.45
BV.14.30	10.61	10.20	0.96	1.67	8.53	0.80	3.25
BV.14.32	9.92	10.37	1.04	1.34	9.03	0.91	3.25
BV.14.34	10.51	10.48	1.00	1.36	9.12	0.87	2.70
BV.14.35	10.01	9.80	0.98	2.84	6.96	0.71	5.37
BV.14.42	10.32	9.60	0.93	3.29	6.31	0.66	6.81

TABLE 10

SHEAR AT FLEXURE-SHEAR CRACKING LOAD: MOVING LOADS

Mark	Load Position	Initiating Cracking Shear V_f kips	Web-Shear Cracking Shear V_s kips	Inclined Cracking Shear		
				Comp. V_c kips	Meas. V_{cm} kips	Meas./Comp. V_{cm}/V_c
B.10.23	4	9.28	15.52	10.32	9.85	0.95
	5	7.53	15.52	8.57	8.35	0.975
	6	6.34	15.52	7.38	6.93	0.94
B.10.24	3	9.36	13.12	10.24	10.09	0.99
	4	7.18	13.12	8.06	7.93	0.98
	5	5.83	13.12	6.71	6.59	0.98
	6	4.90	13.12	5.78	6.26	1.08
	7	5.83	13.12	6.71	6.59	0.98
	8	7.18	13.12	8.06	7.93	0.98
BW.10.22	3	9.69	13.80	10.61	10.80	1.02
	4	7.44	13.80	8.36	8.46	1.01
	5	6.03	13.80	6.95	6.70	0.96
	6	5.08	13.80	6.00	5.85	0.98
	7	6.03	13.80	6.95	7.45	1.07
	8	7.44	13.80	8.36	8.46	1.01
CW.10.26*	4	9.04	8.80	9.63	9.42	0.98
	6	6.12	8.80	6.71	6.00	0.89
	8	9.04	8.80	9.63	9.42	0.98
CW.10.27*	6	6.10	8.84	6.75	5.92	0.88
	7	7.25	8.84	7.90	7.30	0.92

* Other cracks occurred in these beams during very large increases in load.

TABLE 11

COMPUTED AND MEASURED CAPACITIES

Mark	Steel Stress at Ultimate		Total Ult. Bending Moment			$\frac{M_{ut}}{M_{uf}}$	$\frac{M_{ut}}{M_{us}}$ **	Failure Mode***	
	Meas. $f_{su\,m}$ ksi	Comp. $f_{su\,c}$ ksi	Comp. for Flexure M_{uf} k-in.	Comp. for Shear M_{us} k-in.	Meas. from Tests M_{ut} k-in.			Obs.	Pred.
AD.14.37a	123	225	480	-	242	0.51	-	S	S
b	-	-	480	-	307	0.64	-	S	S
AW.14.39	-	218	568	725	512	0.90	-	F	F
AW.14.76	-	202	475	665	410	0.86	-	F	F
AW.24.48	-	206	523	556	528	1.01	-	F	F
AW.24.68	179	189	468	534	446	0.95	-	F	F
B.10.23	202	240	523	-	417	0.80	-	S	S
B.10.24	211	242	400	-	384	0.83	-	S	S
B.14.34	210	237	390	-	328	0.84	-	S	S
B.14.41	175	230	465*	-	354	0.76	-	S	S
BD.14.18	217	235	513	-	448	0.87	-	S	S
BD.14.19	192	242	543	-	410	0.76	-	S	S
BD.14.23	119	231	385	-	208	0.54	-	S	S
BD.14.26	132	230	381	-	236	0.62	-	S	S
BD.14.27	220	230	380	-	354	0.93	-	S	S
BD.14.28	222	230	379	-	366	0.97	-	F	S
BD.14.34	206	227	374	-	324	0.87	-	S	S
BD.14.35	141	227	368	-	240	0.65	-	S	S
BD.14.42	175	224	457*	-	363	0.79	-	S	S
BD.24.32	159	225	486	-	330	0.68	-	S	S
BV.14.30	210	227	490	489	450	0.92	0.92	B	S
BV.14.32a	224	235	506*	487	466	0.92	0.96	B	S
BV.14.32b	-	238	520	487	520	1.00	-	F	S
BV.14.34	225	233	493*	499	470	0.95	-	F	F
BV.14.35	227	232	492*	505	461	0.94	-	F	F
BV.14.42	207	221	453*	490	450	0.99	-	F	F
BW.10.22	231	243	408	410	402	0.99	0.98	F	F
BW.14.20	225	248	290	298	297	1.02	-	F	F
BW.14.22	226	230	508	521	510	1.00	-	F	F
BW.14.23	232	240	522	525	509	0.97	-	F	F
BW.14.26	237	255	422	422	412	0.98	0.98	T	F

TABLE 11 (Cont'd)

Mark	Steel Stress at Ultimate		Total Ult. Bending Moment			$\frac{M_{ut}}{M_{uf}}$	$\frac{M_{ut}}{M_{us}}$ **	Failure Mode ***	
	Meas. $f_{su\,m}$ ksi	Comp. $f_{su\,c}$ ksi	Comp. for Flexure M_{uf} k-in.	Comp. for Shear M_{us} k-in.	Meas. from Tests M_{ut} k-in.			Obs.	Pred.
BW.14.31	212	227	488	507	473	0.98	-	F	F
BW.14.32	221	228	368	366	378	1.03	-	F	S
BW.14.34	206	226	476	427	466	0.98	1.09	S	S
BW.14.38	218	228	476*	469	477	1.00	1.02	S	S
BW.14.39	221	227	470*	528	477	1.01	-	F	F
BW.14.41	202	224	465*	502	438	0.94	-	F	F
BW.14.42	200	223	454*	497	438	0.97	-	F	F
BW.14.43	213	223	454*	566	452	1.00	-	F	F
BW.14.45	193	215	439*	500	447	1.02	0.89	T	F
BW.14.58	174	193	563*	575	551	0.98	0.96	S	F
BW.14.60	180	194	559*	568	525	0.94	0.92	S	F
BW.15.34	213	226	486	506	477	0.98	-	F	F
BW.15.37	-	222	468*	548	472	1.01	-	F	F
BW.16.38	205	222	463*	514	469	1.01	-	F	F
BW.18.15S	223	236	520	514	522	1.00	1.02	S	S
L				534			-	-	F
BW.18.27S	232	237	516	600	516	1.00	-	F	F
L				552			-	F	F
BW.19.28S	235	238	519	548	517	1.00	-	F	F
L				549		0.92	-	F	F
BW.28.26S	206	230	377	368	390	1.03	1.01	T	S
L				385		0.96	1.06	-	F
BW.28.28S	212	229	370	380	393	1.06	-	F	F
L				395		0.98	-	F	F
C.10.27	130	241	398	-	227	0.57	-	S	S
C.10.28	165	237	512	-	311	0.61	-	S	S
C.13.23	128	241	409	-	270	0.66	-	S	S
CD.13.24	130	242	420	-	281	0.67	-	S	S
CD.13.25	131	241	412	-	315	0.76	-	S	S
CD.14.34	128	227	378	-	202	0.53	-	S	S
CW.10.26	218	238	511	568	492	0.96	-	F	F
CW.10.27	229	238	510	569	500	0.98	-	F	F

TABLE 11 (Cont'd)

Mark	Steel Stress at Ultimate		Total Ult. Bending Moment			$\frac{M_{ut}}{M_{uf}}$	$\frac{M_{ut}}{M_{us}}$ **	Failure Mode ***	
	Meas. $f_{su\,m}$ ksi	Comp. $f_{su\,c}$ ksi	Comp. for Flexure M_{uf} k-in.	Comp. for Shear M_{us} k-in.	Meas. from Tests M_{ut} k-in.			Obs.	Pred.
CW.13.28	218	228	495	438	495	1.00	1.13	S	S
CW.13.38	208	225	475	490	466	0.98	-	F	F
CW.14.14	237	243	540	545	515	0.95	-	F	F
CW.14.15	-	250	296	492	294	0.99	-	F	F
CW.14.16	219	238	281	316	288	1.02	-	F	F
CW.14.17	228	249	294	284	284	0.97	1.00	S	S
CW.14.18	238	249	294	577	296	1.01	-	F	F
CW.14.19	237	249	292	342	297	1.02	-	F	F
CW.14.20	-	248	292	344	295	1.01	-	F	F
CW.14.21	236	248	293	299	289	0.99	0.97	T	F
CW.14.22	221	239	524	496	498	0.95	1.00	S	S
CW.14.23	240	247	289	301	287	0.99	0.95	S	F
CW.14.24	238	247	289	351	289	1.00	-	F	F
CW.14.25	223	230	510	608	512	1.00	-	F	F
CW.14.26	240	245	284	361	296	1.04	-	F	F
CW.14.35	213	226	480	546	464	0.97	0.85	T	F
CW.14.36	226	231	481*	562	484	1.00	-	F	F
CW.14.37	208	229	474*	445	464	0.98	1.04	S	S
CW.14.39	180	224	466*	404	394	0.84	0.98	S	S
CW.14.40	215	223	464*	669	473	1.02	-	F	F
CW.14.42	220	220	451*	481	466	1.03	-	F	F
CW.14.45	190	215	440*	527	420	0.96	-	F	F
CW.14.47	200	211	431*	440	430	1.00	0.98	S	F
CW.14.50	185	207	421*	488	437	1.04	0.90	S	F
CW.14.51	158	200	566*	477	466	0.82	0.98	S	S
CW.14.54	145	197	560*	463	484	0.86	1.05	S	S
CW.18.15S	222	235	509	598	522	1.03	-	F	F
L				616			-	F	F
CW.28.26S	203	228	369	389	374	1.01	0.96	T	F
L				396				F	F
CW.28.28S	211	227	368	423	393	1.07	-	F	F
L				401			-	F	F
FW.14.06	223	256	741	645	655	0.88	1.02	S	S
FW.14.07	256	256	741	758	711	0.96	-	F	F

* Value compensated for non-rectangular compression zone

** Tabulated for shear and transition failures only.

*** F:Flexural failure, S:Shear failure, T:Transition failure, B:Bond failure.

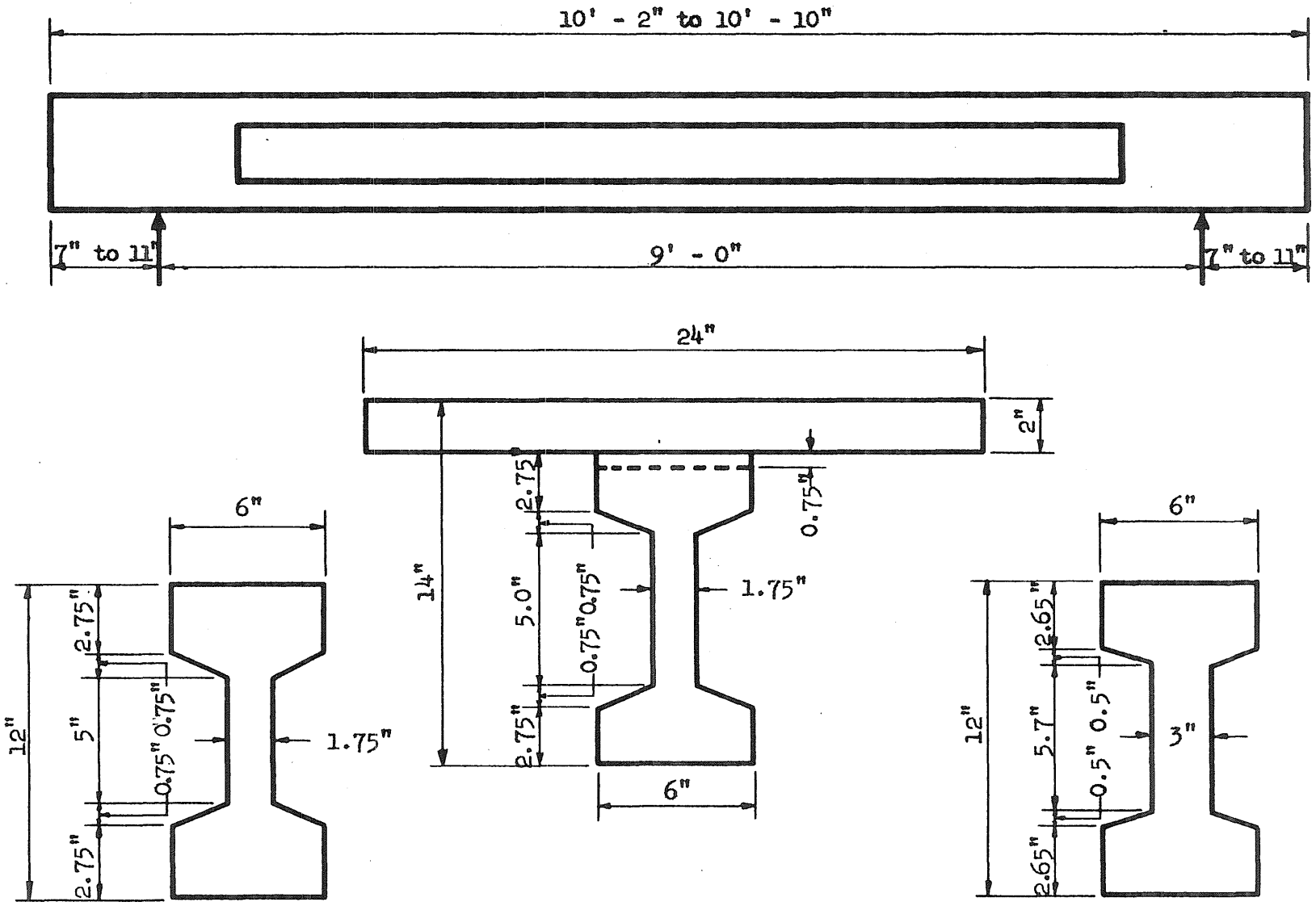

FIG. 1 NOMINAL DIMENSIONS OF BEAMS

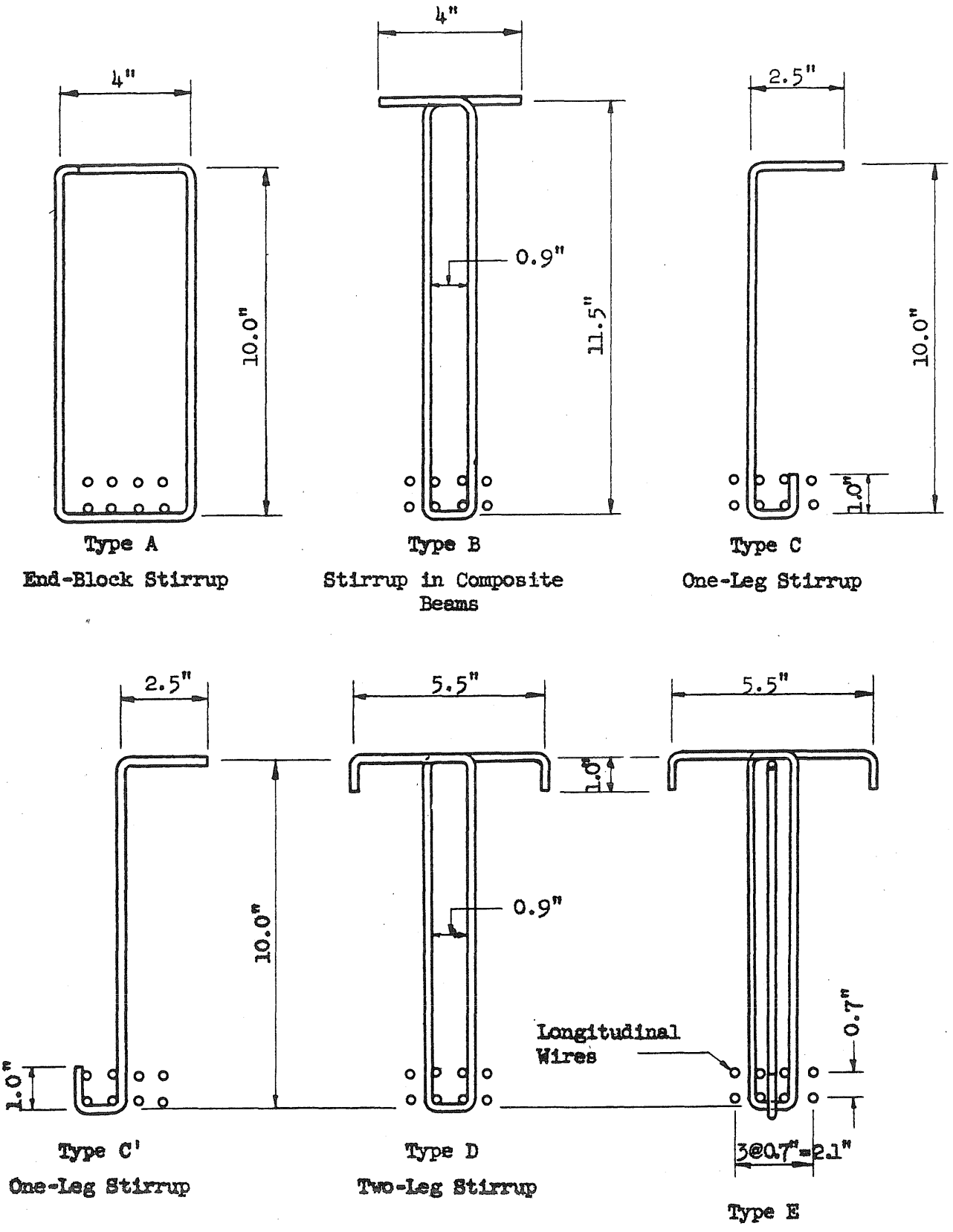

FIG. 2 NOMINAL DIMENSIONS OF STIRRUPS

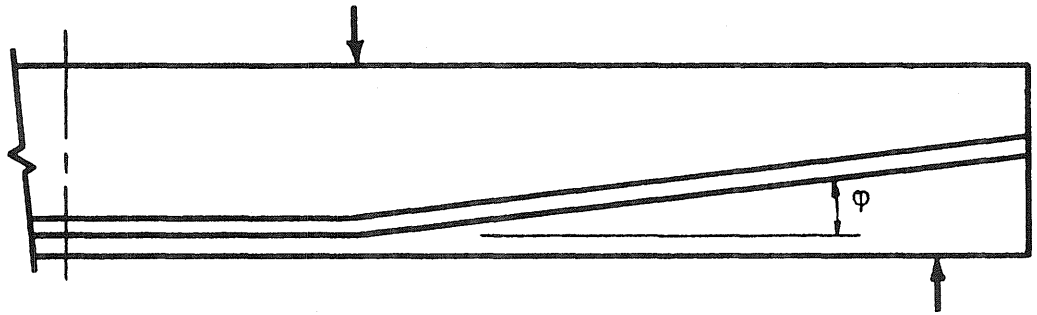

Drape Profiles A Through G

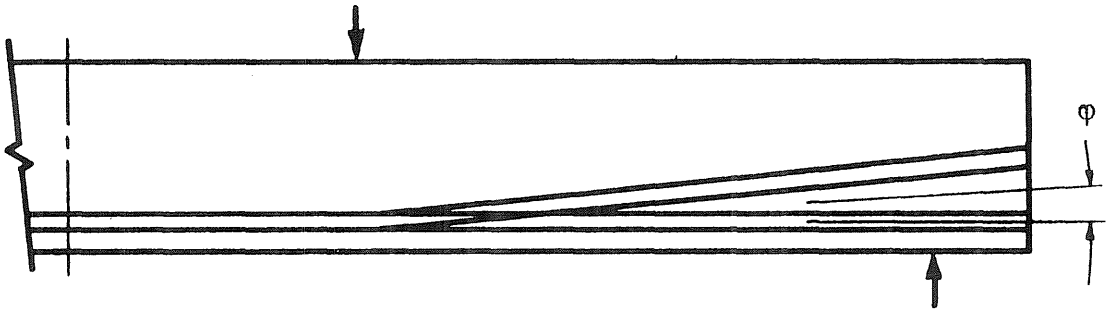

Drape Profiles W Through Z

FIG. 3 TYPICAL DRAPE PROFILES

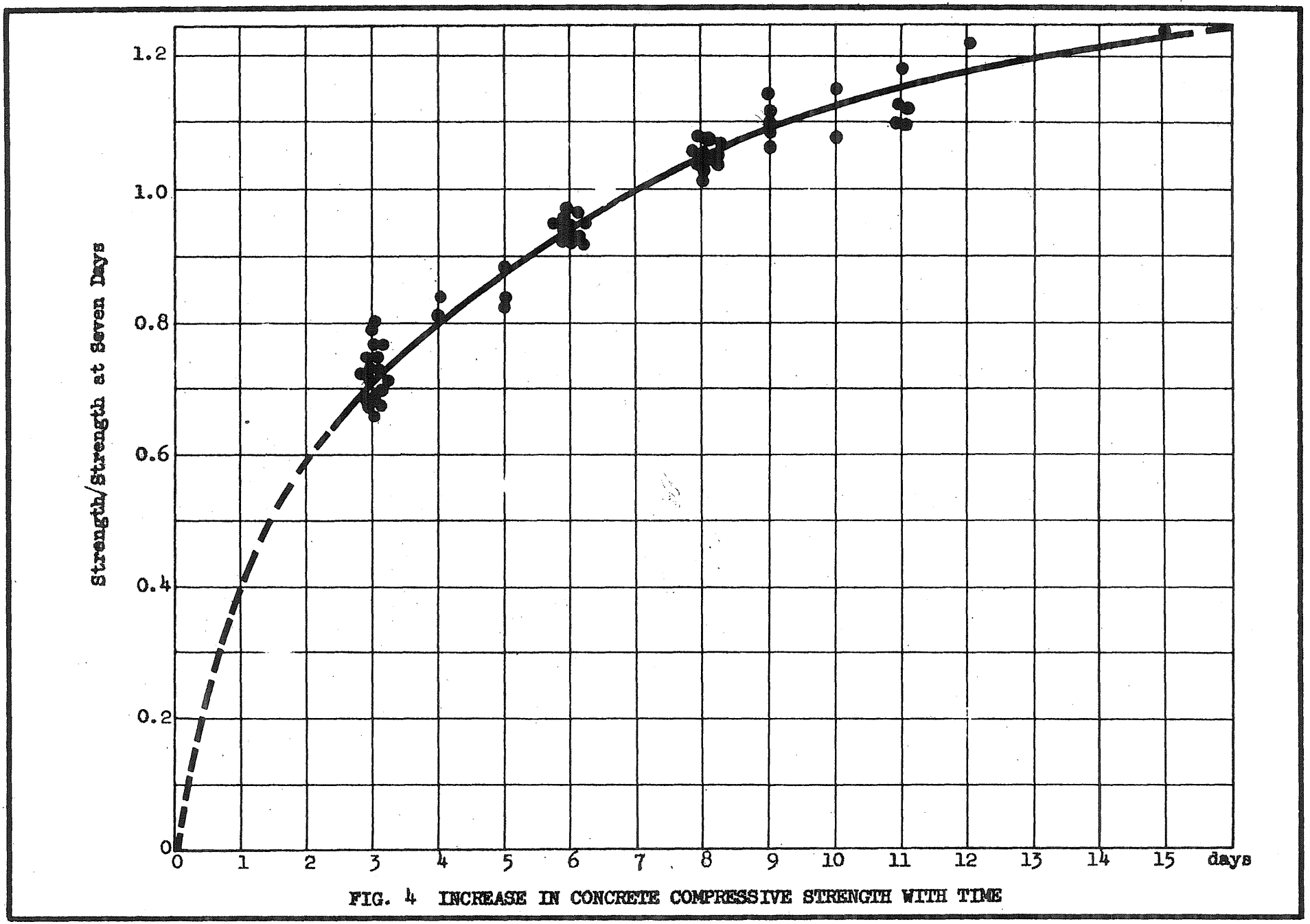

FIG. 4 INCREASE IN CONCRETE COMPRESSIVE STRENGTH WITH TIME

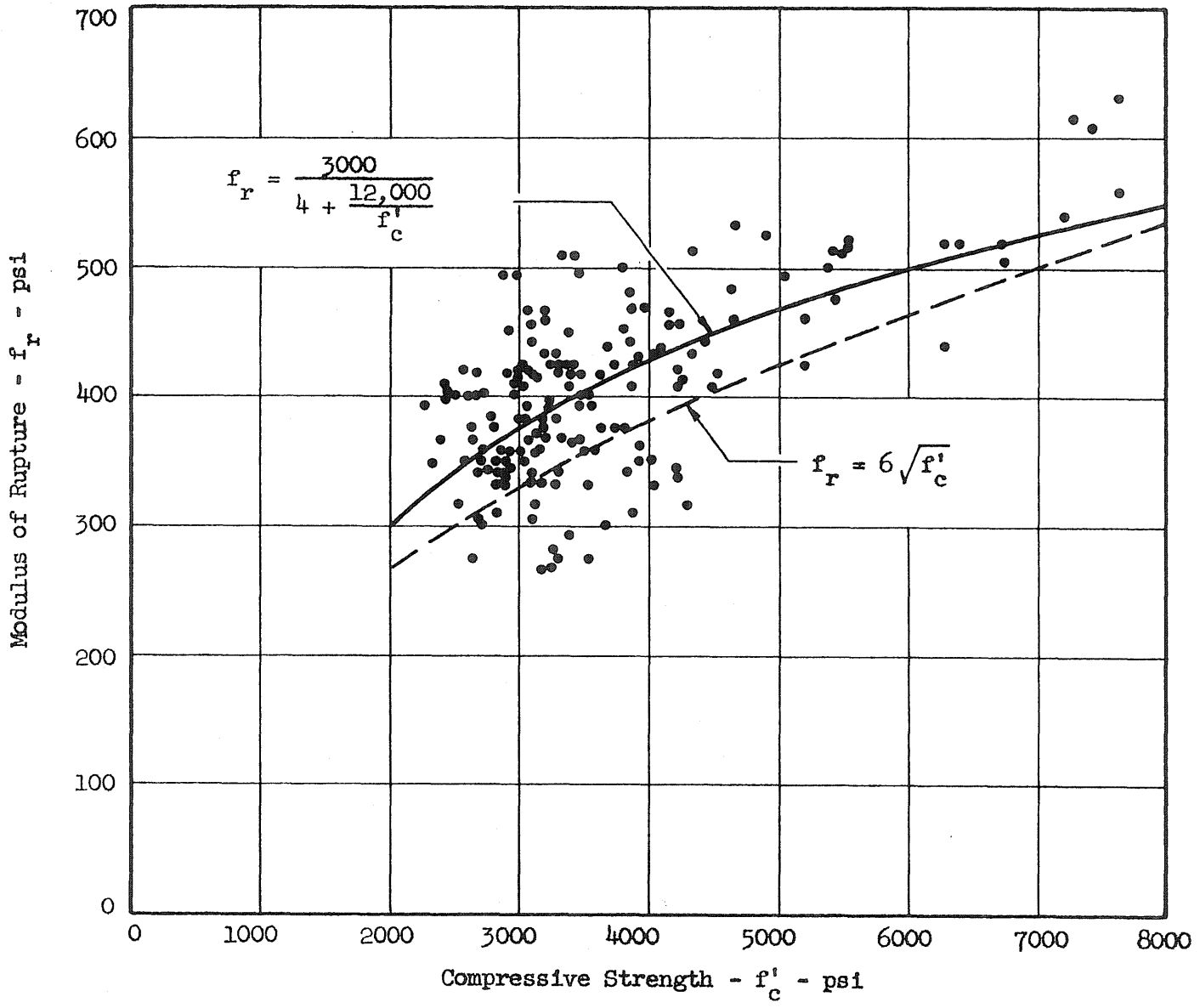

FIG. 5 RELATIONSHIP BETWEEN MODULUS OF RUPTURE AND COMPRESSIVE STRENGTH OF CONCRETE

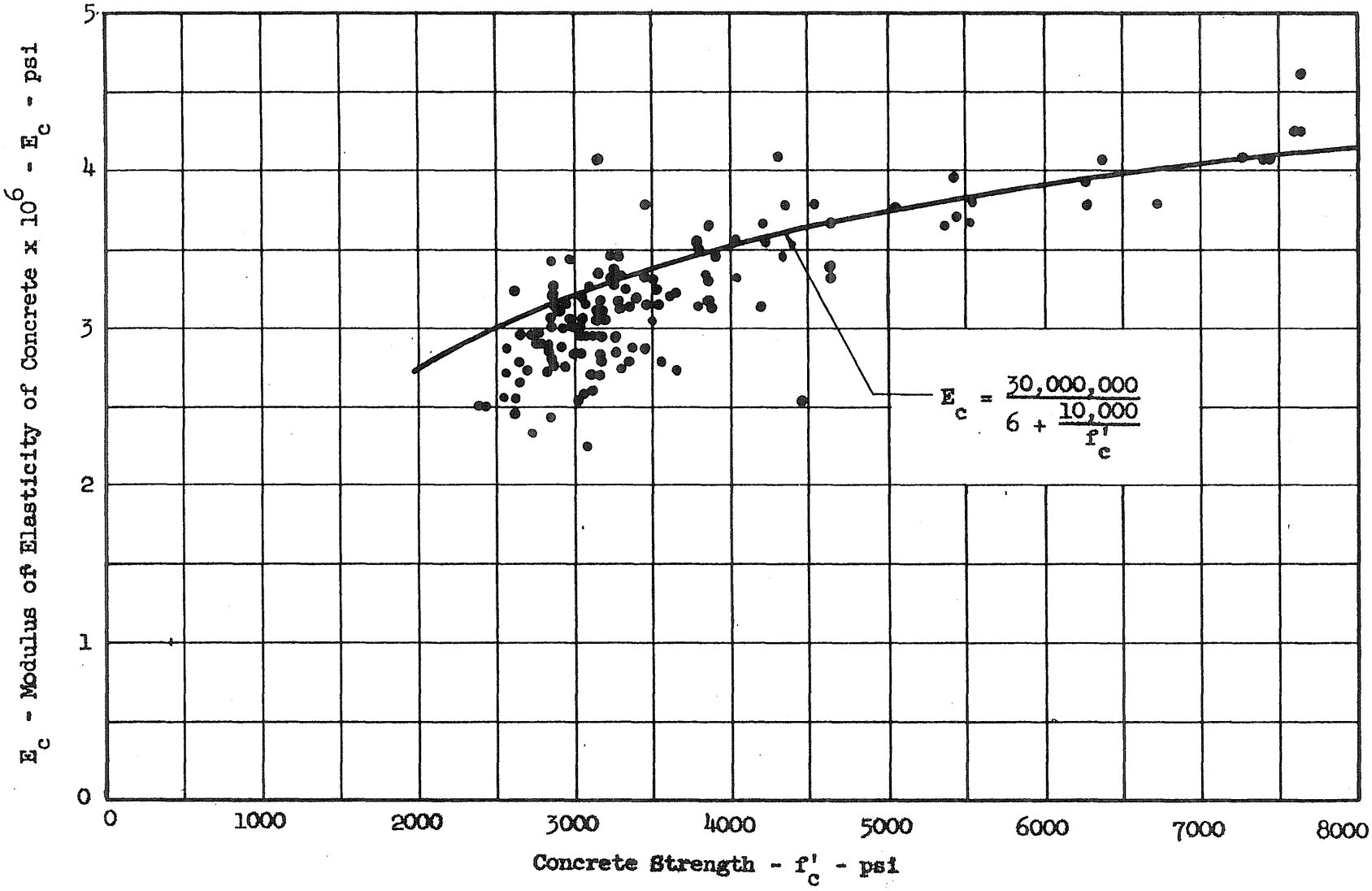

FIG. 6 RELATIONSHIP BETWEEN MODULUS OF ELASTICITY AND CONCRETE STRENGTH

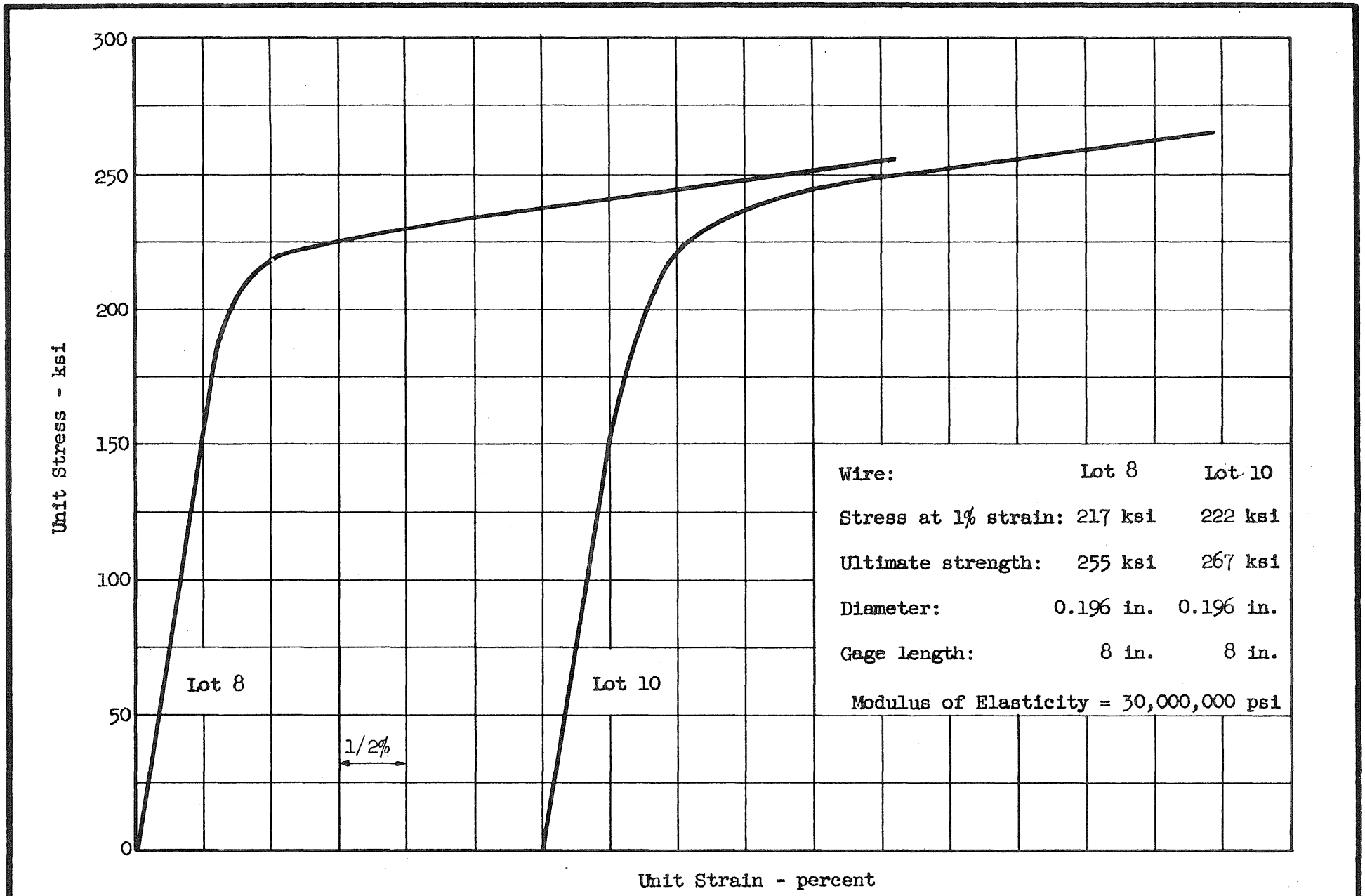

FIG. 7 STRESS-STRAIN RELATIONSHIP FOR LOT 8 AND LOT 10 WIRE

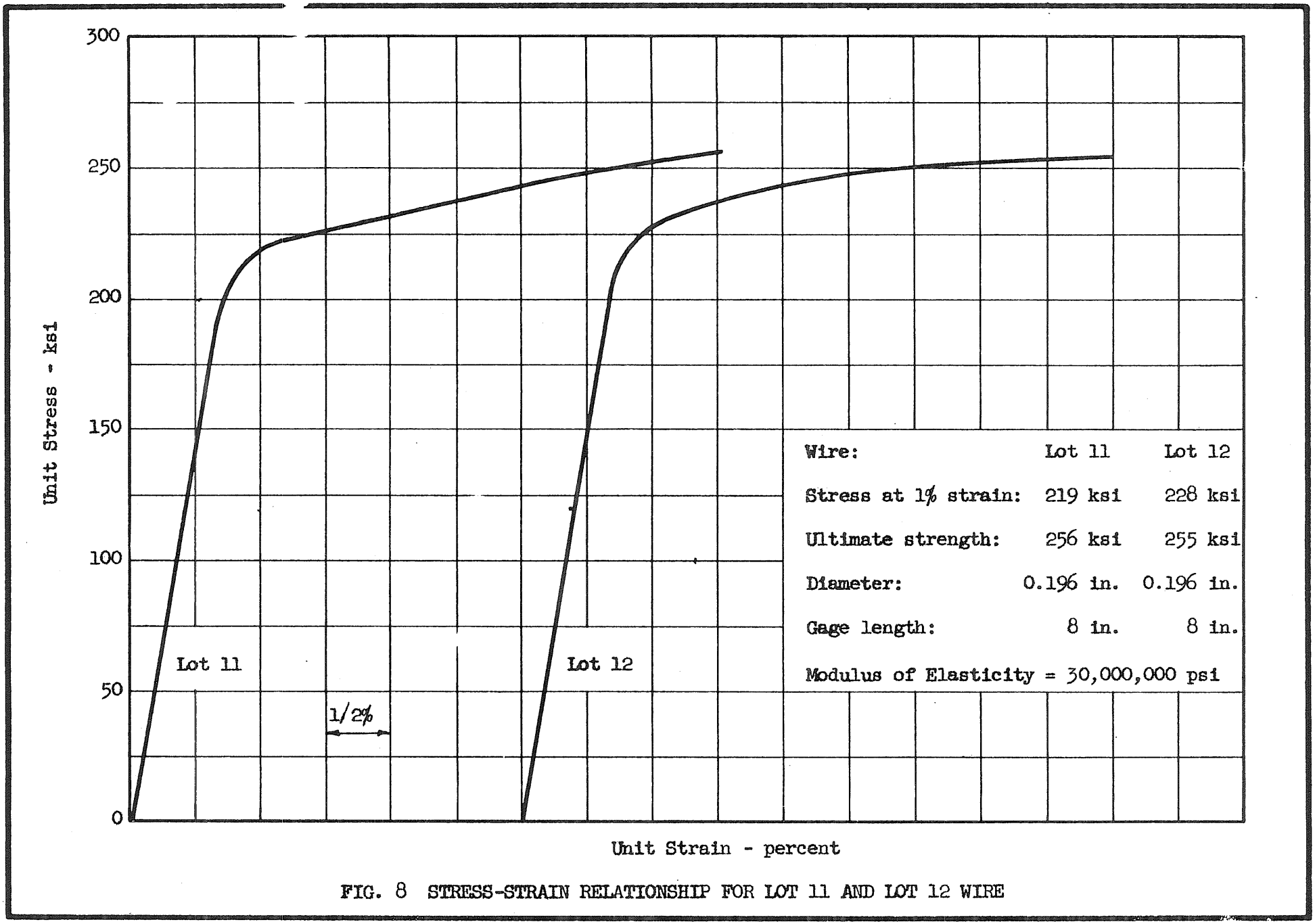

FIG. 8 STRESS-STRAIN RELATIONSHIP FOR LOT 11 AND LOT 12 WIRE

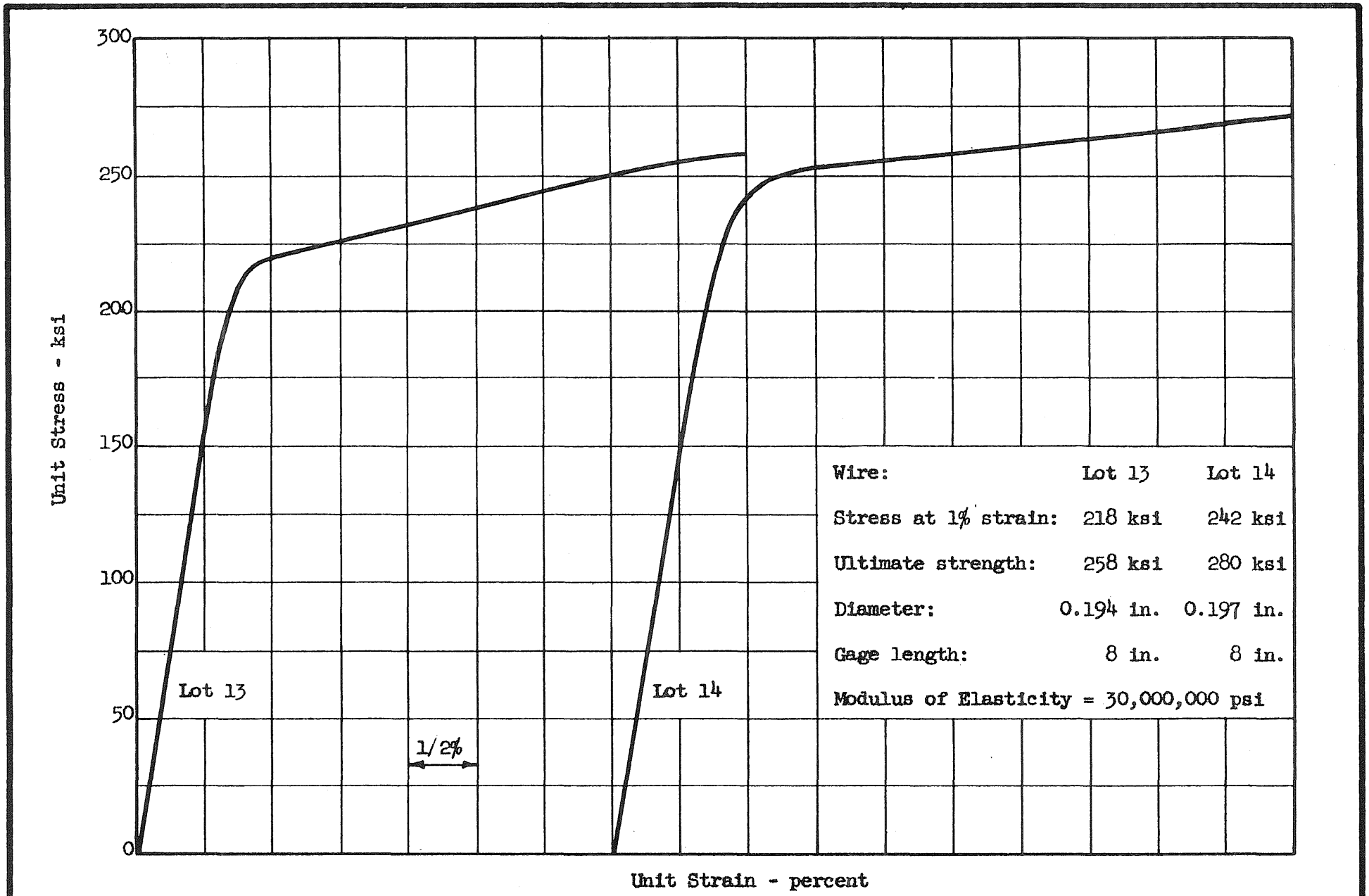

FIG. 9 STRESS-STRAIN RELATIONSHIP FOR LOT 13 AND LOT 14 WIRE

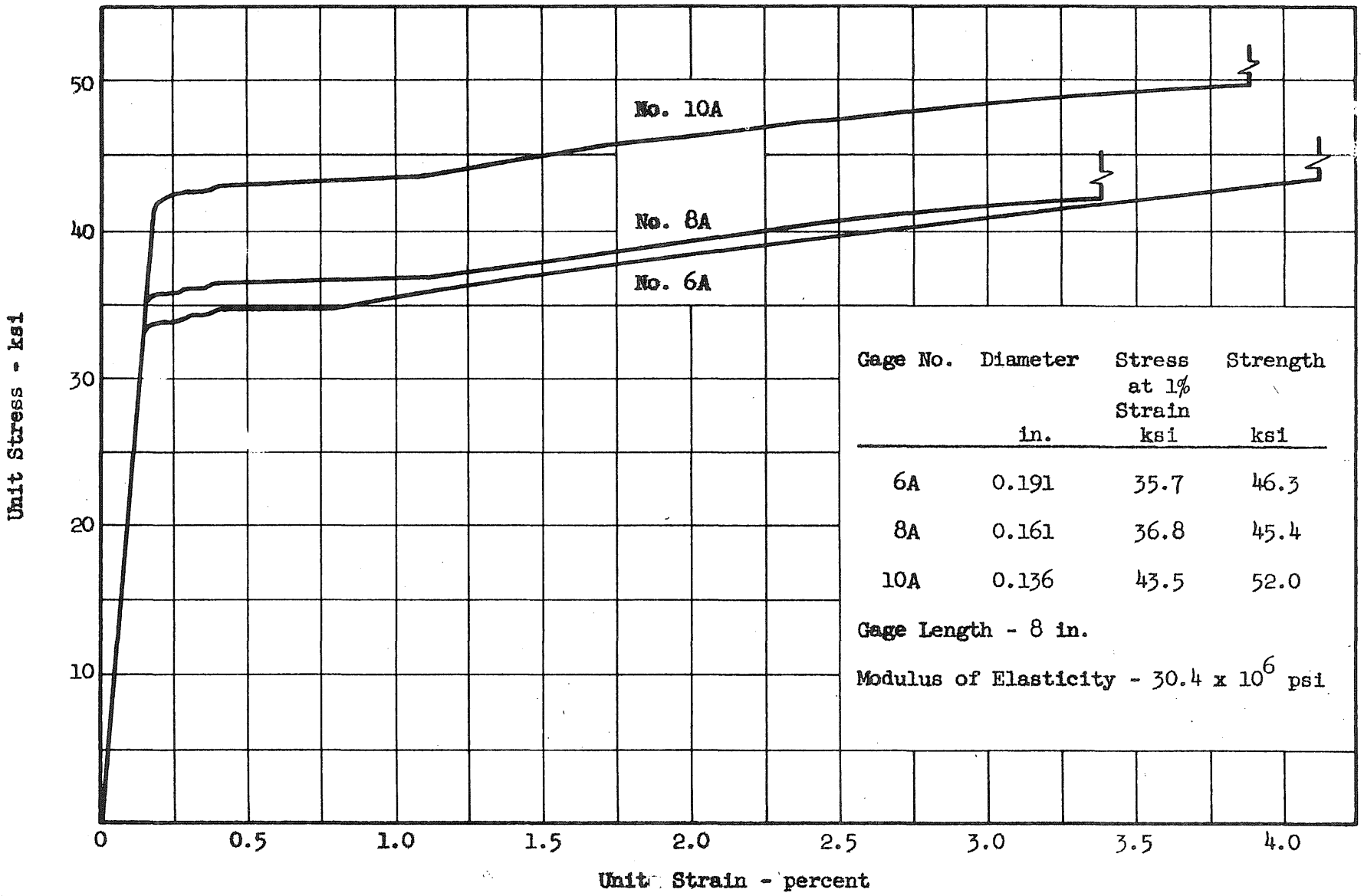

Gage No.	Diameter in.	Stress at 1% Strain ksi	Strength ksi
6A	0.191	35.7	46.3
8A	0.161	36.8	45.4
10A	0.136	43.5	52.0

Gage Length - 8 in.

Modulus of Elasticity - 30.4×10^6 psi

FIG. 10 STRESS-STRAIN RELATIONSHIP FOR BLACK ANNEALED WIRE, LOT A

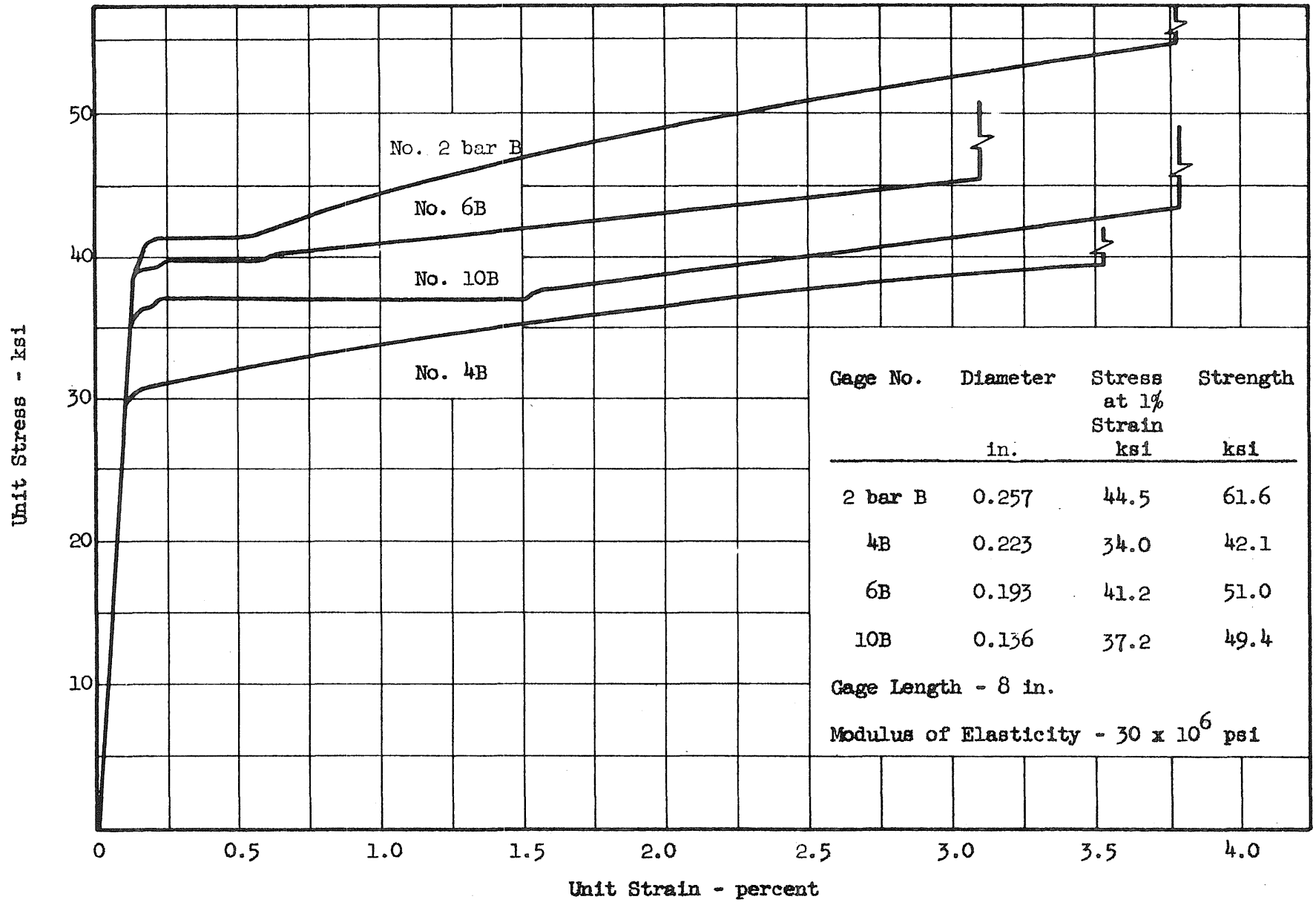

Gage No.	Diameter in.	Stress at 1% Strain ksi	Strength ksi
2 bar B	0.257	44.5	61.6
4B	0.223	34.0	42.1
6B	0.193	41.2	51.0
10B	0.136	37.2	49.4

Gage Length - 8 in.

Modulus of Elasticity - 30×10^6 psi

FIG. 11 STRESS-STRAIN RELATIONSHIP FOR BLACK ANNEALED WIRE, LOT B

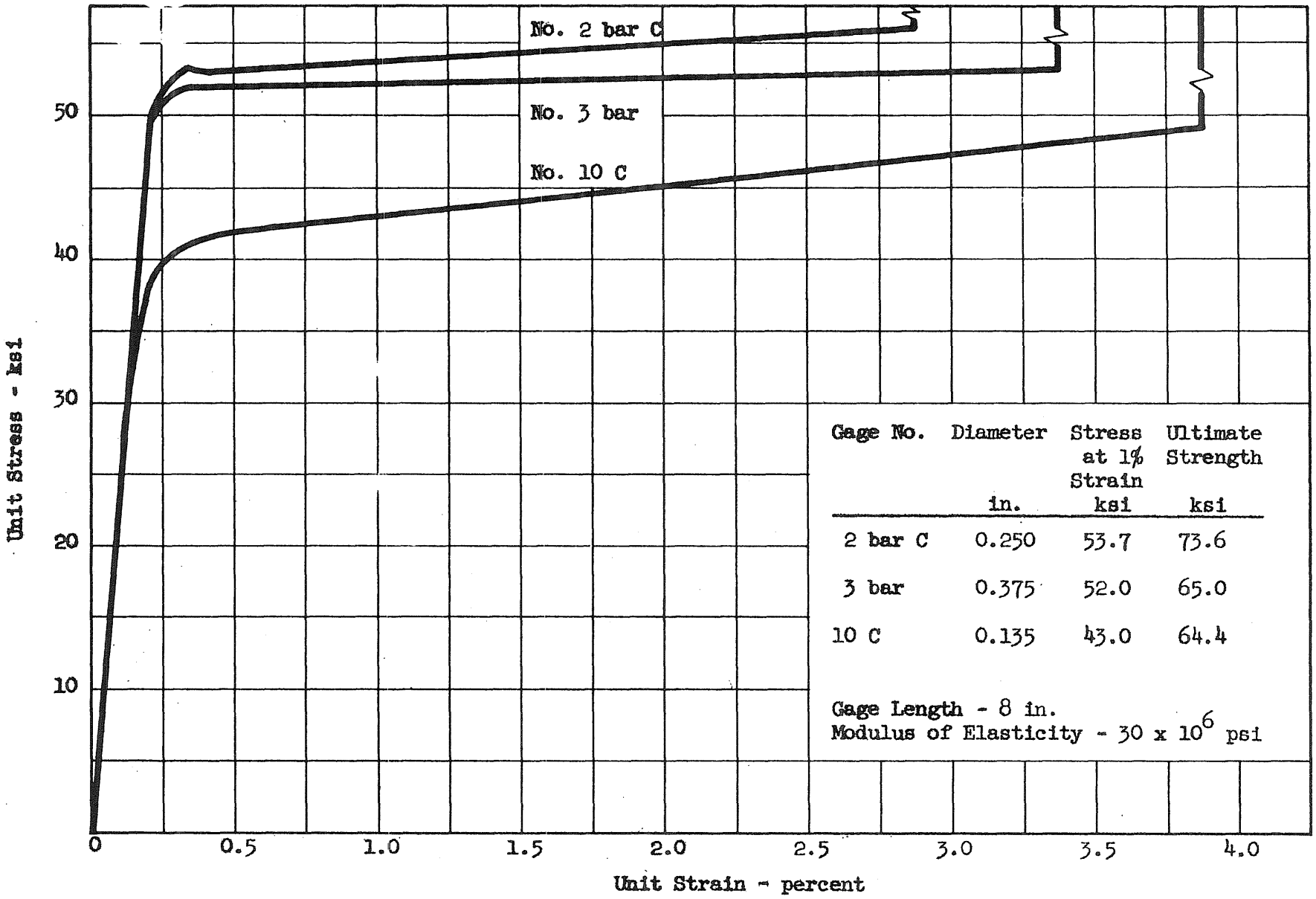

FIG. 12 STRESS-STRAIN RELATIONSHIP FOR BLACK ANNEALED WIRE, LOT C

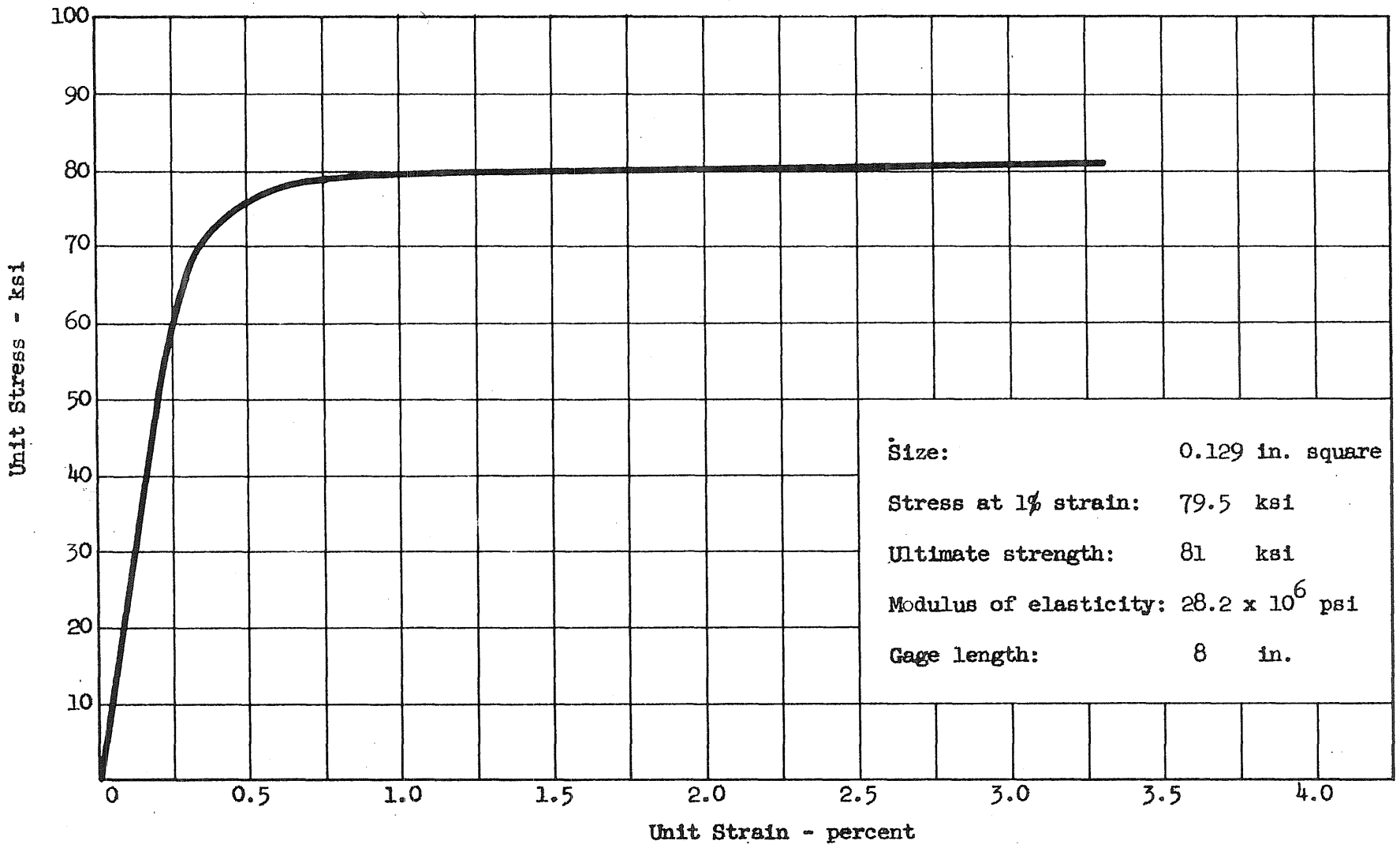

FIG. 13 STRESS-STRAIN RELATIONSHIP FOR COLD DRAWN STIRRUP WIRE

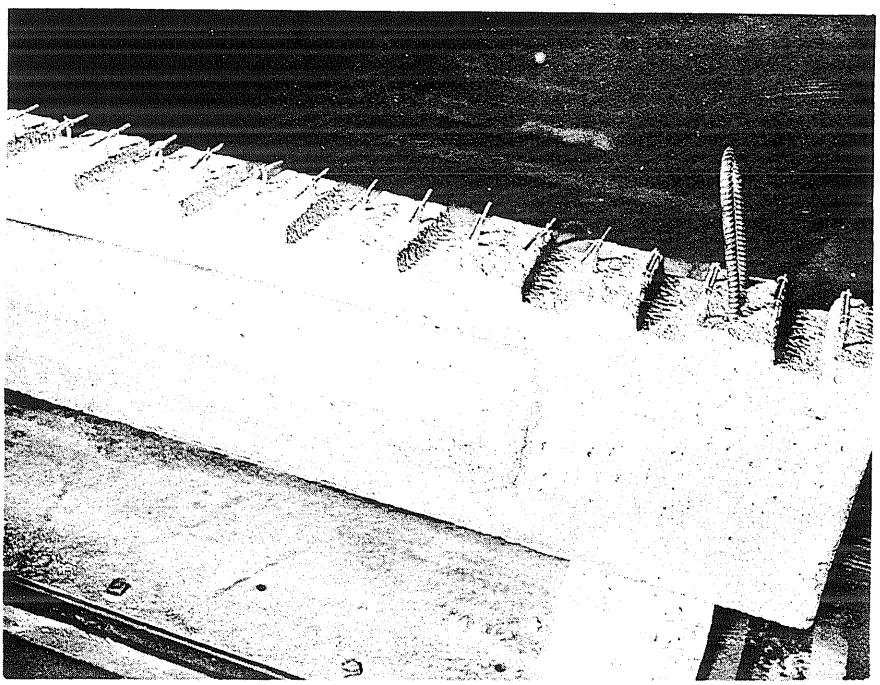

(a) Shear Keys and Protruding Ends of Stirrups in Beam FW.14.06

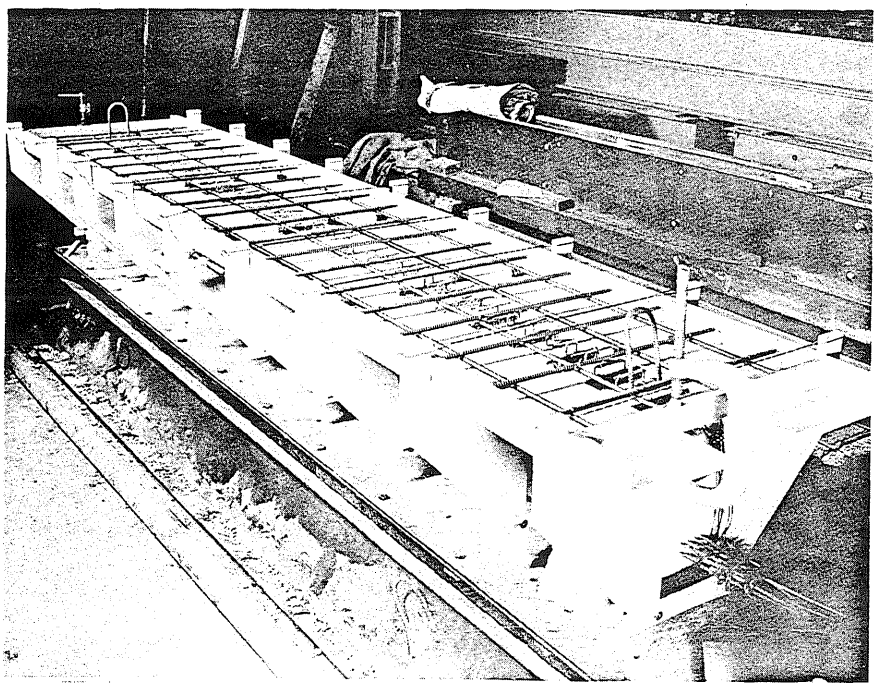

(b) Beam FW.14.06 Before Casting the Slab

FIG. 14 DETAILS OF COMPOSITE BEAMS

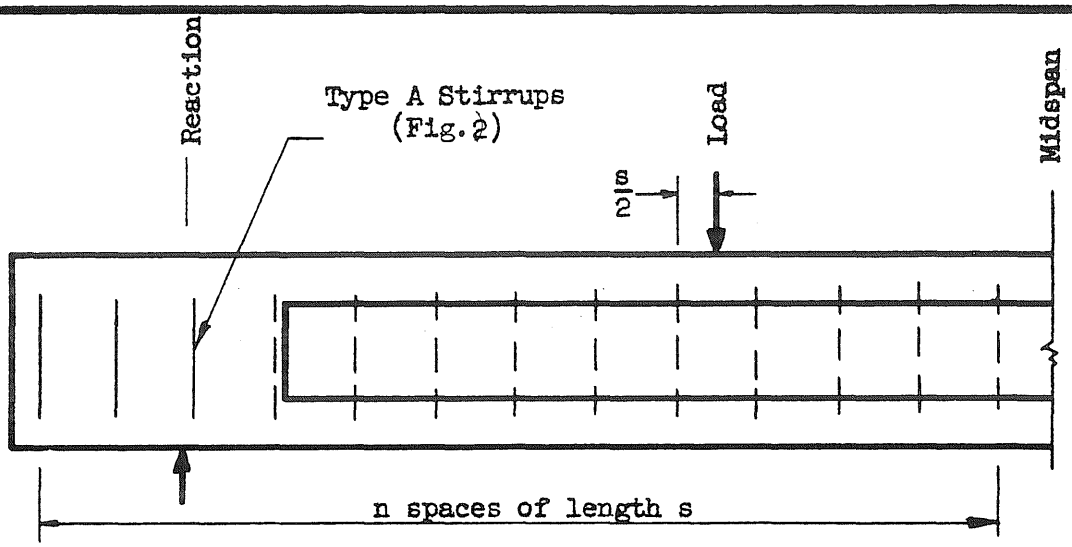

Stirrup Arrangement 1

s = 2.75, 3.5, 3.75, 4.0, 4.5, 5.0, 9.0, 10.0 or 10.5 in.

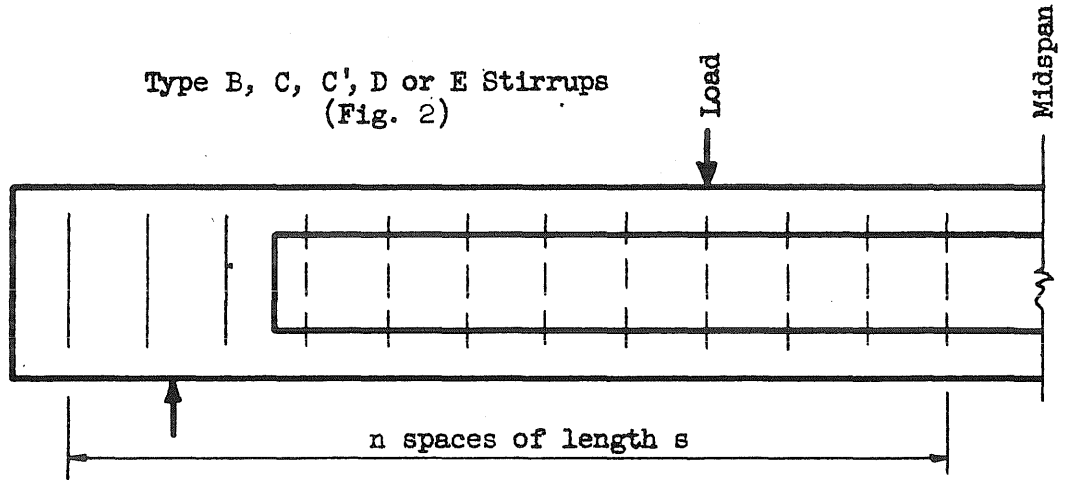

Stirrup Arrangement 2

s = 3.75, 5.0, 6.5 or 7.5 in.

FIG. 15 TYPICAL STIRRUP ARRANGEMENTS: TWO-POINT LOADS

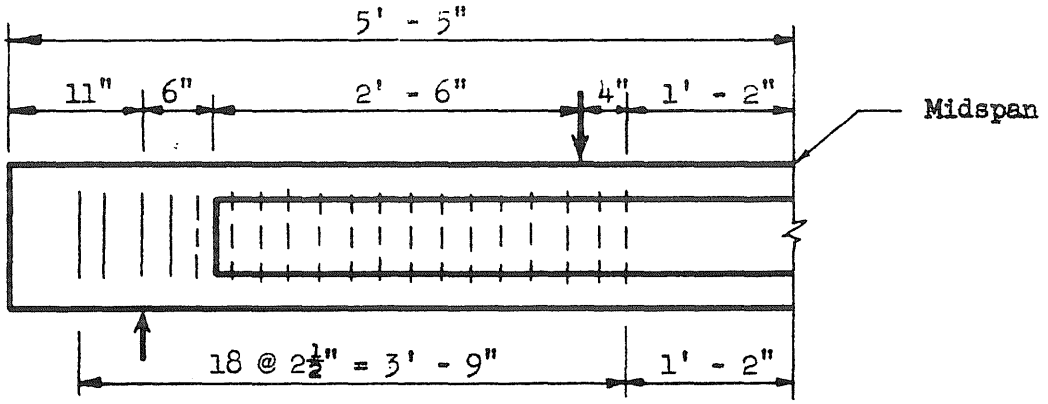

Stirrup Arrangement 3 - s = 2½ in.

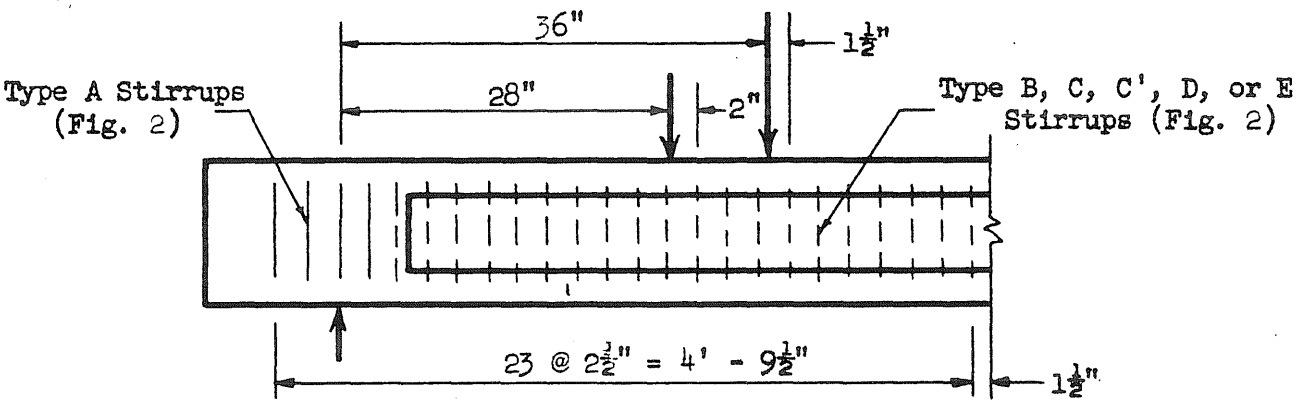

Stirrup Arrangement 4 - s = 2½ in.

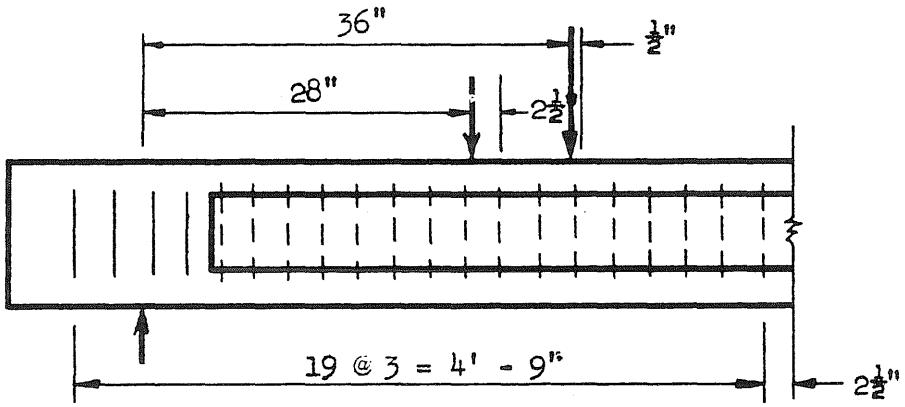

Stirrup Arrangement 5 - s = 3 in.

FIG. 16 TYPICAL STIRRUP ARRANGEMENTS: TWO-POINT LOADS

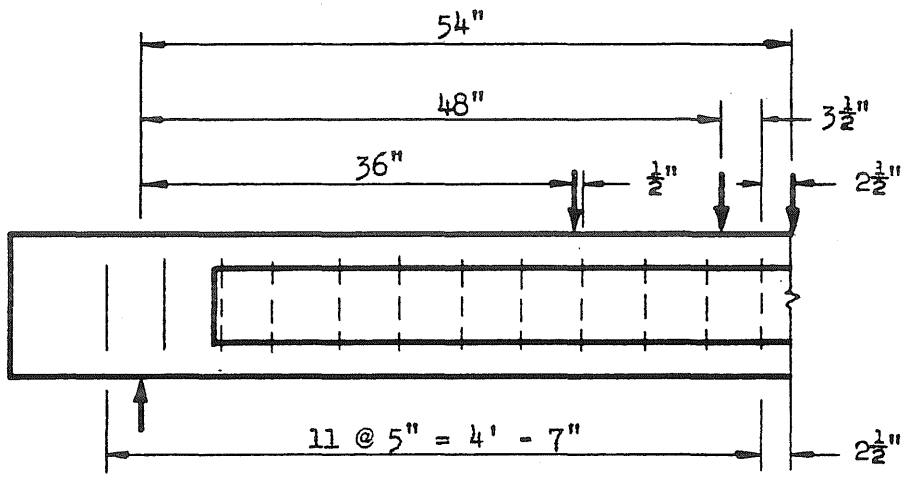

Stirrup Arrangement 6 - s = 5 in.

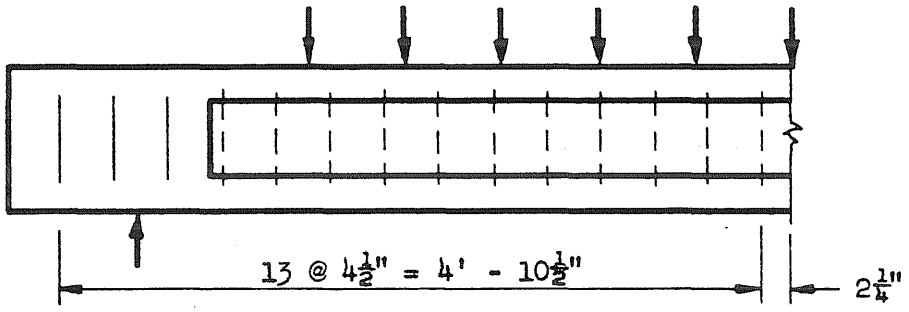

Stirrup Arrangement 7 - Beam CW.10.26
s = 4½ in.

FIG. 17 TYPICAL STIRRUP ARRANGEMENTS

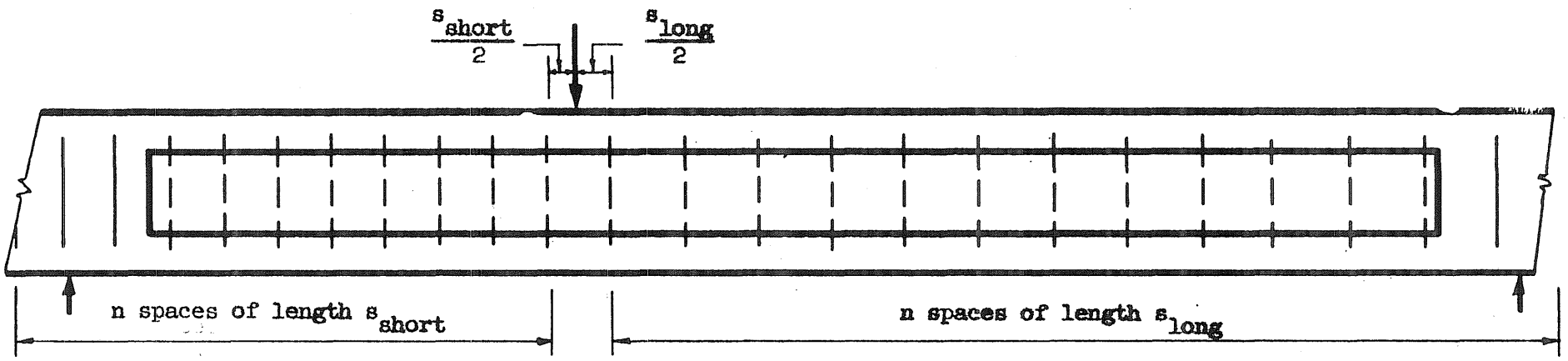

Stirrup Arrangement 8 - Beams BW.28.28 and CW.28.28

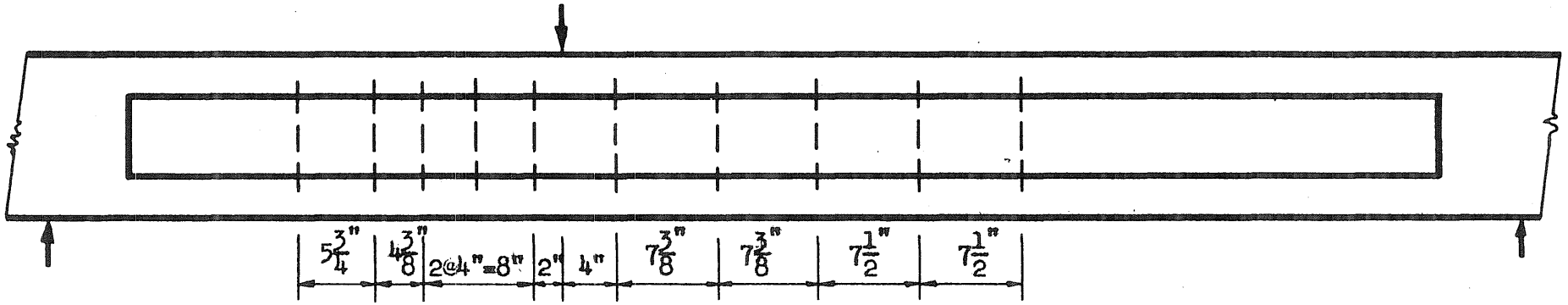

Stirrup Arrangement 9 - Beam BW.18.15

FIG. 18 TYPICAL STIRRUP ARRANGEMENTS

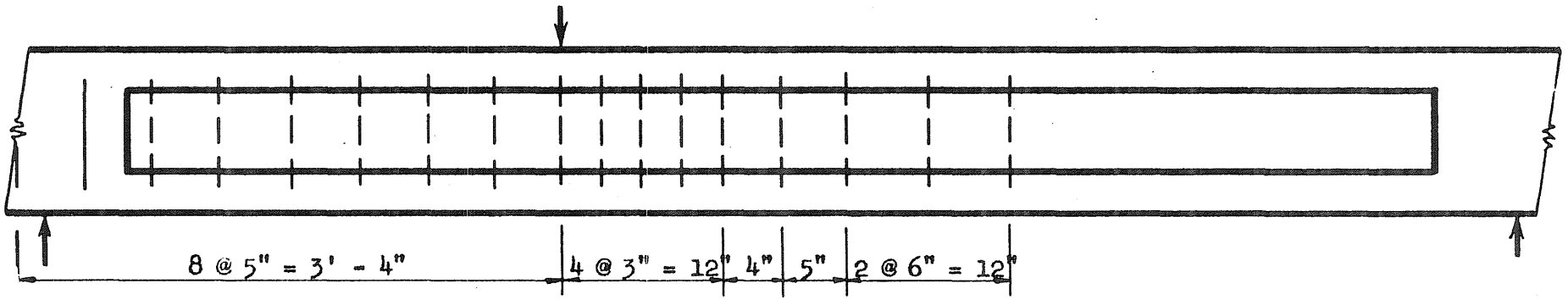

Stirrup Arrangement 10 - Beam BW.18.27

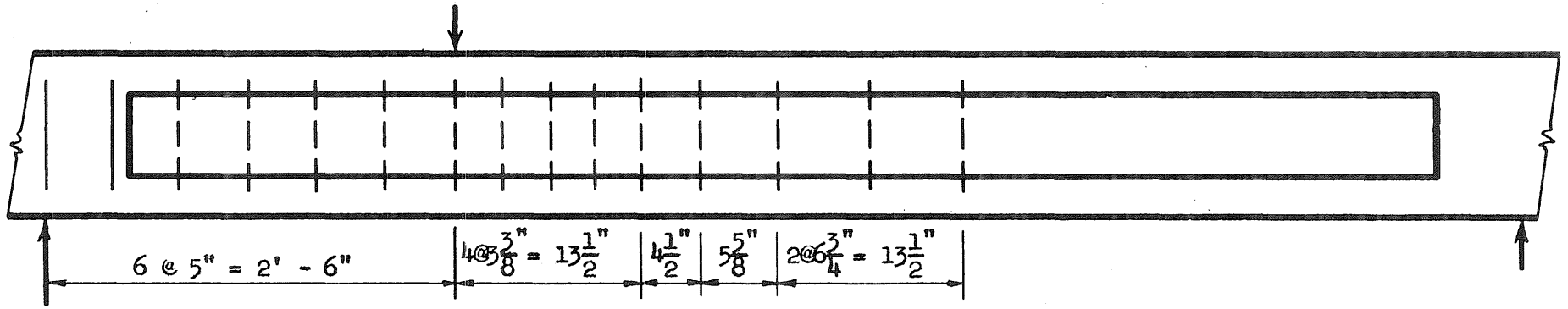

Stirrup Arrangement 11 - Beam BW.19.28

FIG. 19 STIRRUP ARRANGEMENTS IN BEAMS BW.18.27 AND BW.19.27

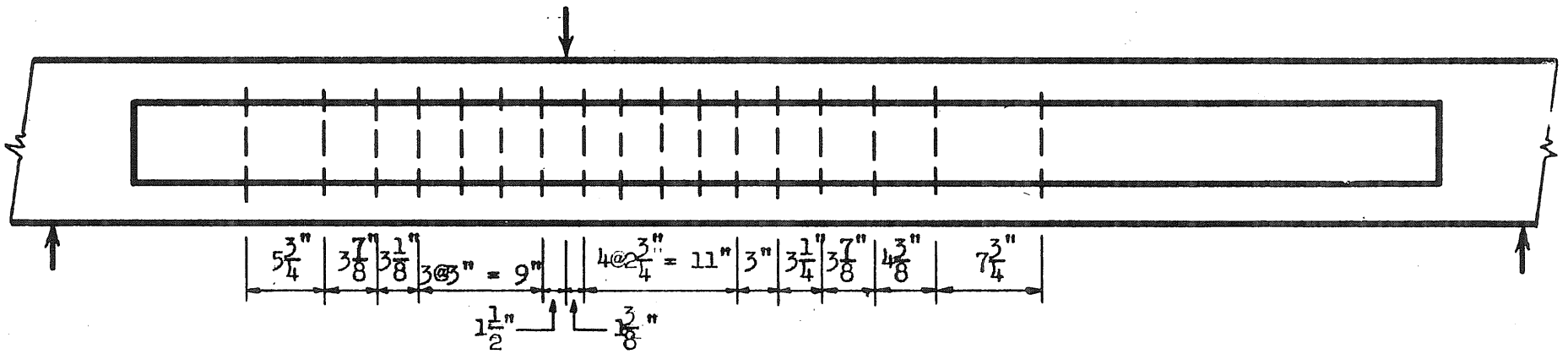

Stirrup Arrangement 12 - Beam BW.28.26

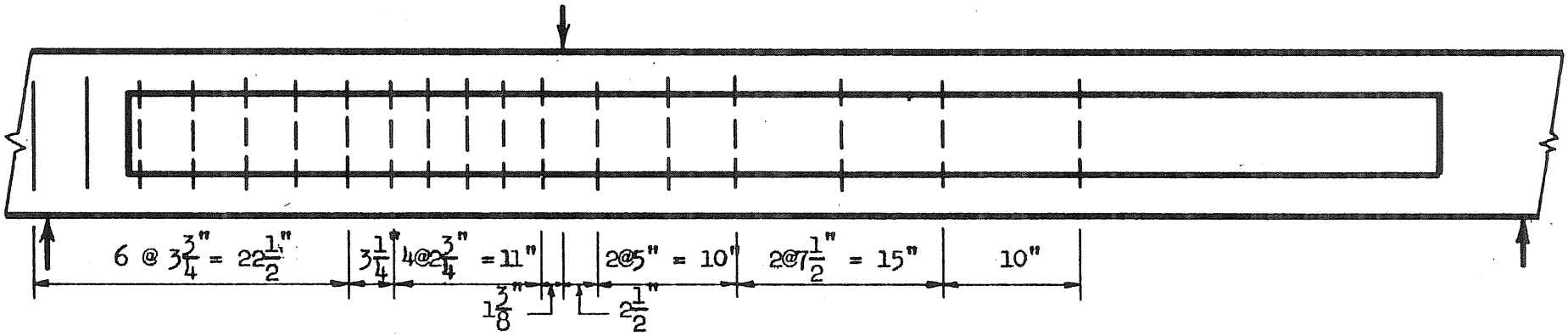

Stirrup Arrangement 13 - Beam CW.18.15

FIG. 20 STIRRUP ARRANGEMENTS IN BEAMS BW.28.26 AND CW.18.15

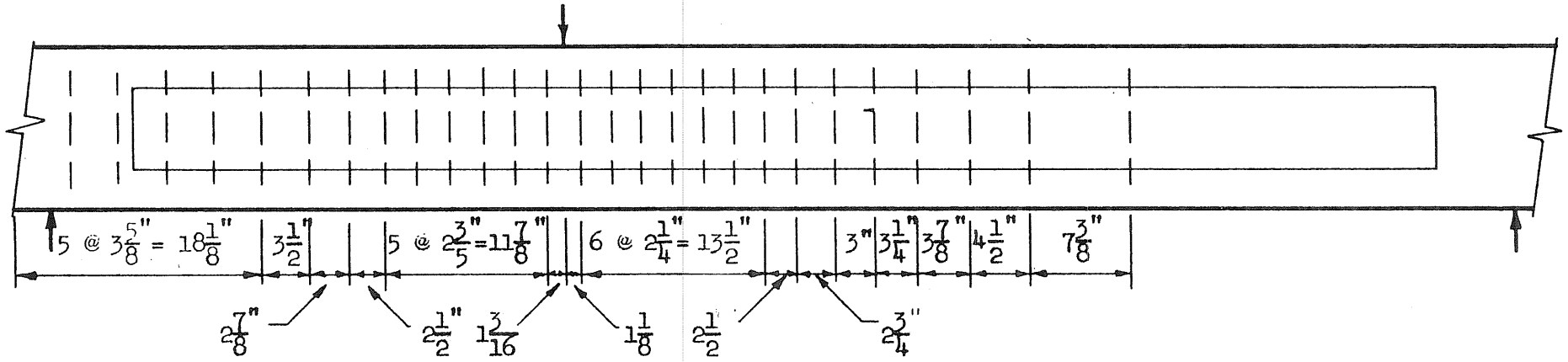

FIG. 21 STIRRUP ARRANGEMENT 14 - BEAM CW.28.26

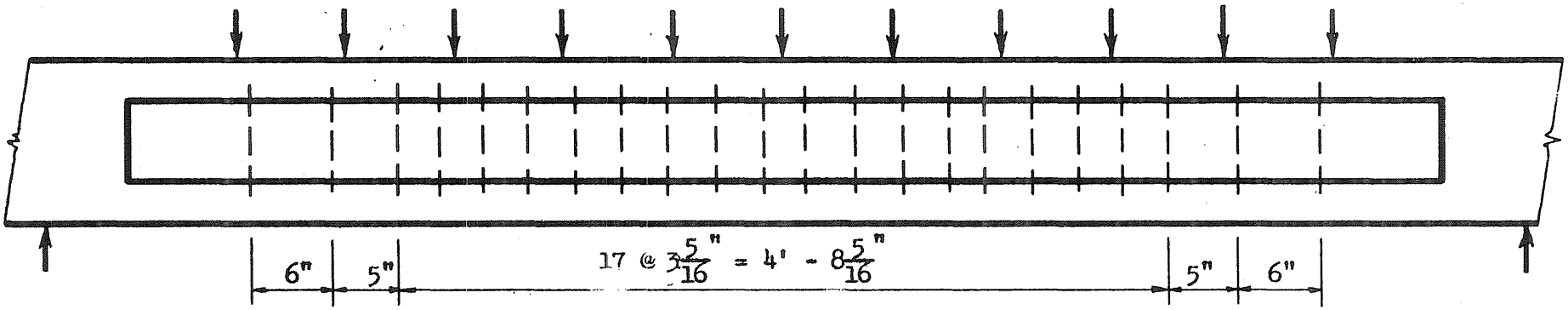

Stirrup Arrangement 15 - Beam BW.10.22

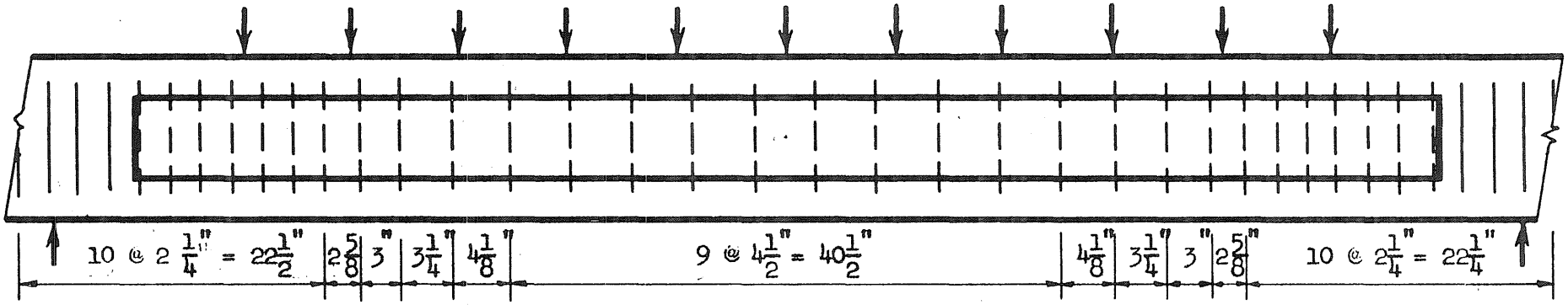

Stirrup Arrangement 16 - Beam CW.10.27

FIG. 22 STIRRUP ARRANGEMENTS IN BEAMS BW.10.22 AND CW.10.27

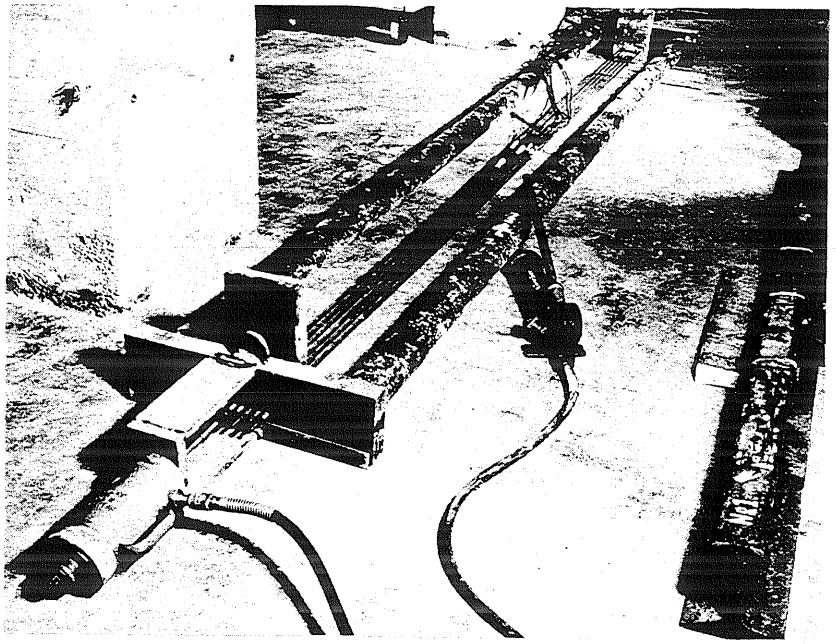

(a) Tensioning Apparatus

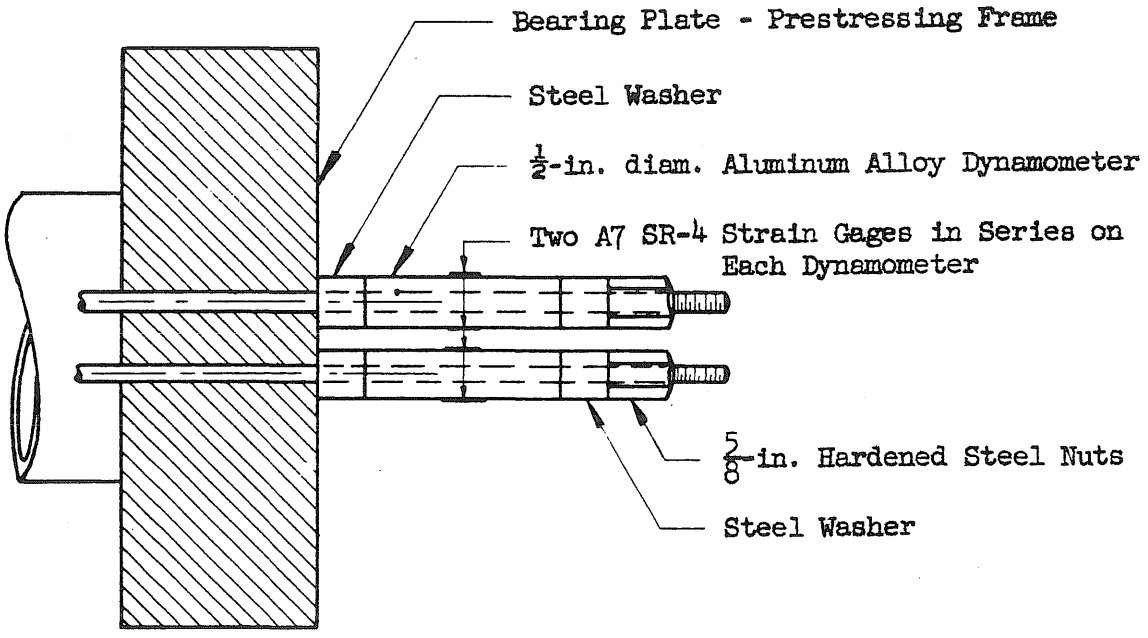

(b) Reinforcement Anchorage and Dynamometers

FIG. 23 TENSIONING APPARATUS

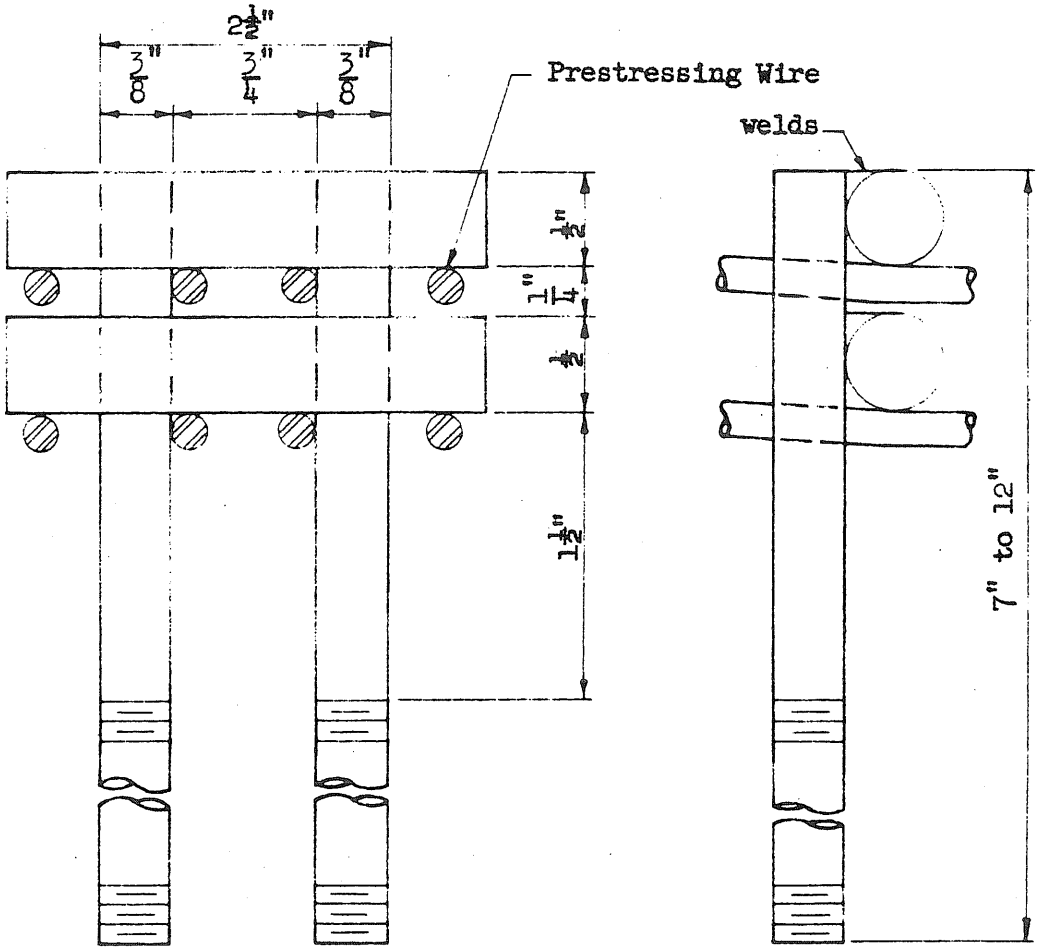

Detail of Draping Saddle

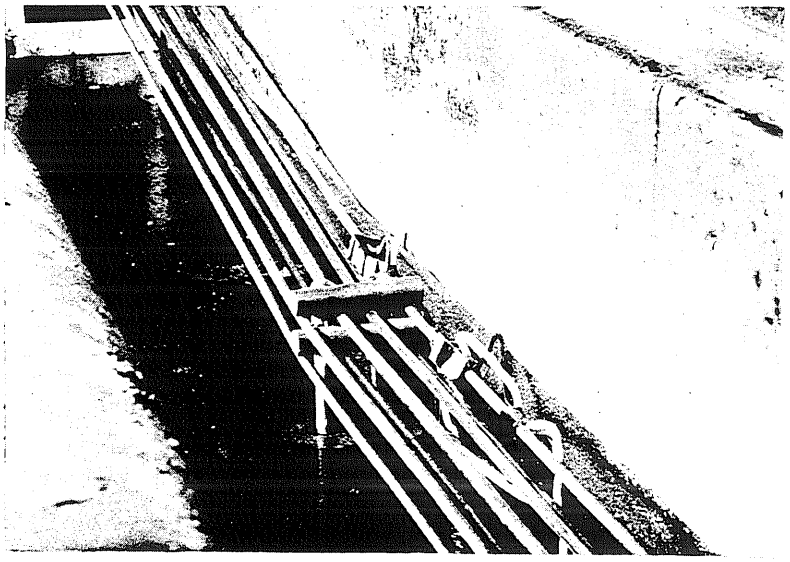

A Draping Saddle in Beam BD.14.42

FIG. 24 DRAPING SADDLES

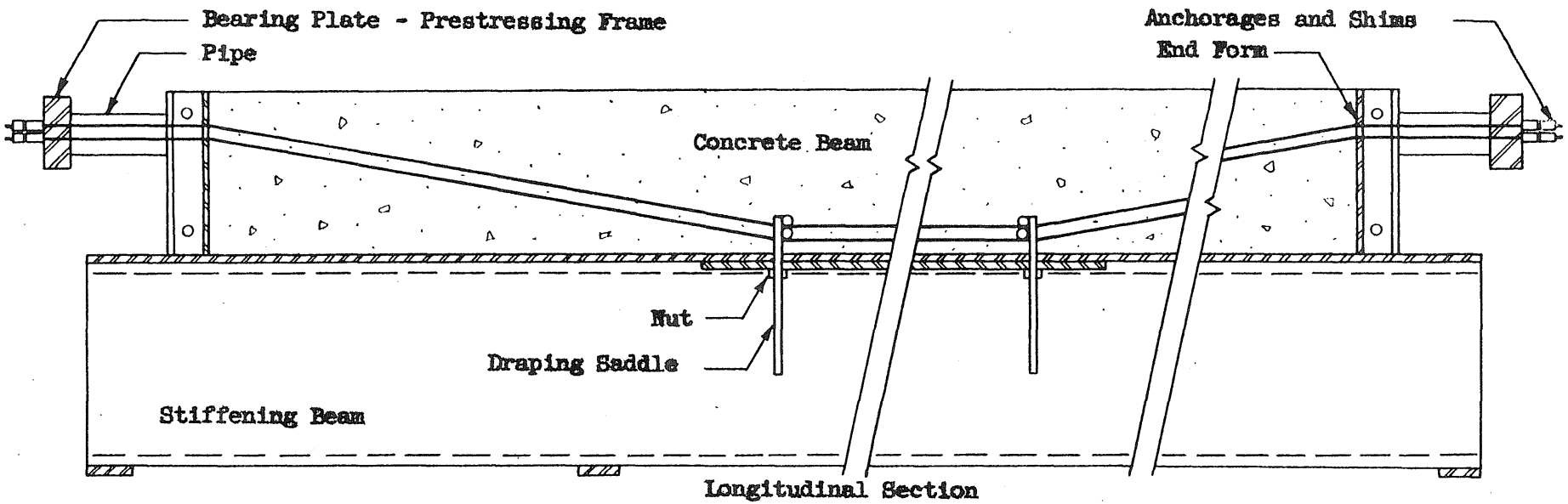

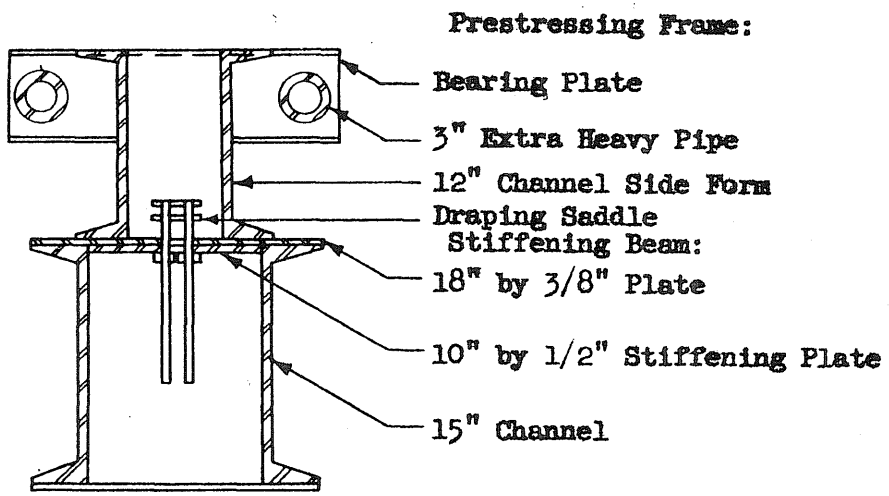

FIG. 25 CROSS SECTIONS OF BEAM AND FORM

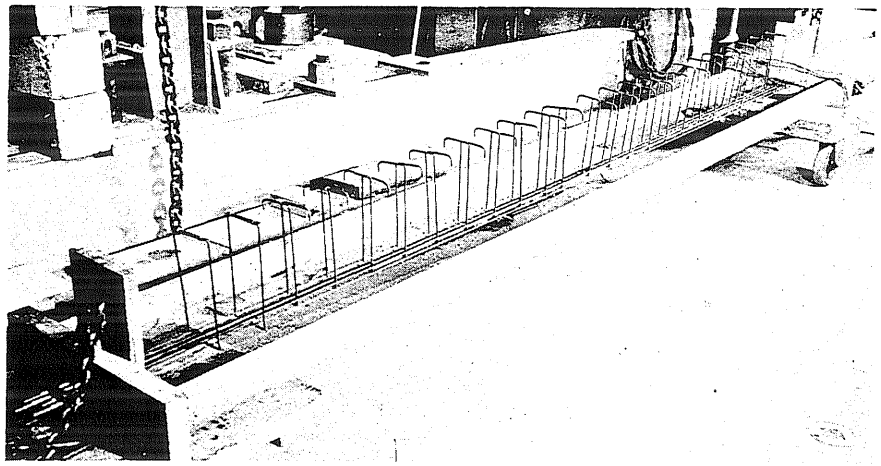

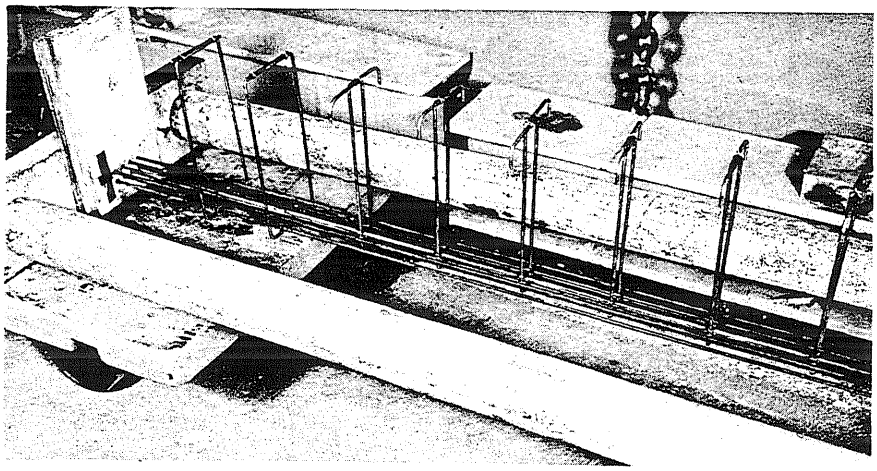

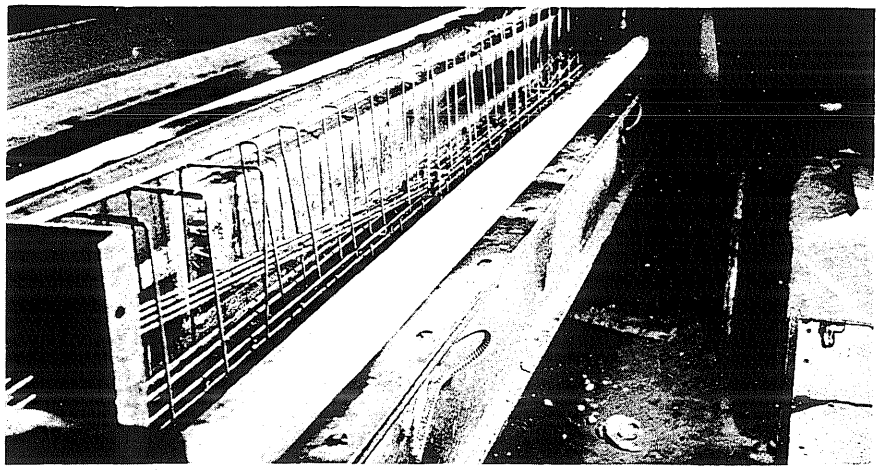

FIG. 26 TYPICAL STIRRUP ARRANGEMENTS

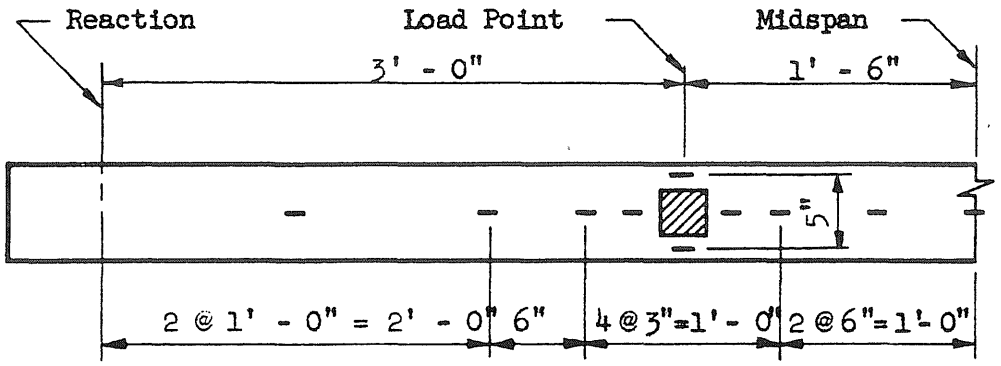

(a) Beams Loaded at Two Points

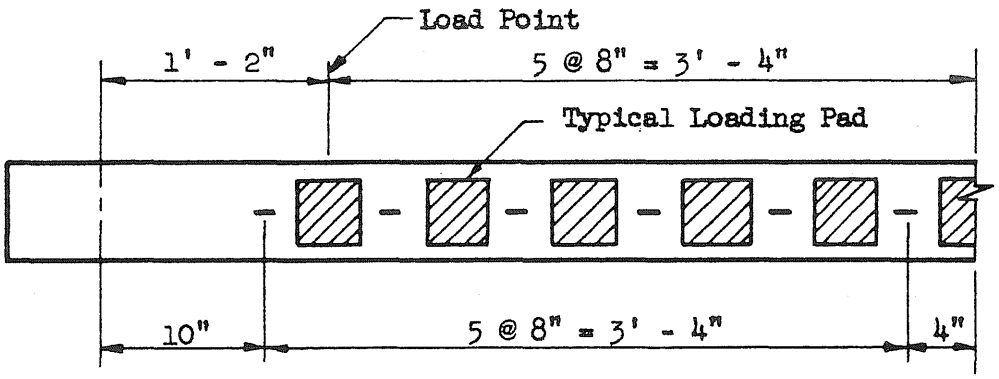

(b) Beams Tested Under Moving Loads

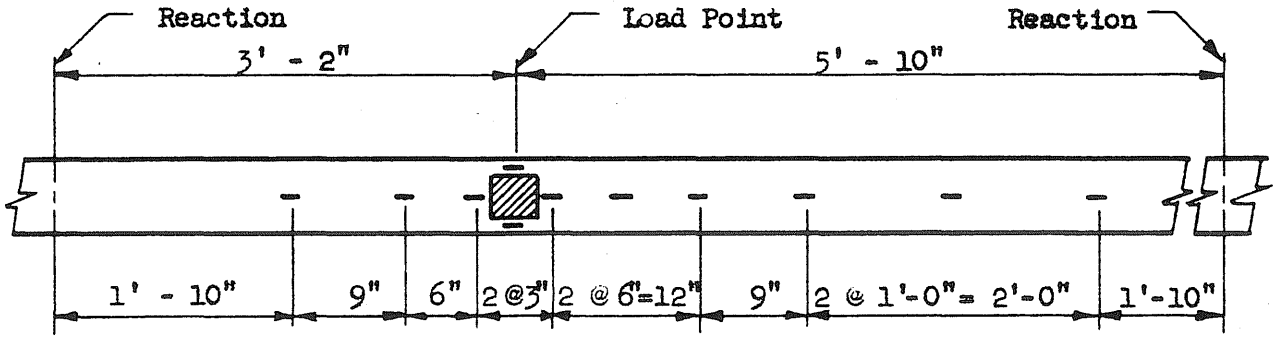

(c) Beam Loaded with Single Concentrated Load

FIG. 27 TYPICAL ARRANGEMENTS OF TOP CONCRETE STRAIN GAGES

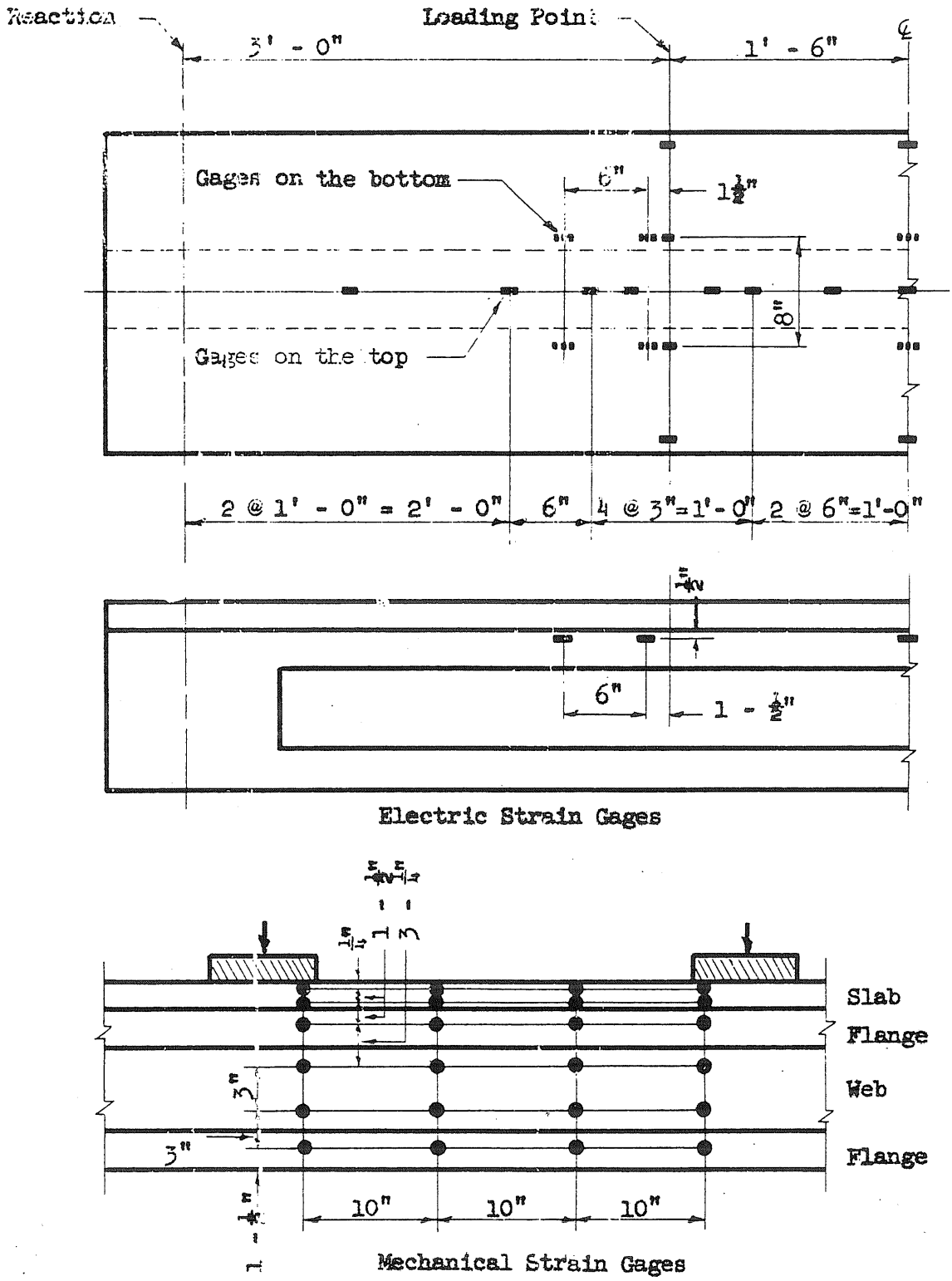

FIG. 28 POSITION OF STRAIN GAGES ON COMPOSITE BEAMS

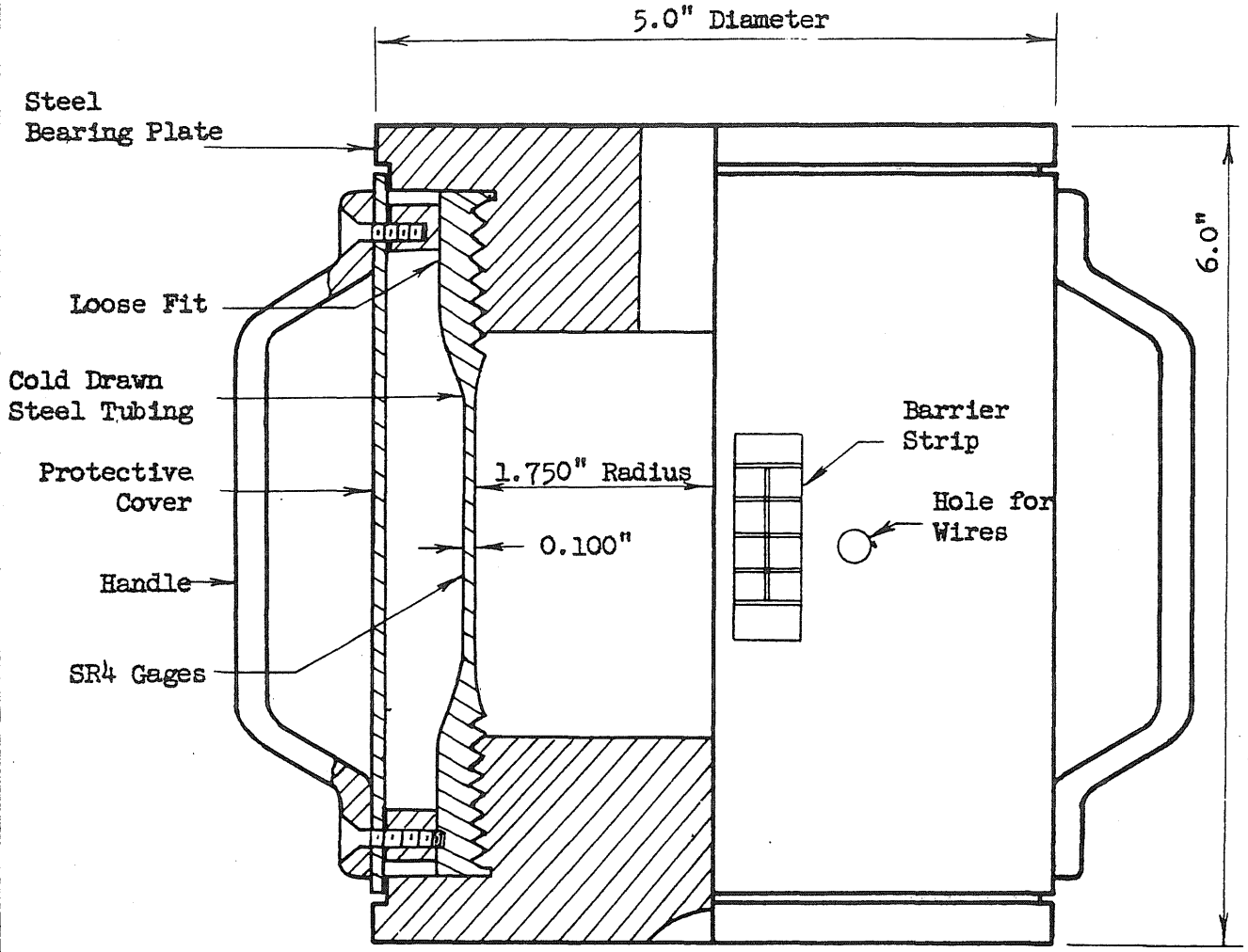

FIG. 29 DETAILS OF LOAD CELLS

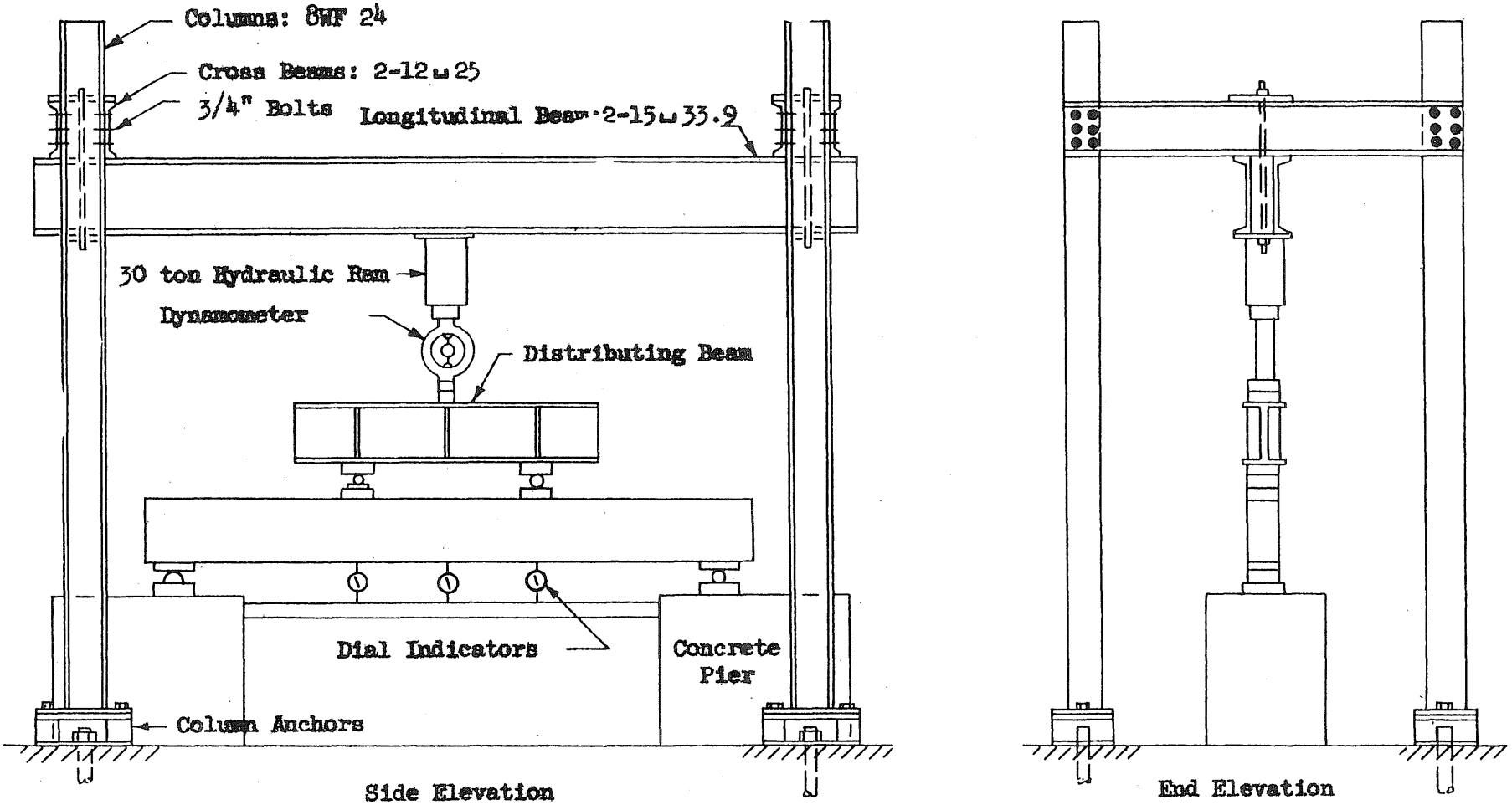

FIG. 30 DETAILS OF TESTING FRAME FOR BEAMS LOADED AT TWO POINTS

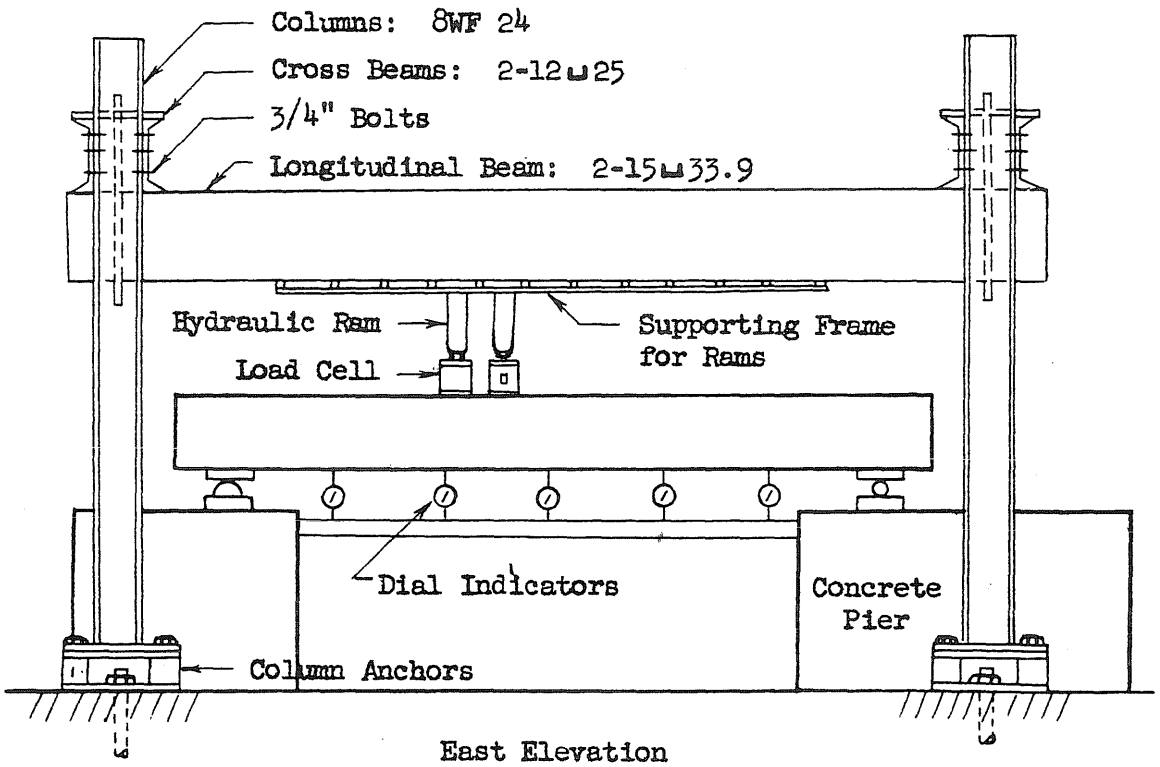

East Elevation

Scale 3/8 in. = 1 ft

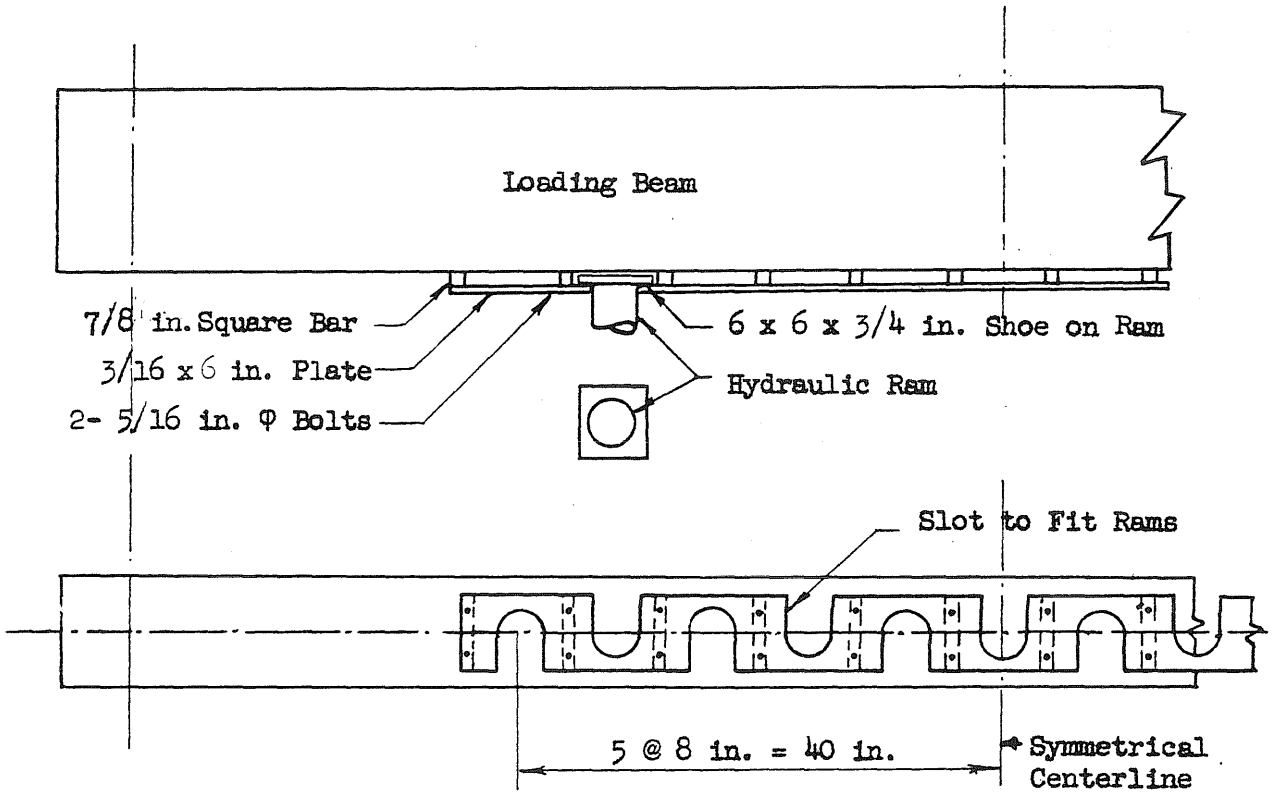

Detail of Supporting Frame for Rams

Scale 3/4 in. = 1 ft

FIG. 31 DETAILS OF MOVING LOAD TEST FRAME

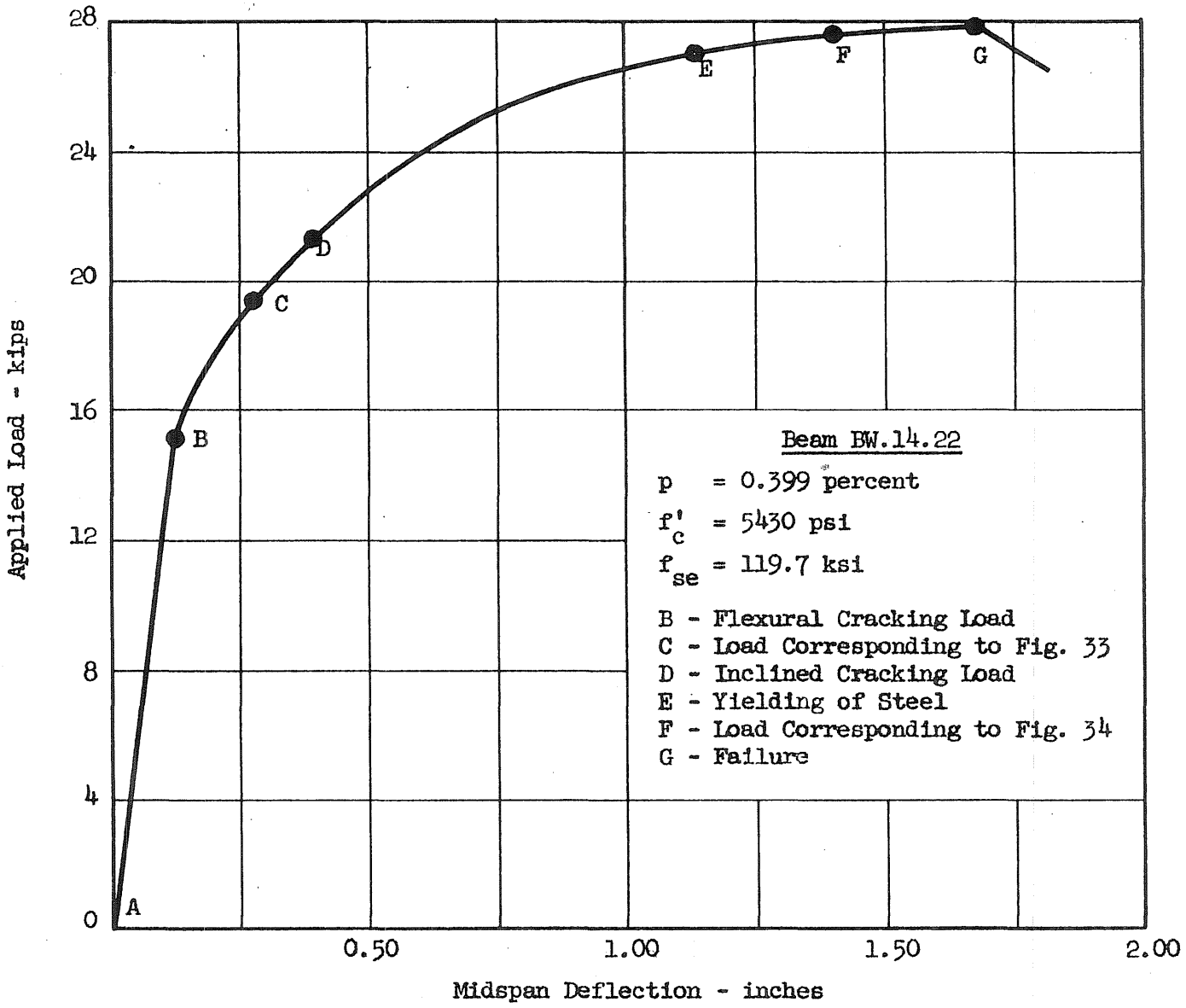

FIG. 32 LOAD-DEFLECTION CURVE FOR A FLEXURAL FAILURE

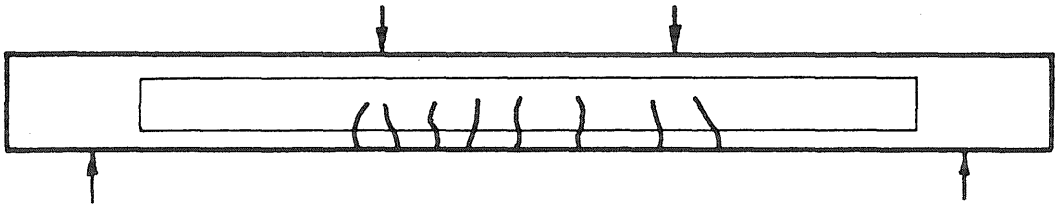

(a) Crack Pattern

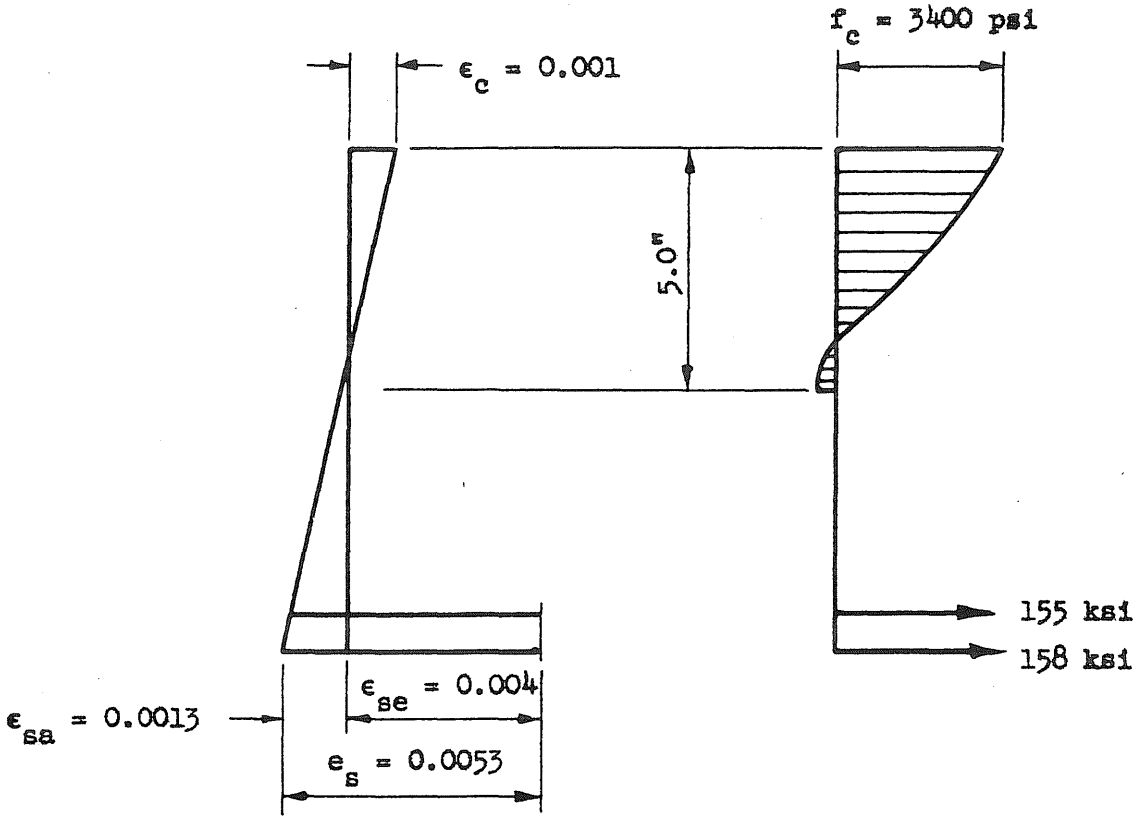

(b) Strain Distribution in Constant Moment Region

(c) Stress Distribution in Constant Moment Region

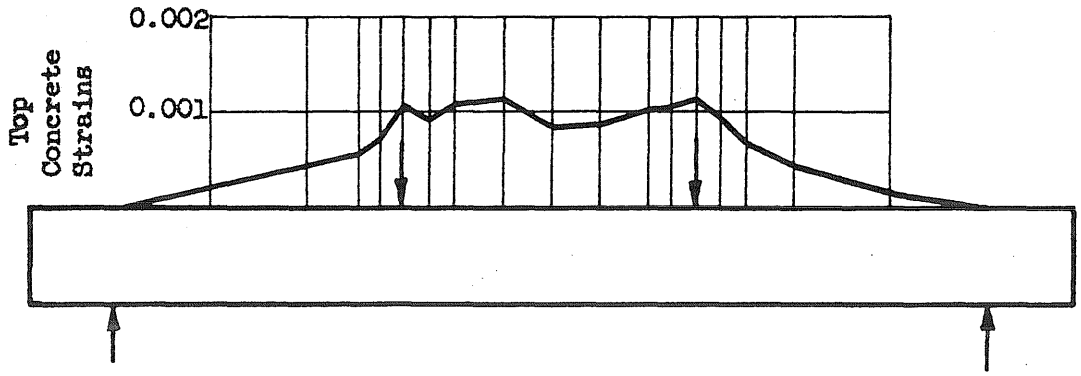

(d) Strain Distribution Along Top of Beam

FIG. 33 STRESSES, STRAINS AND CRACK PATTERN IN BEAM BW.14.22 AT LOAD CORRESPONDING TO POINT C IN FIG. 32

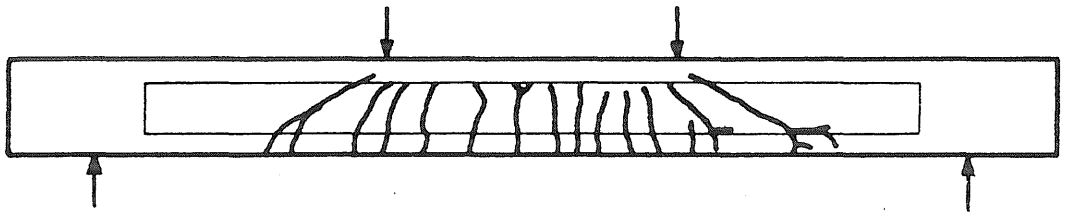

(a) Crack Pattern

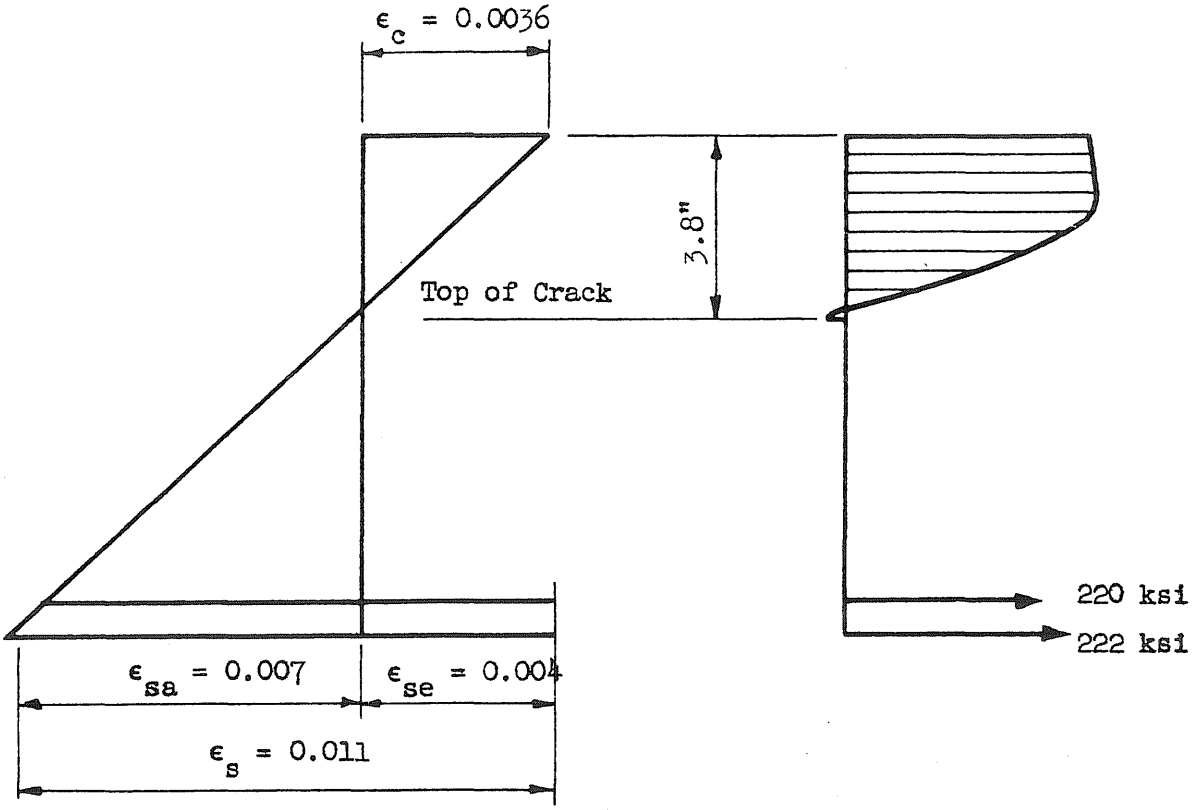

(b) Strain Distribution in Constant Moment Region

(c) Approximate Stress Distribution in Constant Moment Region

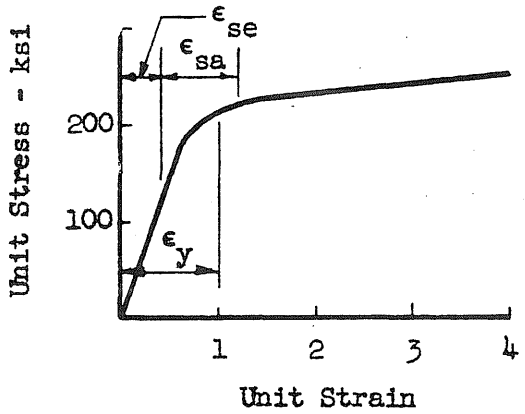

(d) Comparison of Steel Strains and Steel Stress-Strain Curve

FIG. 34 STRESSES, STRAINS AND CRACK PATTERN IN BEAM BW.14.22 AT LOAD CORRESPONDING TO POINT F IN FIG. 32

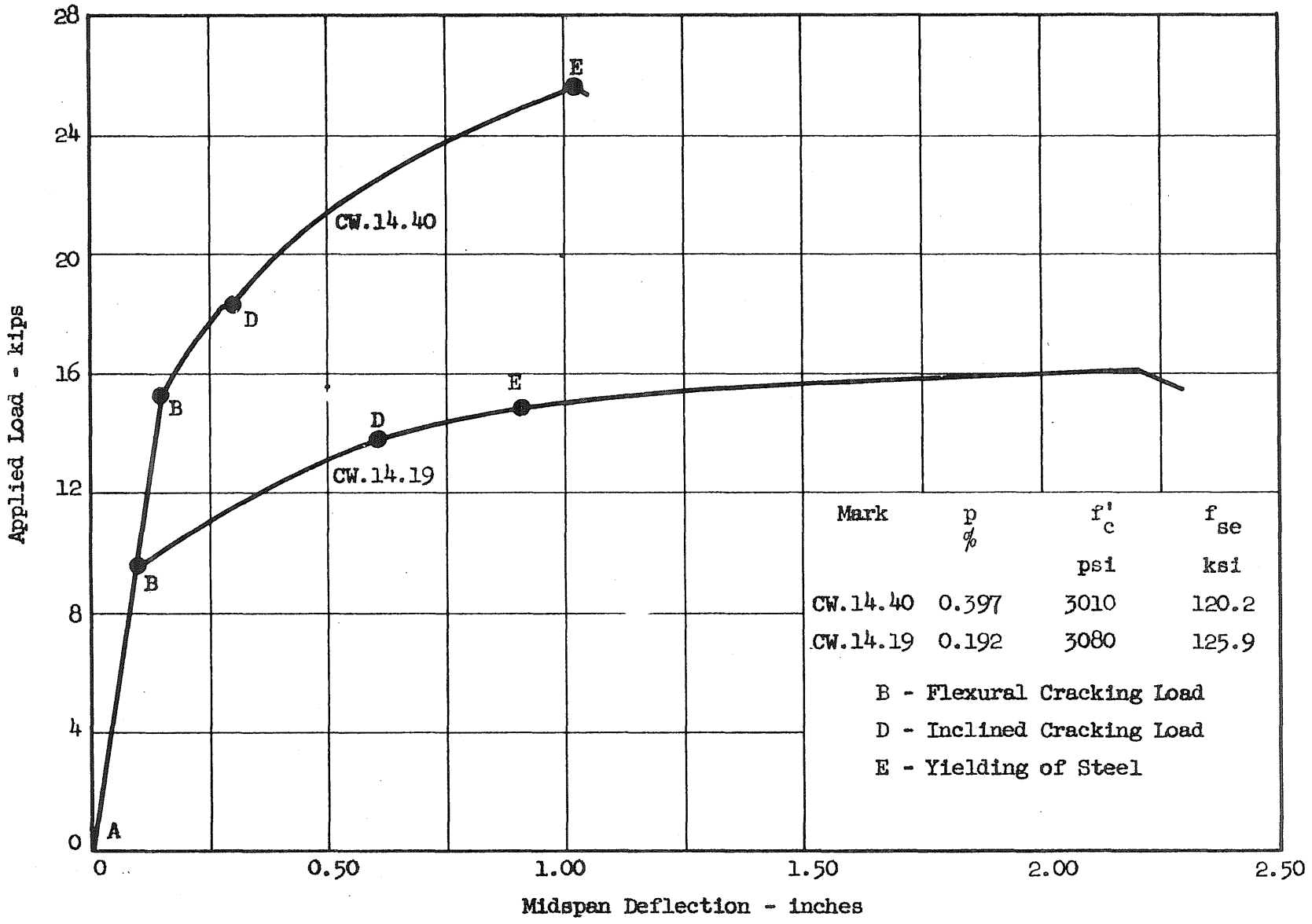

FIG. 35 LOAD-DEFLECTION CURVES FOR BALANCED AND UNDER-REINFORCED FLEXURAL FAILURES

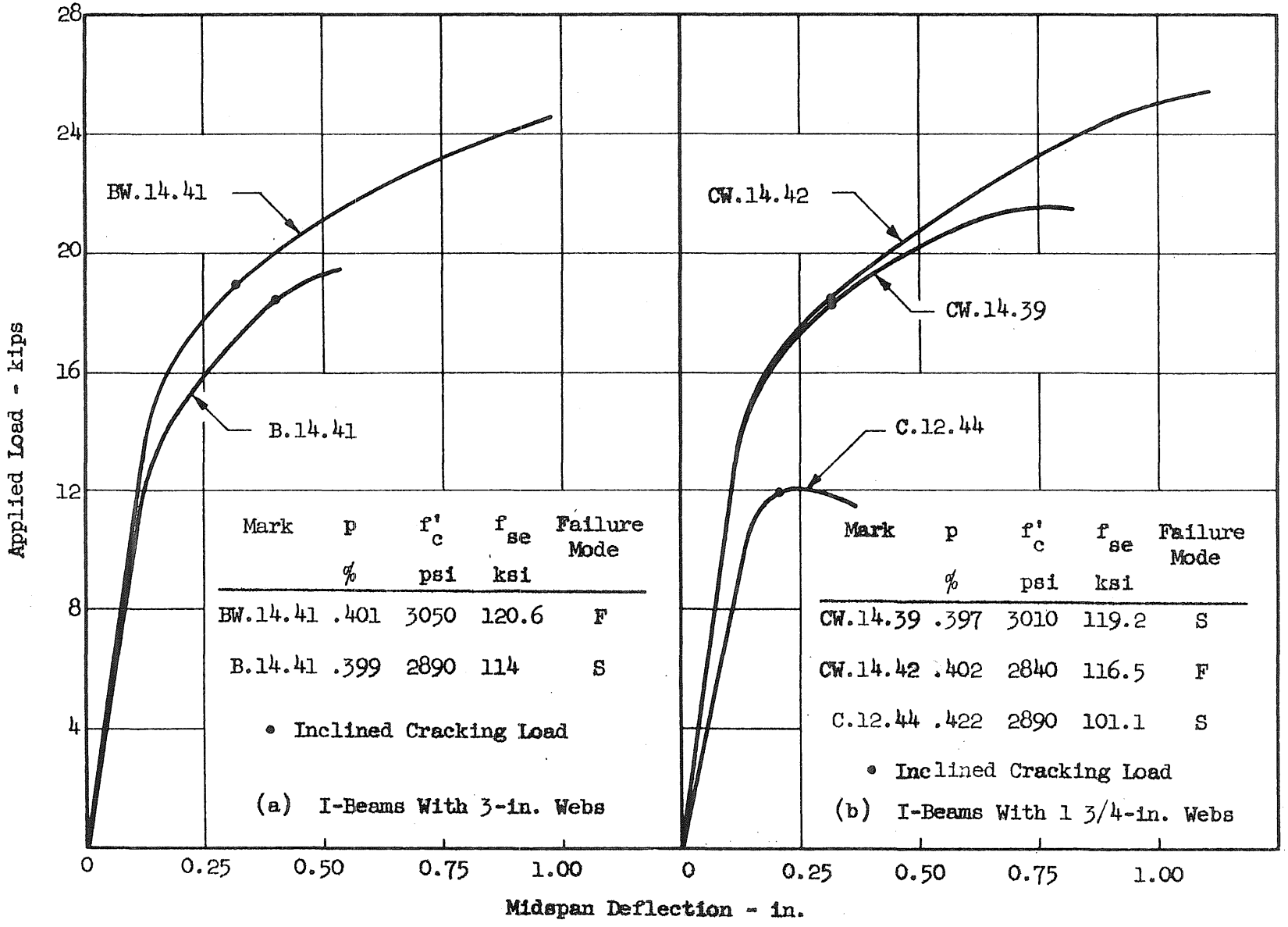

FIG. 36 COMPARISON OF STRENGTH AND DUCTILITY OF BEAMS FAILING IN FLEXURE AND SHEAR

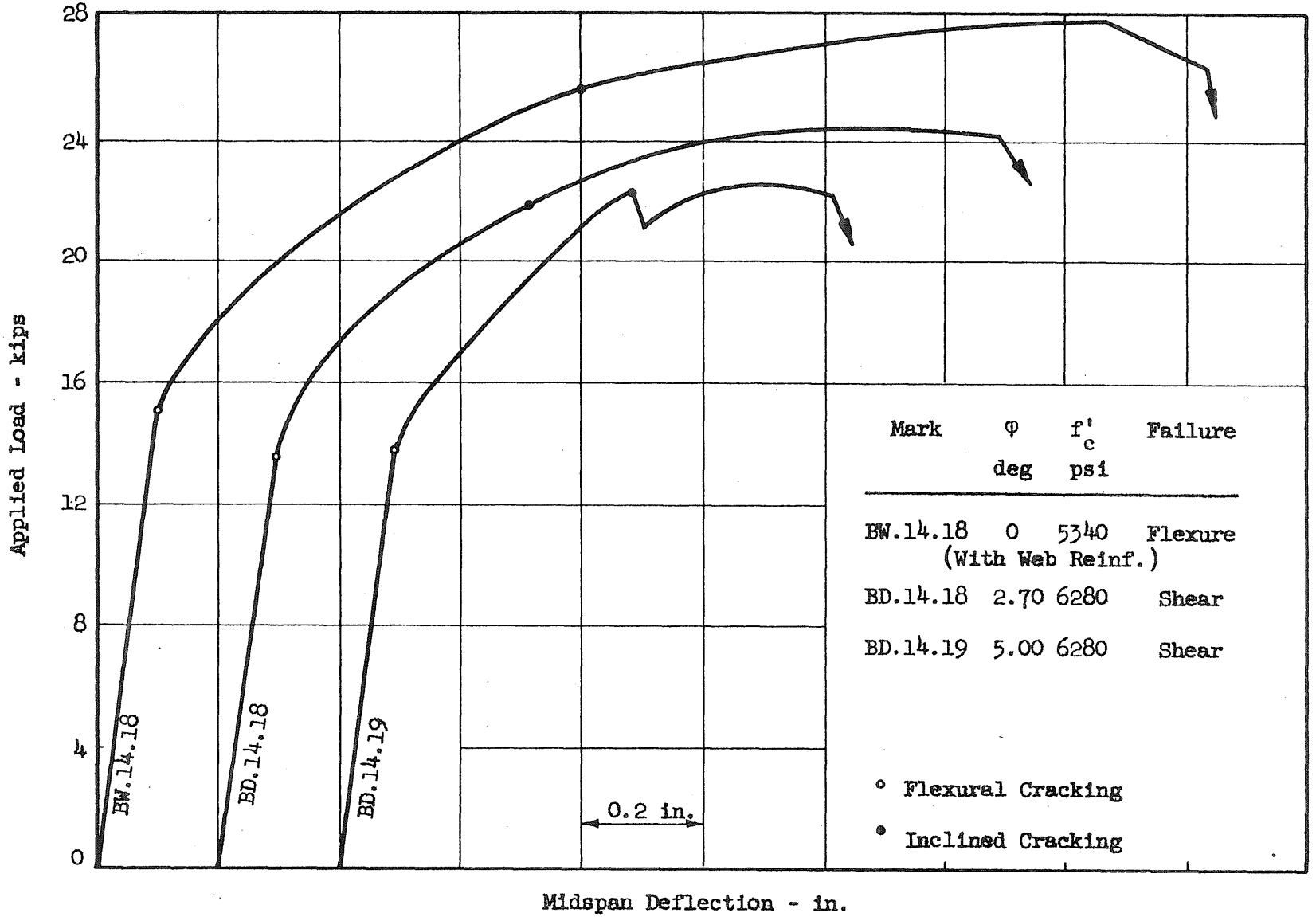

FIG. 37 LOAD-DEFLECTION CURVES SHOWING THE EFFECT OF DRAPE ANGLE ON DUCTILITY

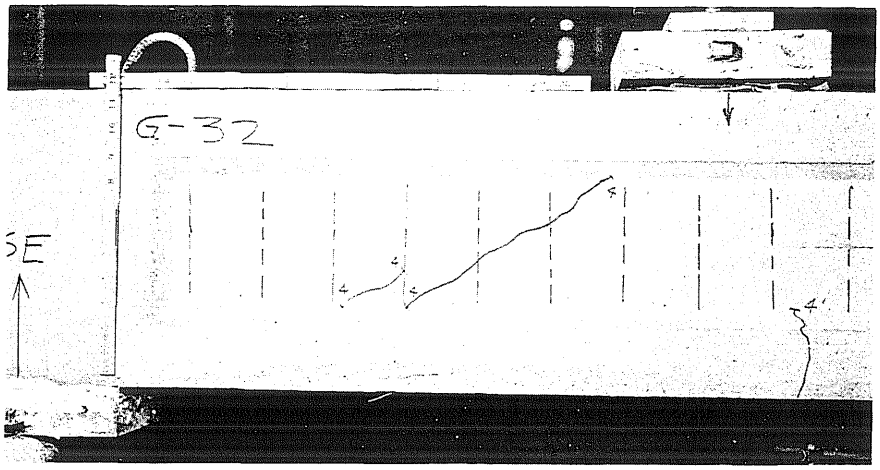

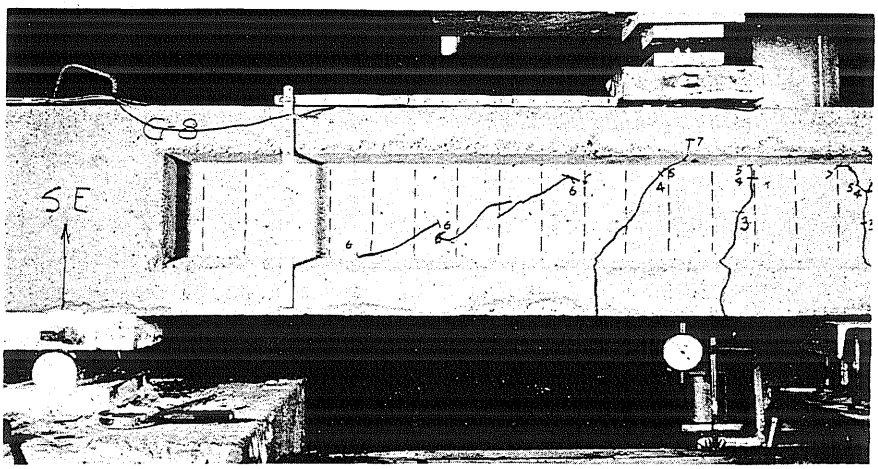

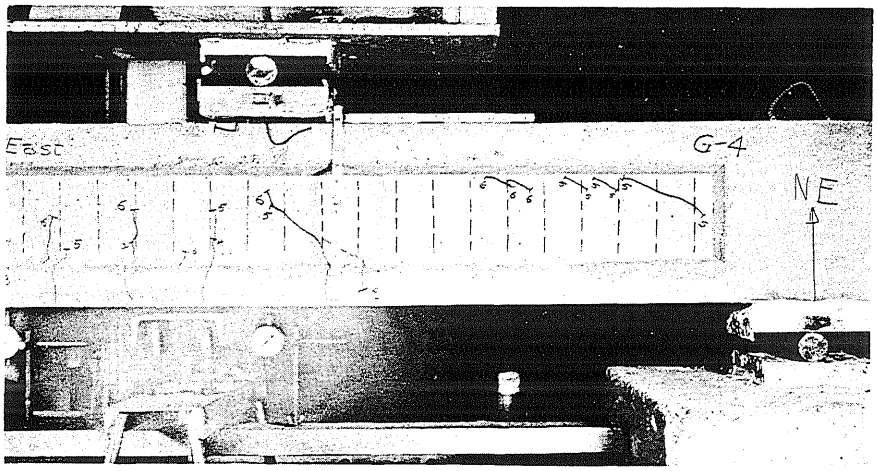

FIG. 38 TYPICAL WEB-SHEAR CRACKS

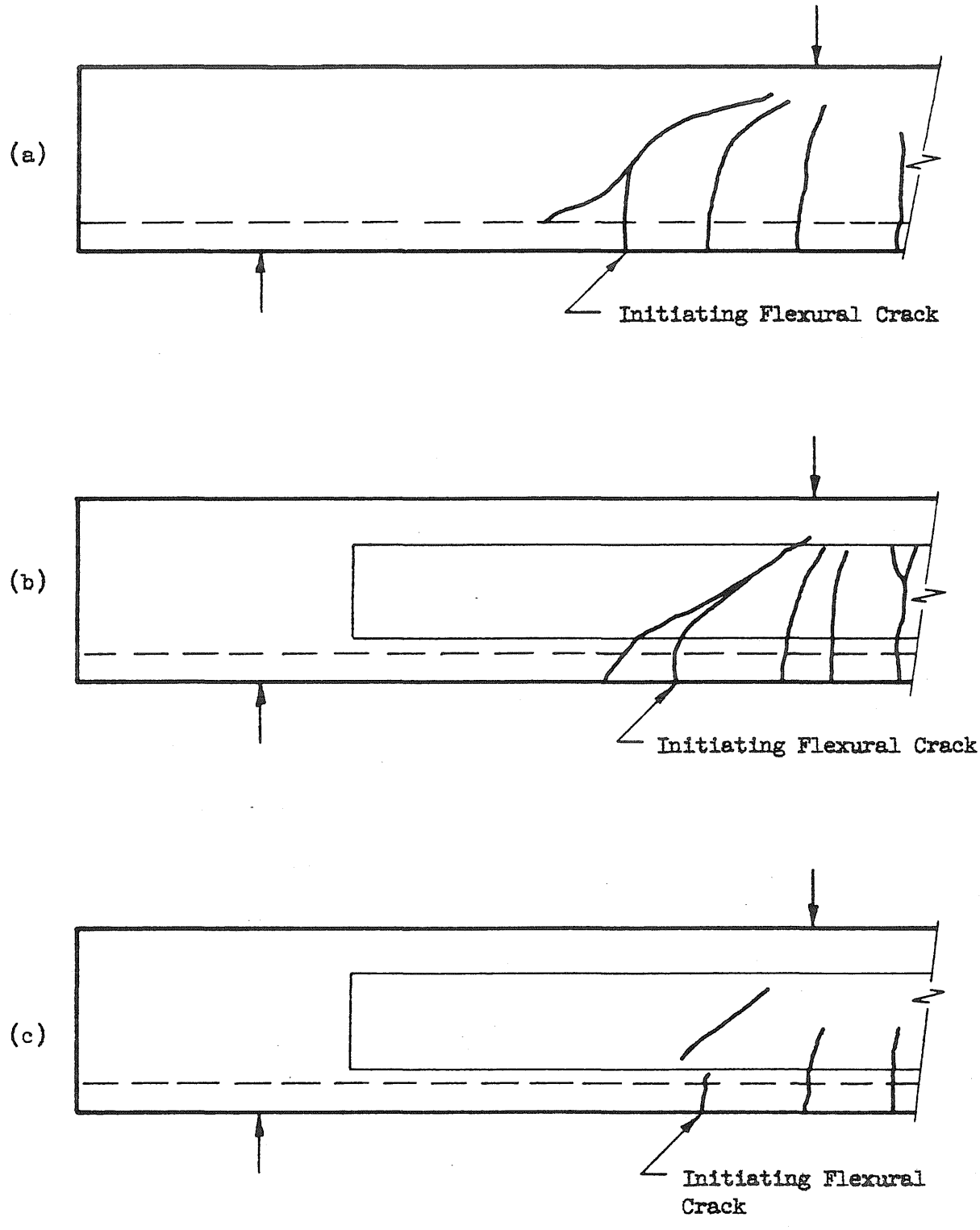

FIG. 39 TYPICAL FLEXURE-SHEAR CRACKS

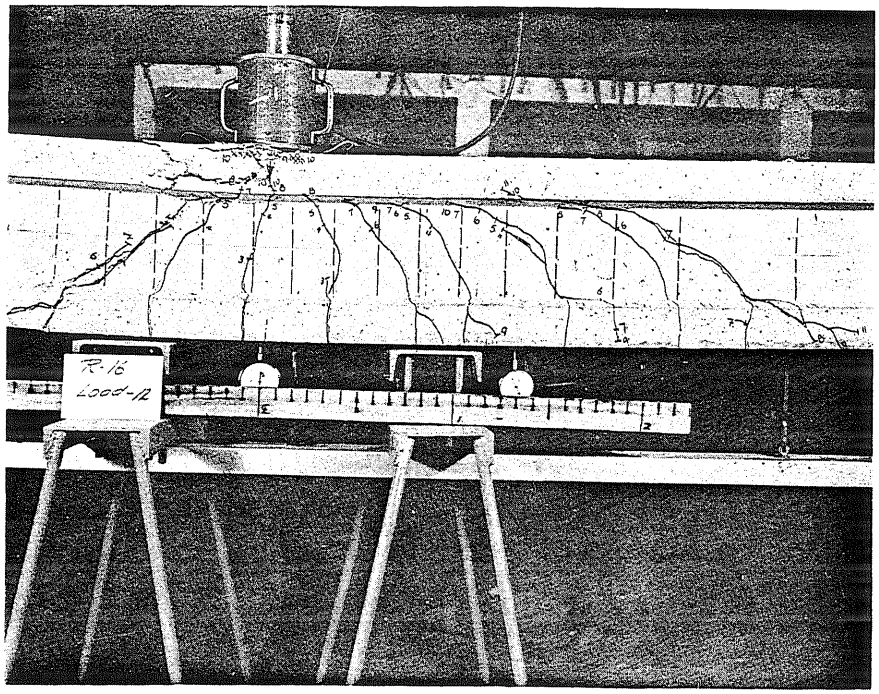

(a) Beam BW.28.26

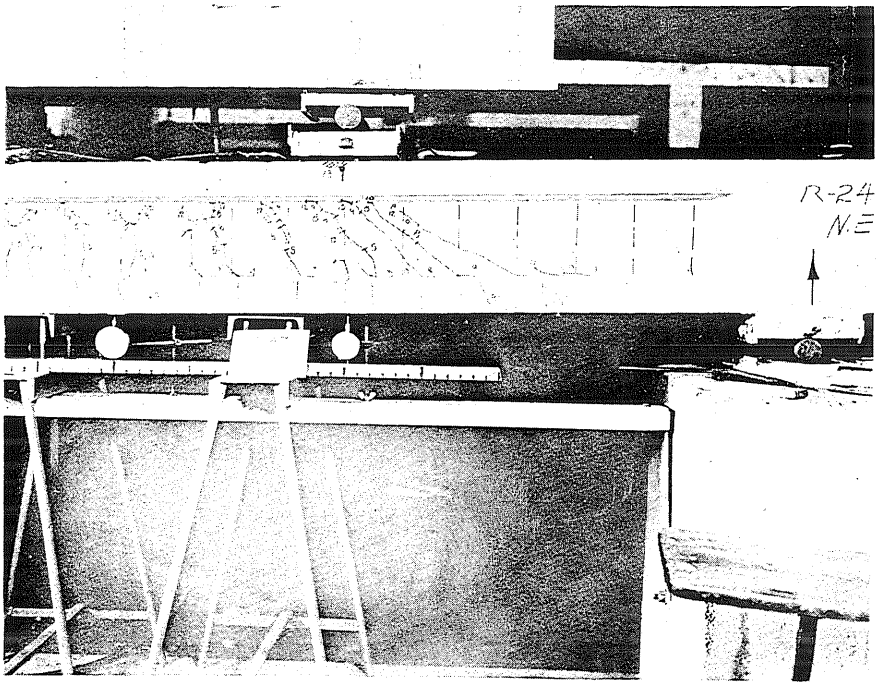

(b) Beam BW.14.26

FIG. 40 TYPICAL FLEXURE-SHEAR CRACKS

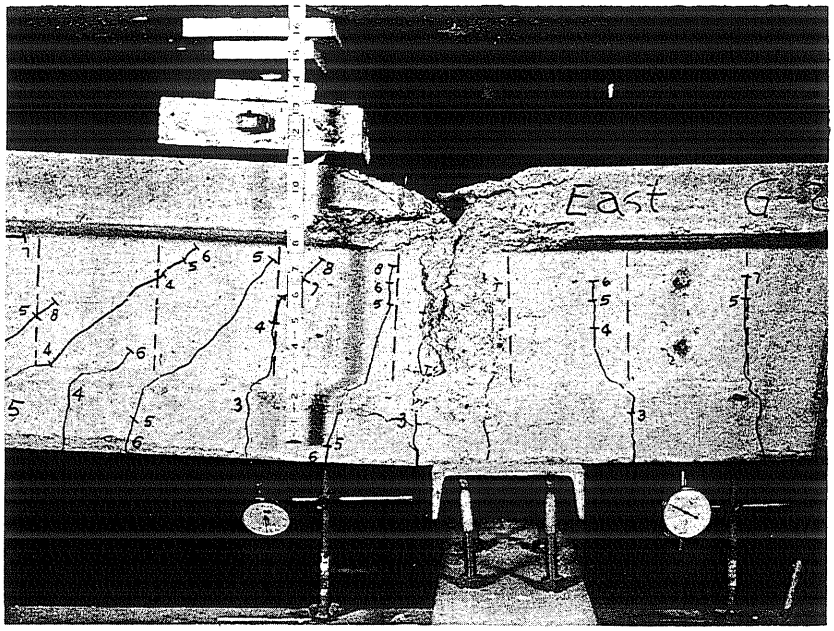

(a) Cracks in South Shear Span After Failure

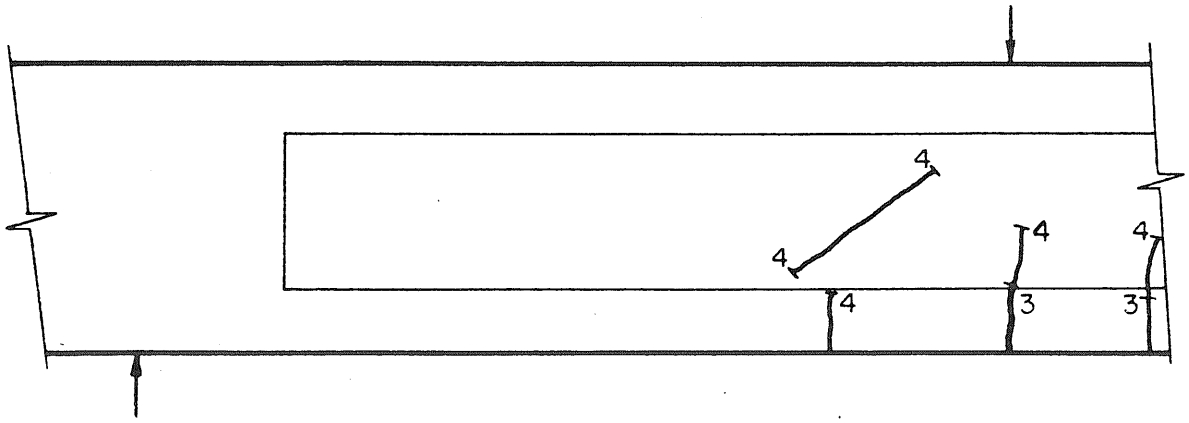

(b) Cracks in South Shear Span at Inclined Cracking Load

FIG. 41 FLEXURE-SHEAR CRACK ORIGINATING IN THE WEB ABOVE AN INITIATING FLEXURAL CRACK IN BEAM CW.14.40

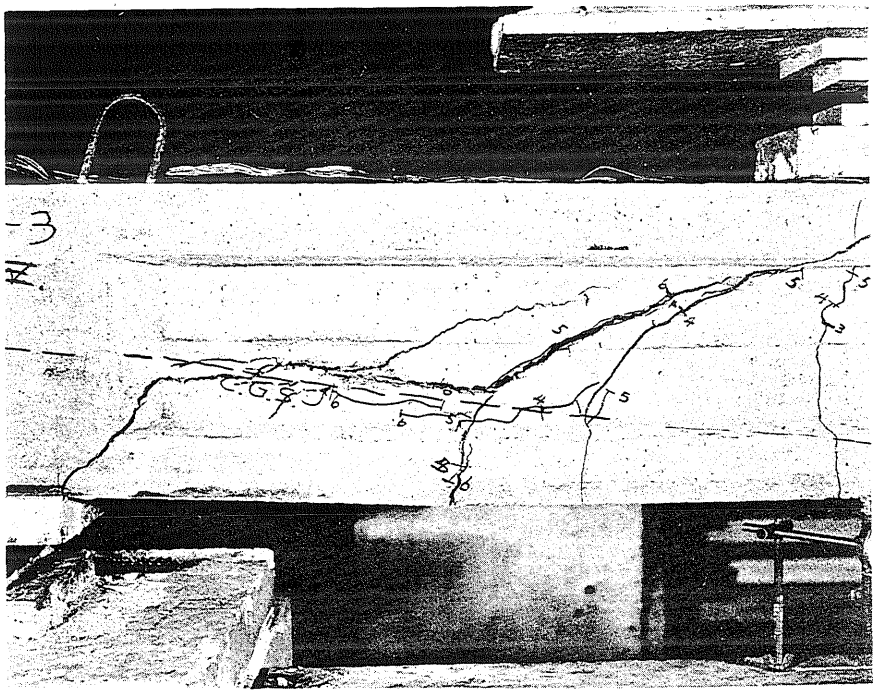

(a) Beam BD.24.32 - Splitting in a Beam With Draped Wires

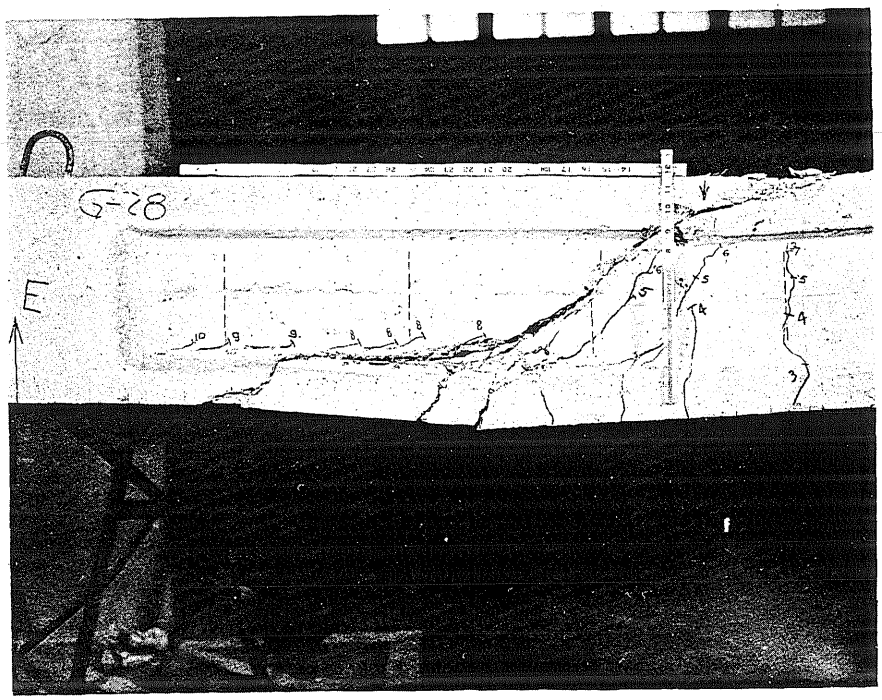

(b) Beam BW.14.31 - Splitting in a Beam With a Large Stirrup Spacing

FIG. 42 CRACKING, OR "SPLITTING", ALONG THE REINFORCEMENT

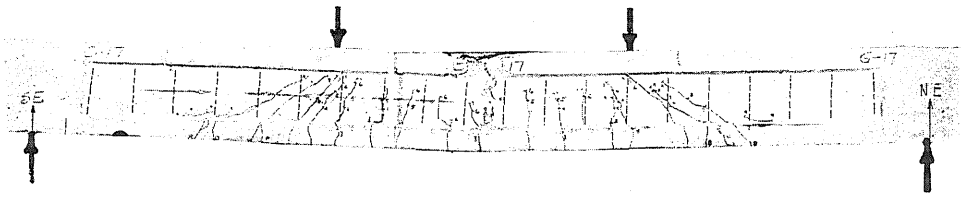

(a) Beam BW.14.43 - Flexure-Shear Cracks in a Beam Loaded at Two Points

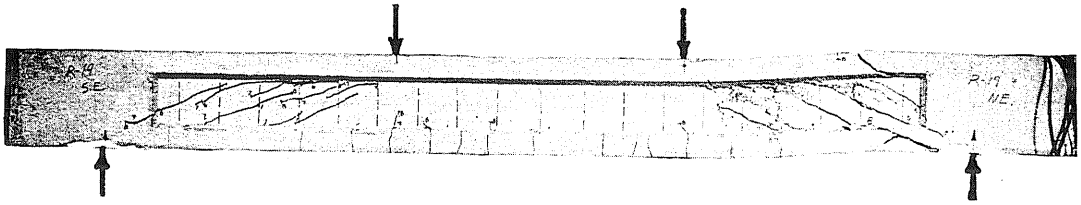

(b) Beam CW.14.54 - Web-Shear Cracks in a Beam Loaded at Two Points

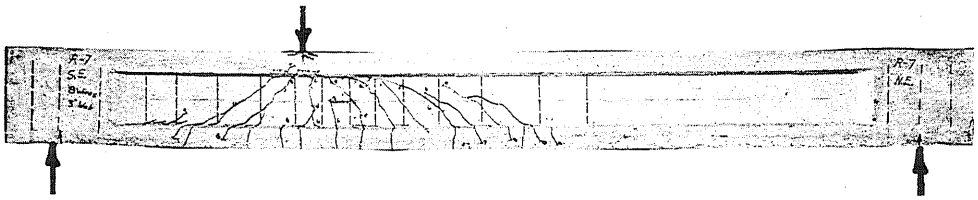

(c) Beam BW.19.28 - Flexure-Shear Cracks in Beam Loaded With a Single Concentrated Load

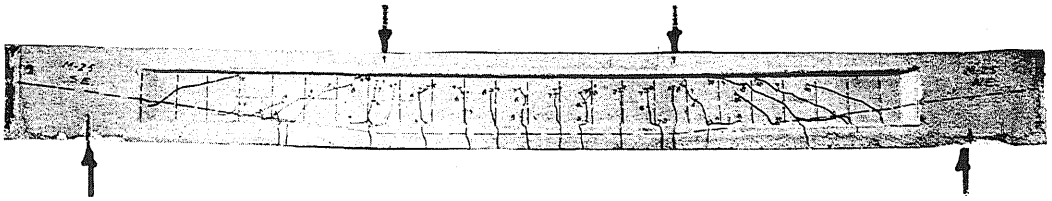

(d) Beam BV.14.42 - Flexure-Shear Cracks in a Beam With Draped Wires

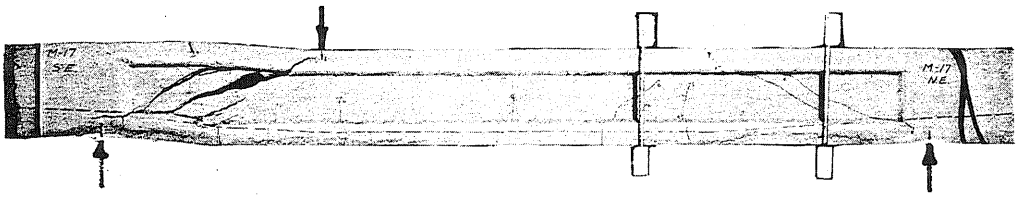

(e) Beam CD.13.24 - Web-Shear Cracks in a Beam With Draped Wires

FIG. 43 TYPICAL CRACK PATTERNS IN BEAMS LOADED WITH STATIONARY LOADS

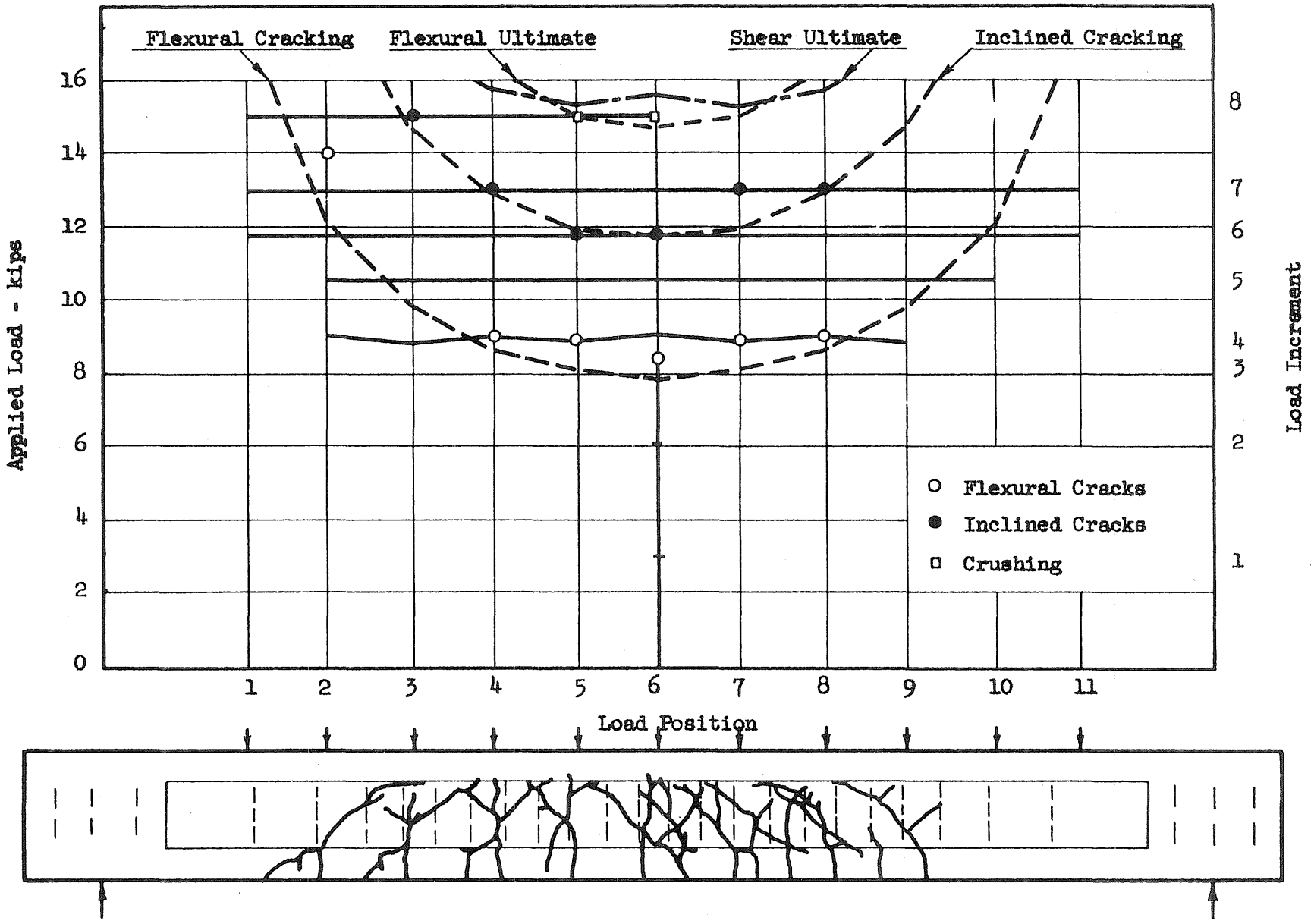

FIG. 44 LOAD RECORD AND CRACK PATTERN FOR BEAM BW.10.22

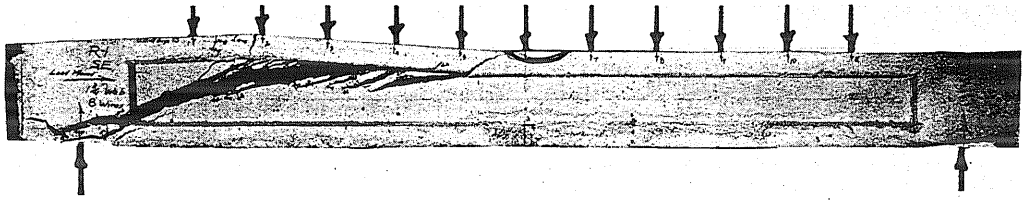

(a) Beam C.10.28 - Web-Shear Cracks in a Beam Without Stirrups

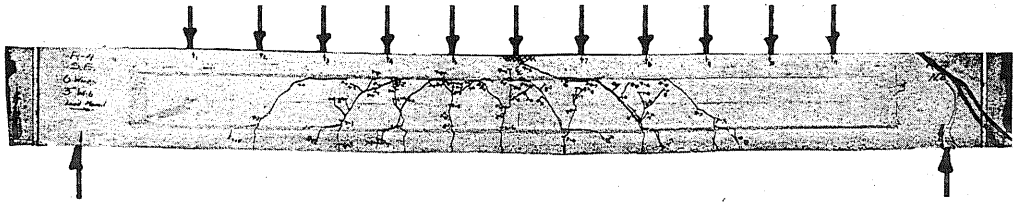

(b) Beam B.10.24 - Flexure-Shear Cracks in a Beam Without Stirrups

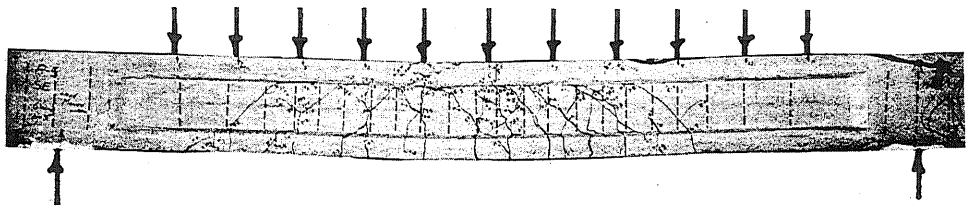

(c) Beam BW.10.22 - Flexure-Shear Cracks in a Beam With Stirrups

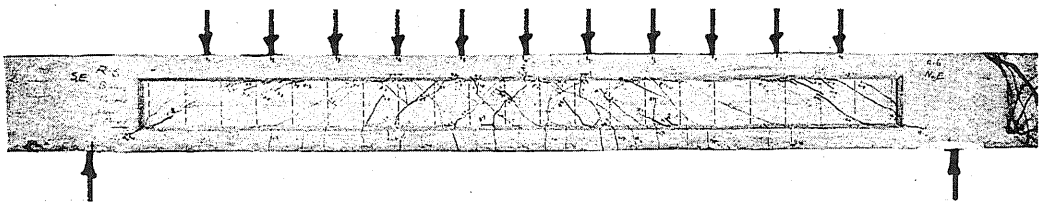

(d) Beam CW.10.26 - Web-Shear and Flexure-Shear Cracks in a Beam With Stirrups

FIG. 45 TYPICAL CRACK PATTERNS IN BEAMS TESTED UNDER A SIMULATED MOVING LOAD

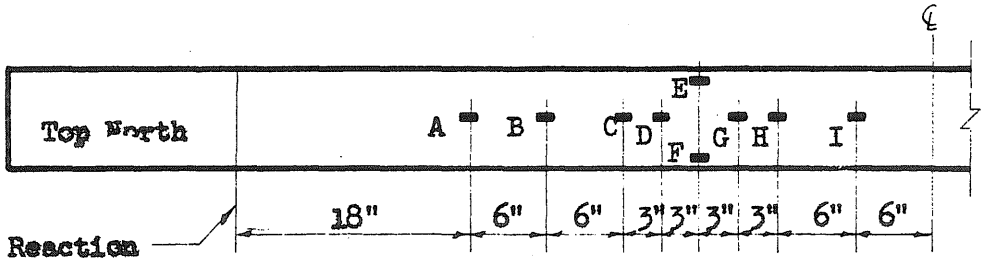

Beam CW.14.21

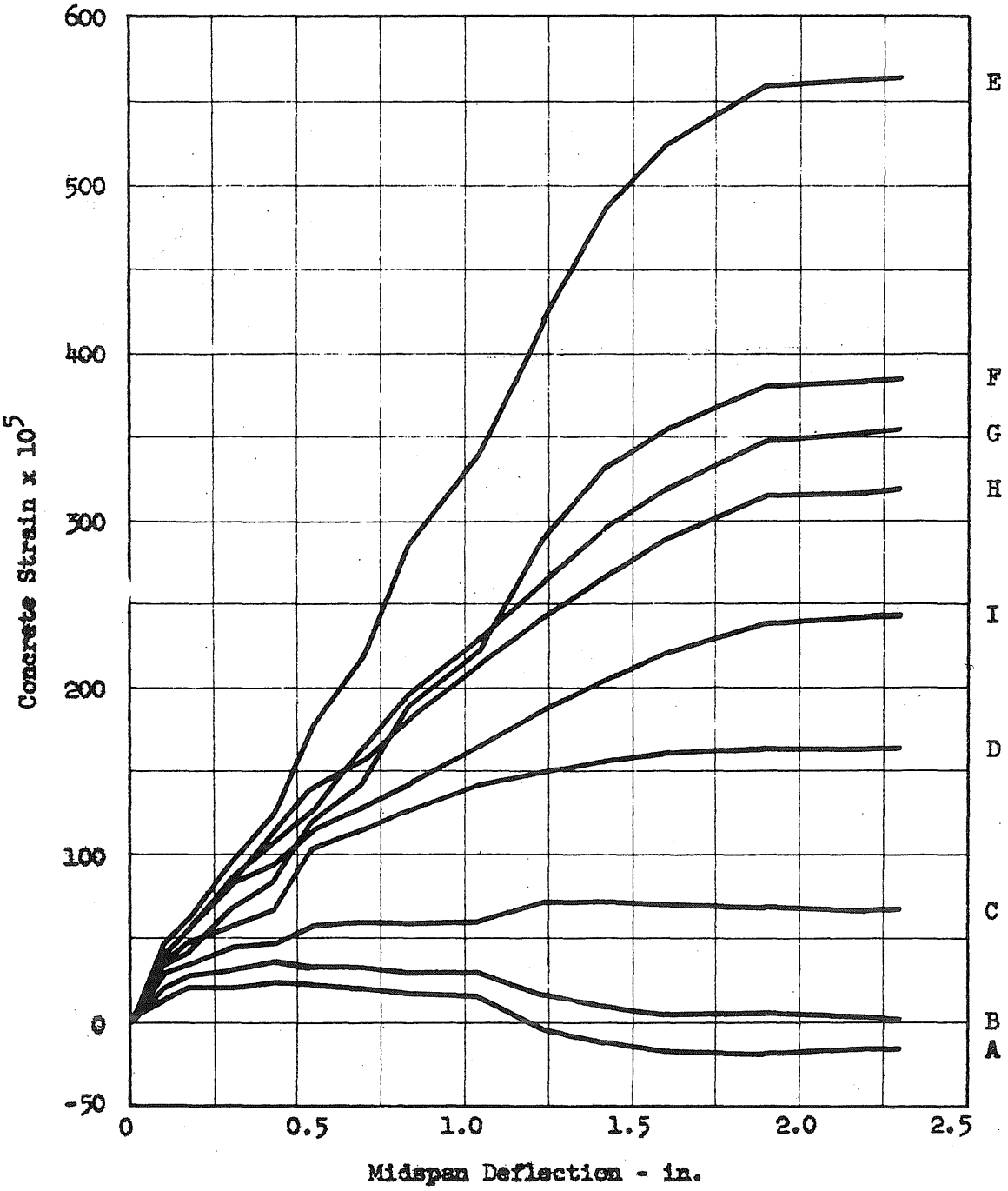

FIG. 46 RELATIONSHIP BETWEEN CONCRETE STRAINS AND DEFLECTIONS

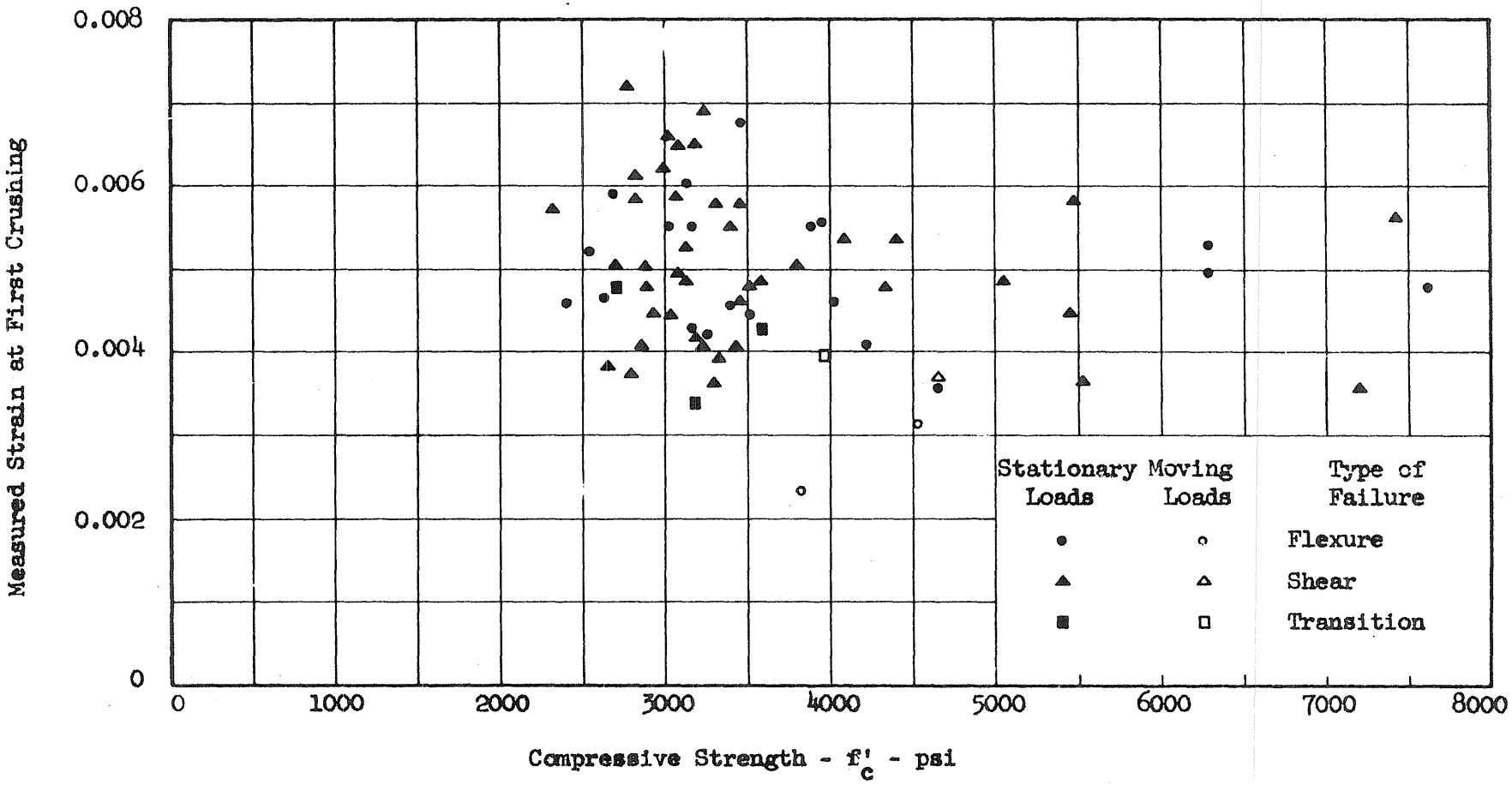

FIG. 47 MEASURED VALUES OF CONCRETE STRAIN AT FIRST CRUSHING

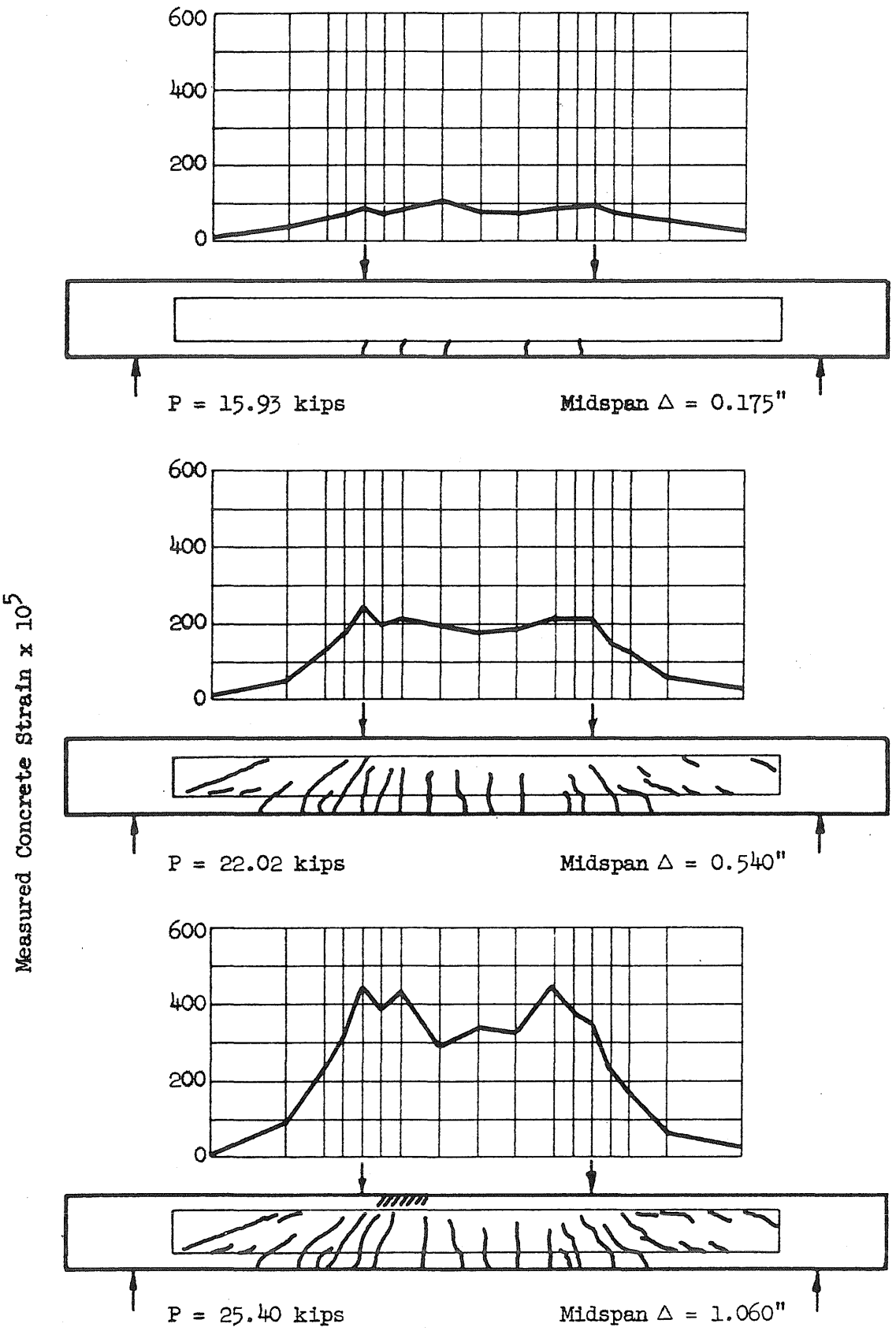

FIG. 48 CRACK PATTERNS AND CORRESPONDING DISTRIBUTIONS OF STRAIN ON TOP SURFACE OF BEAM CW.14.40

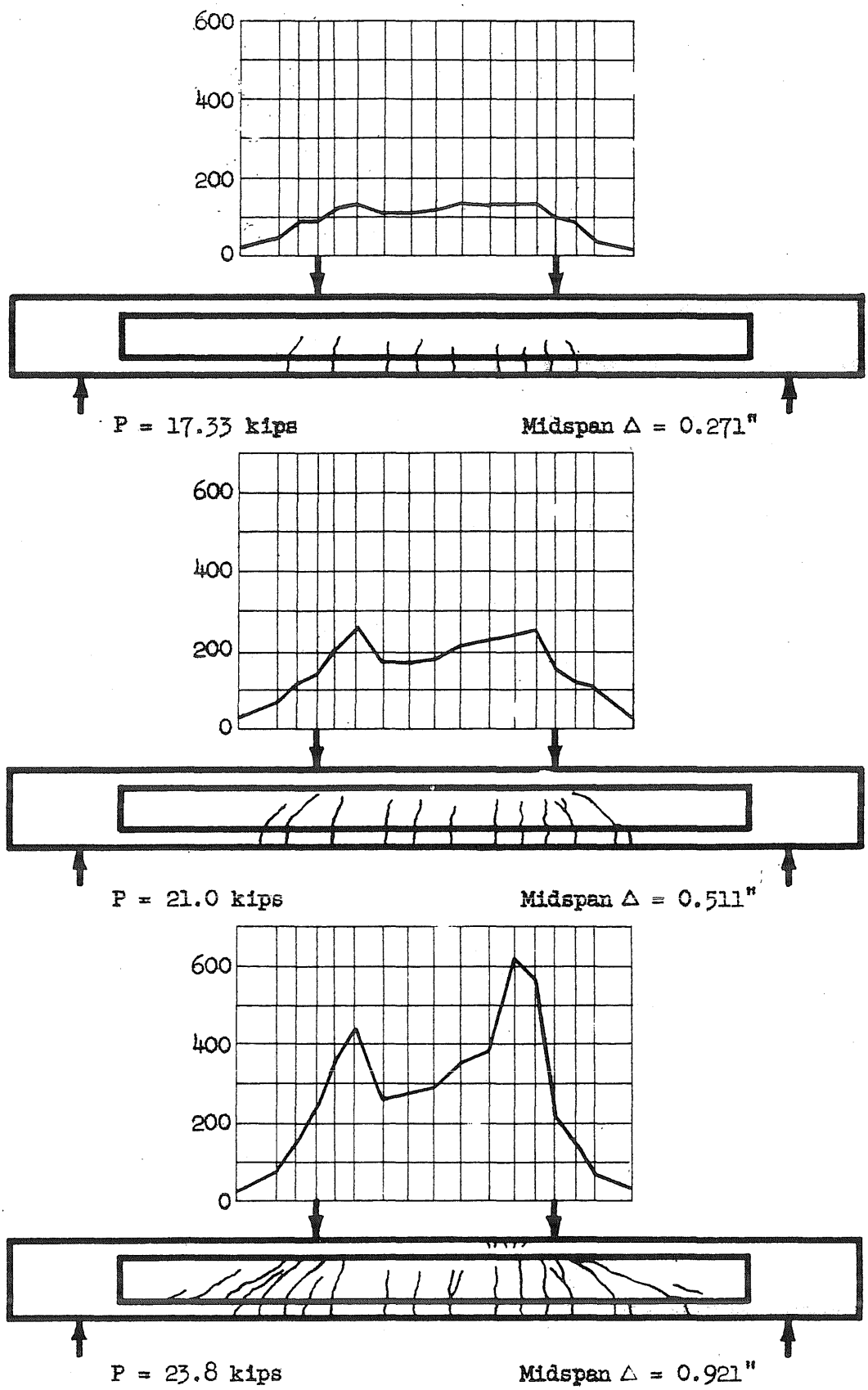

FIG. 49 CRACK PATTERNS AND CORRESPONDING DISTRIBUTIONS OF STRAIN ON TOP SURFACE OF BEAM BW.14.42

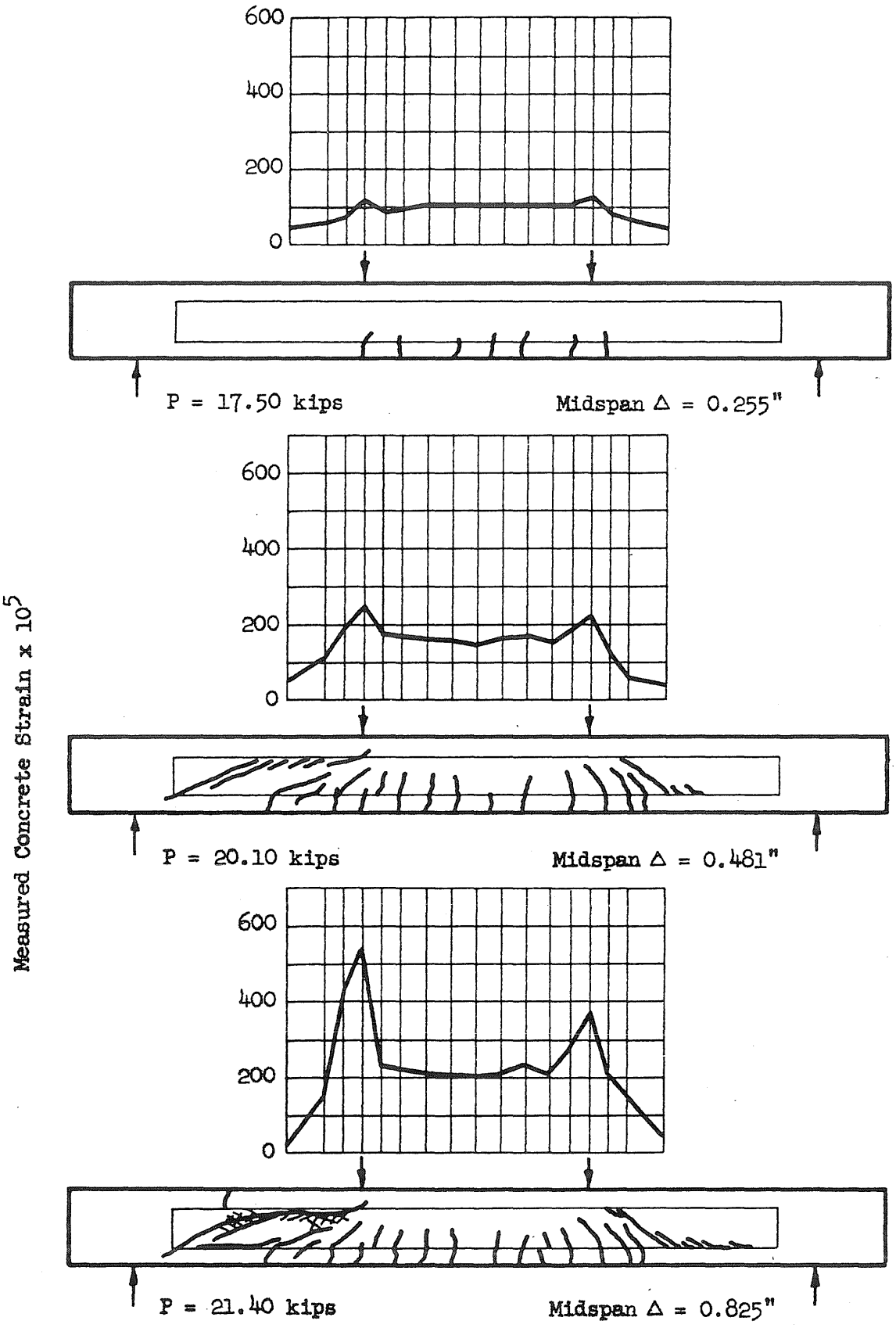

FIG. 50 CRACK PATTERNS AND CORRESPONDING DISTRIBUTIONS OF STRAIN ON TOP SURFACE OF BEAM CW.14.39

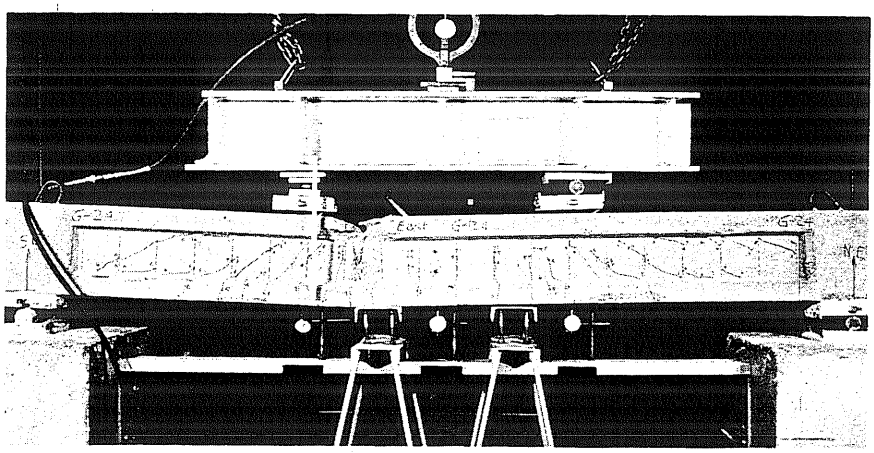

(a) Beam CW.14.40

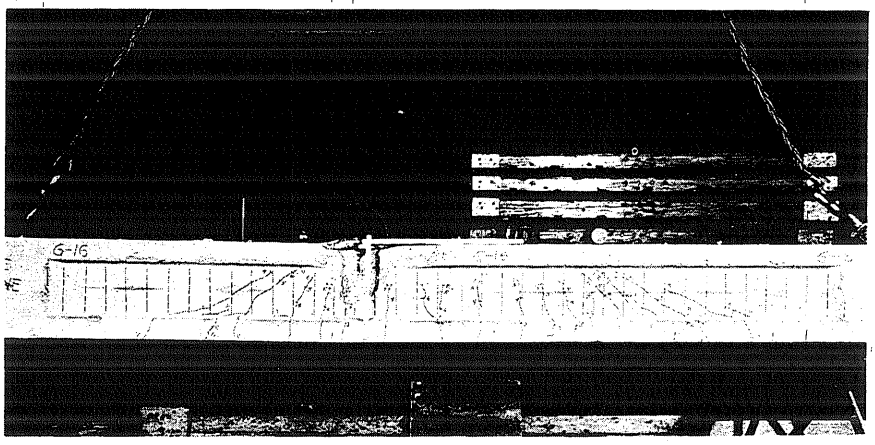

(b) Beam BW.14.42

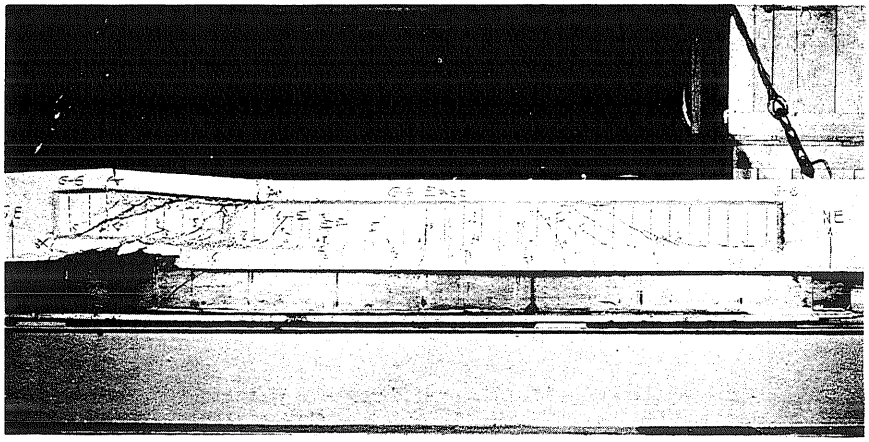

(c) Beam CW.14.39

FIG. 51 BEAMS CW.14.40, BW.14.42 AND CW.14.39 AFTER FAILURE

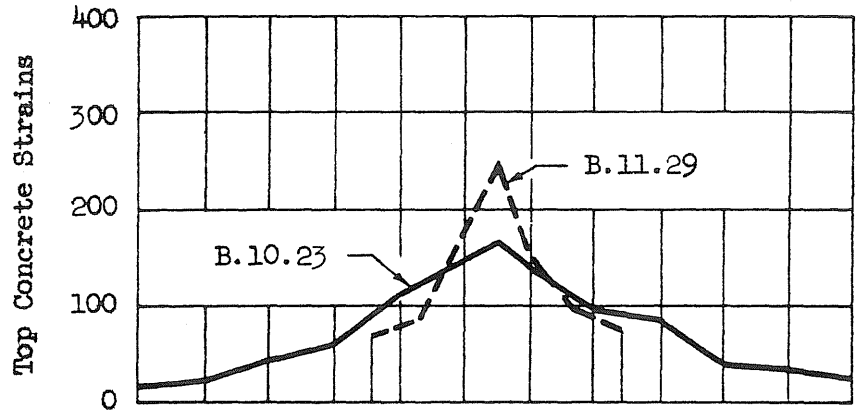

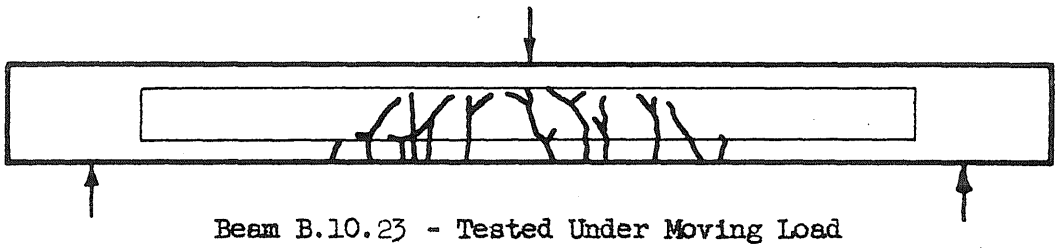

Beam B.10.23 - Tested Under Moving Load

P = 14.67 kips Midspan Δ = 0.321"

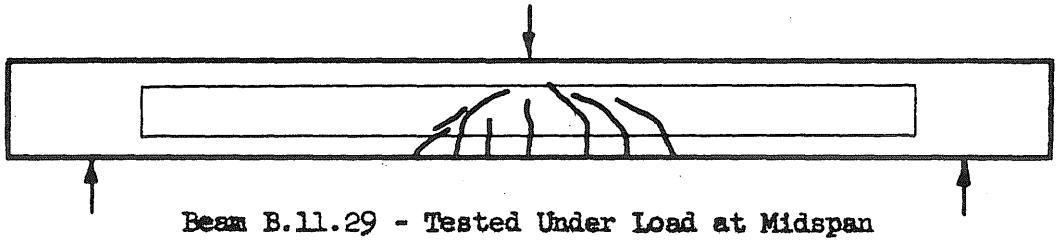

Beam B.11.29 - Tested Under Load at Midspan

P = 14.65 kips Midspan Δ = 0.280"

FIG. 52 COMPARISON OF TOP CONCRETE STRAINS AND CRACK PATTERNS FOR BEAMS TESTED UNDER MOVING AND STATIONARY LOADS

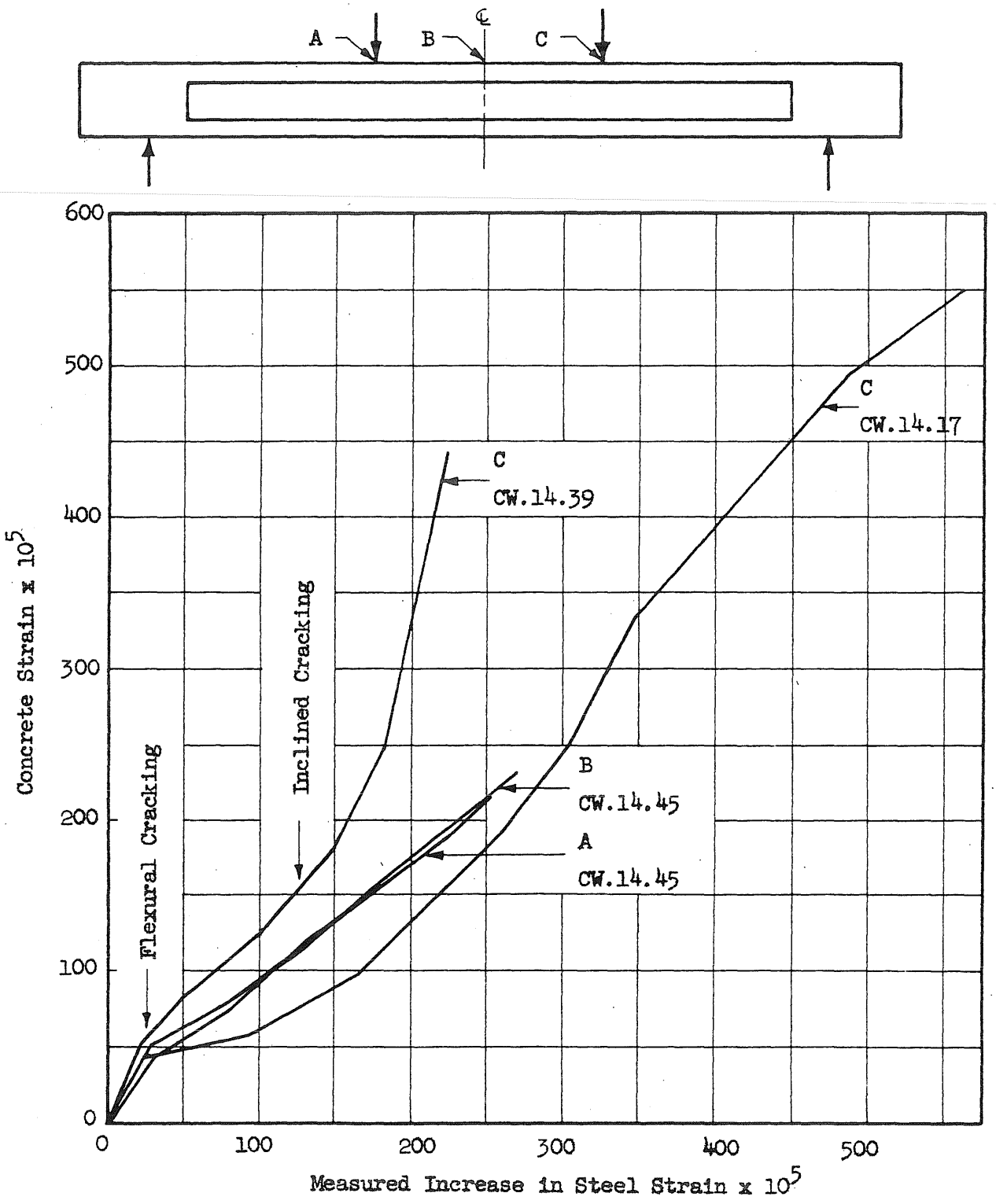

FIG. 53 RELATIONSHIP BETWEEN CONCRETE AND STEEL STRAINS FOR SHEAR AND FLEXURAL FAILURES

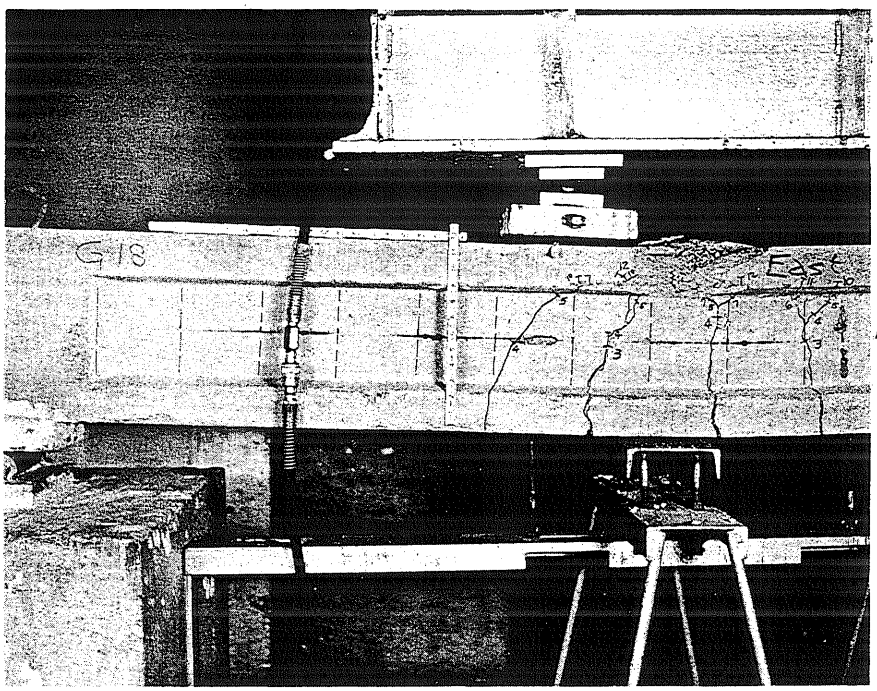

FIG. 54 FLEXURAL FAILURE IN A BEAM WITH FOUR WIRES

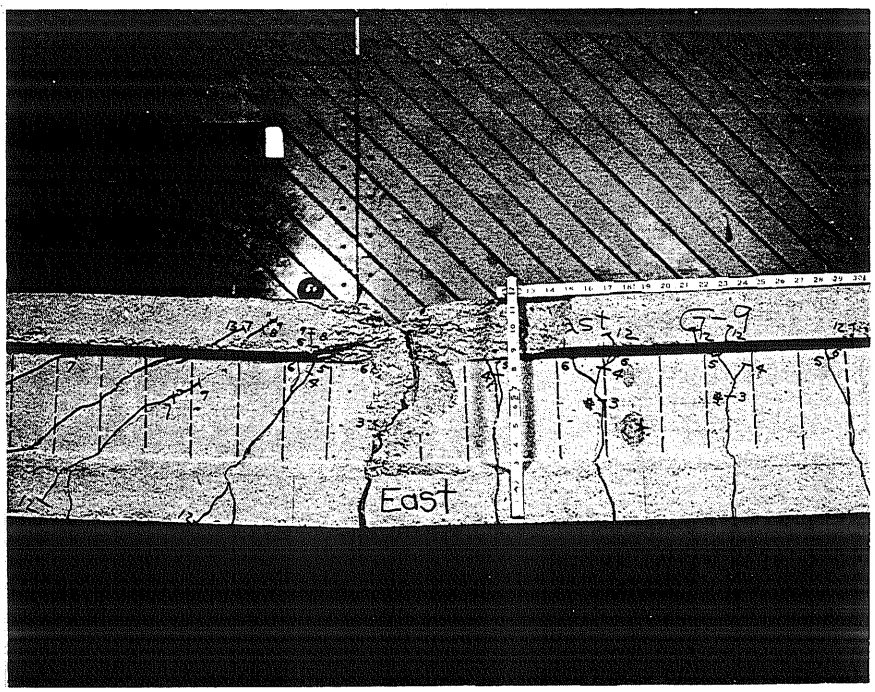

FIG. 55 FLEXURAL FAILURE IN A BEAM WITH EIGHT WIRES

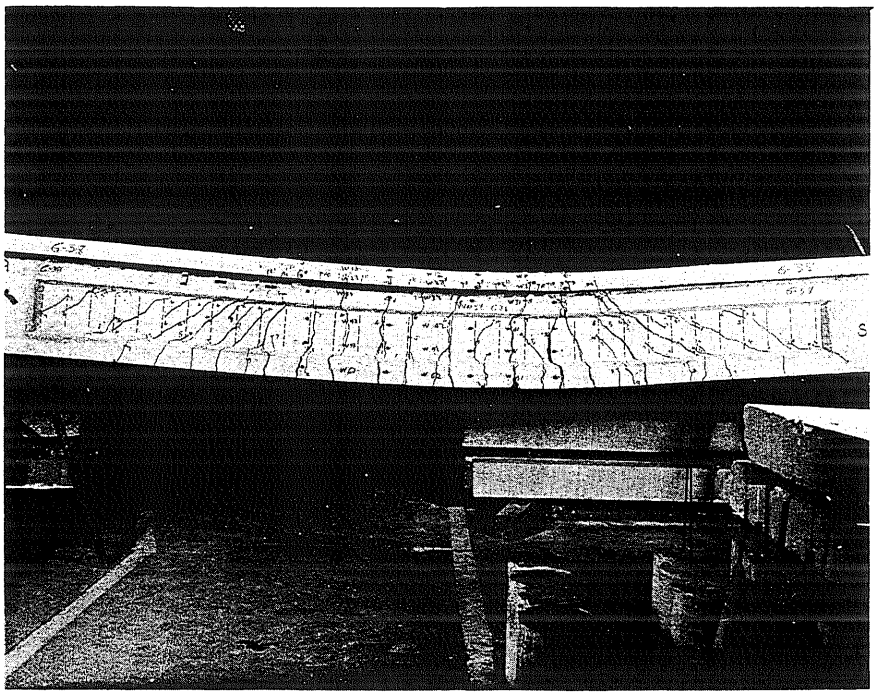

FIG. 56 FLEXURAL FAILURE OF A GREATLY UNDER-REINFORCED BEAM - BEAM FW.14.07

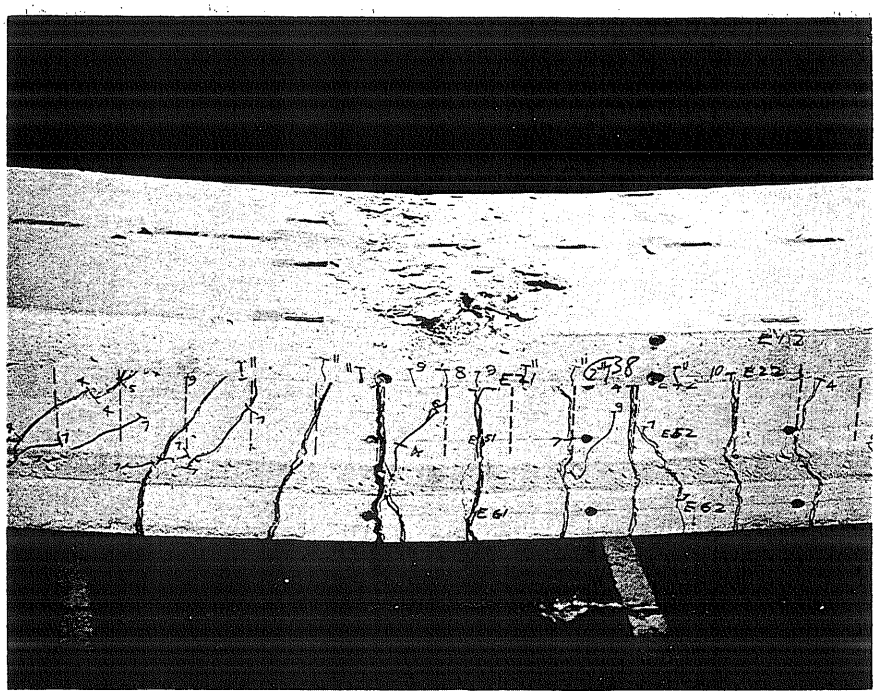

FIG. 57 CRUSHING OF CONCRETE IN THE SLAB - BEAM FW.14.07

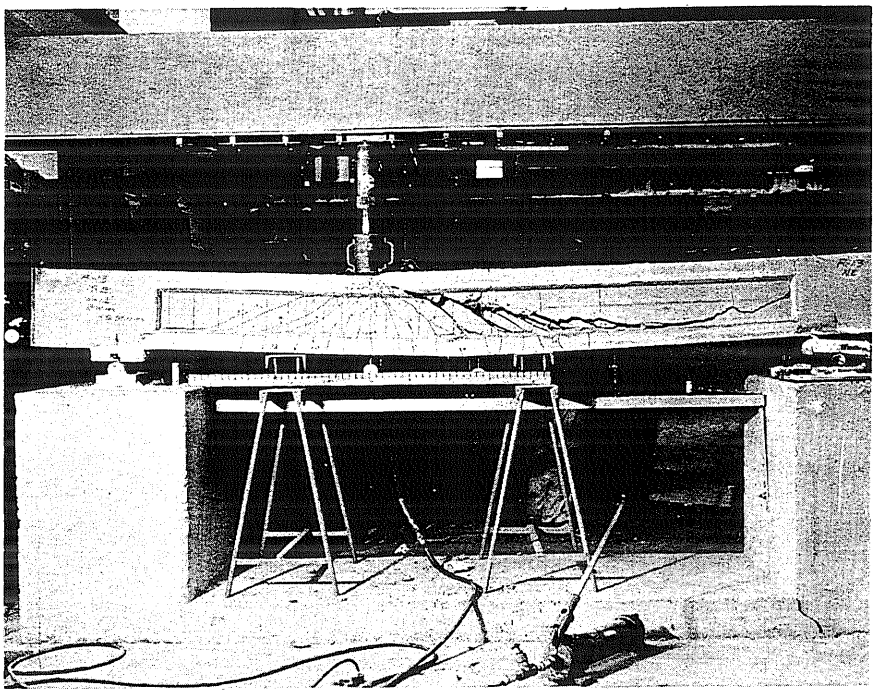

FIG. 58 BEAM CW.18.15 - FLEXURAL FAILURE FOLLOWED BY RELIEVING OF PRESTRESS IN LONG SHEAR SPAN

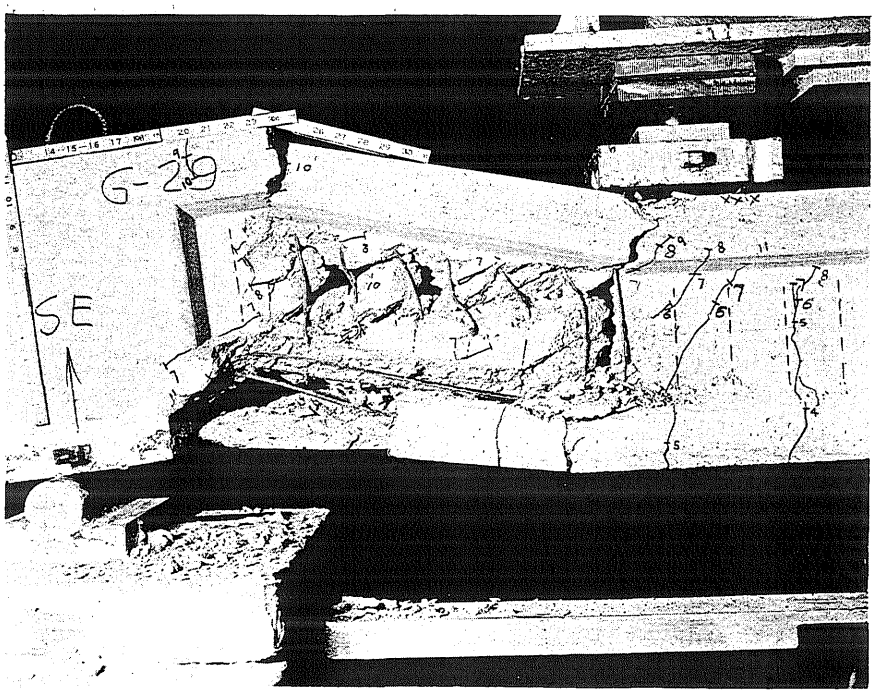

FIG. 59 BEAM CW.13.28 - SHEAR FAILURE ACCOMPANIED BY CRUSHING OF WEB UNDER LOAD POINT

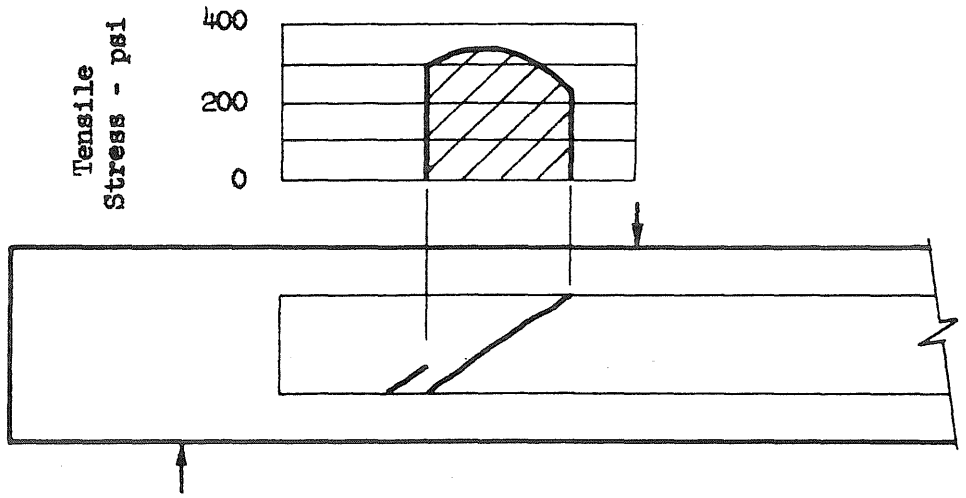

Beam CW.13.38

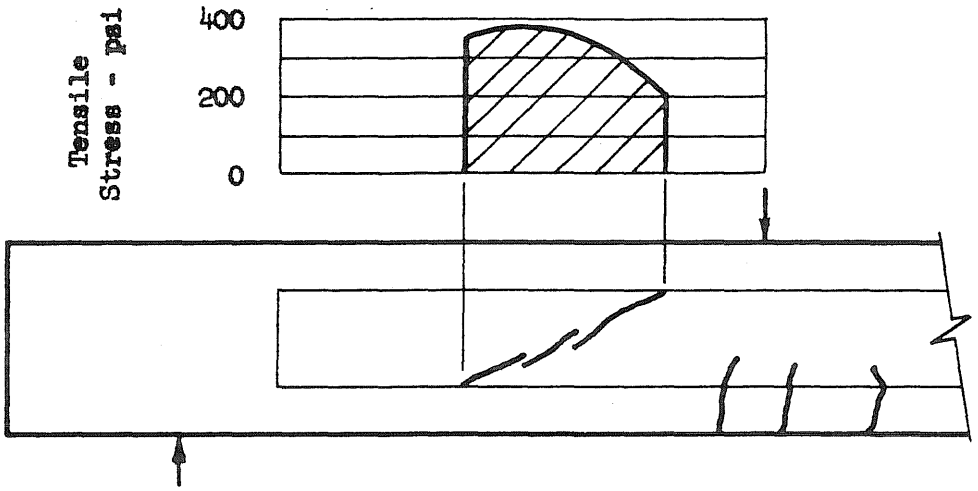

Beam CW.14.47

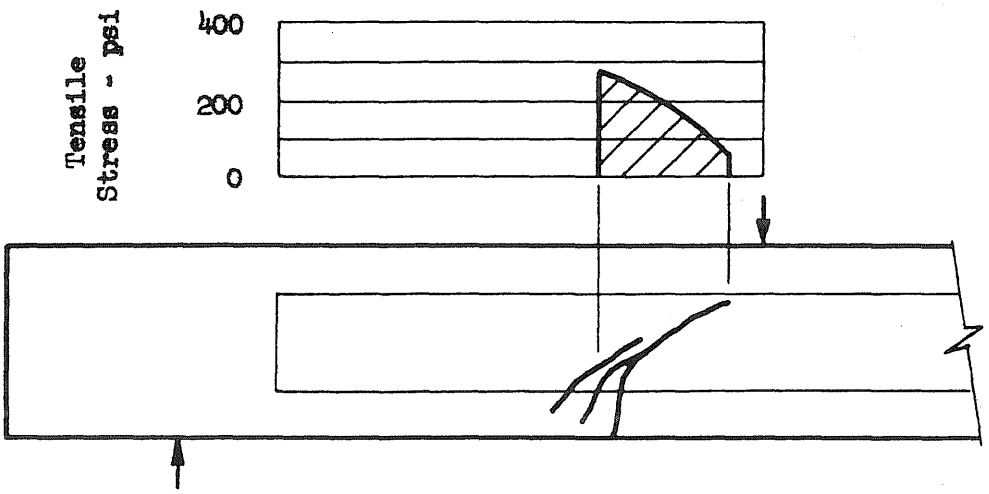

Beam BW.14.41

FIG. 60 DISTRIBUTION OF PRINCIPAL TENSILE STRESSES ALONG TRAJECTORIES OF INCLINED CRACKS

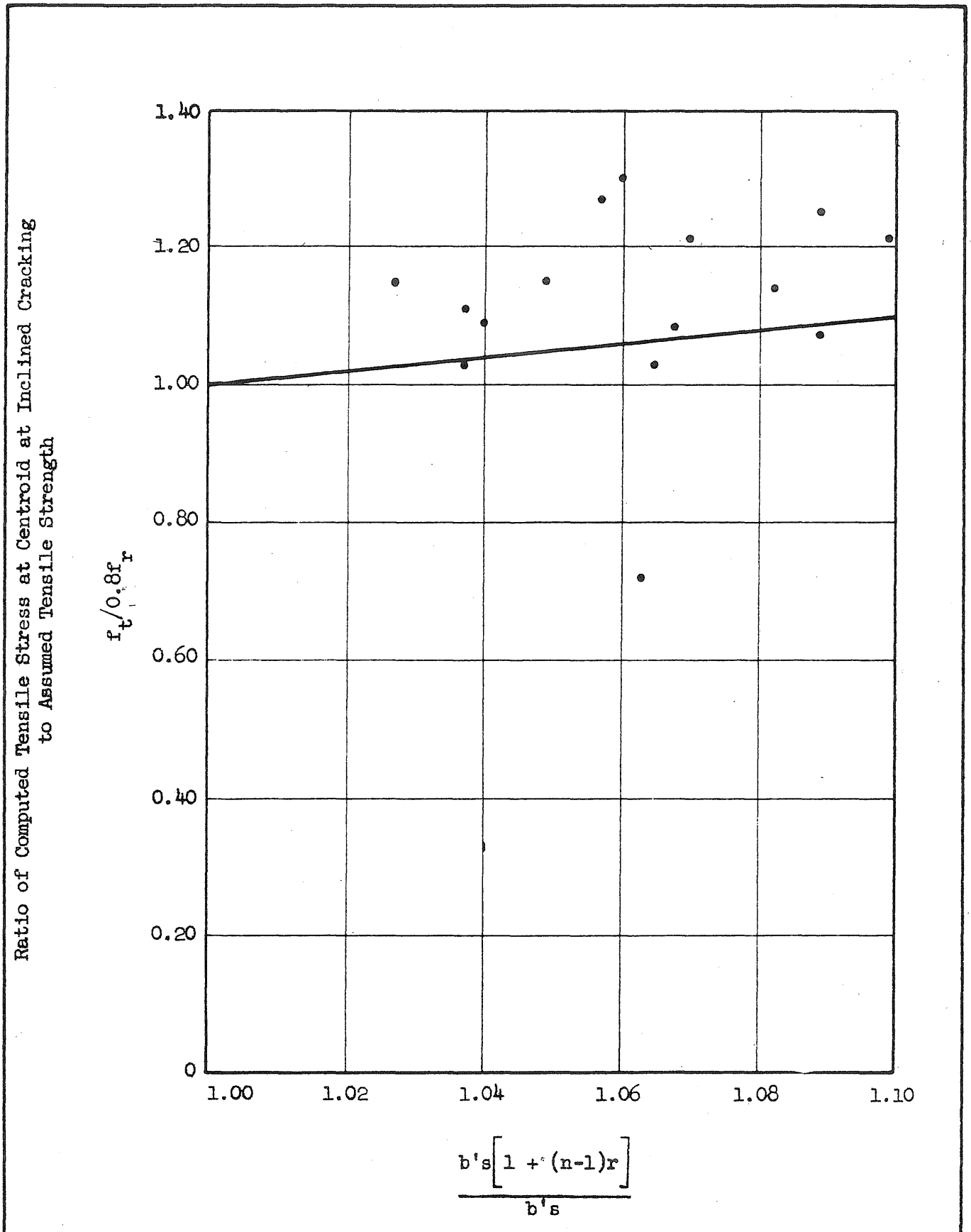

FIG. 61 EFFECT OF STIRRUPS ON APPARENT TENSILE STRENGTH OF CONCRETE

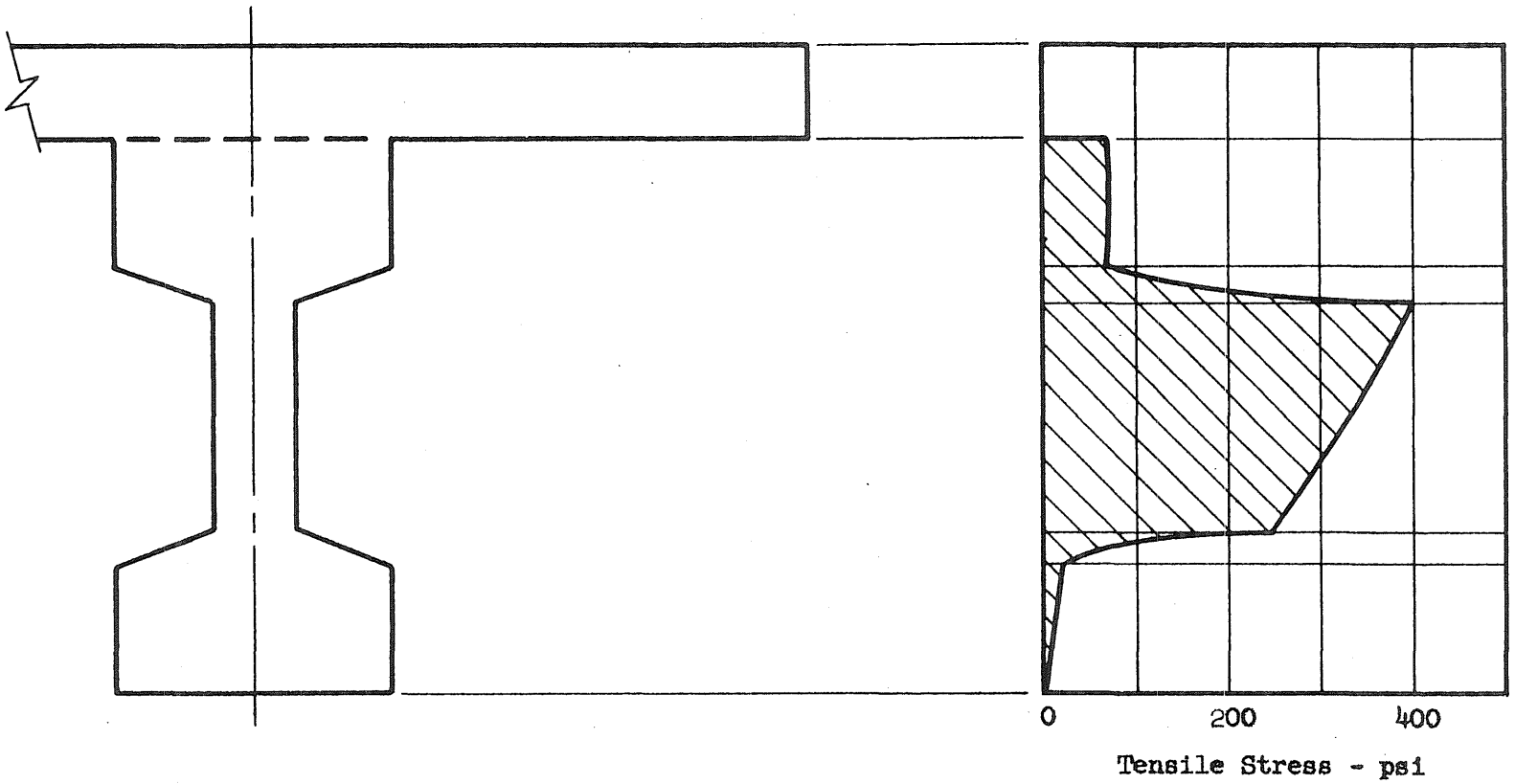

(a) Cross Section

(b) Distribution of Principal Tensile Stresses

FIG. 62 PRINCIPAL TENSILE STRESSES IN BEAM FW.14.06 AT WEB-SHEAR CRACKING LOAD

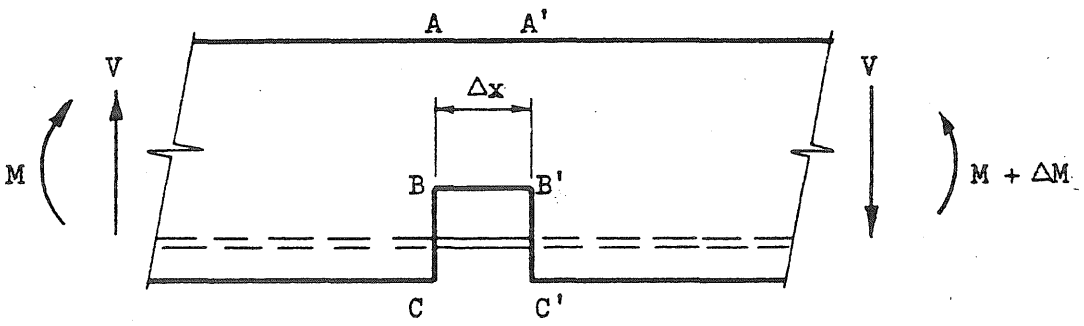

(a) Gap in Bottom of Beam

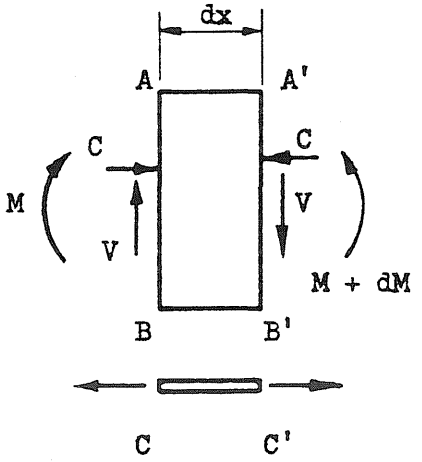

(b) Forces on Block ABB'A'

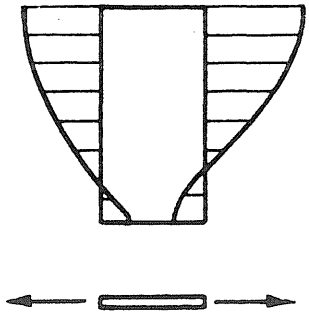

(c) Stresses on Block ABB'A'

(d) Difference in Stresses

(e) Shear Stresses on Section A'B'

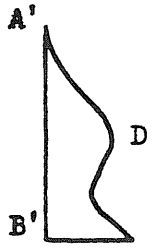

(f) Principal Tensile Stresses on Section A'B'

FIG. 63 ANALYSIS OF STRESSES ABOVE A FLEXURAL CRACK IN A REGION OF COMBINED SHEAR AND FLEXURE

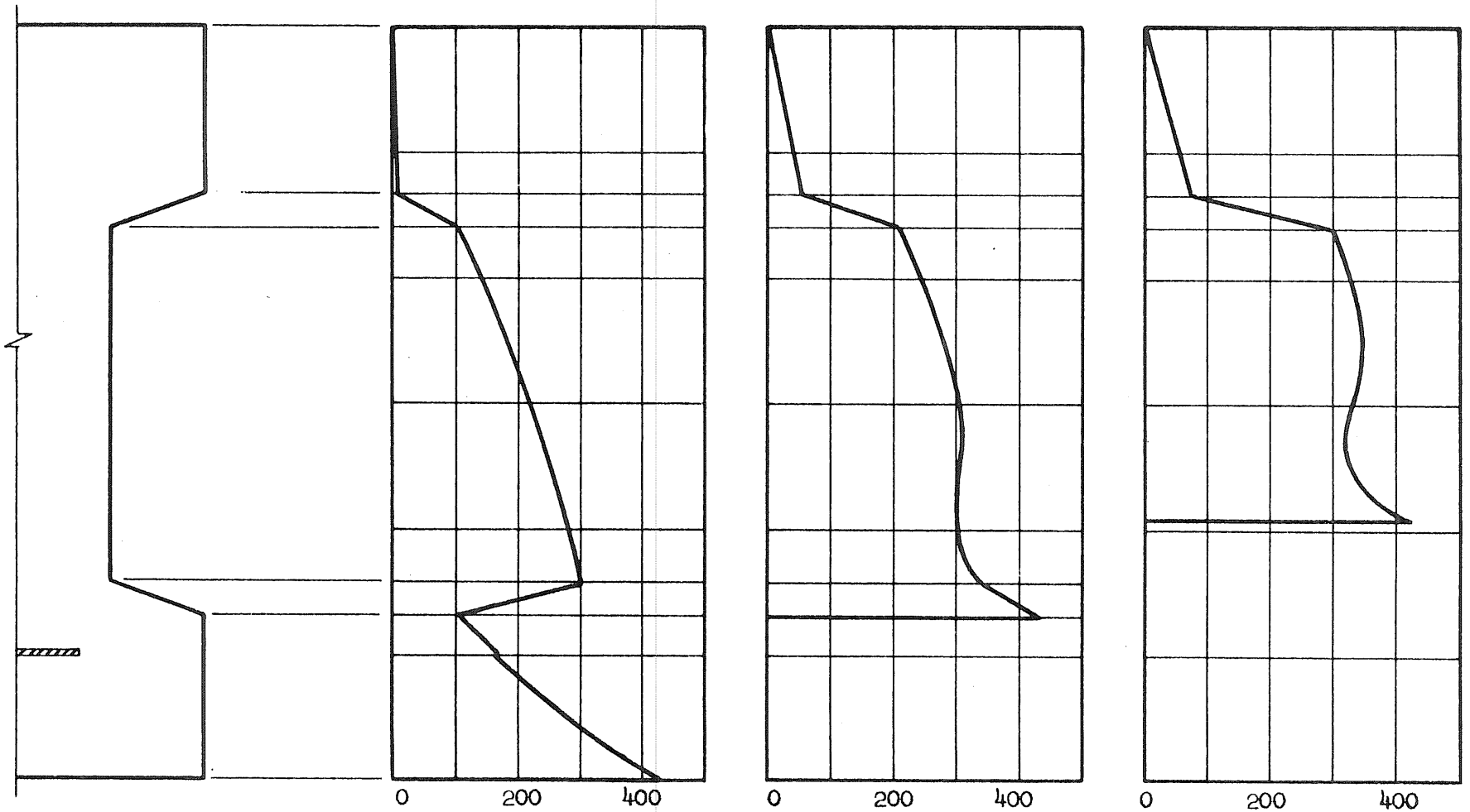

FIG. 64 PRINCIPAL TENSILE STRESSES ABOVE A FLEXURAL CRACK IN A REGION OF COMBINED SHEAR AND FLEXURE

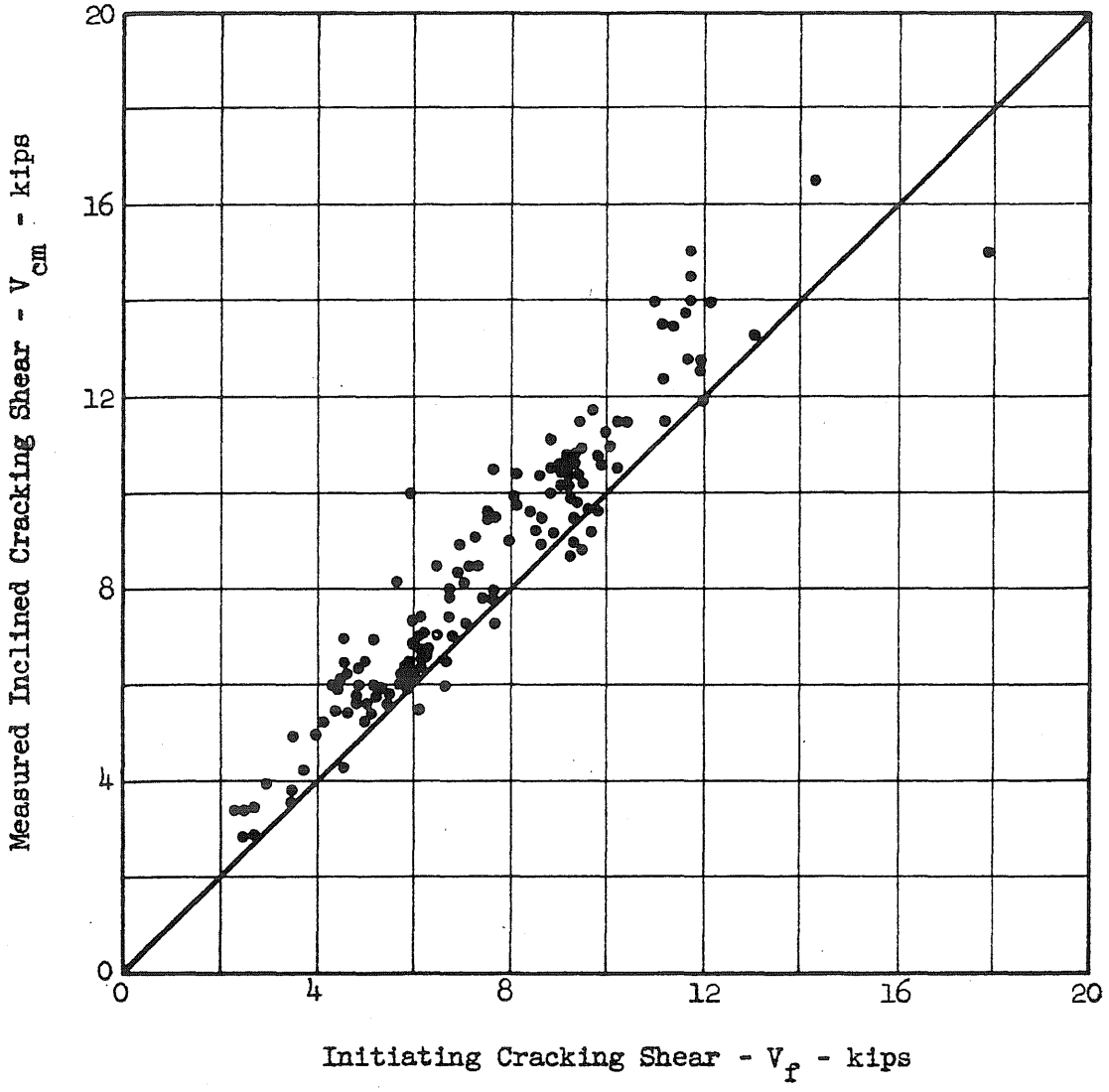

FIG. 65 COMPARISON OF THE MEASURED INCLINED CRACKING SHEAR AND THE COMPUTED SHEAR CORRESPONDING TO INITIATING CRACKS

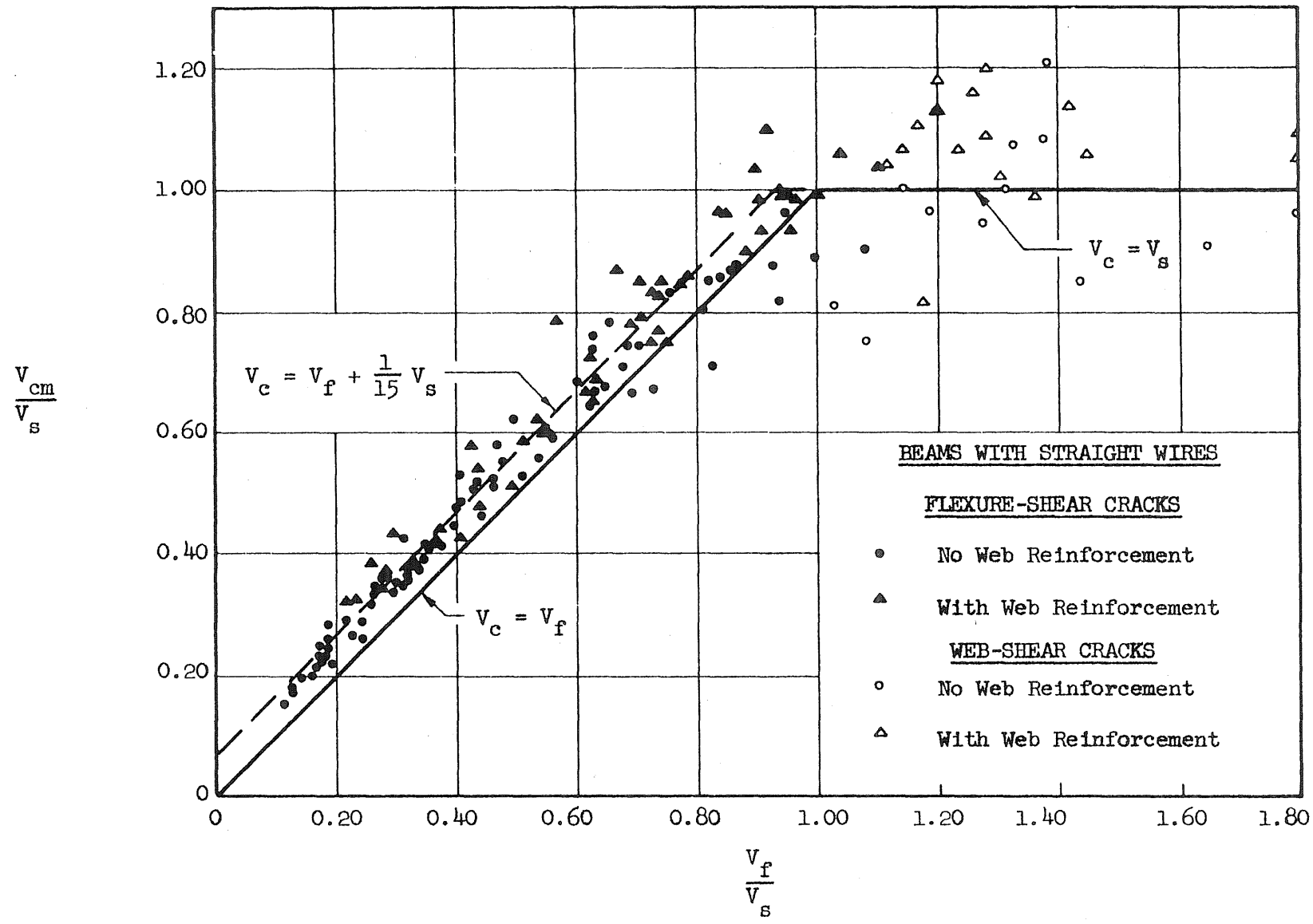

FIG. 66 COMPARISON OF THE DIMENSIONLESS QUANTITIES V_{cm}/V_s AND V_f/V_s FOR BEAMS WITH STRAIGHT WIRES

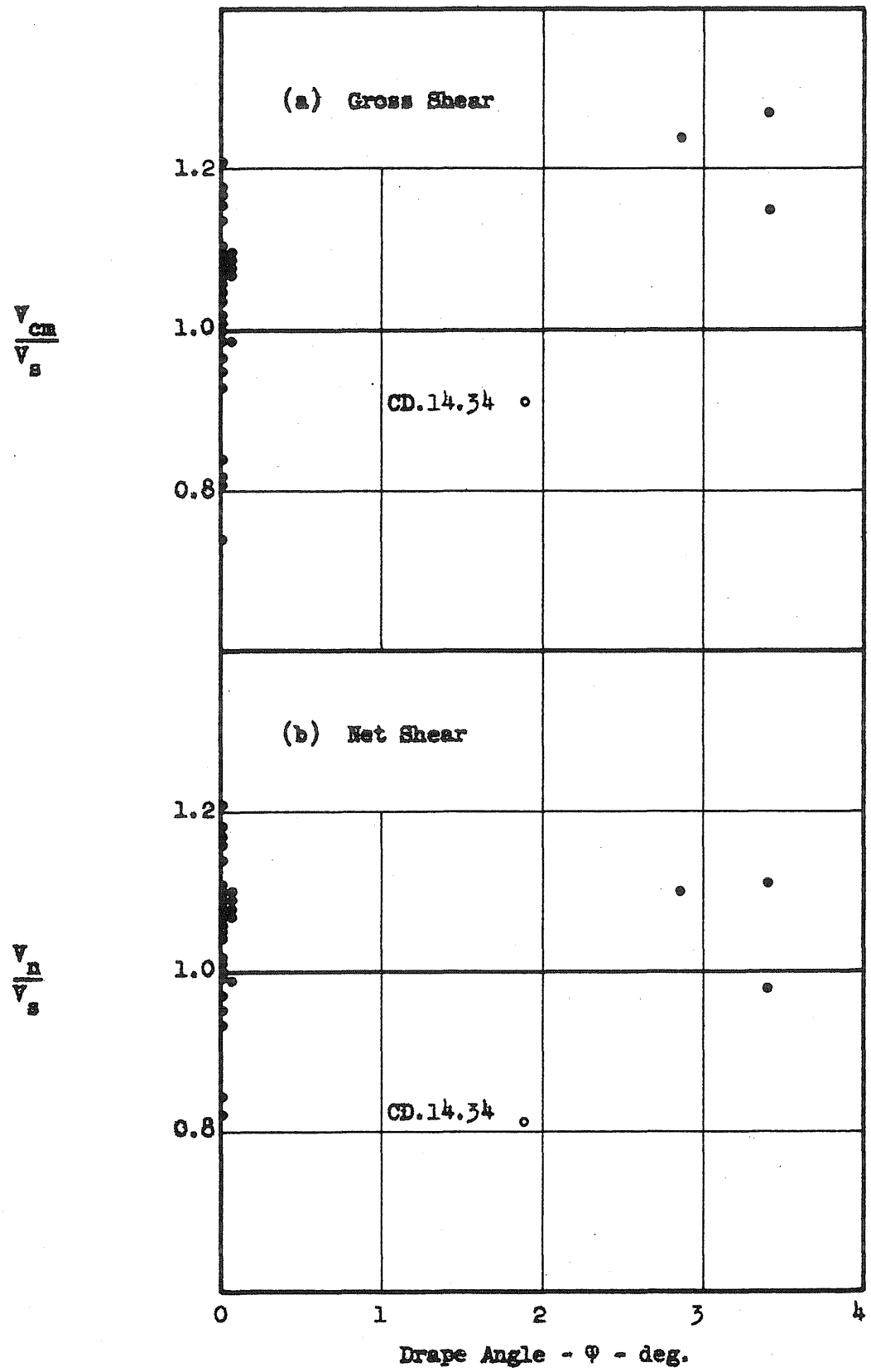

FIG. 67 EFFECT OF DRAPE ANGLE ON SHEAR AT WEB-SHEAR CRACKING

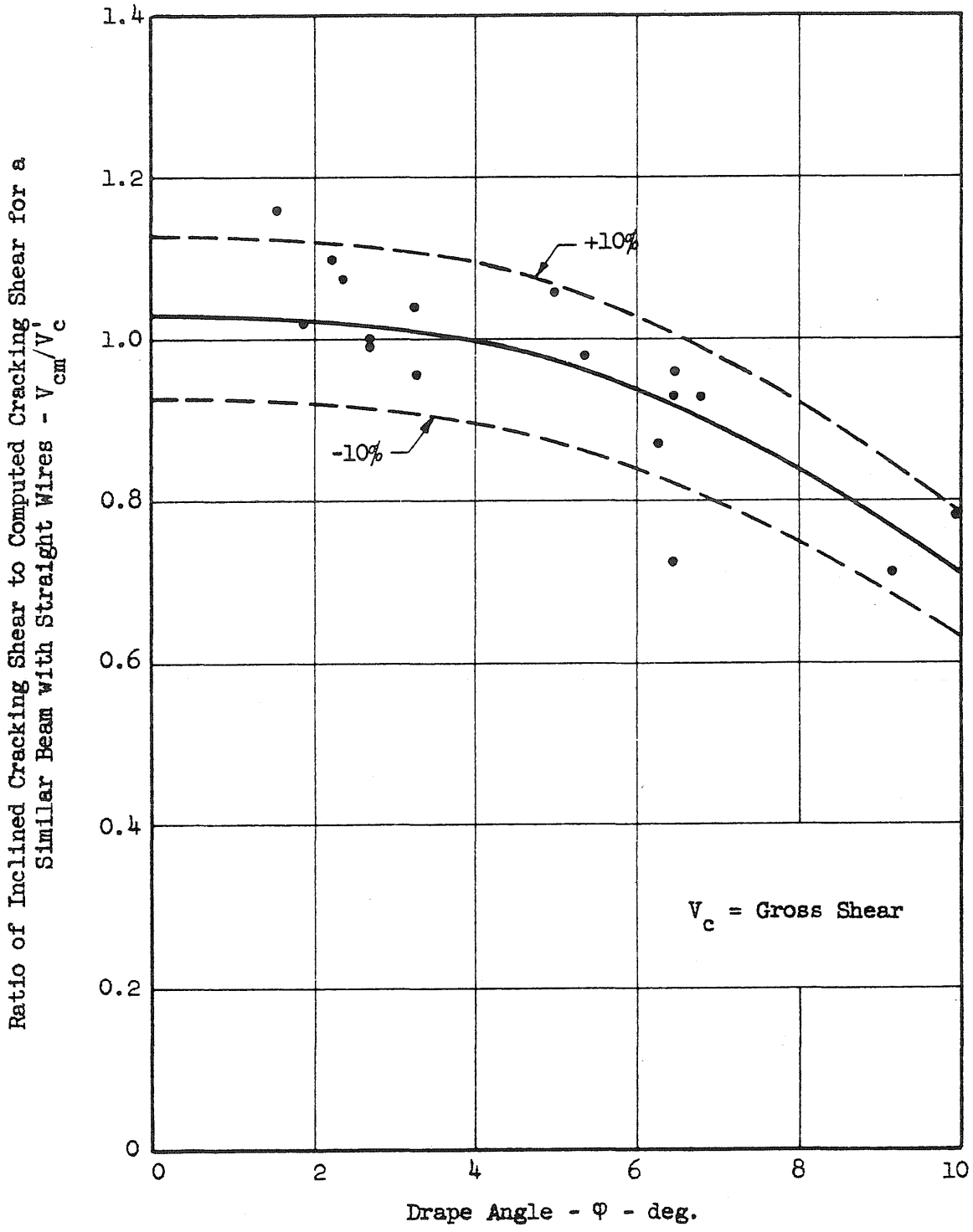

FIG. 68 EFFECT OF DRAPED REINFORCEMENT ON SHEAR AT FLEXURE-SHEAR CRACKING

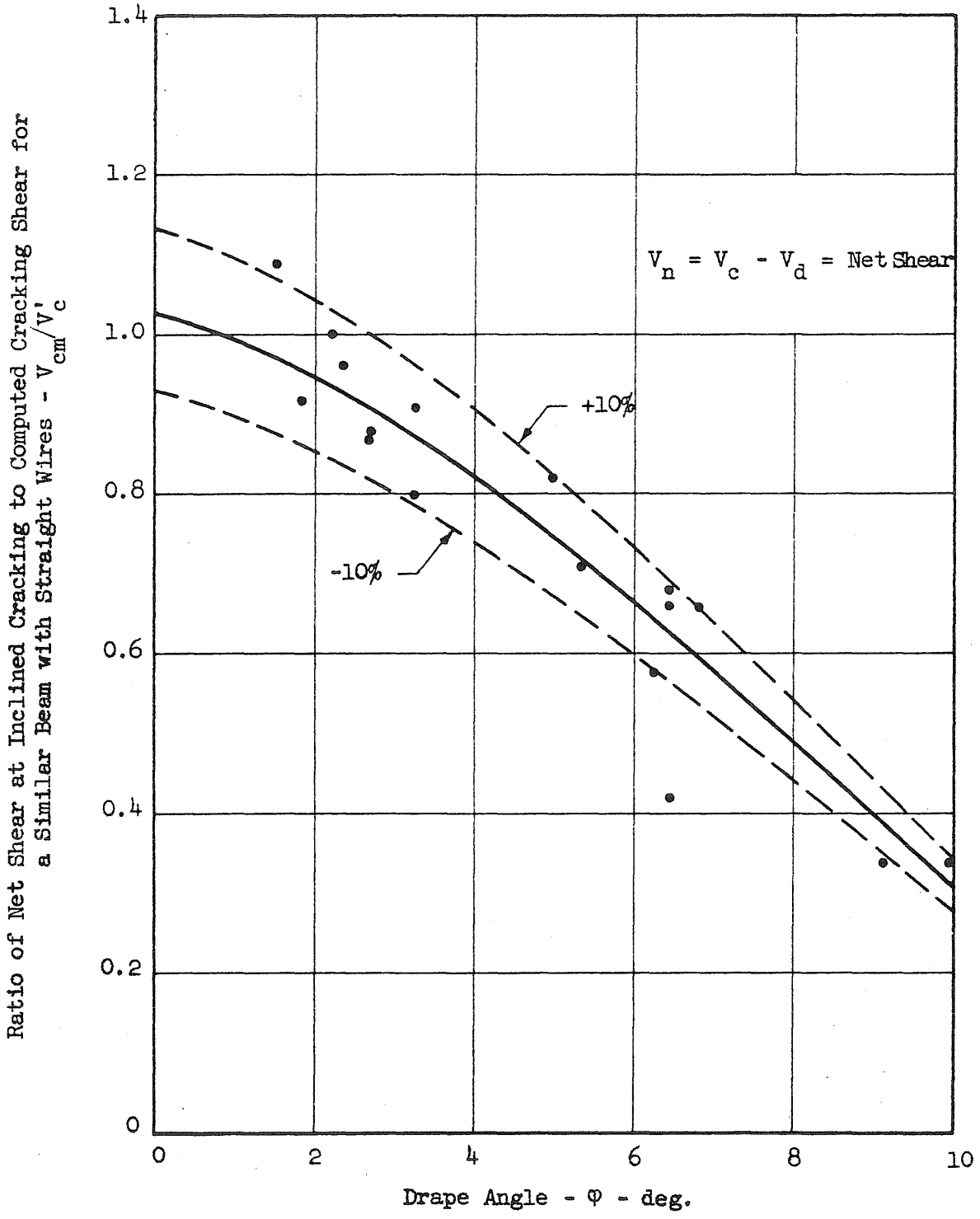

FIG. 69 EFFECT OF DRAPED REINFORCEMENT ON NET SHEAR AT FLEXURE-SHEAR CRACKING

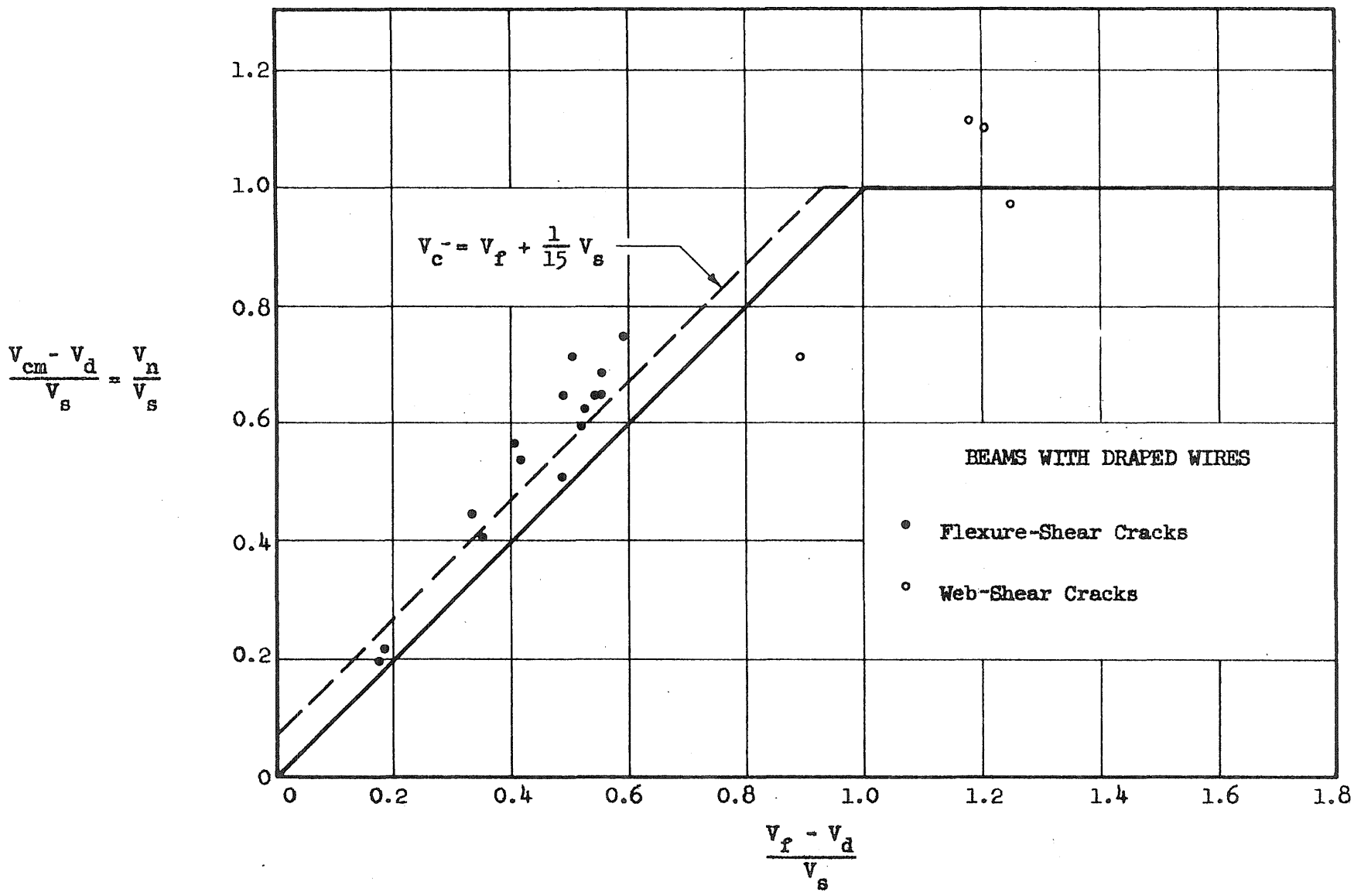

FIG. 70 COMPARISON OF THE DIMENSIONLESS QUANTITIES V_n/V_s AND $(V_f-V_d)/V_s$ FOR BEAMS WITH DRAPED WIRES

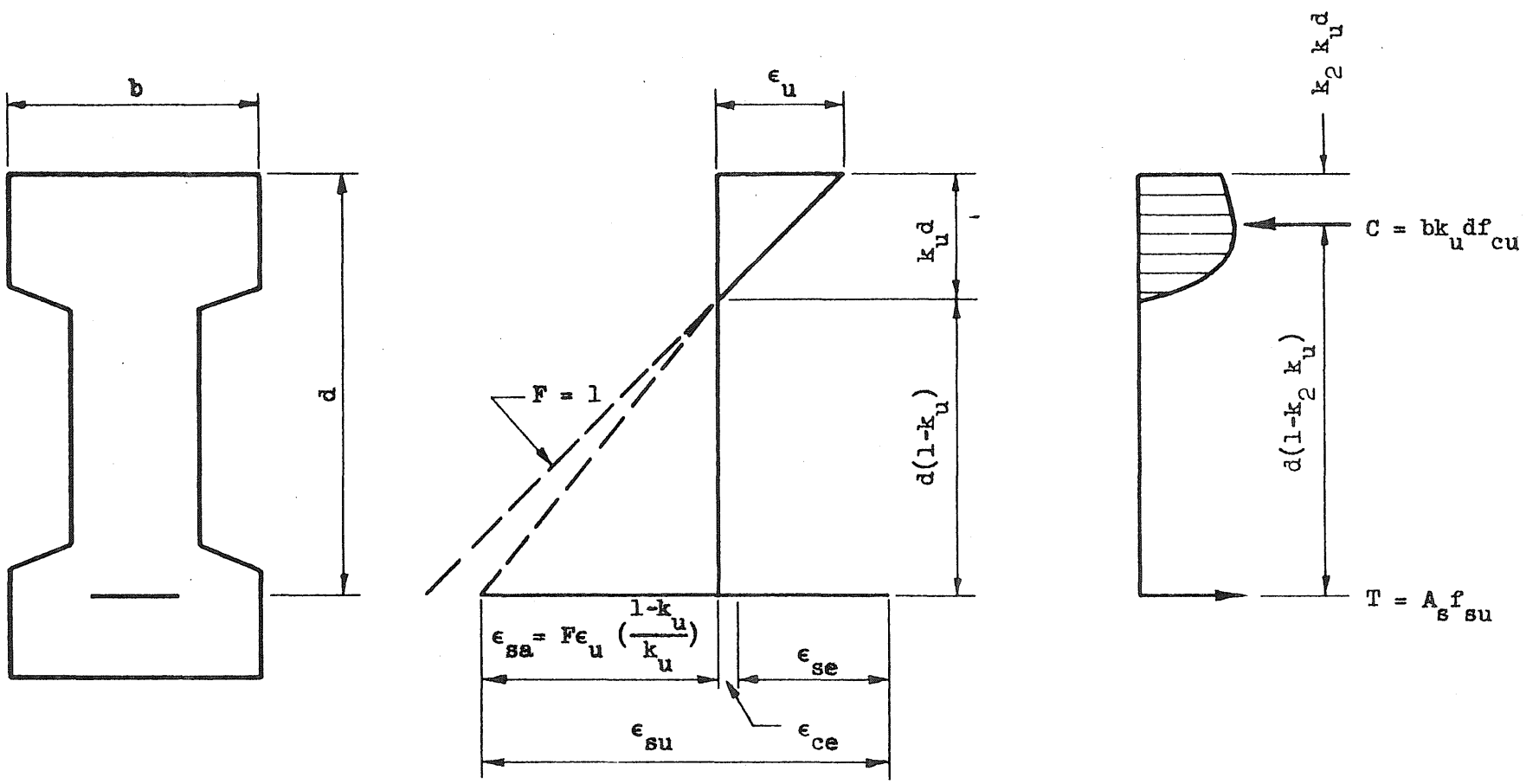

(a) Strain Distribution

(b) Stress Distribution

FIG. 71 ASSUMED STRAIN AND STRESS DISTRIBUTIONS AT ULTIMATE FOR A FLEXURAL FAILURE IN A PRESTRESSED CONCRETE BEAM

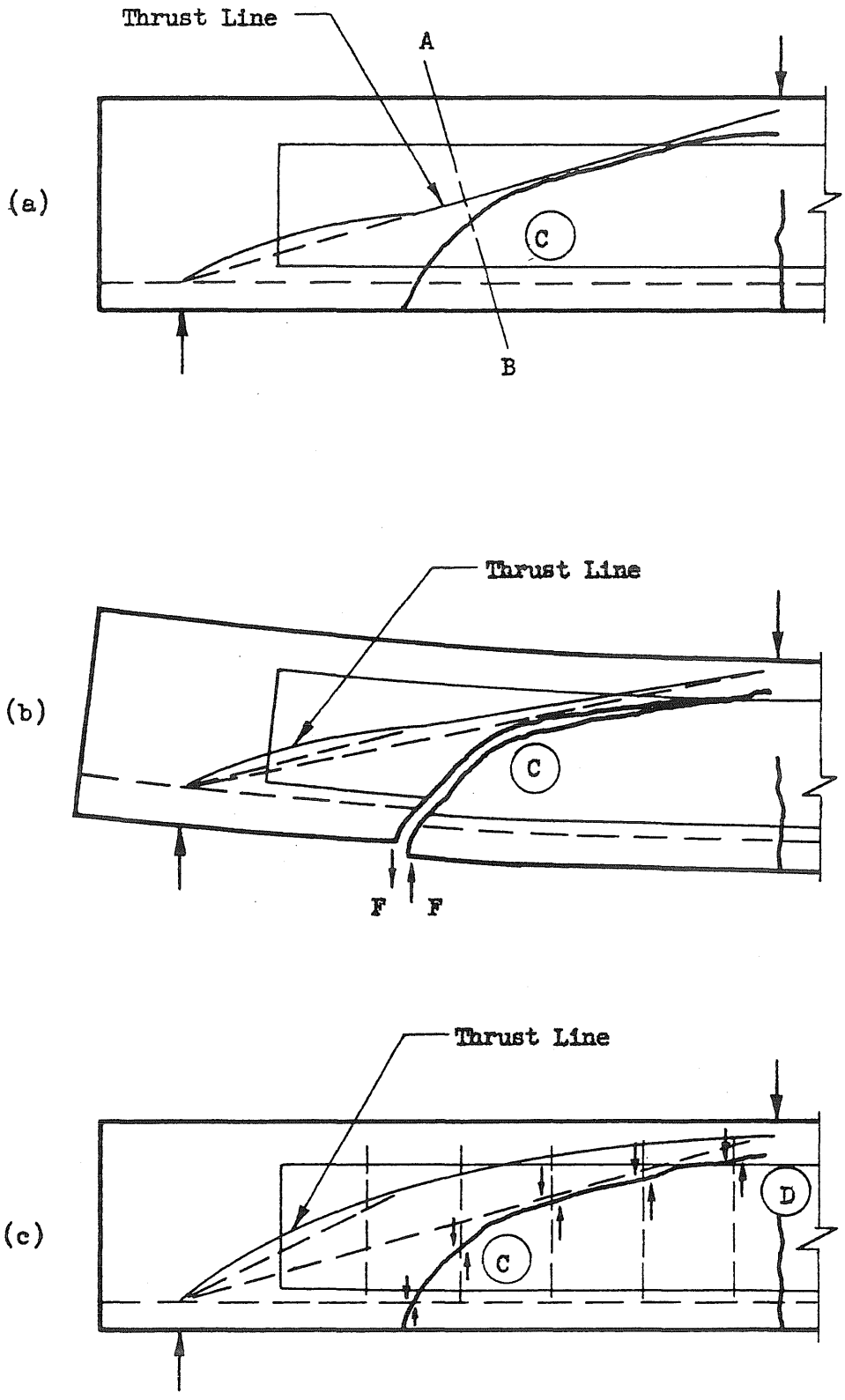

FIG. 72 IDEALIZED CONDITIONS AFTER INCLINED CRACKING

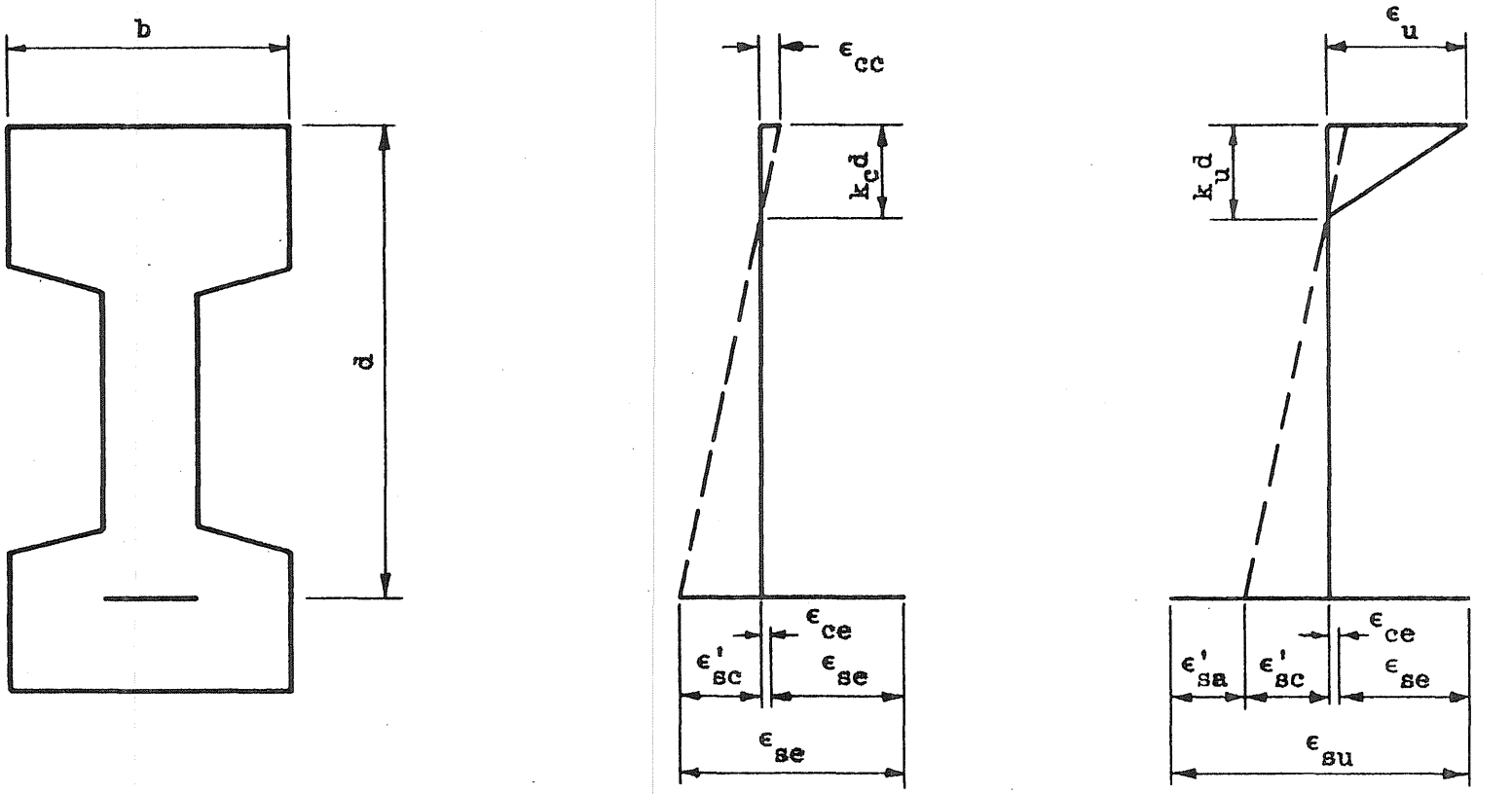

(a) Strains at Inclined Cracking

(b) Strains at Ultimate

FIG. 73 ASSUMED STRAIN DISTRIBUTIONS AT INCLINED CRACKING AND ULTIMATE

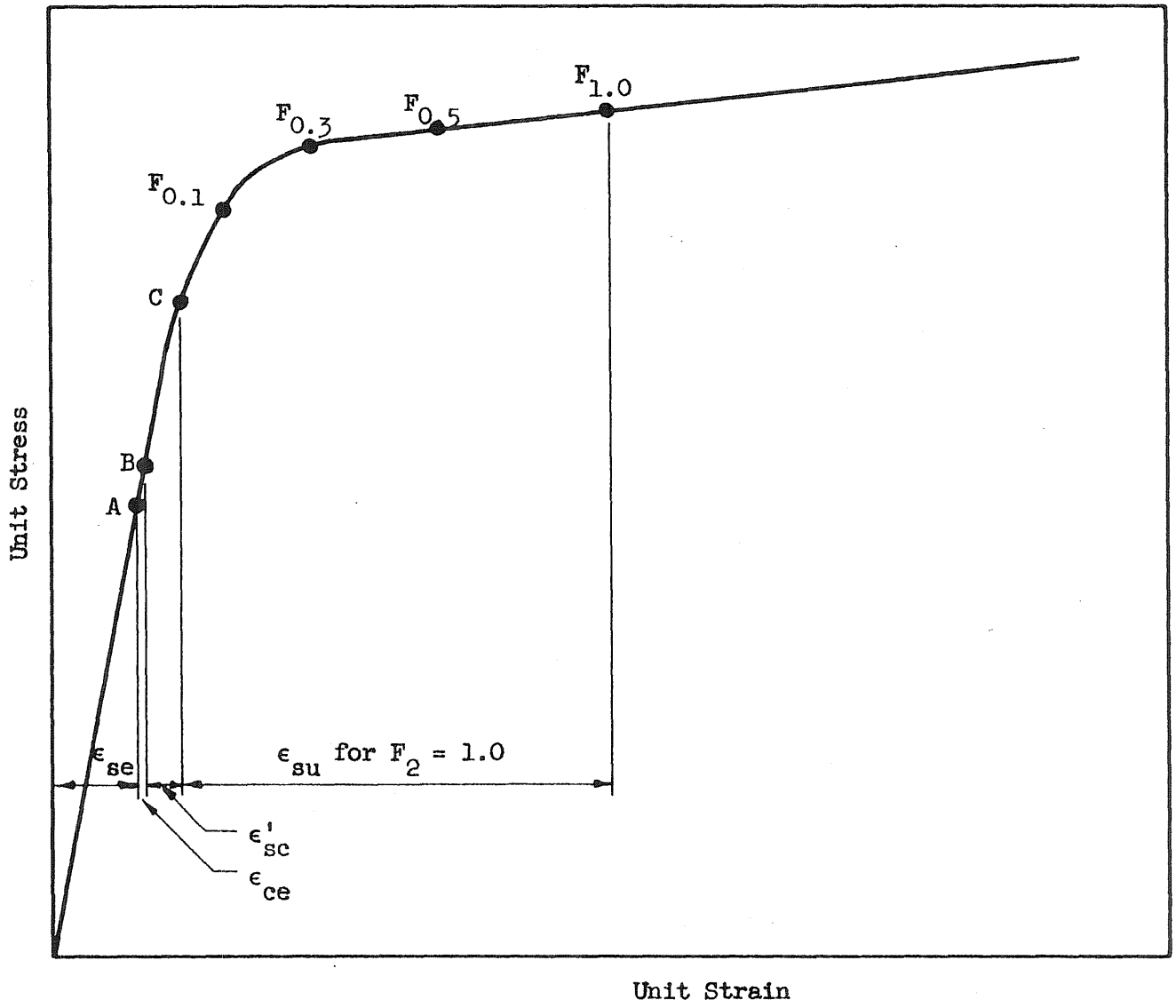

FIG. 74 EFFECT OF STRAIN COMPATIBILITY FACTOR, F_2, ON ULTIMATE STEEL STRESS

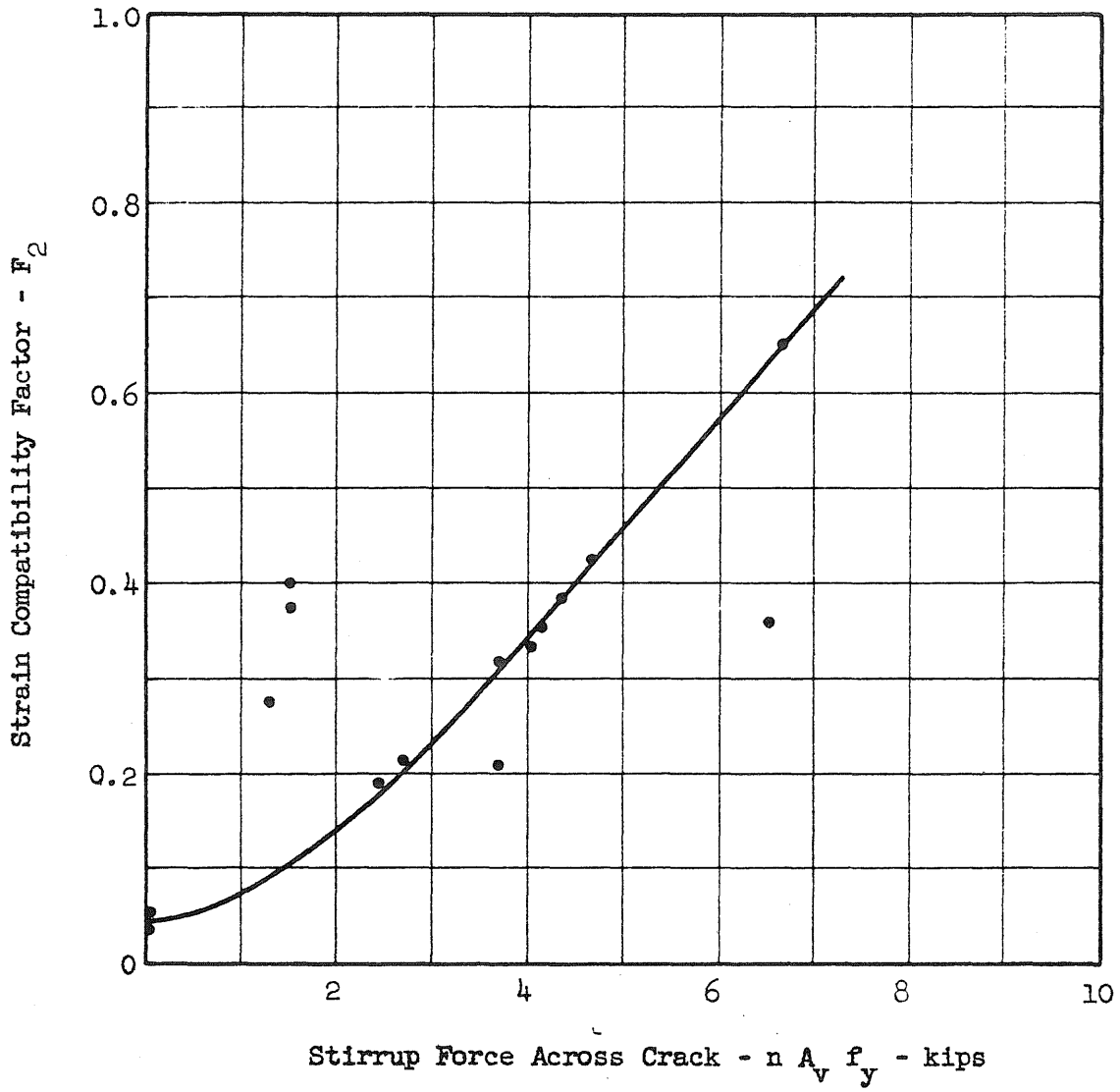

FIG. 75 RELATIONSHIP BETWEEN STRAIN COMPATIBILITY FACTOR AND STIRRUP FORCE ACROSS CRACK IN BEAMS FAILING IN SHEAR

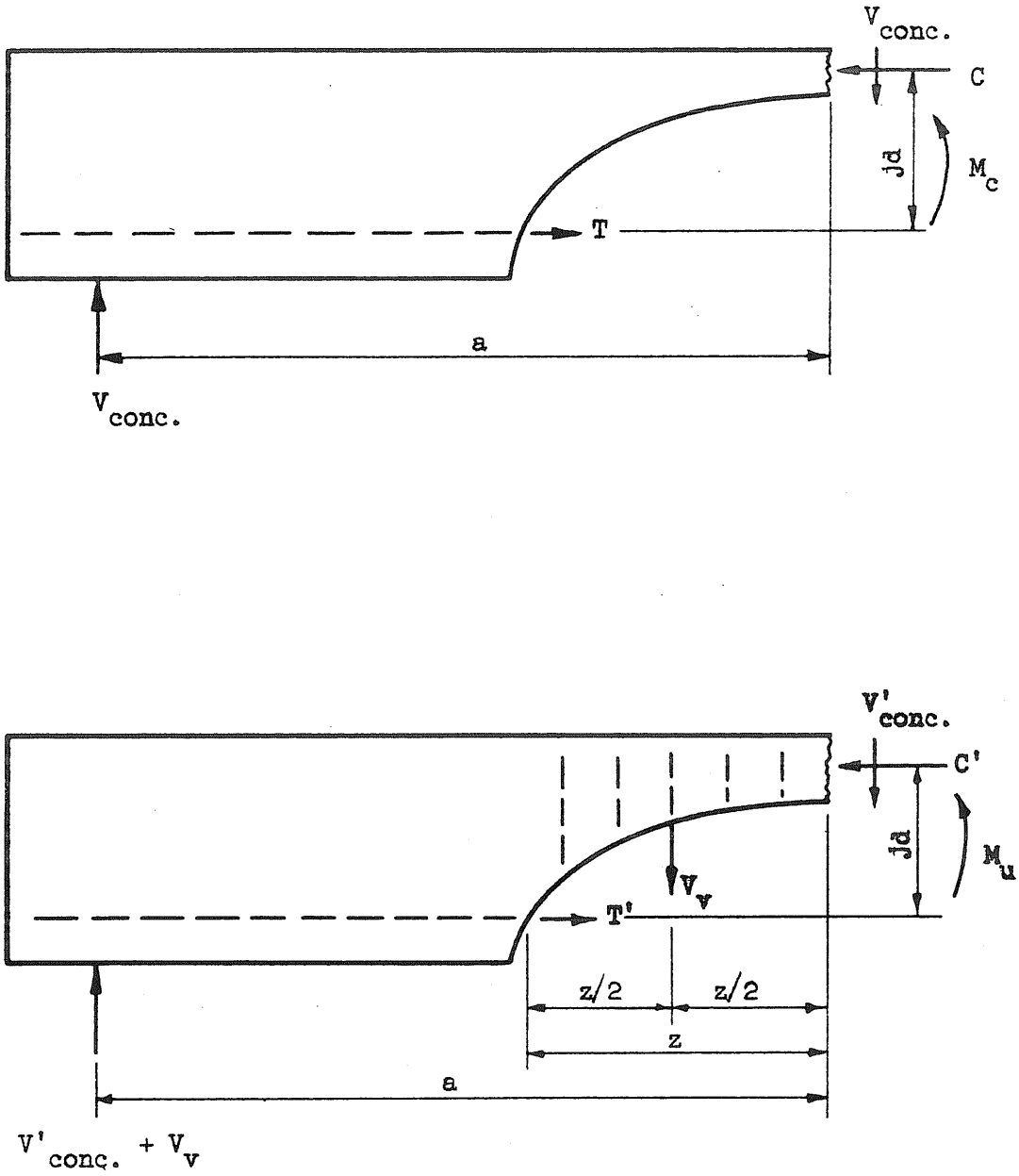

FIG. 76 FORCES ACTING IN A BEAM WITH AN INCLINED CRACK

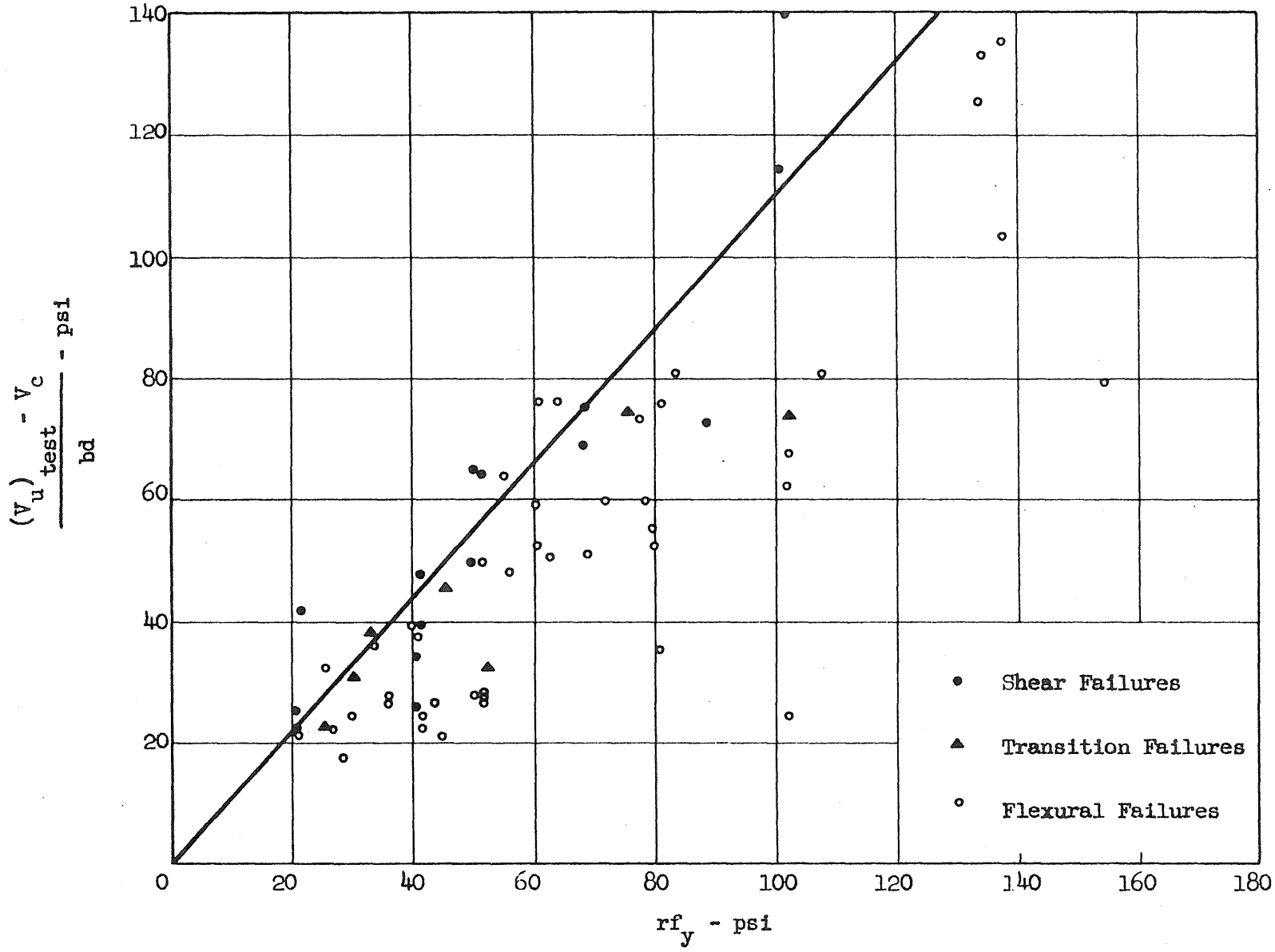

FIG. 77 EFFECT OF WEB REINFORCEMENT ON THE INCREASE IN SHEAR BEYOND INCLINED CRACKING

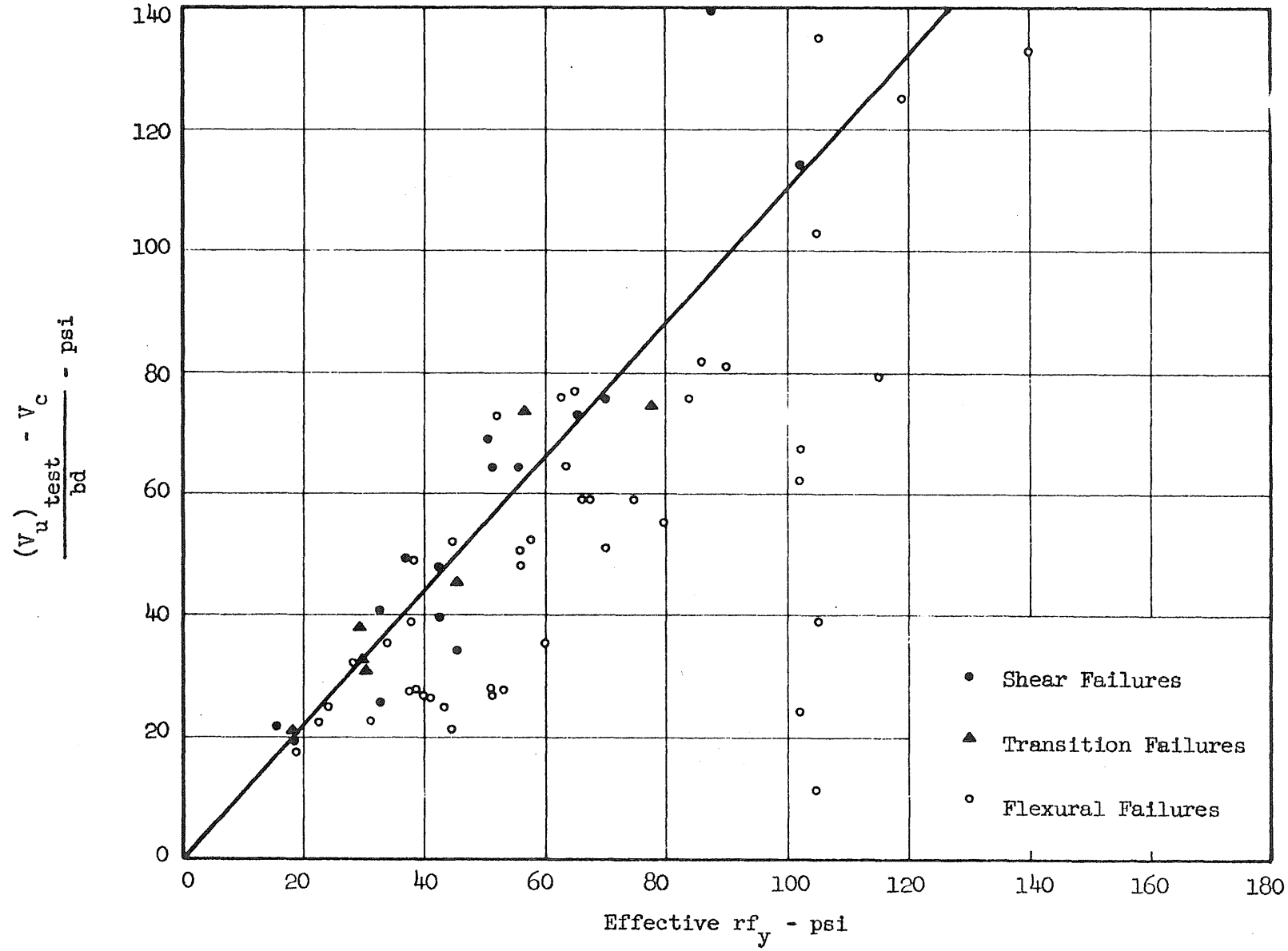

FIG. 78 EFFECT OF WEB REINFORCEMENT ON THE INCREASE IN SHEAR BEYOND INCLINED CRACKING

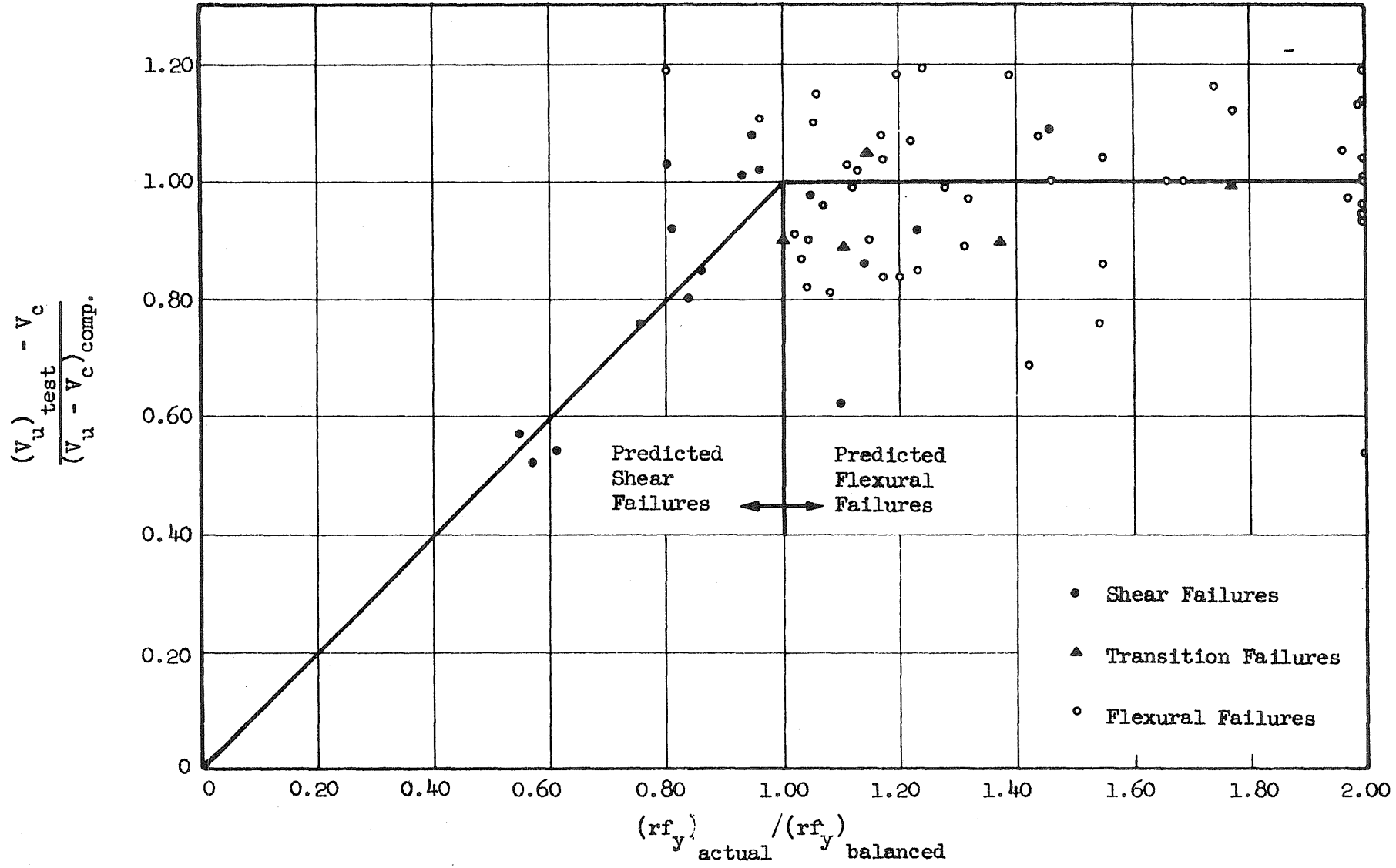

FIG. 79 RELATION BETWEEN THE AMOUNT OF WEB REINFORCEMENT AND THE INCREASE IN SHEAR BEYOND INCLINED CRACKING

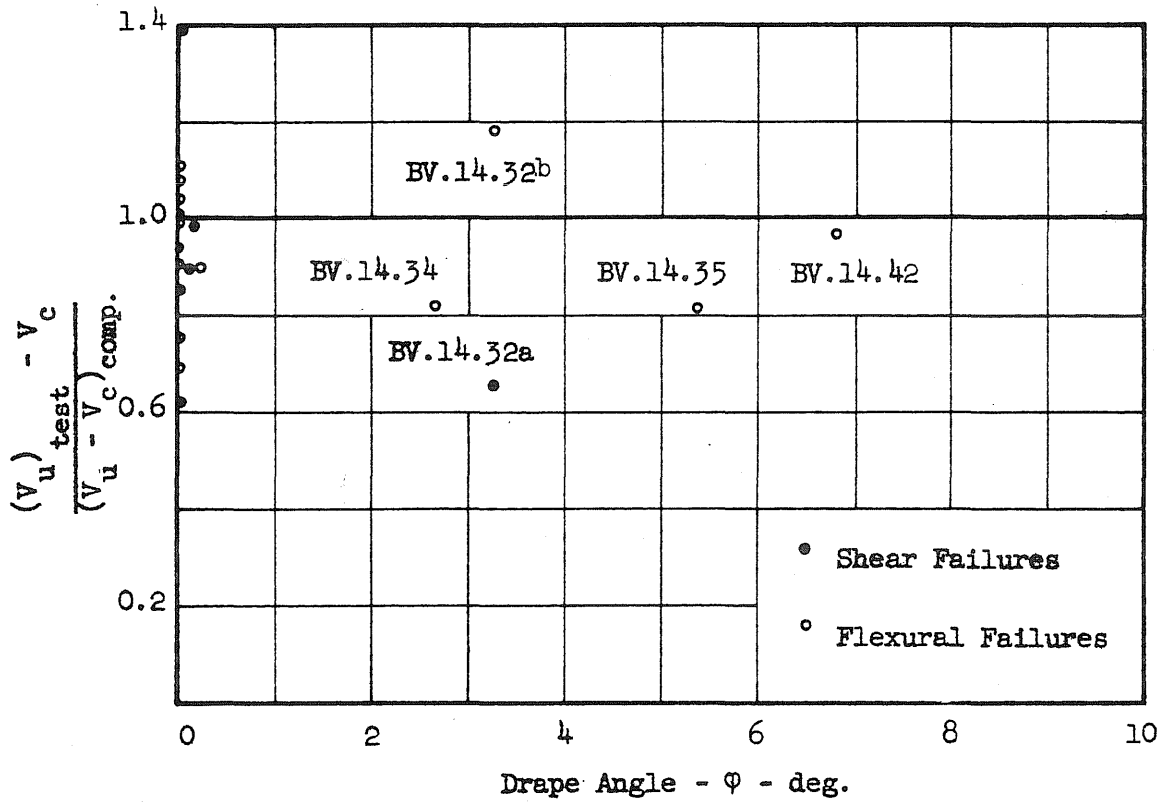

FIG. 80 EFFECT OF DRAPE ANGLE ON EFFICIENCY OF WEB REINFORCEMENT

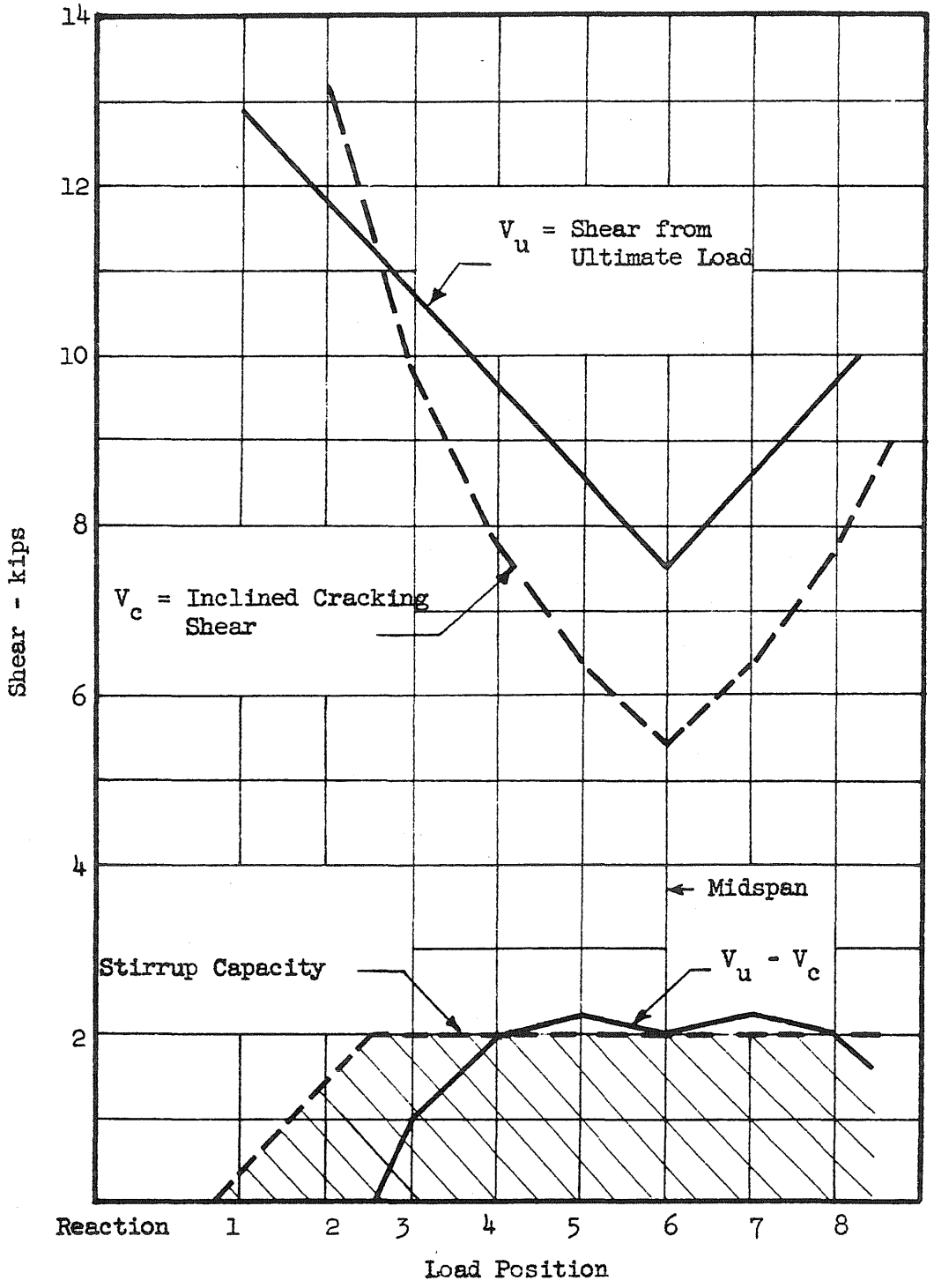

FIG. 81 STIRRUP DESIGN PROCEDURE FOR BEAM BW.10.22

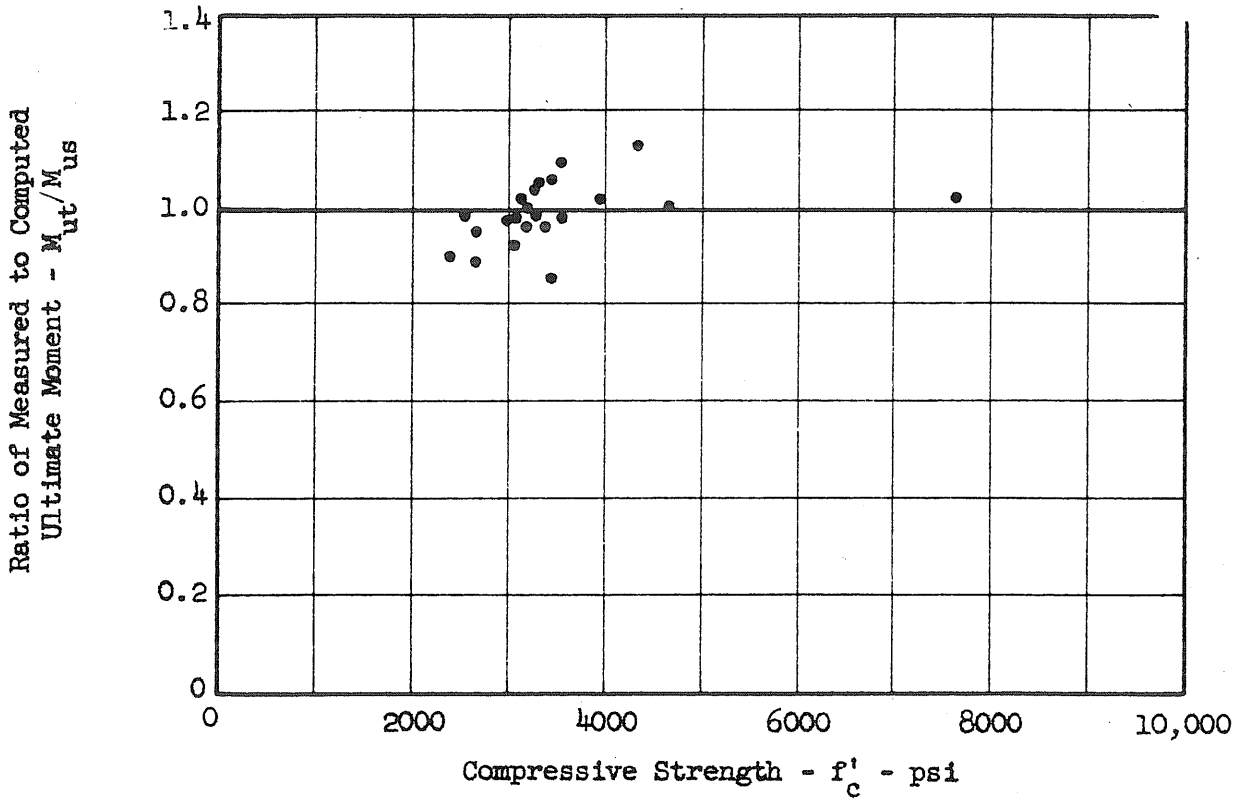

(a) Effect of Concrete Strength

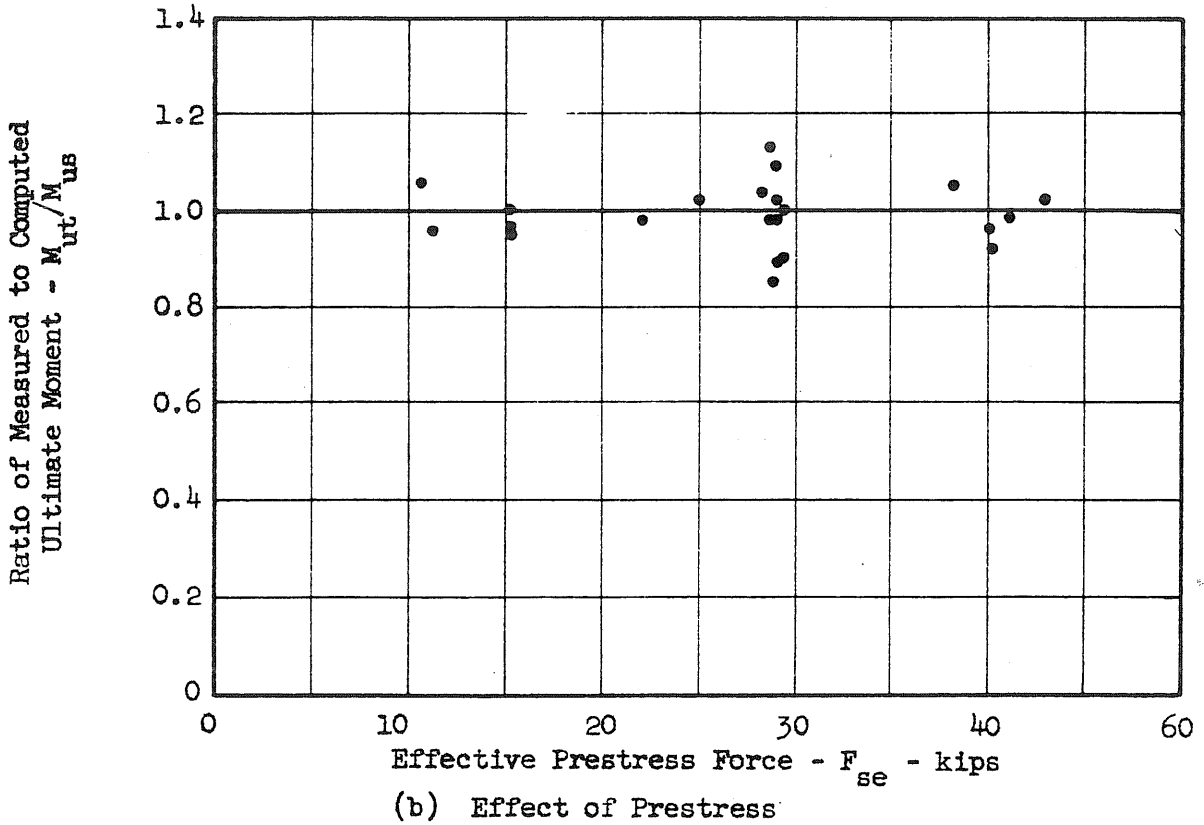

(b) Effect of Prestress

FIG. 82 EFFECT OF VARIABLES ON EFFICIENCY OF WEB REINFORCEMENT FOR SHEAR OR TRANSITION FAILURES

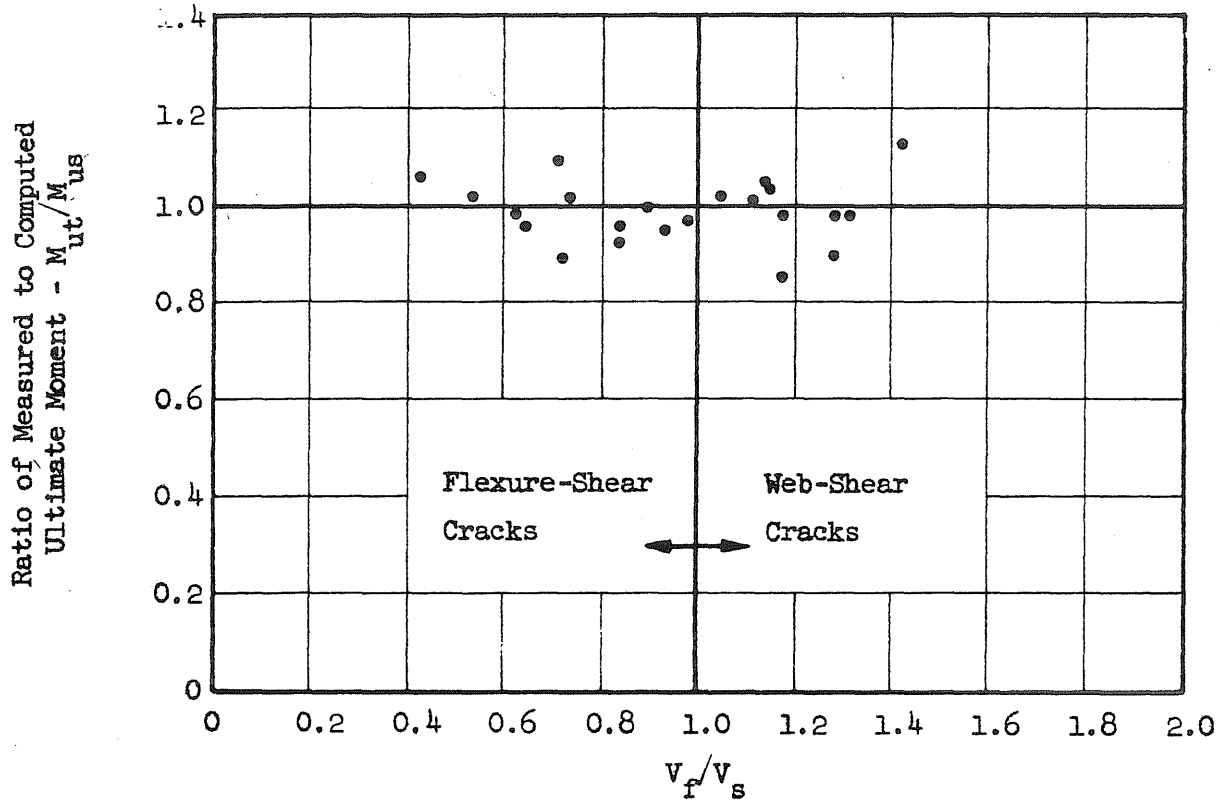

(a) Effect of Type of Inclined Crack

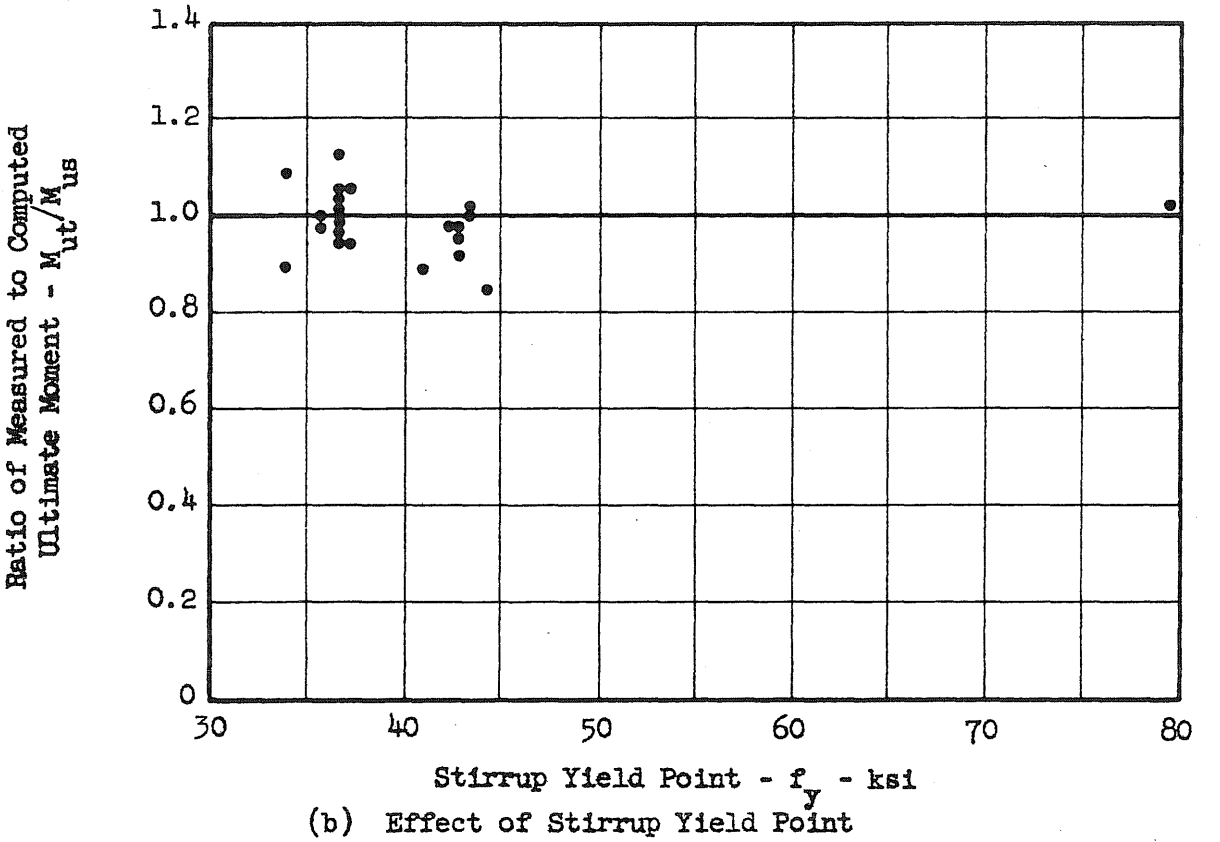

(b) Effect of Stirrup Yield Point

FIG. 83 EFFECT OF VARIABLES ON EFFICIENCY OF WEB REINFORCEMENT FOR SHEAR OR TRANSITION FAILURES

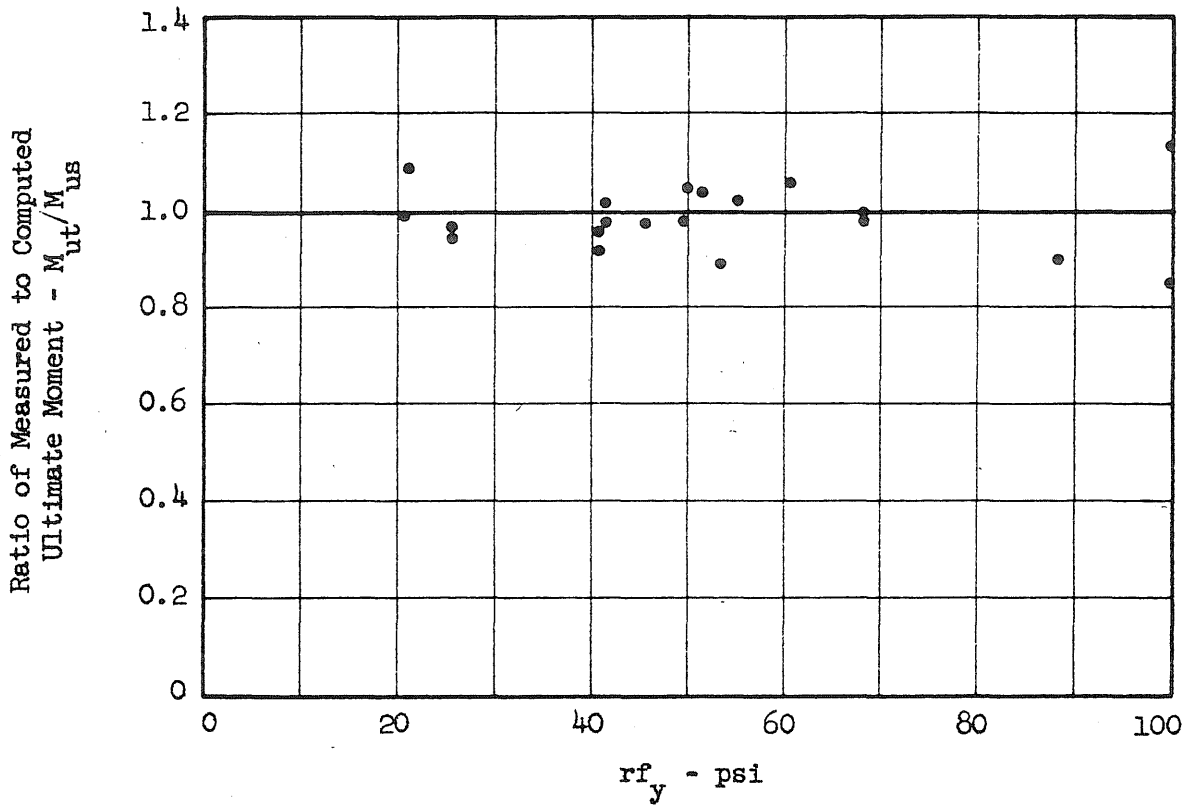

(a) Effect of Amount of Web Reinforcement

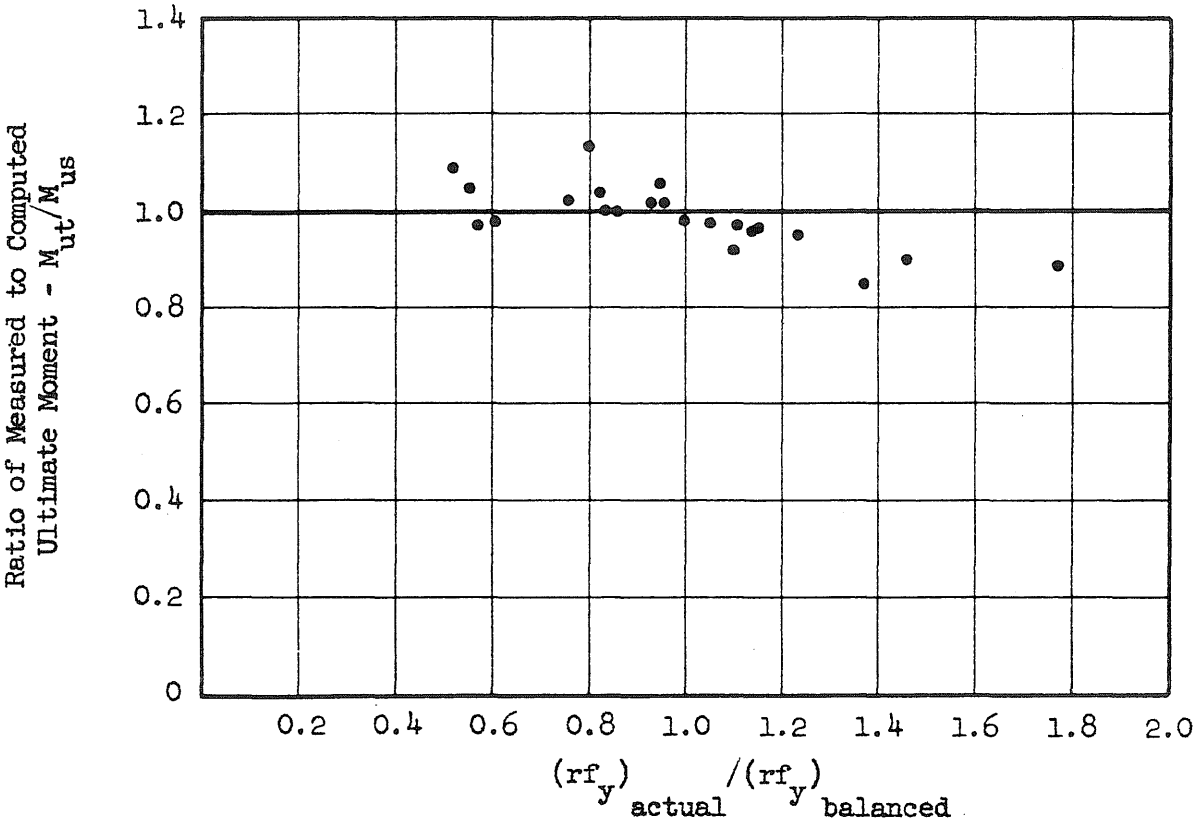

(b) Effect of Over- and Under-Designed Web Reinforcement

FIG. 84 EFFECT OF VARIABLES ON EFFICIENCY OF WEB REINFORCEMENT FOR SHEAR OR TRANSITION FAILURES

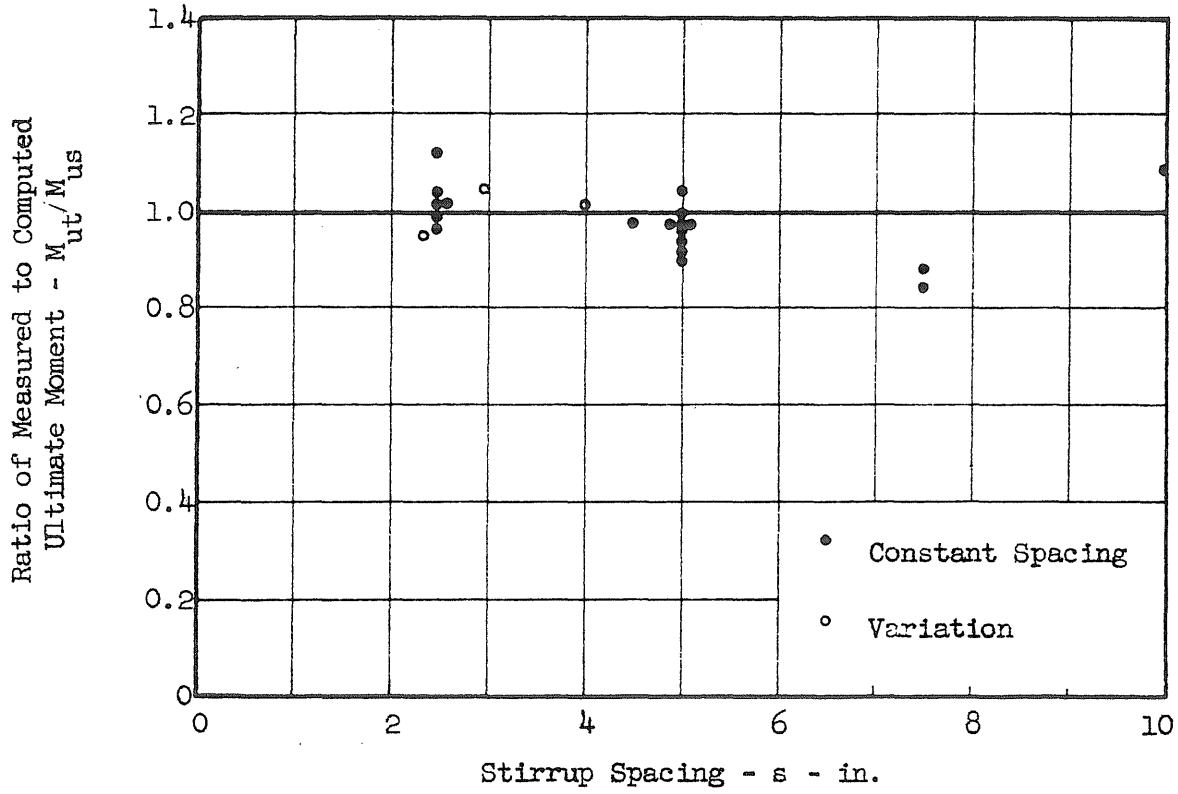

(a) Effect of Stirrup Spacing

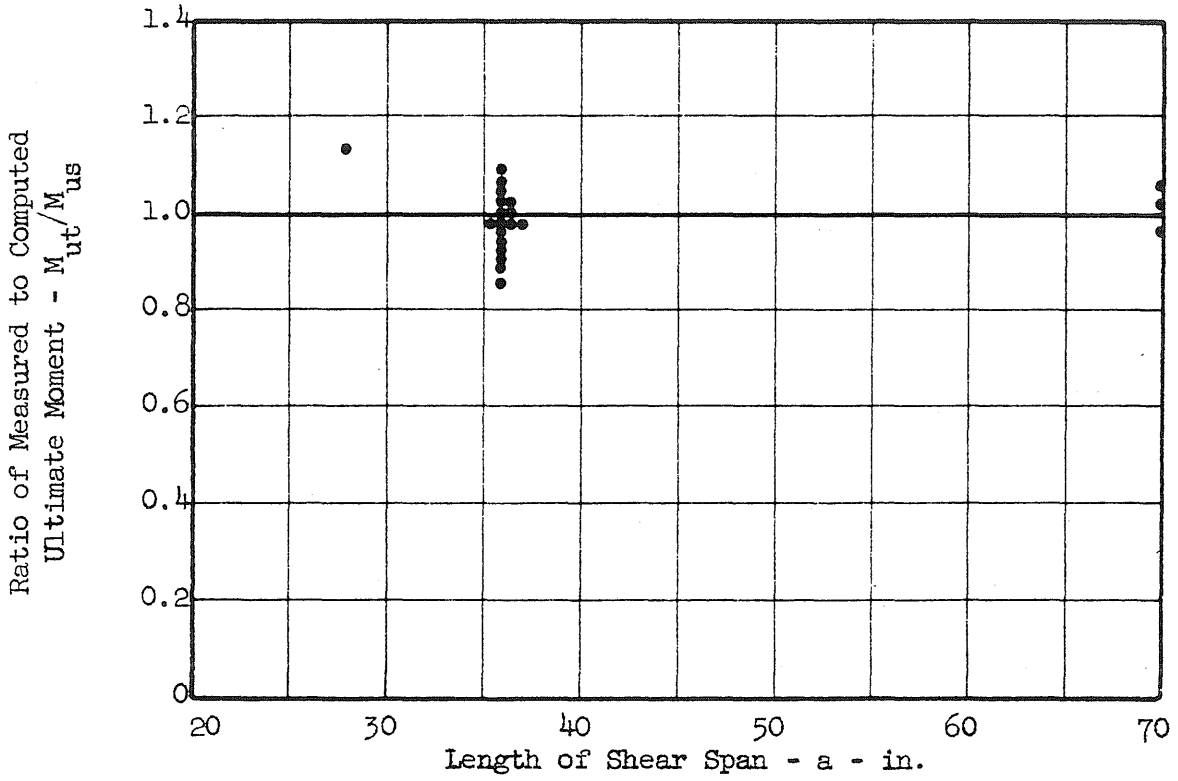

(b) Effect of Length of Shear Span

FIG. 85 EFFECT OF VARIABLES ON EFFICIENCY OF WEB REINFORCEMENT FOR SHEAR OR TRANSITION FAILURES

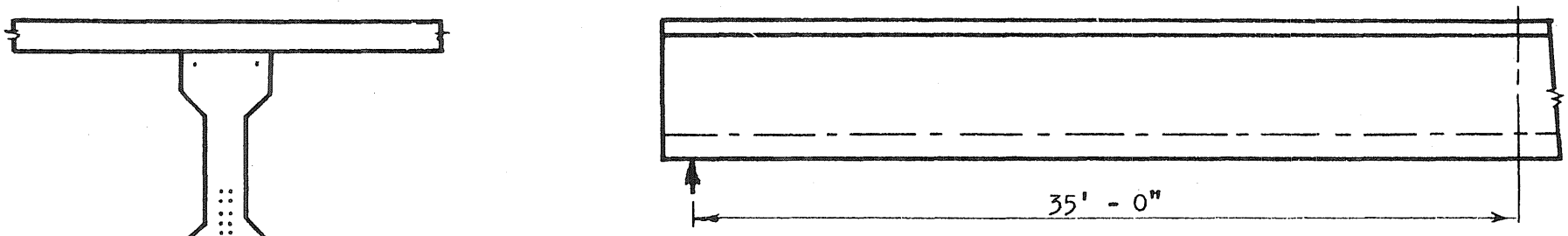

Beam No. 1 - 46 Straight, Pretensioned Strands

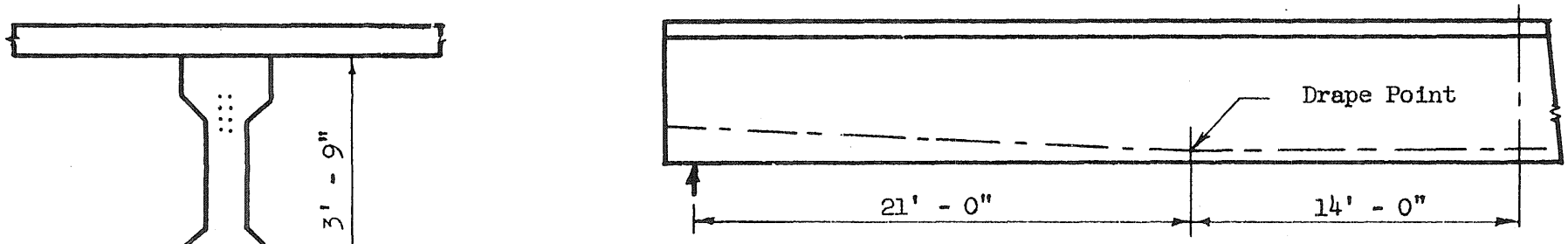

Beam No. 2 - 28 Straight Strands, 8 Draped Strands

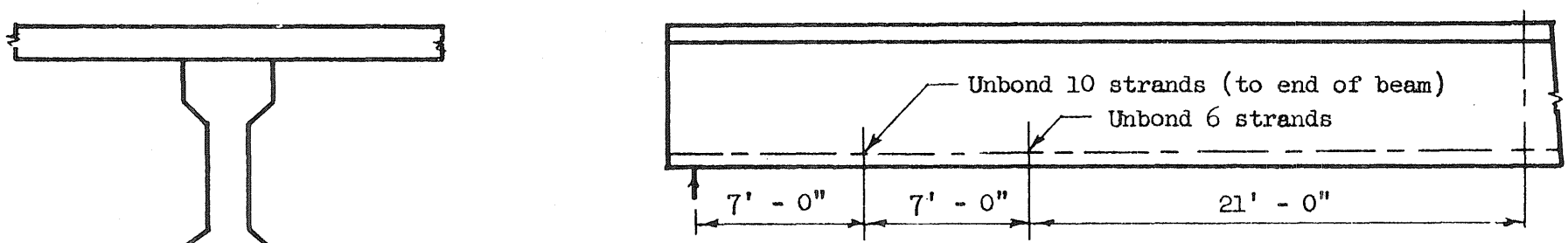

Beam No. 3 - 20 Straight Fully Bonded Strands, 16 Partially Unbonded Strands

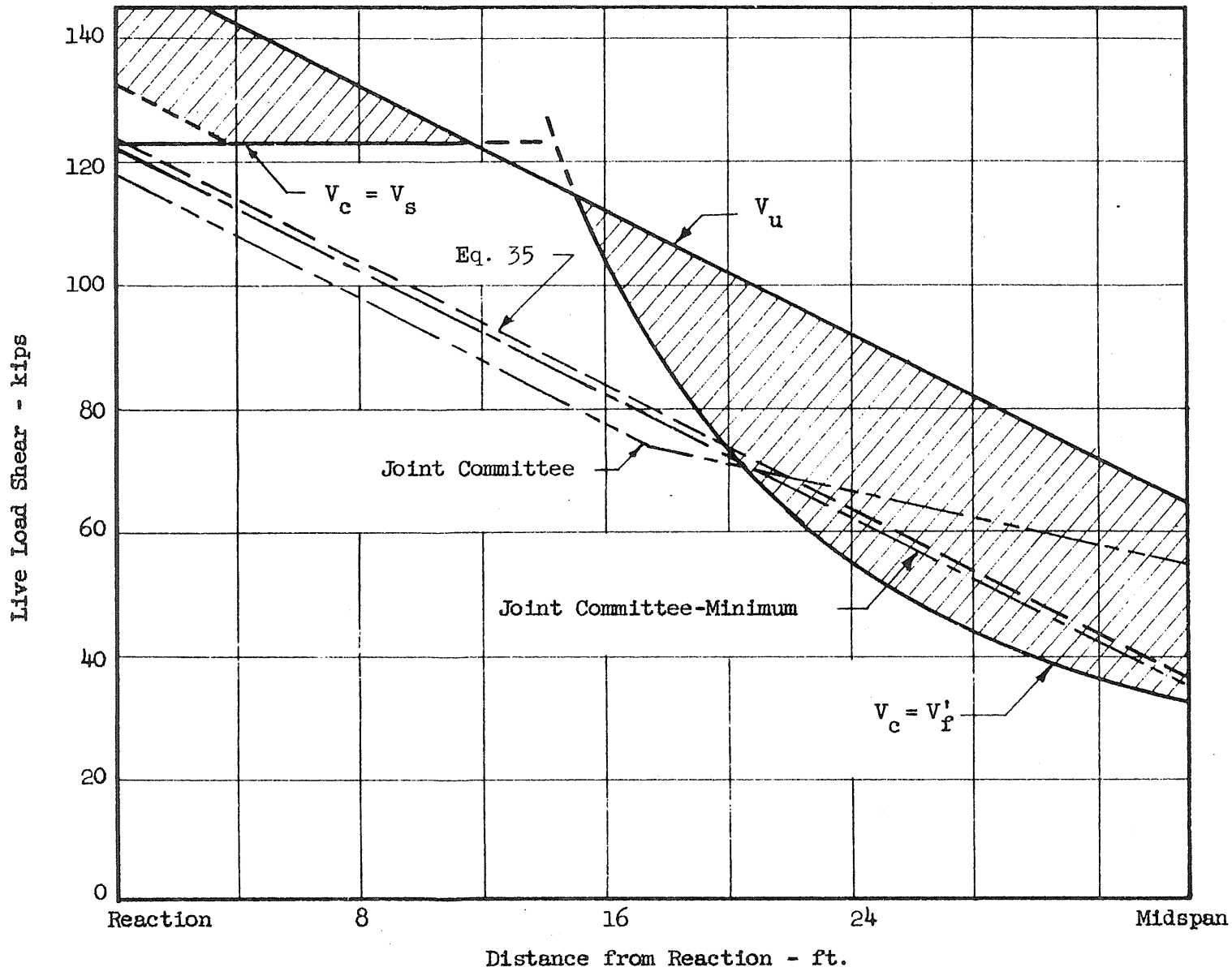

FIG. 87 STIRRUP DESIGN PROCEDURE FOR BEAM NO. 1 WITH STRAIGHT FULLY BONDED REINFORCEMENT

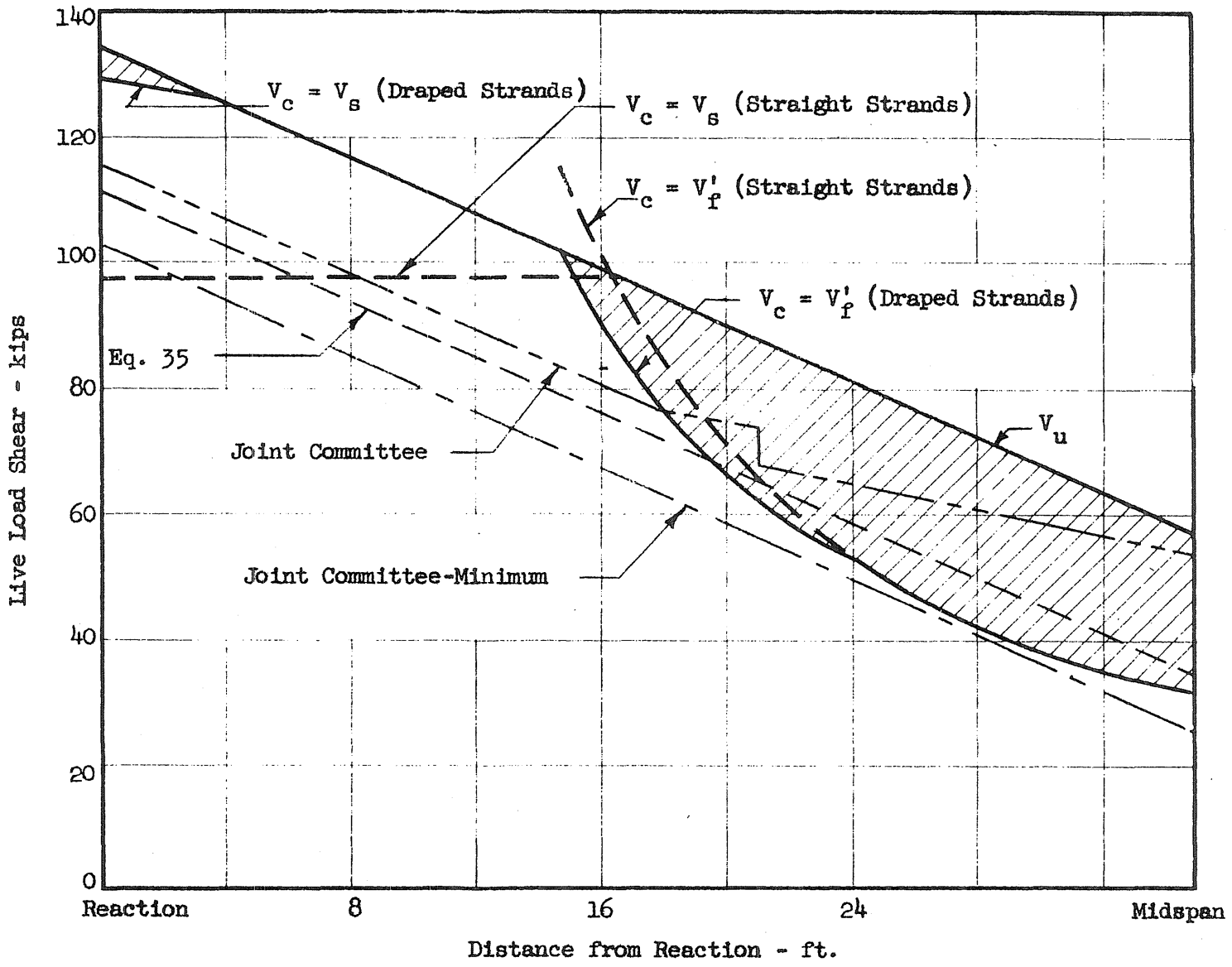

FIG. 88 STIRRUP DESIGN PROCEDURE FOR BEAM NO. 2 WITH DRAPED REINFORCEMENT

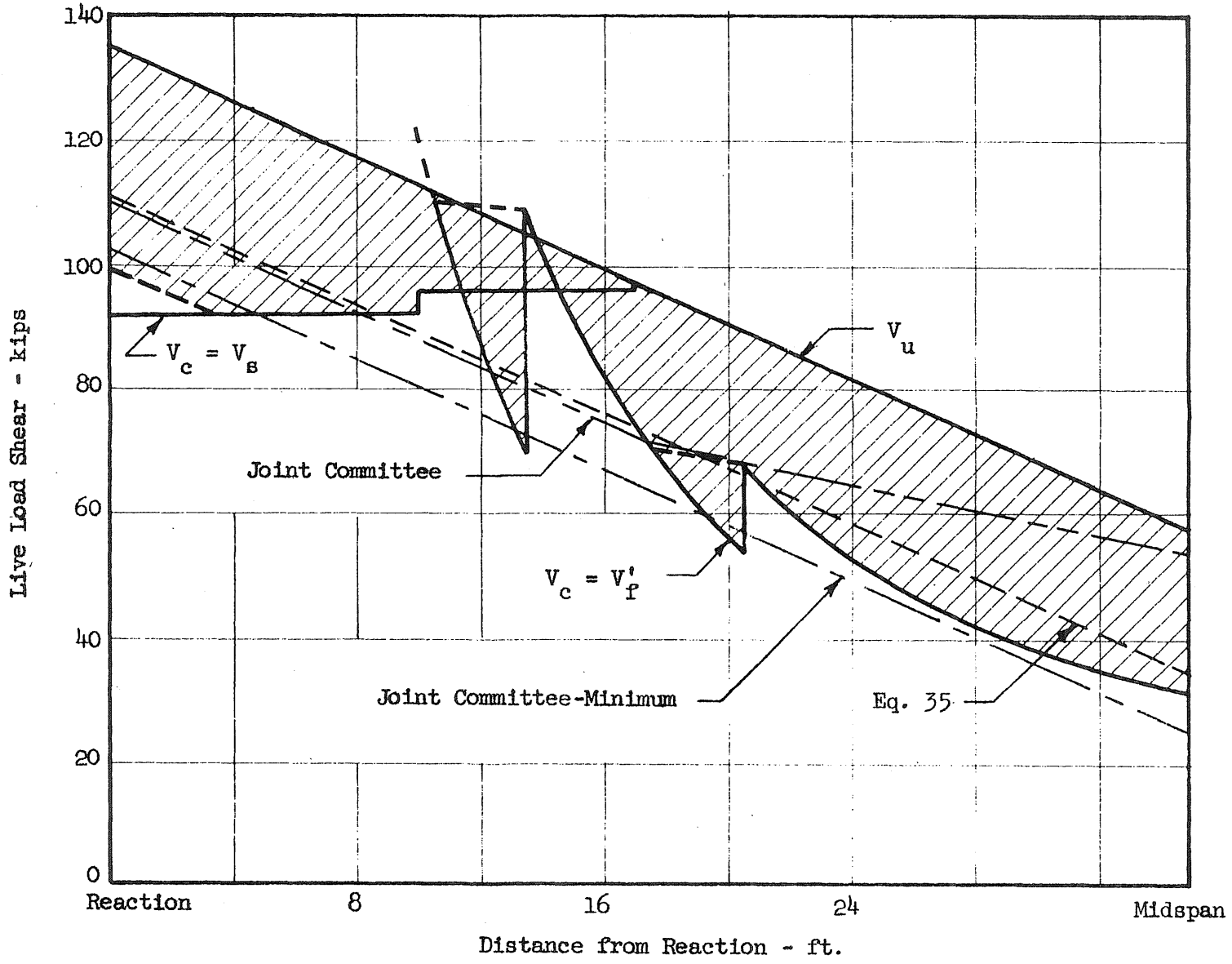

FIG. 89 STIRRUP DESIGN PROCEDURE FOR BEAM NO. 3 WITH PARTIALLY UNBONDED STRAIGHT REINFORCEMENT

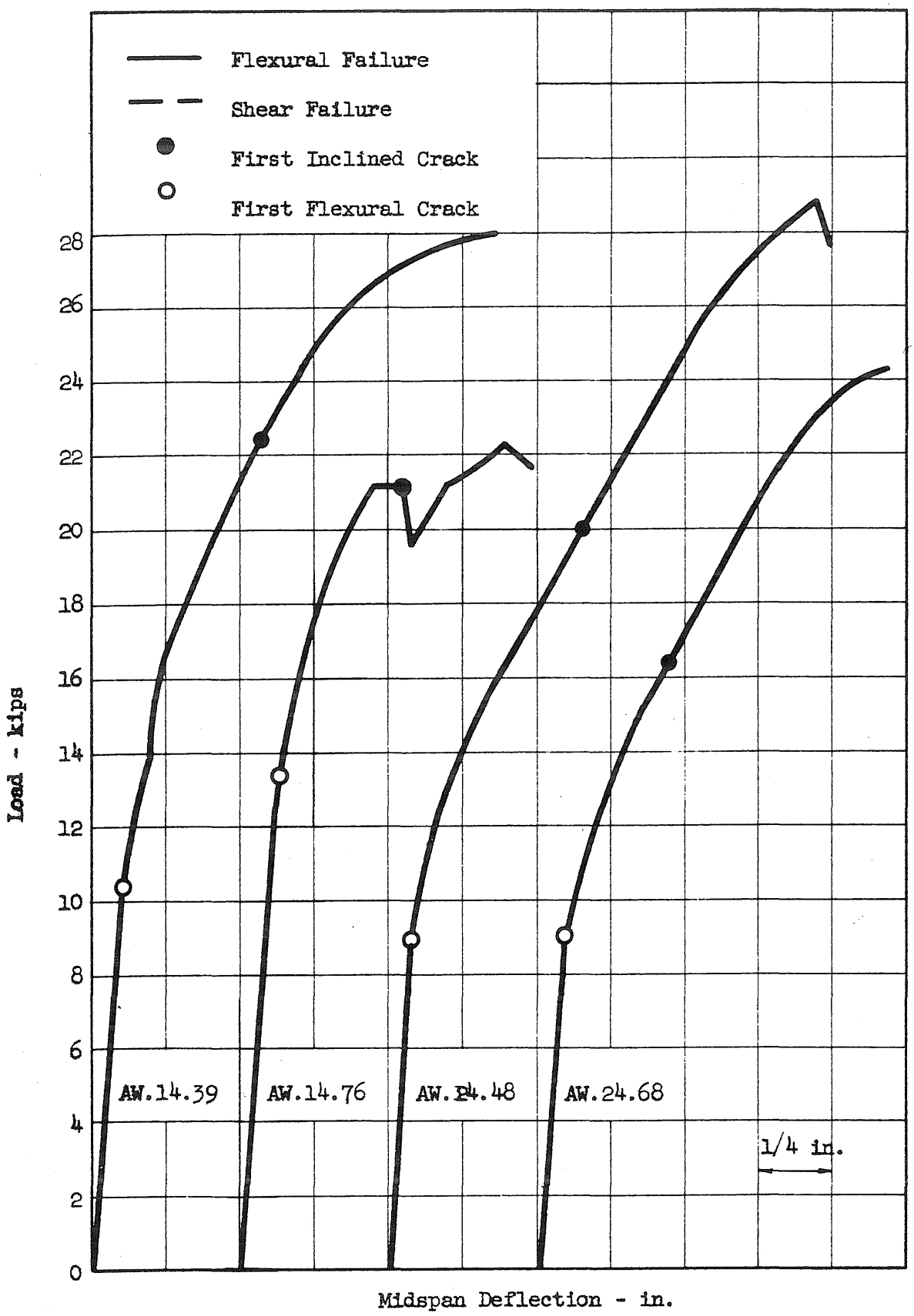

FIG. A1 LOAD-DEFLECTION CURVES - RECTANGULAR BEAMS

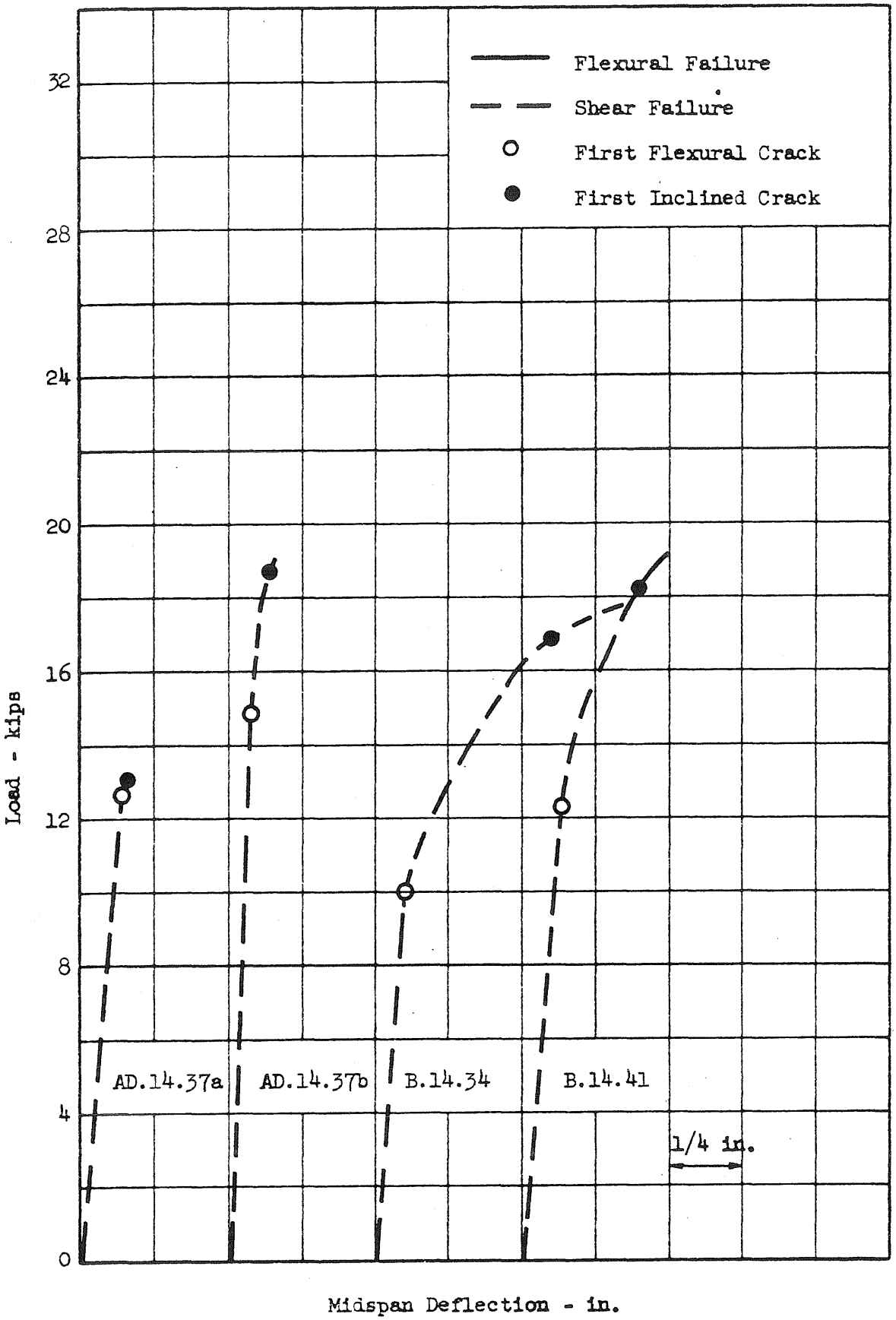

FIG. A2 LOAD-DEFLECTION CURVES - BEAMS WITHOUT WEB REINFORCEMENT

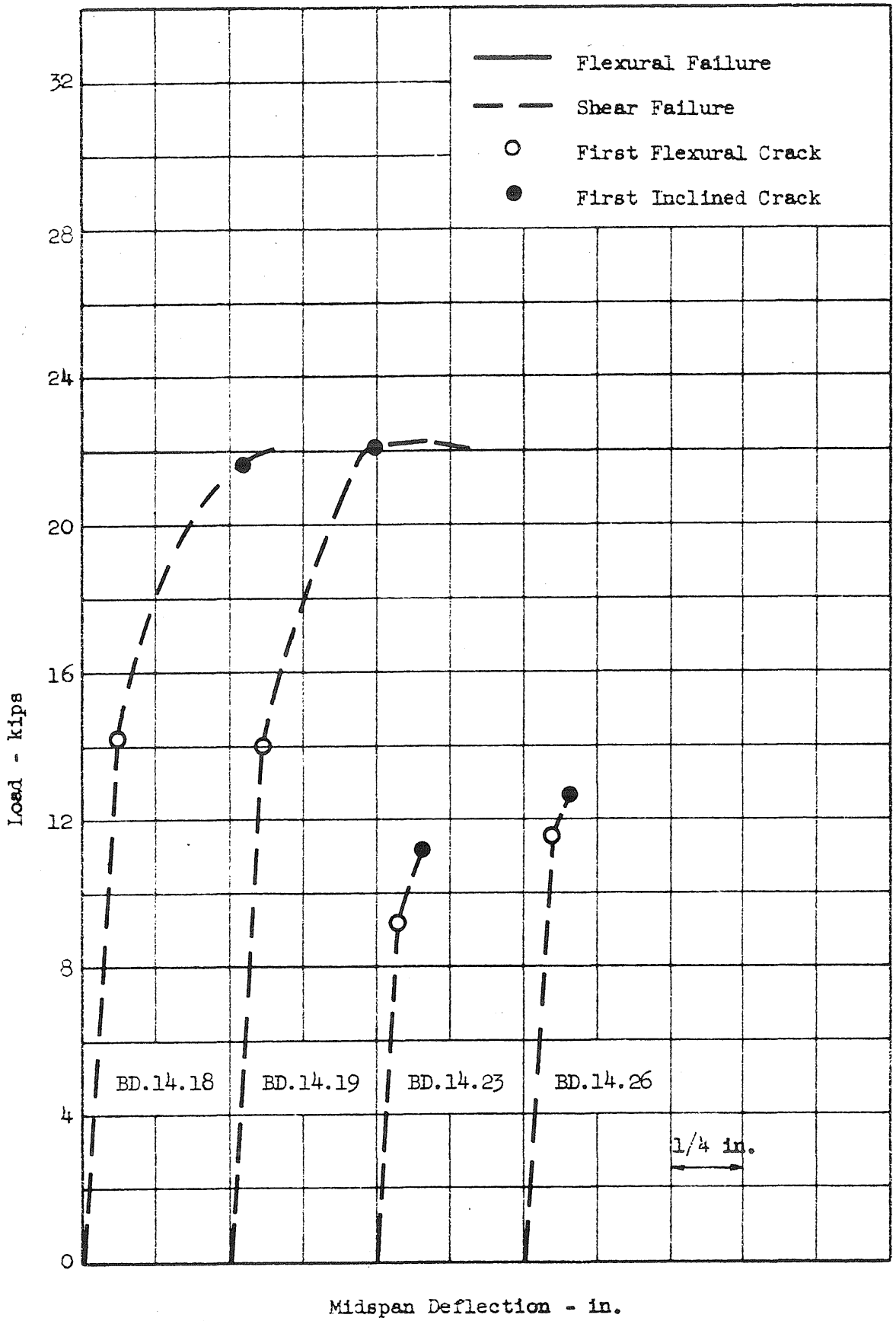

FIG. A3 LOAD-DEFLECTION CURVES - BEAMS WITH DRAPED REINFORCEMENT

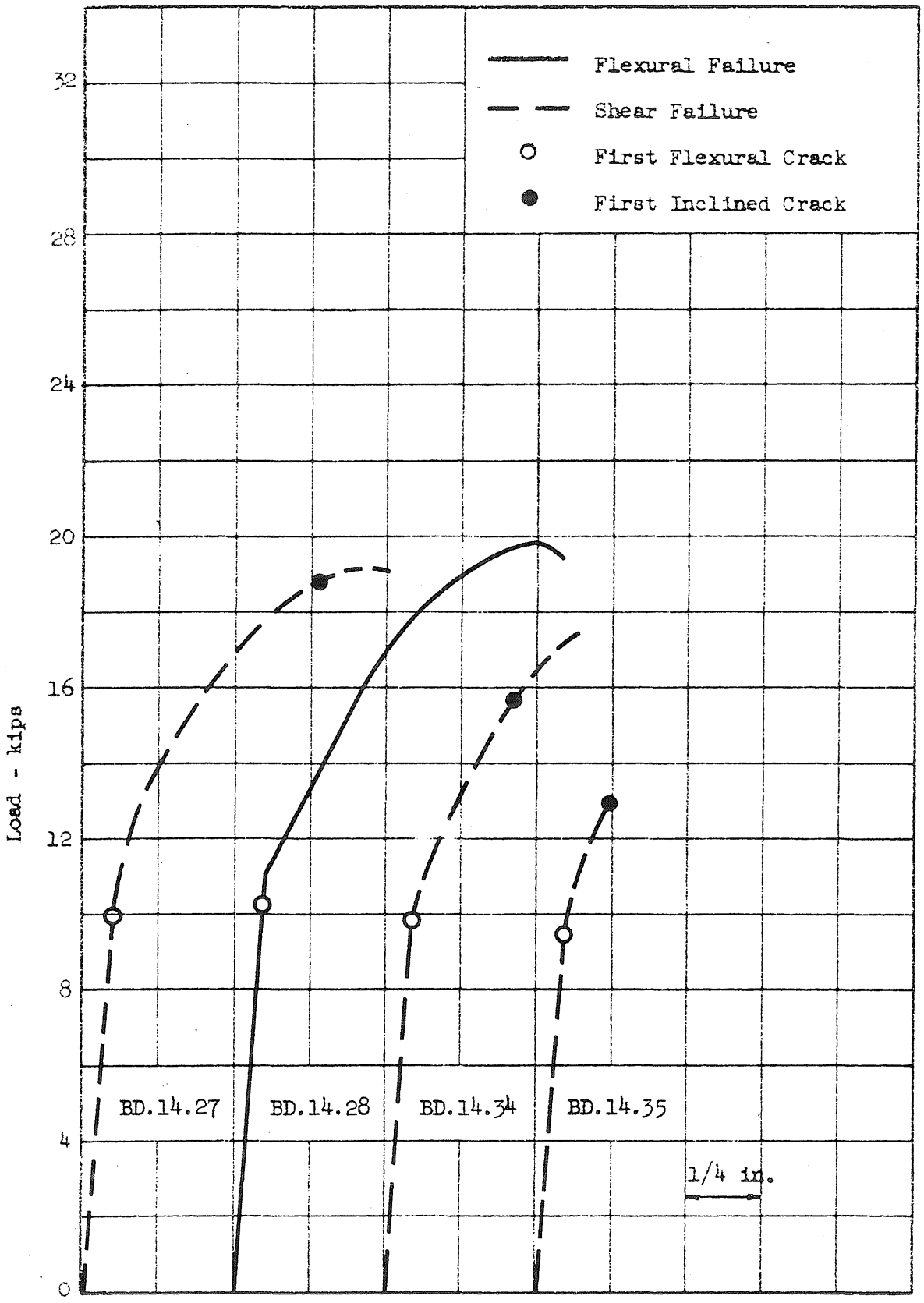

FIG. A4 LOAD-DEFLECTION CURVES - BEAMS WITH DRAPED REINFORCEMENT

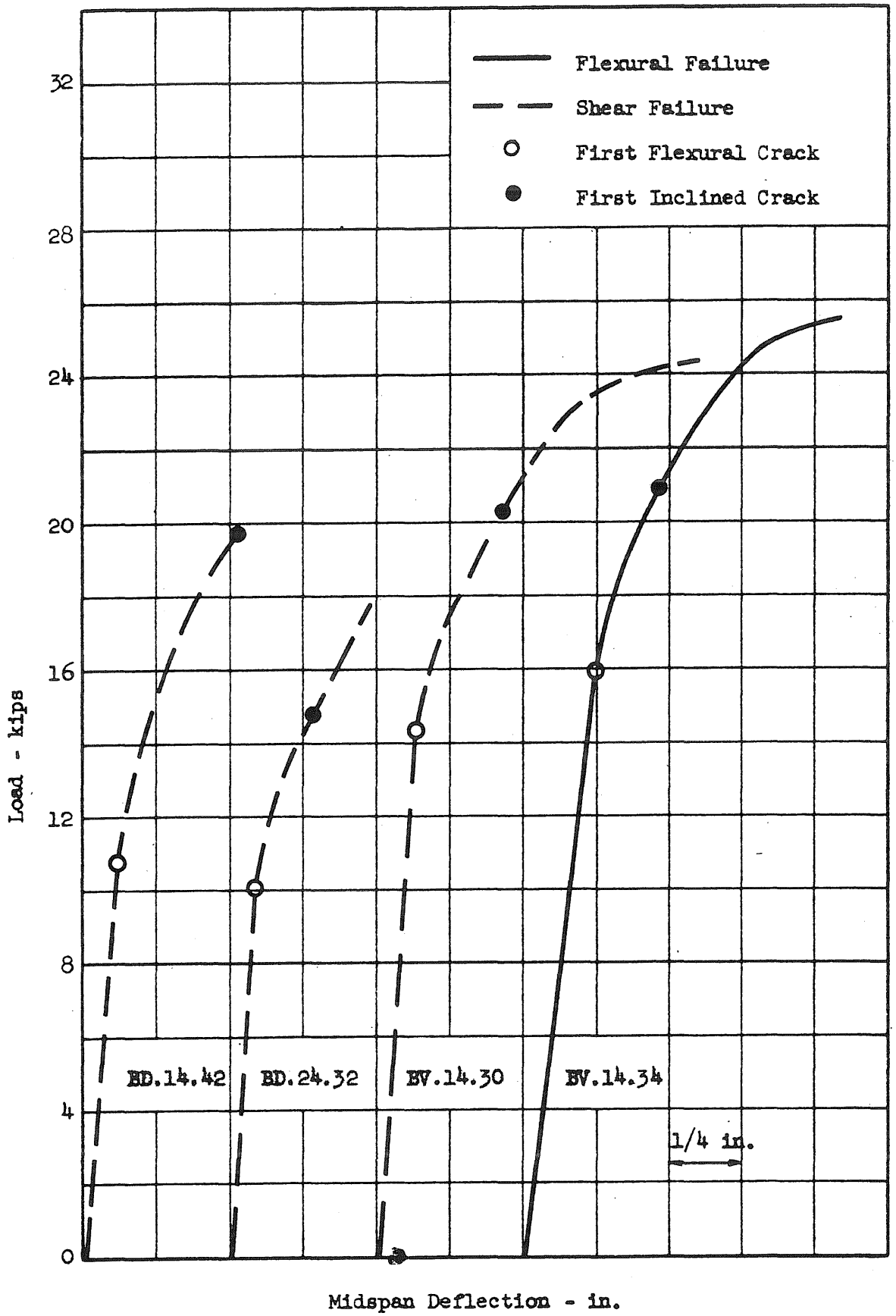

FIG. A5 LOAD-DEFLECTION CURVES - BEAMS WITH DRAPED REINFORCEMENT

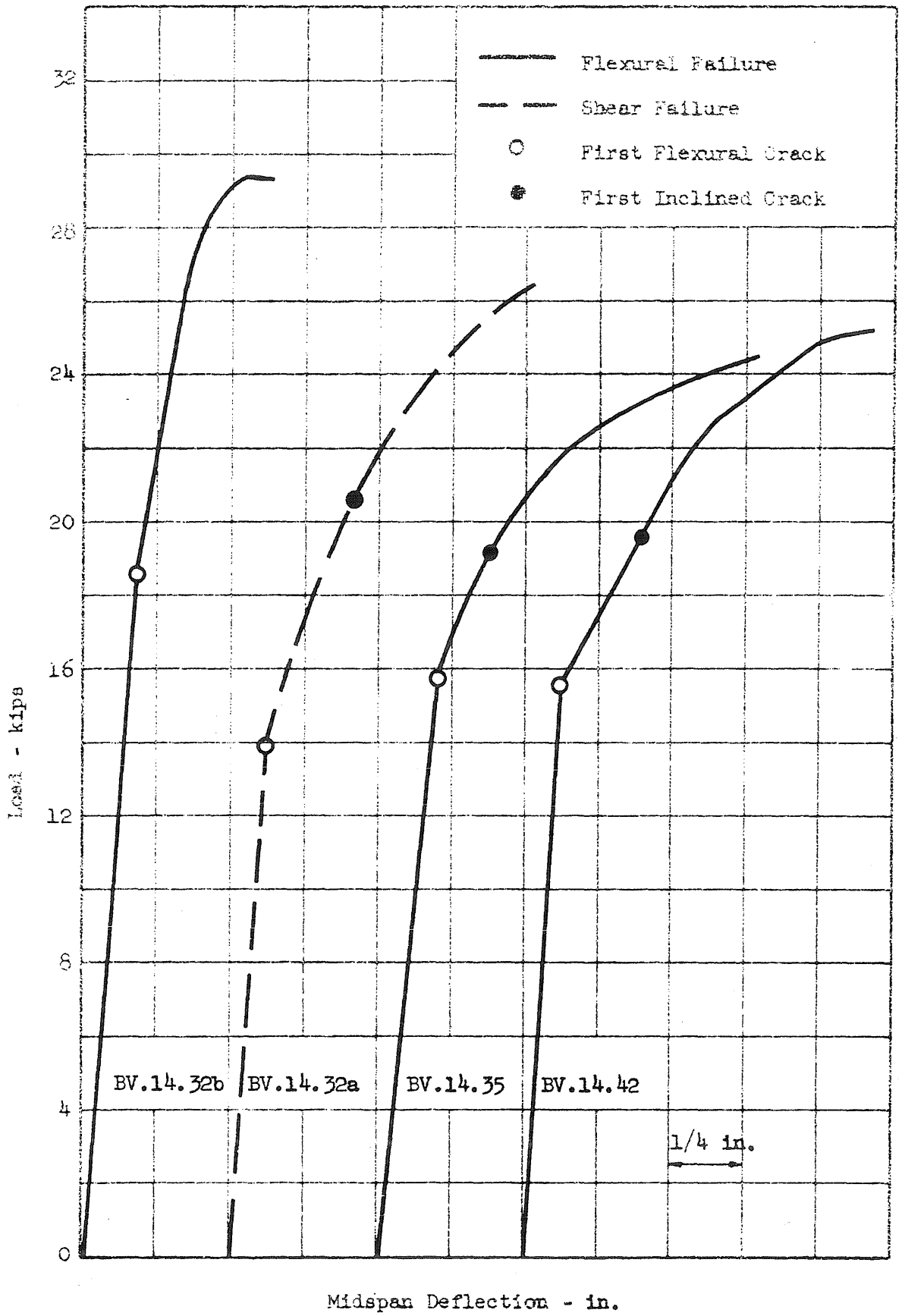

FIG. A6 LOAD-DEFLECTION CURVES - BEAMS WITH DRAPED REINFORCEMENT AND WEB REINFORCEMENT

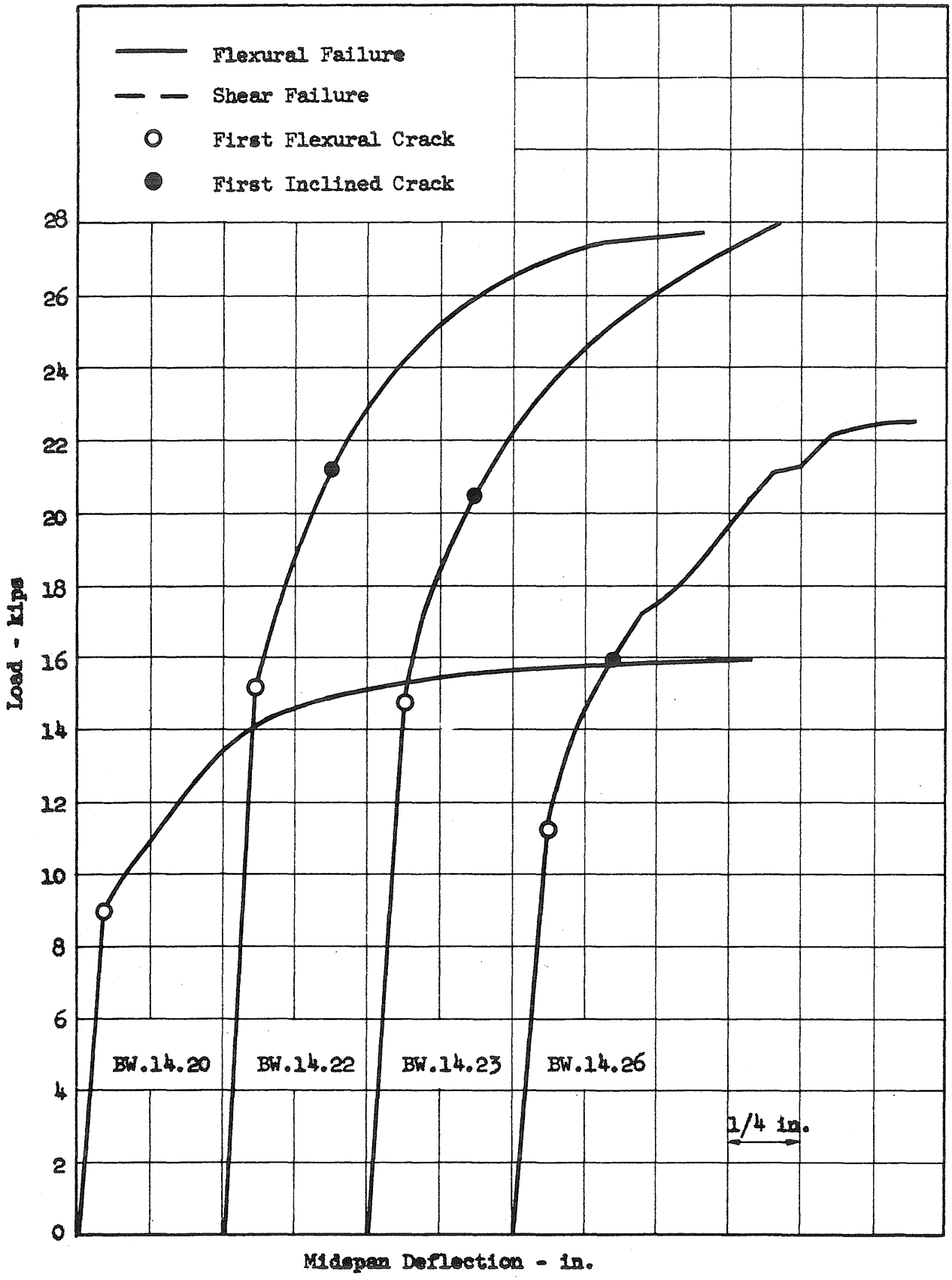

FIG. A7 LOAD DEFLECTION CURVES - 3-IN. I-BEAMS WITH WEB REINFORCEMENT AND 36-IN. SHEAR SPANS

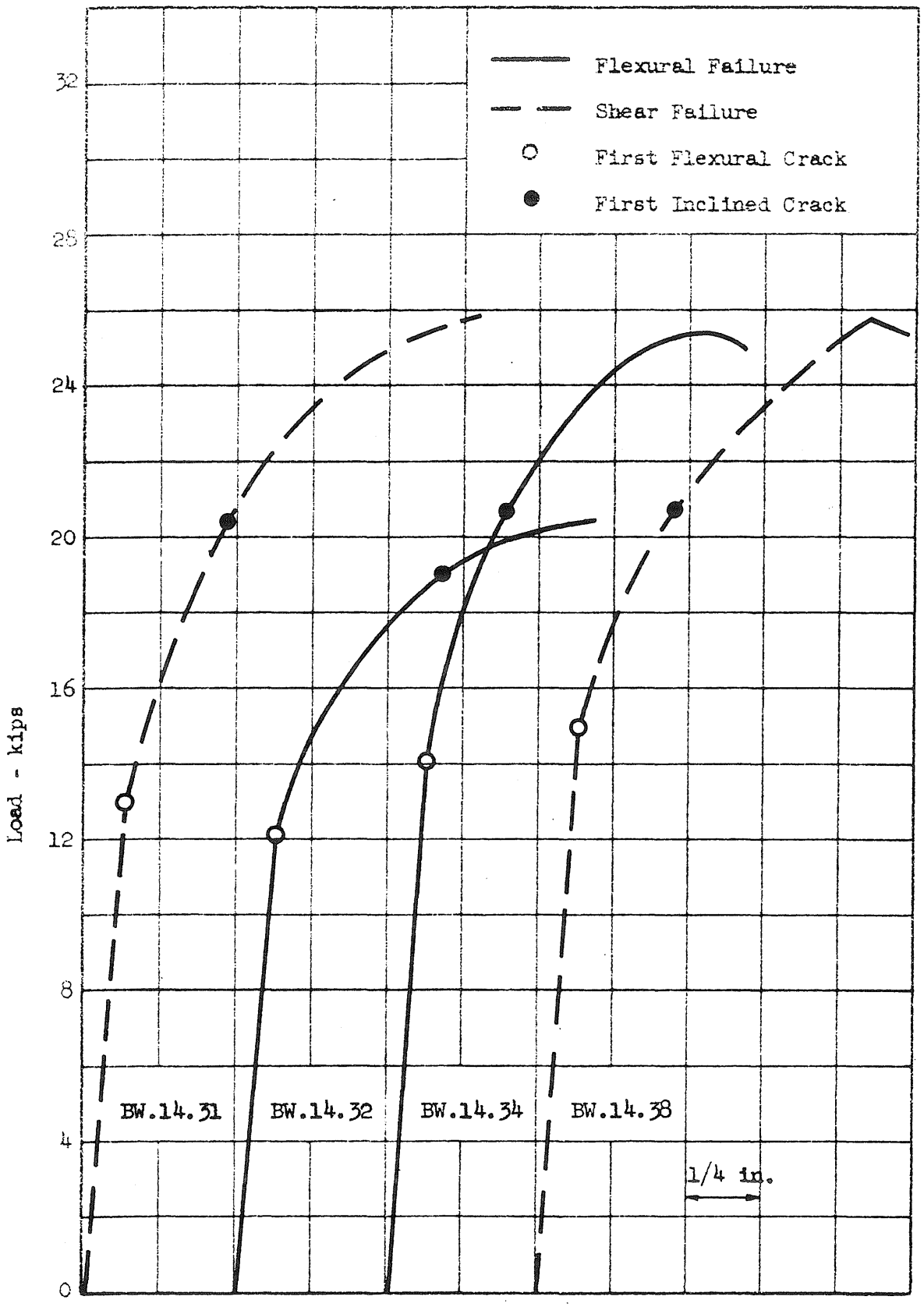

FIG. A8 LOAD-DEFLECTION CURVES - 3-IN. I-BEAMS WITH WEB REINFORCEMENT AND 36-IN. SHEAR SPANS

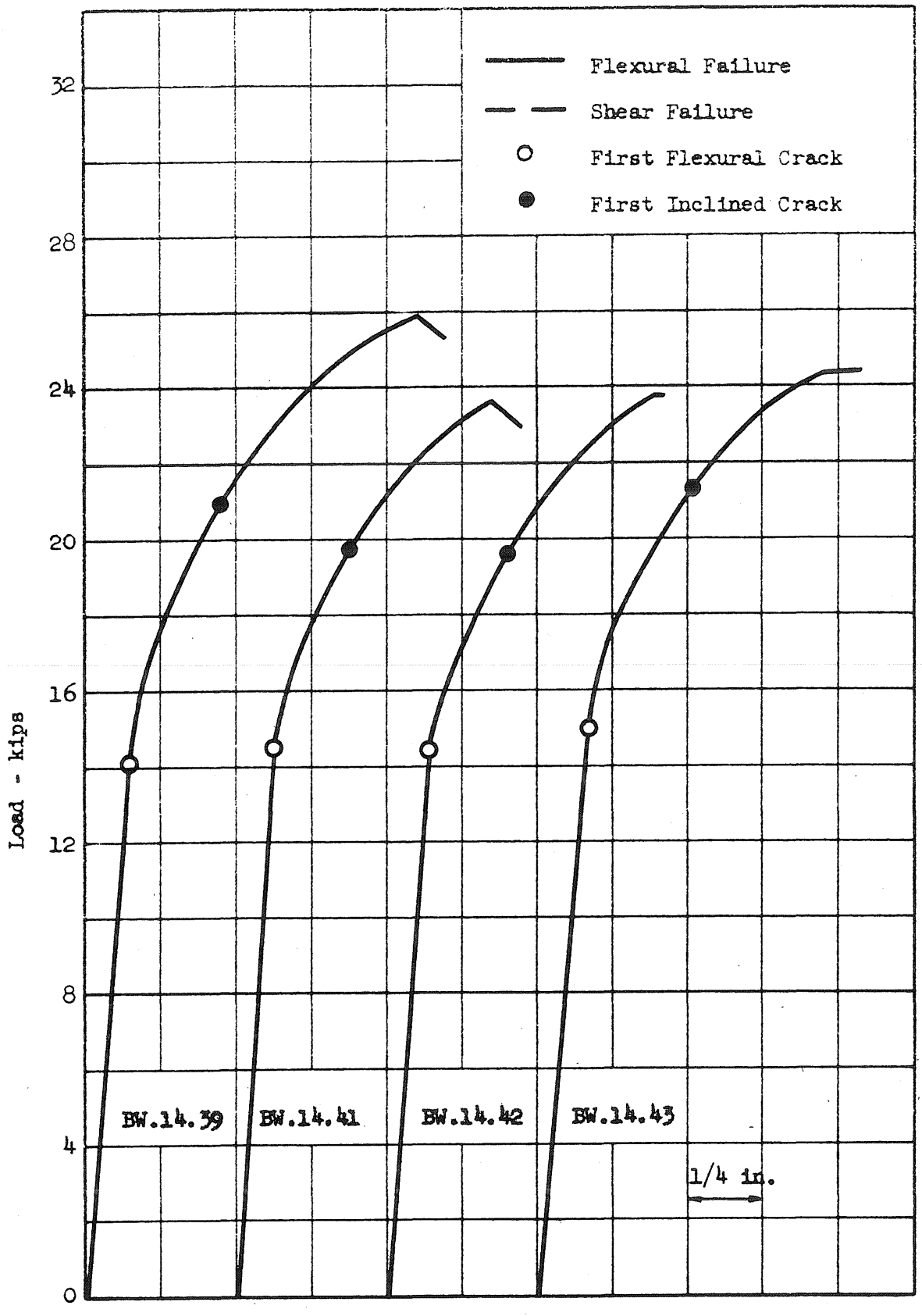

FIG. A9 LOAD-DEFLECTION CURVES - 3-IN. I-BEAMS WITH WEB REINFORCEMENT AND 36-IN. SHEAR SPANS

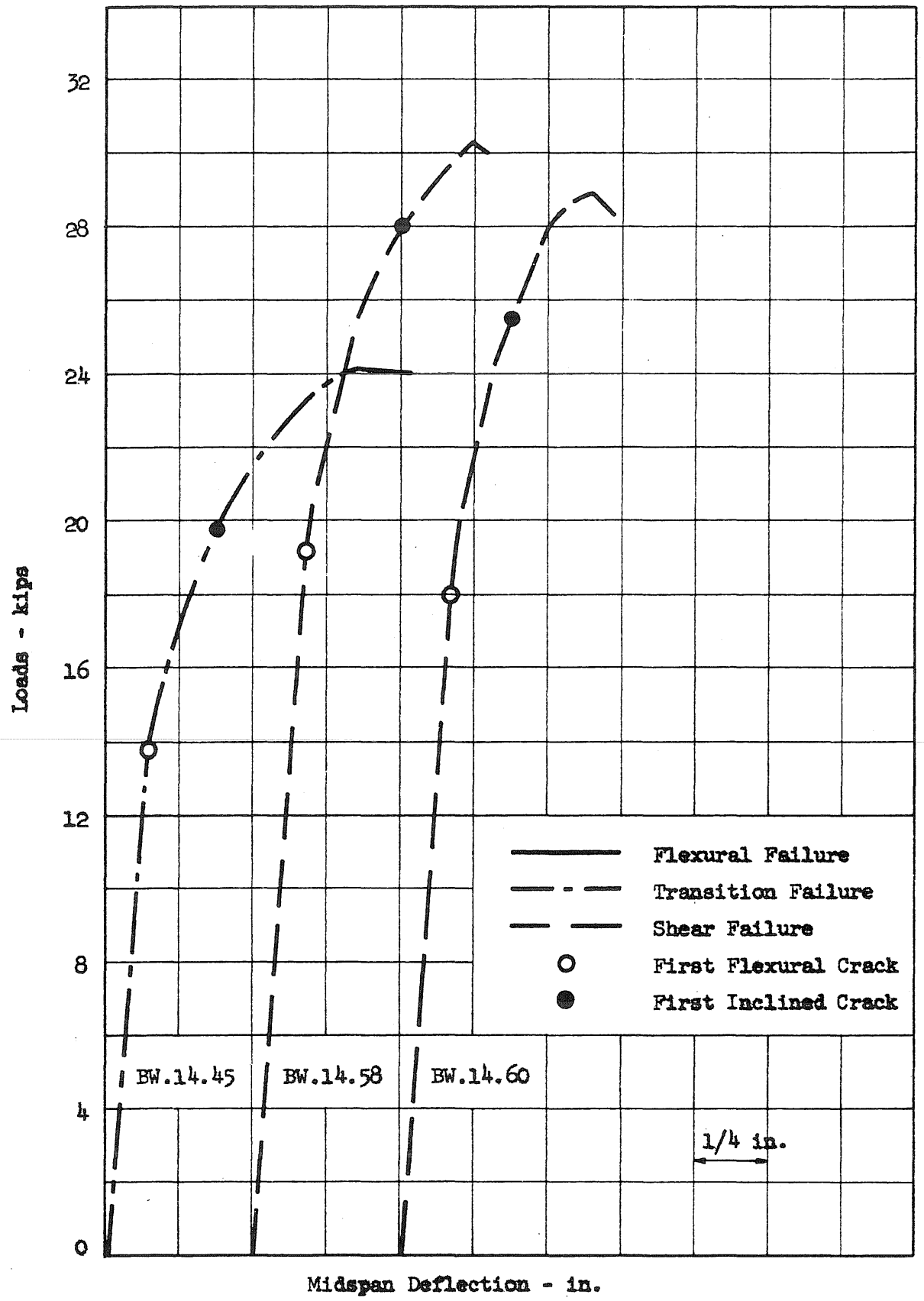

FIG. A10 LOAD-DEFLECTION CURVES - 3-IN. I-BEAMS WITH WEB REINFORCEMENT AND 36-IN. SHEAR SPANS

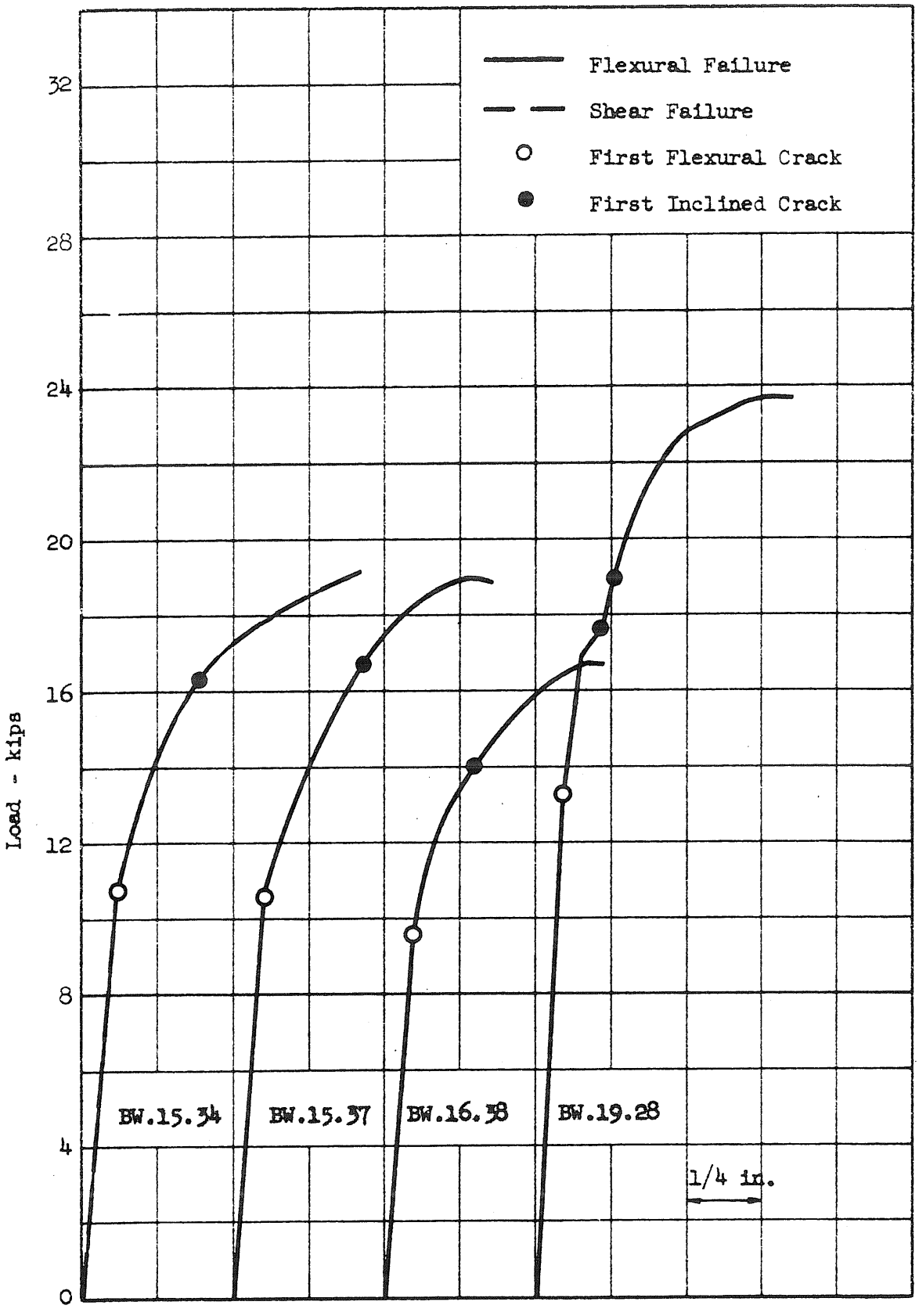

FIG. A11 LOAD-DEFLECTION CURVES - 3-IN. I-BEAMS WITH WEB REINFORCEMENT AND 48, 54, and 78-IN. SHEAR SPANS

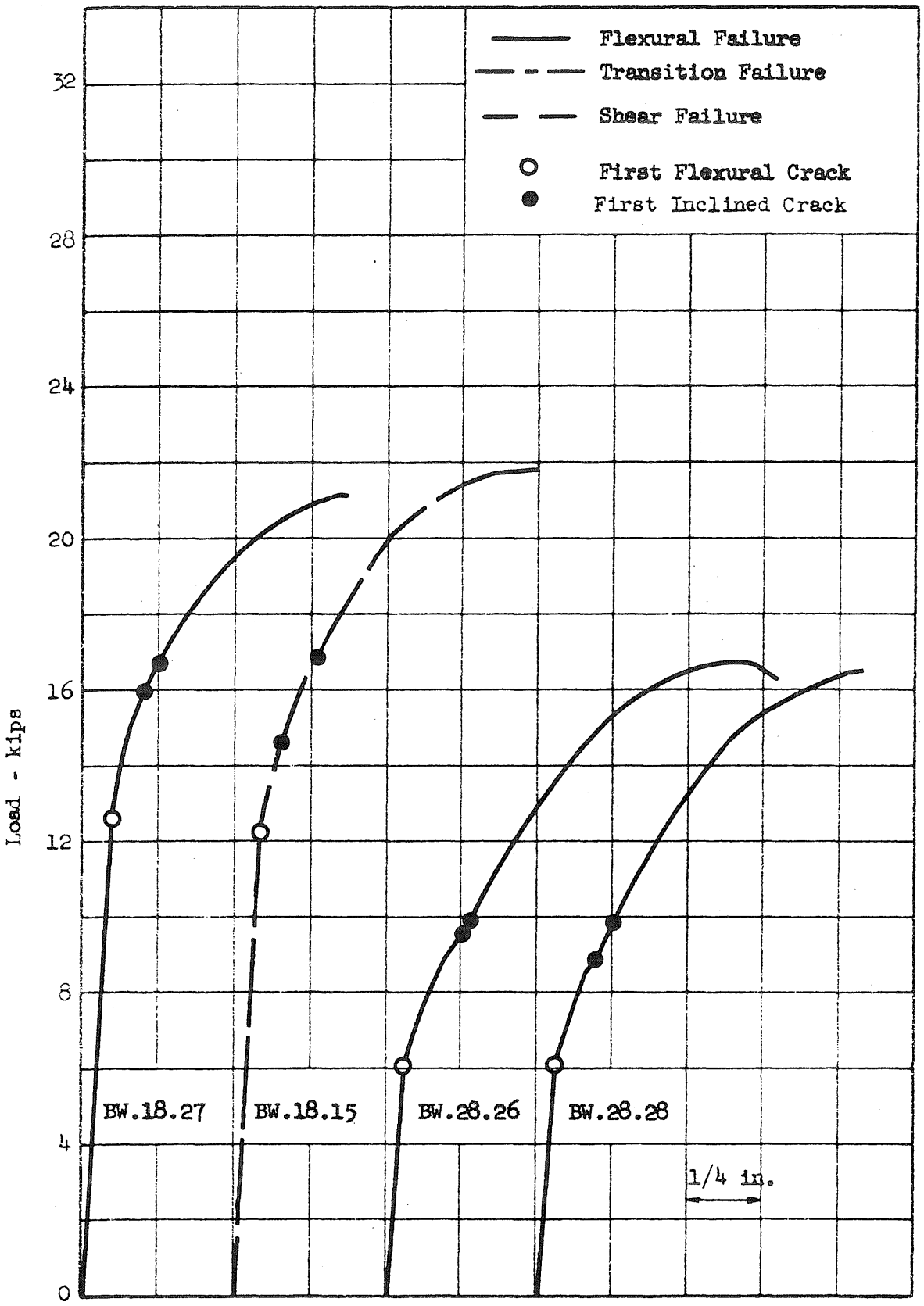

FIG. A12 LOAD-DEFLECTION CURVES - 3-IN. I-BEAMS WITH WEB REINFORCEMENT AND 70-IN. SHEAR SPANS

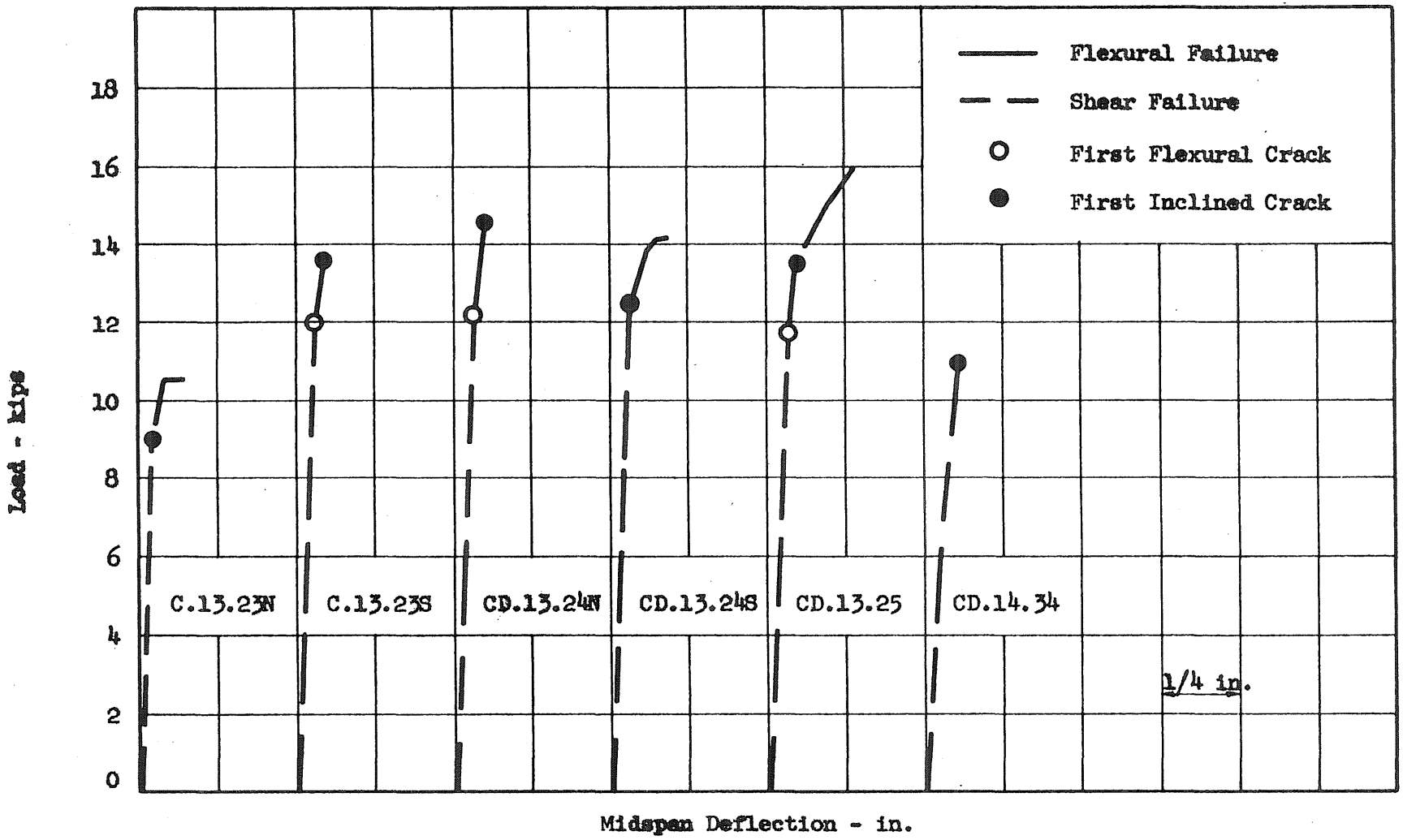

FIG. A13 LOAD-DEFLECTION CURVES - 1 3/4-IN. I-BEAMS WITH STRAIGHT AND DRAPED REINFORCEMENT

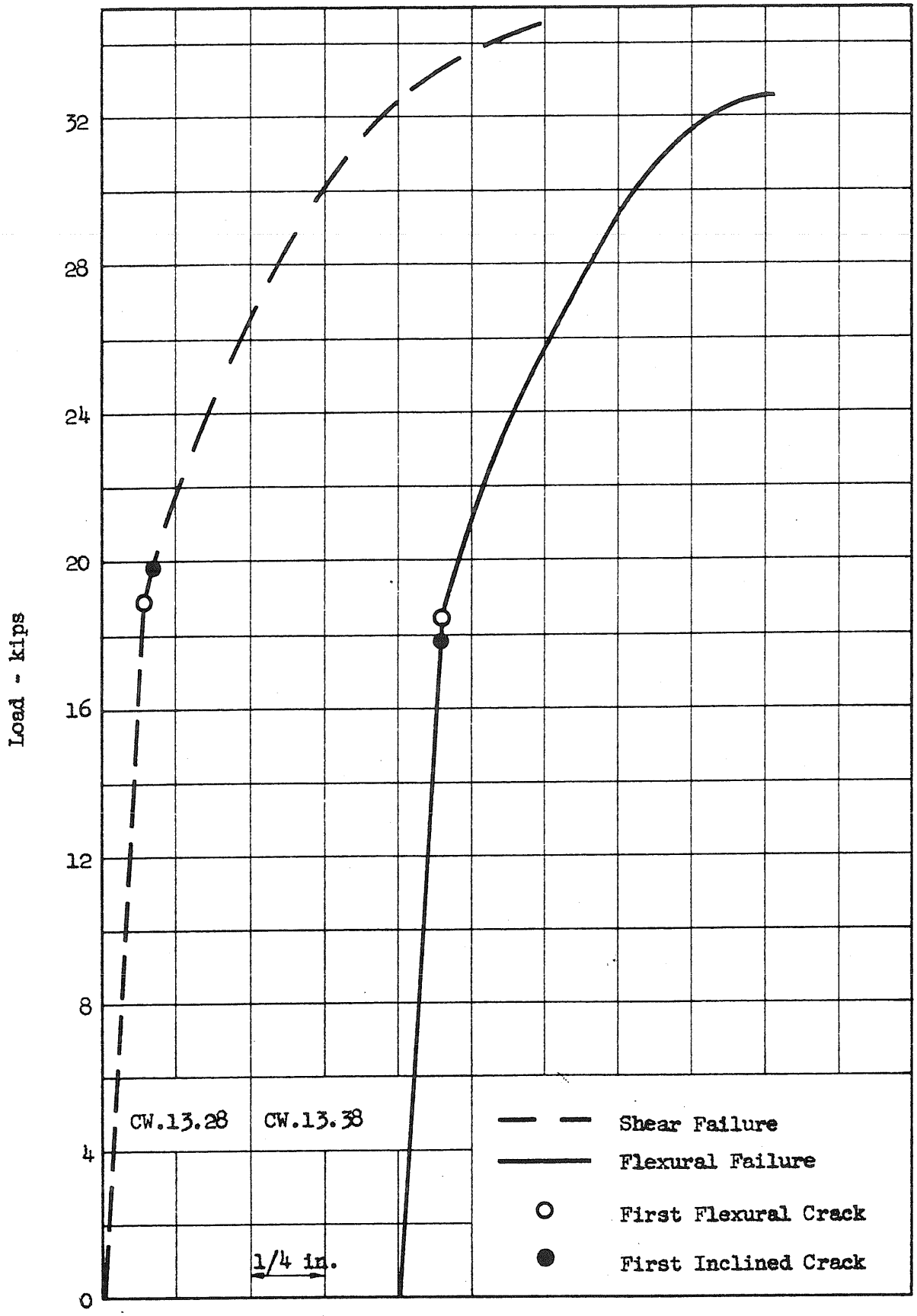

FIG. A14 LOAD-DEFLECTION CURVES - 1 3/4-IN. I-BEAMS WITH WEB REINFORCEMENT AND 28-IN. SHEAR SPANS

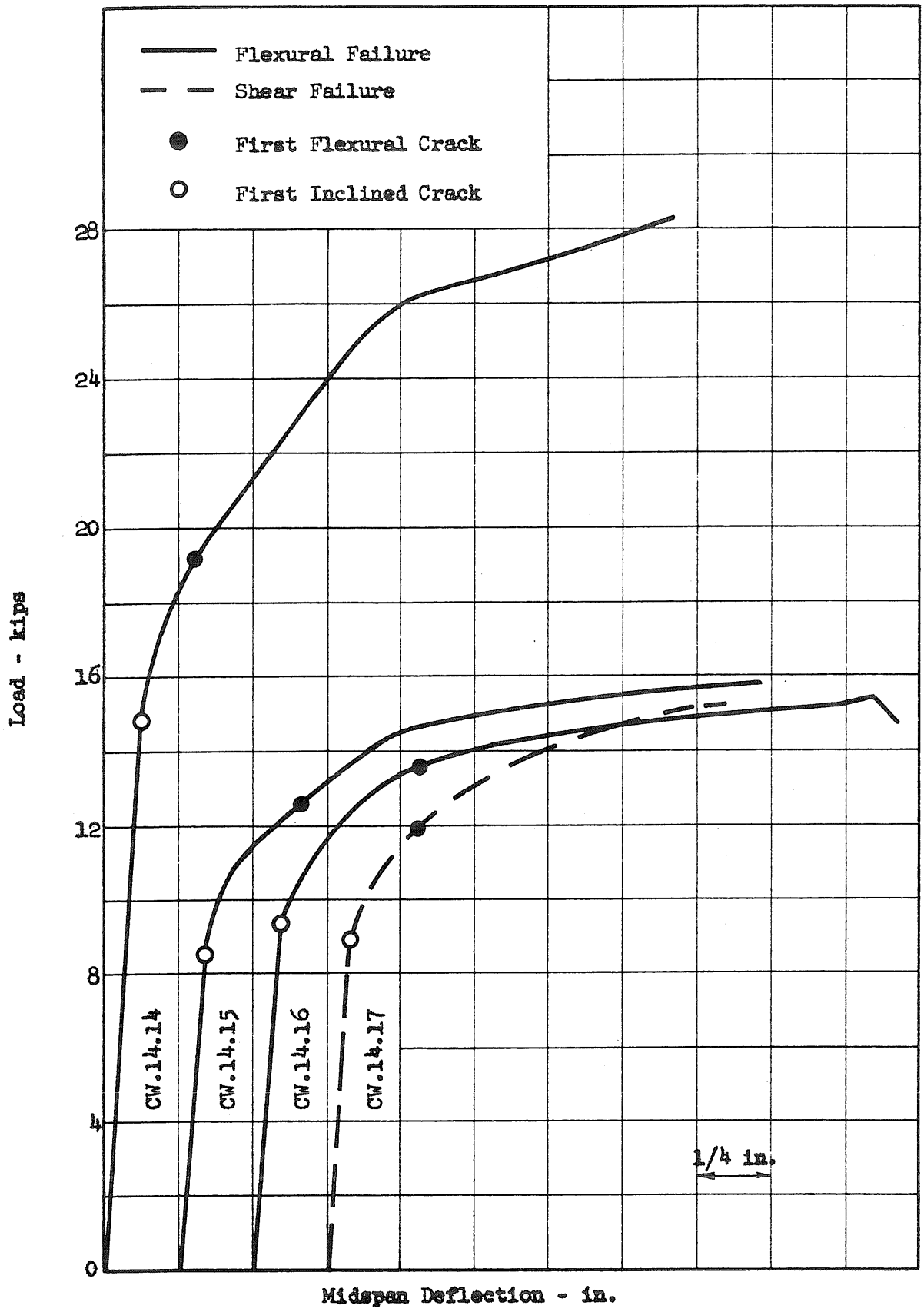

FIG. A15 LOAD-DEFLECTION CURVES - 1 3/4-IN. I-BEAMS WITH WEB REINFORCEMENT AND 36-IN. SHEAR SPANS

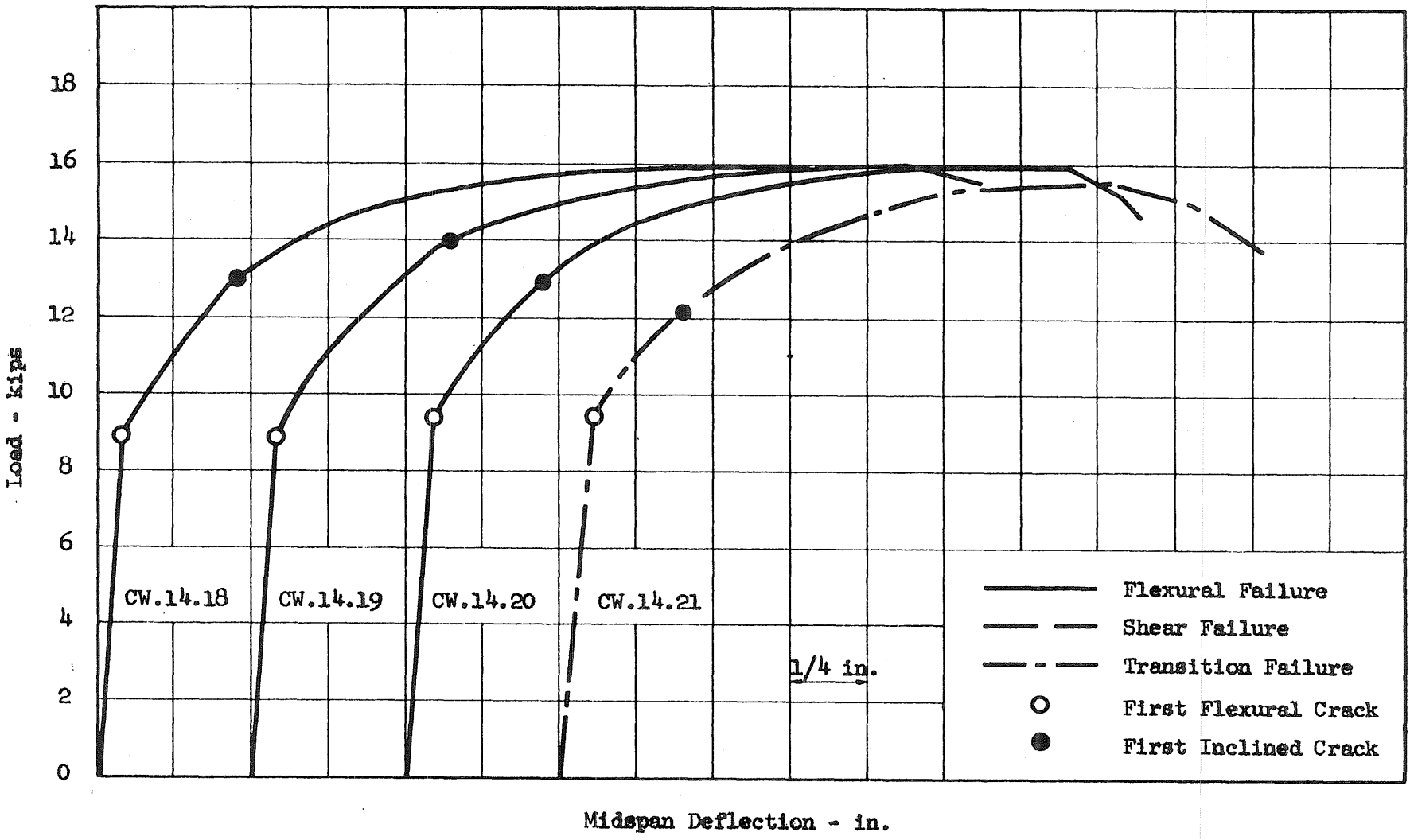

FIG. A16 LOAD-DEFLECTION CURVES - 1 3/4-IN. I-BEAMS WITH WEB REINFORCEMENT AND 36-IN. SHEAR SPANS

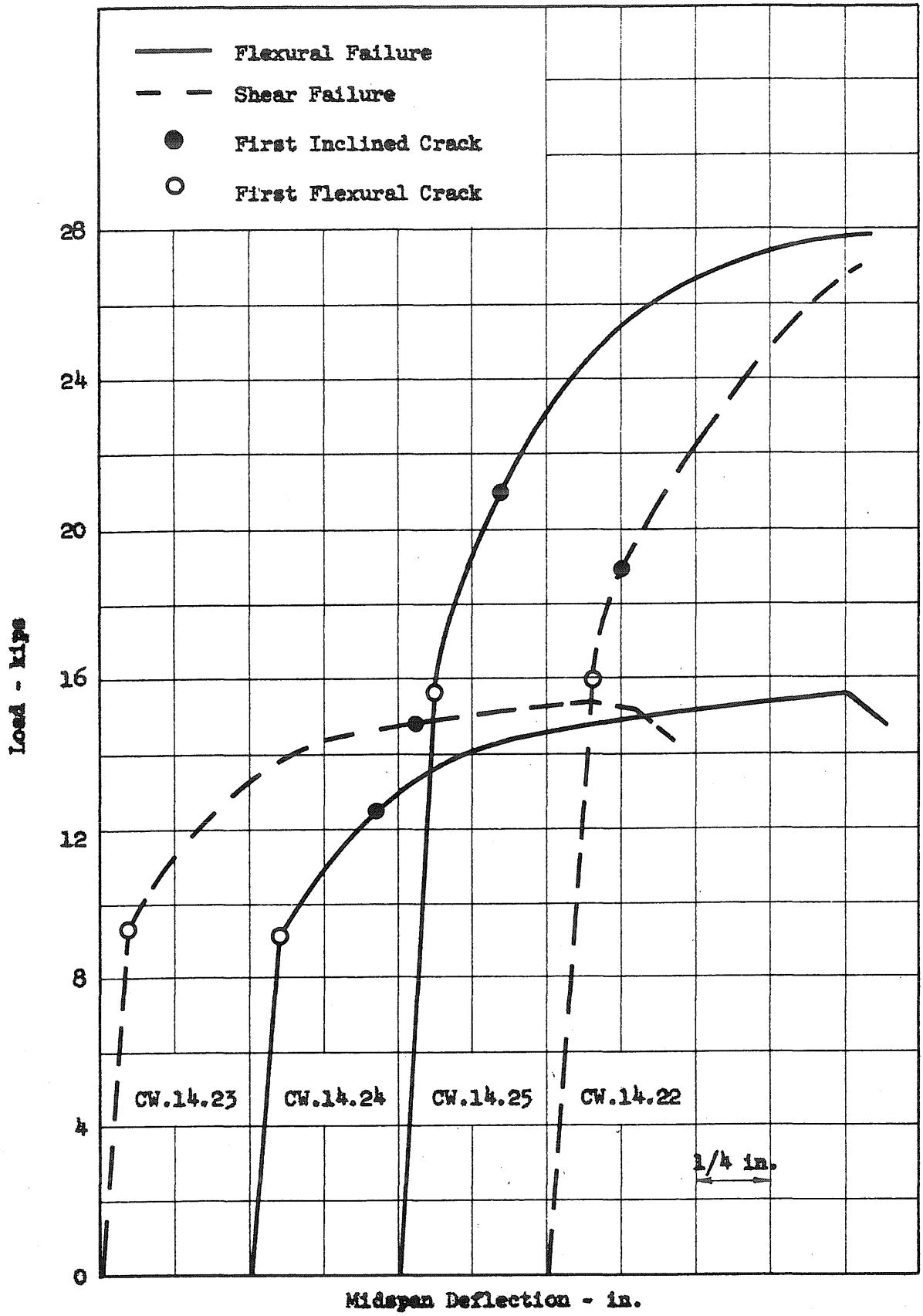

FIG. A17 LOAD-DEFLECTION CURVES - 1 3/4-IN. I-BEAMS WITH WEB REINFORCEMENT AND 36-IN. SHEAR SPANS

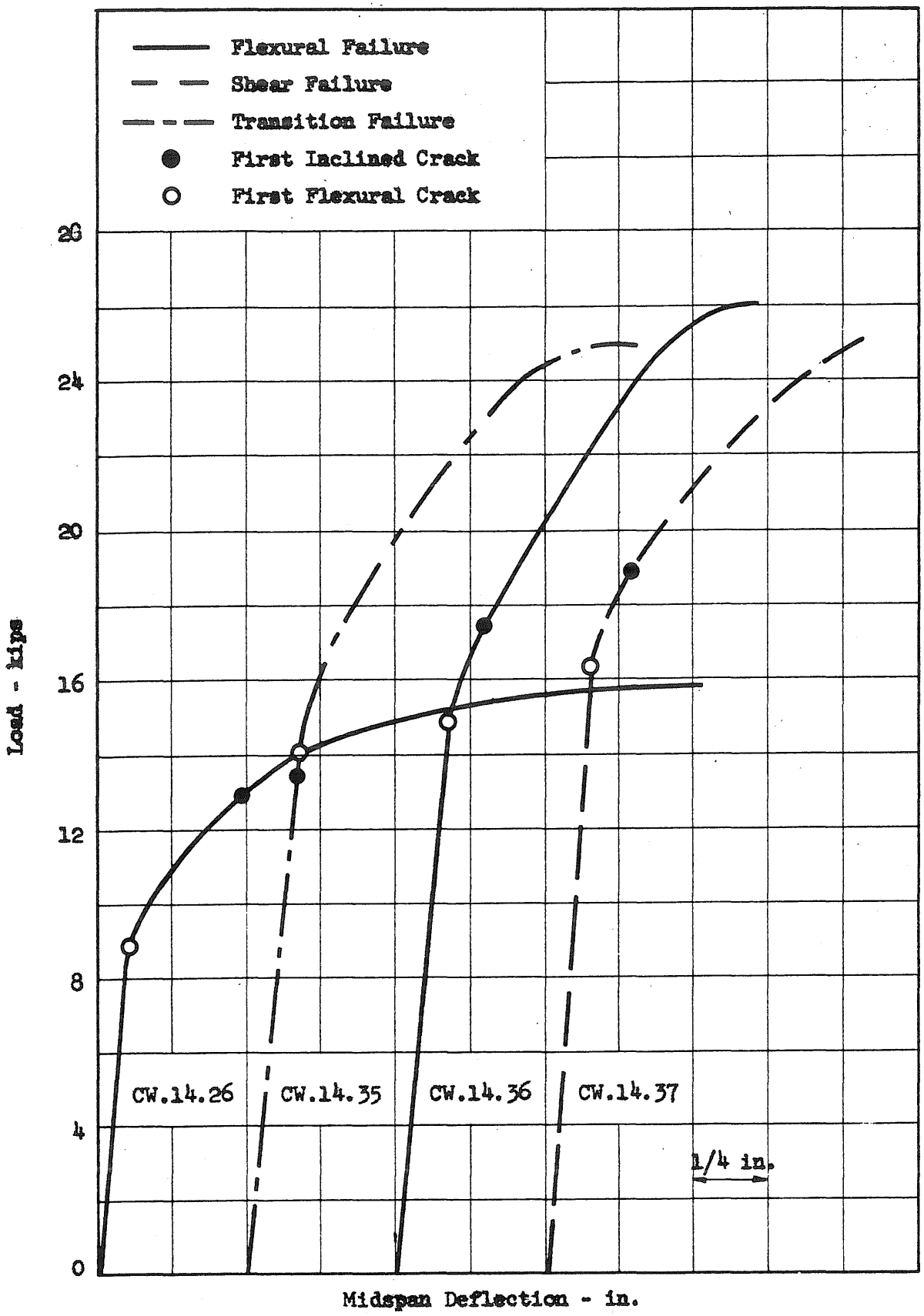

FIG. A18 LOAD-DEFLECTION CURVES - 1 3/4-IN. I-BEAMS WITH WEB REINFORCEMENT AND 36-IN. SHEAR SPANS

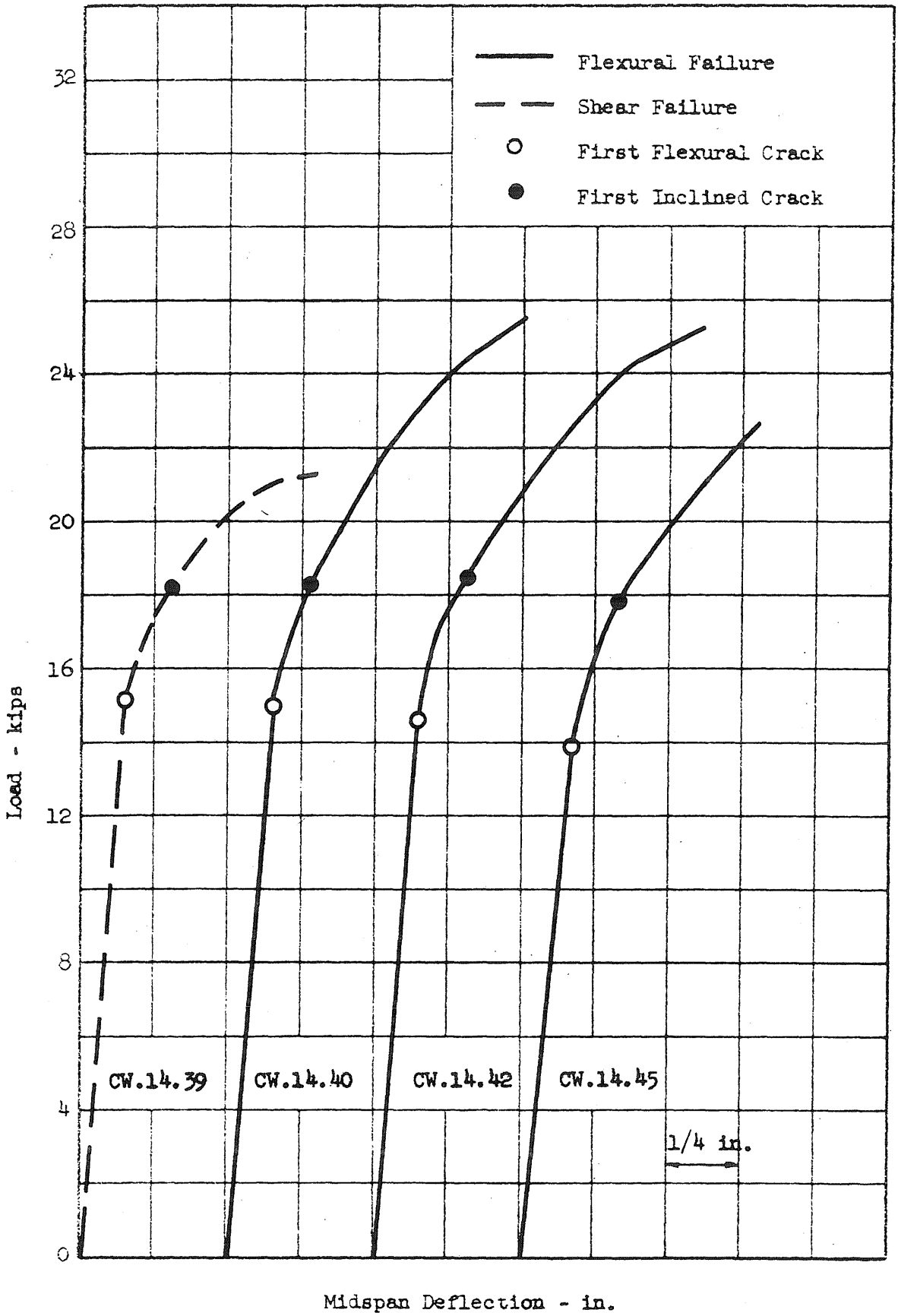

FIG. A19 LOAD-DEFLECTION CURVES - 1 3/4-IN. I-BEAMS WITH WEB REINFORCEMENT AND 36-IN. SHEAR SPANS

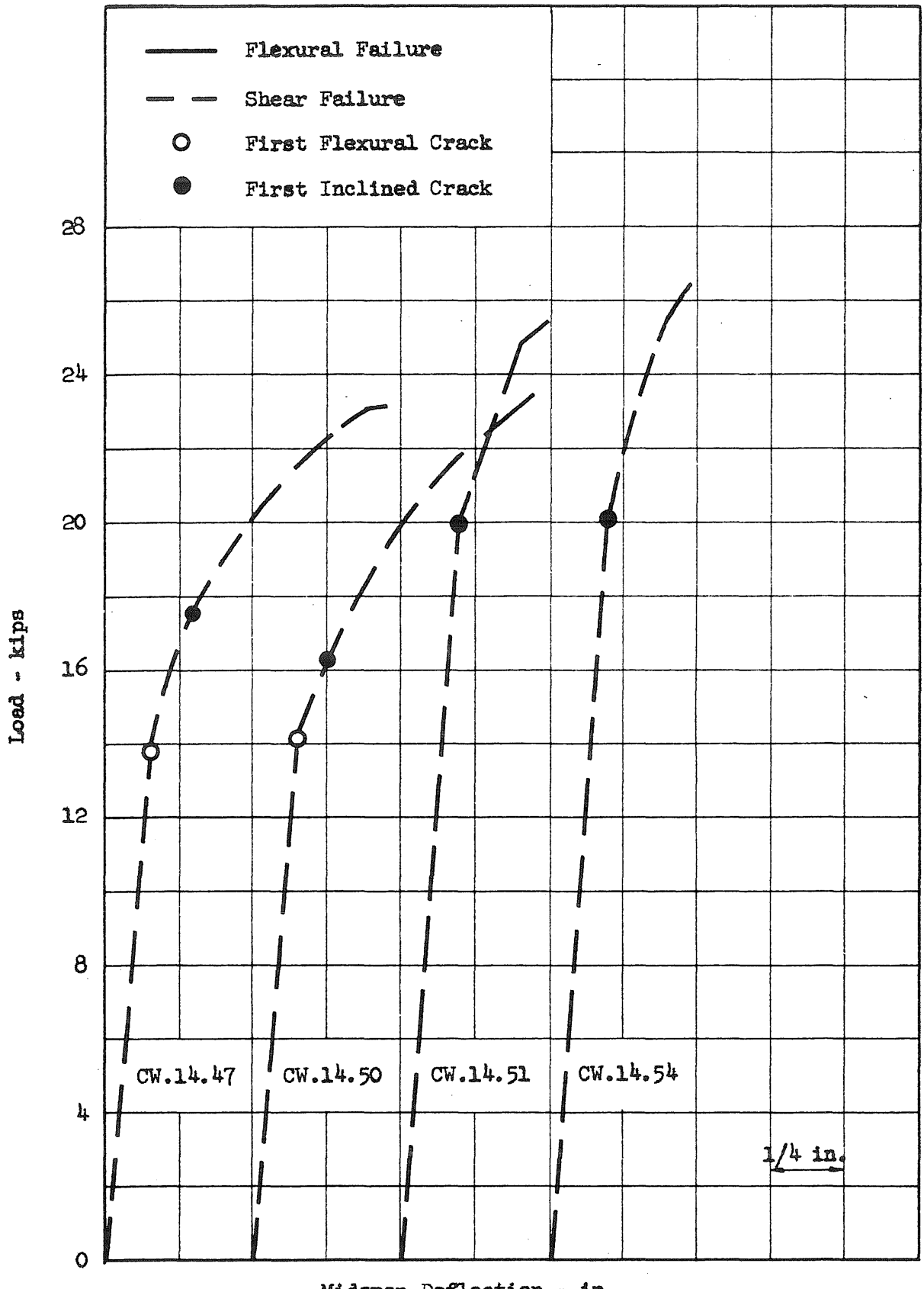

FIG. A20 LOAD-DEFLECTION CURVES - 1 3/4-IN. I-BEAMS WITH WEB REINFORCEMENT AND 36-IN. SHEAR SPANS

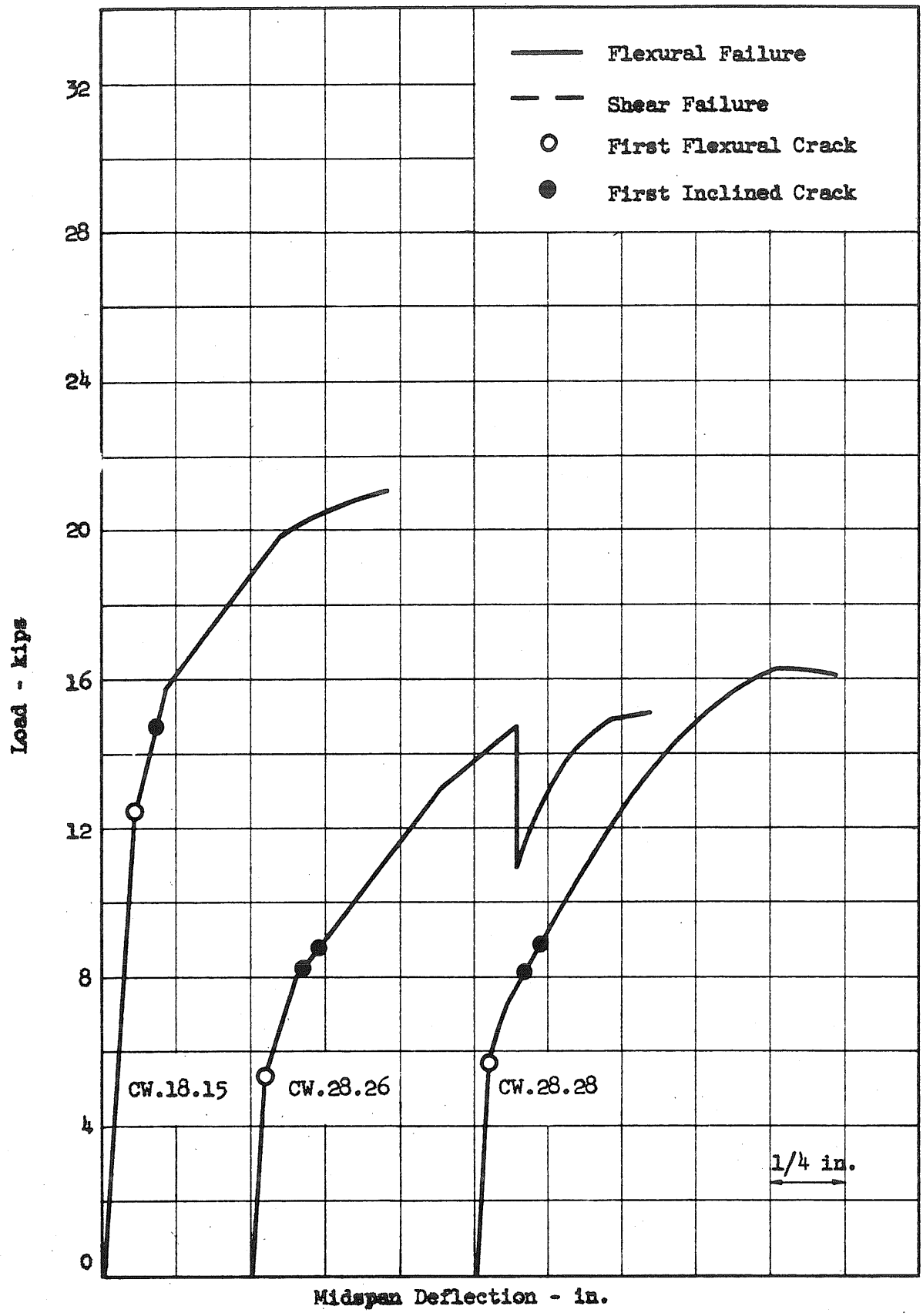

FIG. A21 LOAD-DEFLECTION CURVES - 1 3/4-IN. I-BEAMS WITH WEB REINFORCEMENT AND 70-IN. SHEAR SPANS

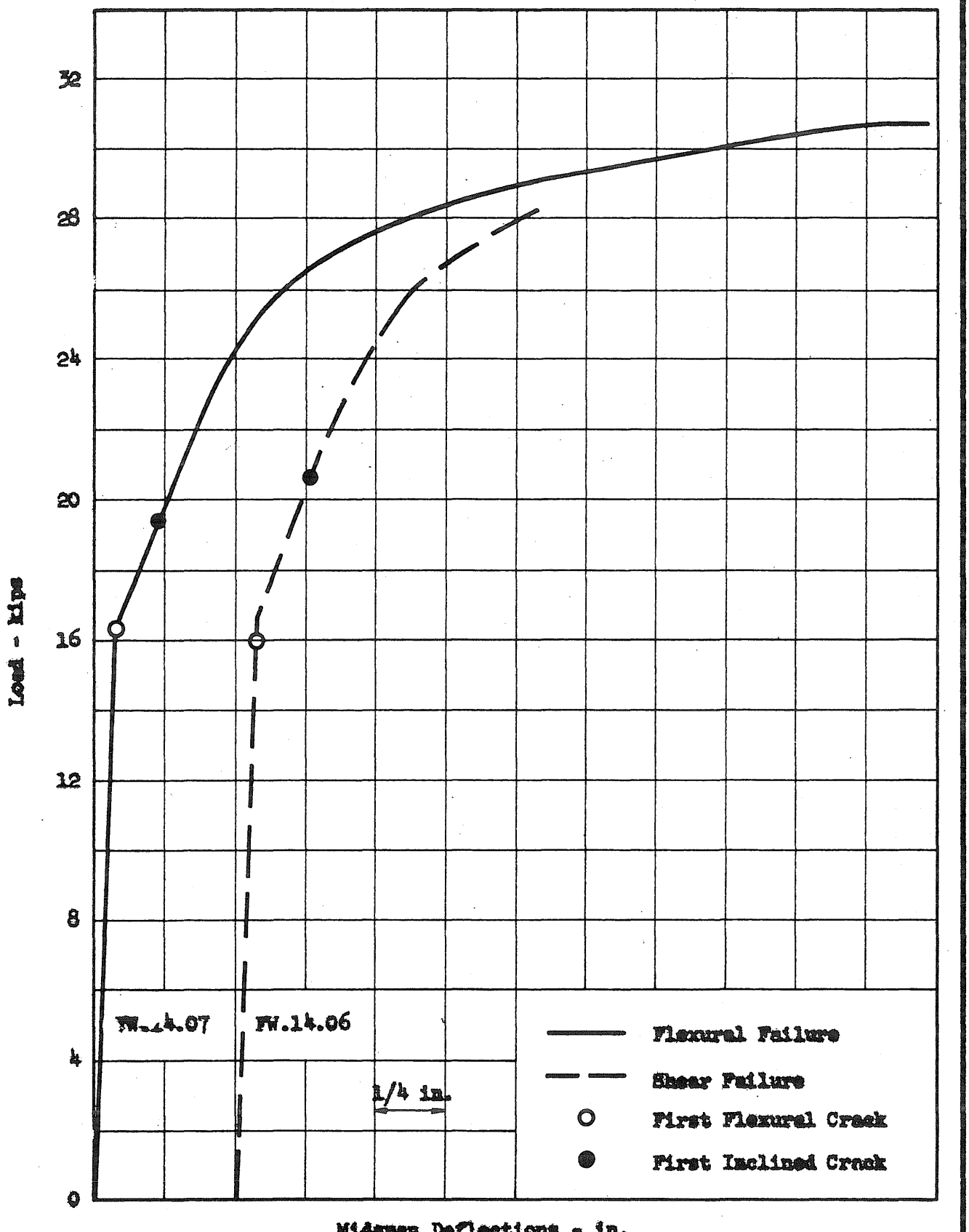

FIG. A22 LOAD-DEFLECTION CURVES - BEAMS WITH WEB REINFORCEMENT AND CAST-IN-PLACE SLABS